Seabirds in 3D: A Framework to Evaluate Collision Vulnerability with Future Offshore Wind Developments

Interim Project Report #1: Estimating Collision Vulnerability of the Seabird Community Across a Segment of the California Current System

This report was prepared by H. T. Harvey & Associates, the Schatz Energy Research Center, R. G. Ford Consulting Company, NOAA Southwest Fisheries Science Center and Oregon State University. This report was prepared for the California Energy Commission and Published by the Schatz Energy Research Center in October 2024.

http://schatzcenter.org/wind/

Disclaimer

This project was funded by the California Energy Commission. The content does not represent the official views of policies of the State of California. This report was created under agreement number: EPC-19-011

About H. T. Harvey & Associates

H. T. Harvey & Associates is an ecological consulting firm whose mission is to create ecologically sound solutions to complex natural resource challenges. We apply our expertise in wildlife ecology, aquatic ecology, plant ecology, restoration ecology, and landscape architecture in pursuit of this mission and we have delivered exceptional consulting services to public agencies, private entities, and nonprofit organizations since 1970. Our staff expertise encompasses a wide range of biological and design disciplines (wildlife ecology, aquatic ecology, plant ecology, restoration ecology, and landscape architecture). Learn more about our work at harveyecology.com

About the Schatz Energy Research Center

The Schatz Energy Research Center at Cal Poly Humboldt advances clean and renewable energy. Our projects aim to reduce climate change and pollution while increasing energy access and resilience. Our work is collaborative and multidisciplinary, and we are grateful to the many partners who together make our efforts possible. Learn more about our work at schatzcenter.org

Rights and Permissions

Schneider, Stephanie R., Eli Wallach, Charles Chamberlin, Sophie B. Bernstein, Sadie Trush, David G. Ainley, Scott B. Terrill, Sharon H. Kramer, R. Glenn Ford, Janet Casey, Jarrod A. Santora, Lisa Ballance, and Arne Jacobson. 2024. *Seabirds in 3D: A Framework to Evaluate Collision Vulnerability with Future Offshore Wind Developments—Interim Project Report #1: Estimating Collision Vulnerability of the Seabird Community Across a Segment of the California Current System.* Prepared by H. T. Harvey & Associates, the Schatz Energy Research Center, R. G. Ford Consulting Company, NOAA Southwest Fisheries Science Center, and Oregon State University. Prepared for the California Energy Commission and published by the Schatz Energy Research Center: Humboldt, CA. schatzcenter.org/publications.

Abstract

Since the 1970s, extensive vessel and aerial surveys have provided comprehensive data on seabird diversity, abundance and distribution across the California Current System (CCS), primarily focusing on horizontal (2D) characterizations of the community. While these surveys have supported identification of seabird 'hotspots' in 2D, there are currently no assessments that include the vertical (3D) distribution. Addressing knowledge gaps regarding seabird distribution patterns from a 3D perspective, however, will be required if California (CA) is to take advantage of its offshore wind (OSW) resources for purposes of reaching its 2045 renewable energy goals. Such assessments would allow the seabirds' vertical distribution to be more explicitly considered in assessments of potential OSW impacts. For offshore wind turbines, the rotor swept zones (RSZ) typically start at 30 meters (m) and extend upwards by an additional 230 m. Collision vulnerability is greatest for birds flying at heights that overlap this zone, with the probability of collision influenced by seabird morphology, flight-style, and wind speed. This report presents a novel 3D Seabird Collision Vulnerability Framework (3D Framework) that integrates several decades of at-sea seabird observations and the offshore windscape to predict densities and vertical distribution of the 44 seabird species most widely encountered in at-sea surveys to allow a 3D perspective of what is expected below, versus at, RSZ-height. Predicting the proportion of seabirds moving at RSZ heights was achieved by quantifying: (1) flight height and wind speed relationships for seabirds grouped by similar morphologies and flight styles, (2) 2D density predictions for each species, and (3) the density of seabird species flying at RSZ heights based on the above factors combined with a comprehensive characterization of the windscape. The study region included all offshore waters capable of supporting current OSW mooring technologies (up to 1,300 m depth), covering the continental shelf and upper continental slope of CA north through southern Oregon (OR). Going forward, it will be possible to apply this 3D Framework to new data and new locations to help decide which areas to lease to the expanding OSW industry. The outcome supports the broader goals of the '3D Seabird Project', to identify sites off CA that maximize energy generation while minimizing seabird exposure to RSZs.

Keywords: California Current System, community composition, density, flight height, marine ecosystem, offshore, seabirds, wind energy

Table of Contents

Tables

Figures

Appendices

List of Preparers

H. T. Harvey & Associates

Stephanie R. Schneider, M.S.

Sophie B. Bernstein, M.S.

Sadie Trush, Ph. D.

David G. Ainley, Ph. D.

Scott B. Terrill, Ph. D.

Sharon H. Kramer, Ph. D.

Schatz Energy Research Center

Eli Wallach, B.S.

Charles Chamberlin, Ph. D.

Arne Jacobson, Ph. D.

R. G. Ford Consulting Company

R. Glenn Ford, Ph. D.

Janet Casey

National Oceanic and Atmospheric Administration, Southwest Fisheries Science Center

Jarrod A. Santora, Ph. D.

Oregon State University

Lisa Ballance, Ph. D.

List of Abbreviations

2D – planar space (e.g., latitude and longitude)
3D – planar plus vertical space (e.g., altitude)
3D Framework – 3D Seabird Collision Vulnerability Framework
ASL – above sea level
BOEM – Bureau of Ocean Energy Management
CA – California
CCS – California Current System
CEC – California Energy Commission
CUTI – Cumulative Upwelling Transport Index
EQN – equation
ESA – Endangered Species Act
FG – flight-style groupings
GW – gigawatts
IDW – Inverse Distance Weighting
km – kilometers (1 kilometer = 0.6 miles)
LOO-CV – leave-one-out cross validation
m – meters (1 meter = ~ 3 feet)
m/s – meters per second
NREL – National Renewable Energy Lab
OCS – outer continental shelf
OR – Oregon
OSW – offshore wind
Project – 3D Seabird Project (inclusive of the Optimization Analysis)
RSZ – rotor swept zone
SB – Senate Bill
WEA – wind energy areas

Highlights

- The goal of this '3D Seabird Project' was to identify locations along the U.S. West Coast, particularly off California (CA), where seabird exposure to rotor swept zones (RSZs) associated with offshore wind (OSW) turbines could be minimized while maintaining strong wind power generation potential. Such information could help assess the suitability of sites selected for future OSW commercialization from a seabird perspective. In this interim task report, we focus on a novel '3D Seabird Collision Vulnerability Framework' (hereafter, 3D Framework).

- This Project is the first to offer a 3D perspective of the California Current System (CCS) seabird community, incorporating the vertical dimension alongside the traditional 2D view, inclusive of a significant portion of the seabird community off CA and southern OR. Due to its global importance, the seabird fauna of the CCS has been extensively surveyed, meaning that various long-term and spatially extensive datasets were available to be compiled and analyzed in relation to the windscape.

- Specifically, the 3D Framework partitioned the seabird community into species 'below risk height' and 'at risk height' by integrating: (1) the relationship between flight height and wind speed for seabirds grouped by similar morphologies and flight styles, (2) 2D density predictions for each species, and (3) the density of seabird species flying at RSZ-height based on the above factors, combined with a comprehensive characterization of the windscape.

- The modeled seabird community, including 44 of the 109 observed species with sufficient data for quantitative assessment, was found to: (1) consist of 18 distinct FGs; (2) mostly fly near the sea surface (<10 m [33 feet]) and concentrate over the inner continental shelf (within ~25 km [15 miles] of the coastline); (3) have much greater densities below the RSZ than within it; (4) include many species from FGs unlikely to fly at RSZ height (e.g., storm-petrels, phalaropes, cormorants, small and medium alcids); (5) include species from FGs more likely to fly at RSZ height (e.g., large diving shearwaters, gulls, small albatross, surface-feeding shearwaters, pelicans); (6) FGs with the strongest wind response use 'dynamic soaring,' where they harness the wind to swoop upward and then use gravity for forward movement.

- Dynamic soaring seabirds are most prevalent in outer continental shelf and inner slope waters, including those already leased for CA OSW development. Depending on the vagaries of prey availability, they are markedly less abundant in shallower, inner shelf waters, including those where OSW facilities currently exist globally. Thus, there's a critical knowledge gap regarding how likely it is that dynamic soaring species might interact with OSW infrastructure.

- The 3D Framework visualizes the overall CCS seabird community versus those 'at risk height', crucial for identifying areas of lesser and greater collision vulnerability across the broader seascape. The 3D Framework presented here can be further refined, updated with new data, and applied to other regions to support planning for expansion of OSW.

Introduction

Context and Background

To achieve the goal of powering CA with clean, renewable energy by 2045, in accordance with the 100% Clean Energy Act of 2018 (Senate Bill [SB] 100), the state will need to rely on a diversified set of energy sources. OSW stands out as a cost-competitive option (Rose et al. 2022) that holds the potential to contribute significantly to meeting the SB 100 targets. The windscape across CA's coastal and Outer Continental Shelf (OCS) regions, which are characterized by seasonally strong winds, has been deemed favorable for OSW energy generation potential. In alignment with SB 100, the California Energy Commission (CEC) has outlined plans to achieve 2 to 5 gigawatts (GW) of OSW capacity by 2030, with an ambitious increase to 25 GW by 2045 (Flint et al. 2022).

The successful deployment of OSW facilities, however, necessitates thorough environmental assessment, permitting, construction, and operational planning. In particular, the siting and permitting of floating OSW facilities will require assessing potential impacts of OSW facilities to marine communities, including the bird community. This will especially be true for seabird species associated with the deeper OCS waters, which have a distinct suite of species relative to the shallow-water OSW facilities currently operating elsewhere. Many seabird species that frequent windy regions of the deeper OCS waters, like those of the CCS, engage in a flight-style known as 'dynamic soaring', which is a flight strategy where an individual cycles through an extraction of energy from wind to gain elevation, then an extraction of energy from gravity to make forward progress with minimal flapping (Pennycuick 1978a, b; Ainley et al. 2015). Wind energy is as important as food energy to these species and it allows them to travel quite rapidly across vast distances in search of prey.

Decades of at-sea surveys, and associated analyses, have provided a baseline understanding of the spatial diversity and abundance of seabirds across the CCS (e.g., Briggs et al. 1987; Mason et al. 2007; Ainley and Hyrenbach 2010; Nur et al. 2011; Adams et al. 2014, 2016; Joyce 2016; Ford et al. 2021; Leirness et al. 2021). These efforts focused on identifying seabird activity 'hotspots' in 2D. However, there has not yet been a vertical component incorporated into prediction maps of seabird occurrence.

Despite the insights gained from 2D predictions, which might be used to shift OSW areas away from seabird 'hotspots' (e.g., Leirness et al. 2021), most seabird fatalities from OSW development are expected to result from collisions with rotating turbine blades which are vertically quite distant from the sea surface (~25 to 30 m [~80 to 100 ft]). To assess seabird vulnerability to collision, it is crucial to consider the degree to which species-specific flight altitudes overlap with potential OSW developments, specifically the RSZs of turbines associated with such developments. Therefore, shifting the dimensionality of predictions from 2D to 3D is imperative for a more accurate understanding of the vulnerability of the CCS seabird community to RSZ collisions.

Previous attempts to model seabird species abundance and distribution have lacked a vertical dimension because only a limited subset of at-sea surveys have flight altitude data for each encountered seabird. Estimating precise and accurate bird altitude above sea level (ASL) is challenging, particularly because the precision and accuracy of such estimates diminish with increasing vertical distances between observers and seabirds (Cook et al. 2018, Harwood et al. 2018, Webb and Nehls 2019, Largey et al. 2021). Because most observations are made from low-lying vessels, at or near the sea surface, estimating distances of birds anywhere above 10 m is challenging for human observers. Additionally, prior 2D assessments have only provided relative metrics of density, owing to a lack of adjustment for seabird movement relative to observer movement (i.e., flux-corrected counts; Spear et al. 1992). Those corrections are needed to accurately determine seabird density. We currently can adjust some historical at-sea counts for flux to estimate density, using the procedures in Clarke et al. (2003), as long as vessel speed and direction, and wind speed and direction (see Spear & Ainley 1997a, b), are logged. Various methods to generate 2D density predictions exist, and there is already a framework and CCS-specific data to predict seabird flight height based on FG and wind speed (Ainley et al. 2015). Thus, it is possible to make predictions about the composition and density of CA's seabird community at heights overlapping RSZs.

As the OSW industry extends into deeper waters where wind facilities have yet to be sited, there is a growing need to understand potential impacts to the seabird populations that occur in those newly impacted habitats. This necessitates investigations focused on the composition and density of birds flying at heights overlapping RSZs, particularly in comparison to shallower waters where OSW facilities currently operate. Initiating the development of a predictive framework for seabird composition and density at altitudes intersecting RSZs in the CCS represents a crucial first step. Such a framework would provide valuable insights, aiding in the identification of sites with reduced seabird presence. This information addresses current knowledge gaps relevant to the environmental permitting process for floating OSW facilities. Furthermore, with advancements in technologies for monitoring seabird movements in remote offshore environments (e.g., Schneider et al. 2024), there is potential for significant enhancements in the precision and reliability of predictions generated through such a framework.

Purpose and Goals

The purpose of this interim report was to provide an overview of a 3D Framework developed and applied by this Project. This 3D Framework predicted the 2D and 3D density of the 44 most abundant seabird species across areas capable of supporting OSW mooring infrastructure between Point Conception, in southern CA, and Yaquina Head, in central OR. Leveraging datasets of the offshore seabird community and windscape spanning the last few decades, the results contribute to the broader Project goal of implementing a multi-objective optimization to identify sites that best minimize seabird collision vulnerability while maintaining relatively robust energy generation potential (Figure 1).

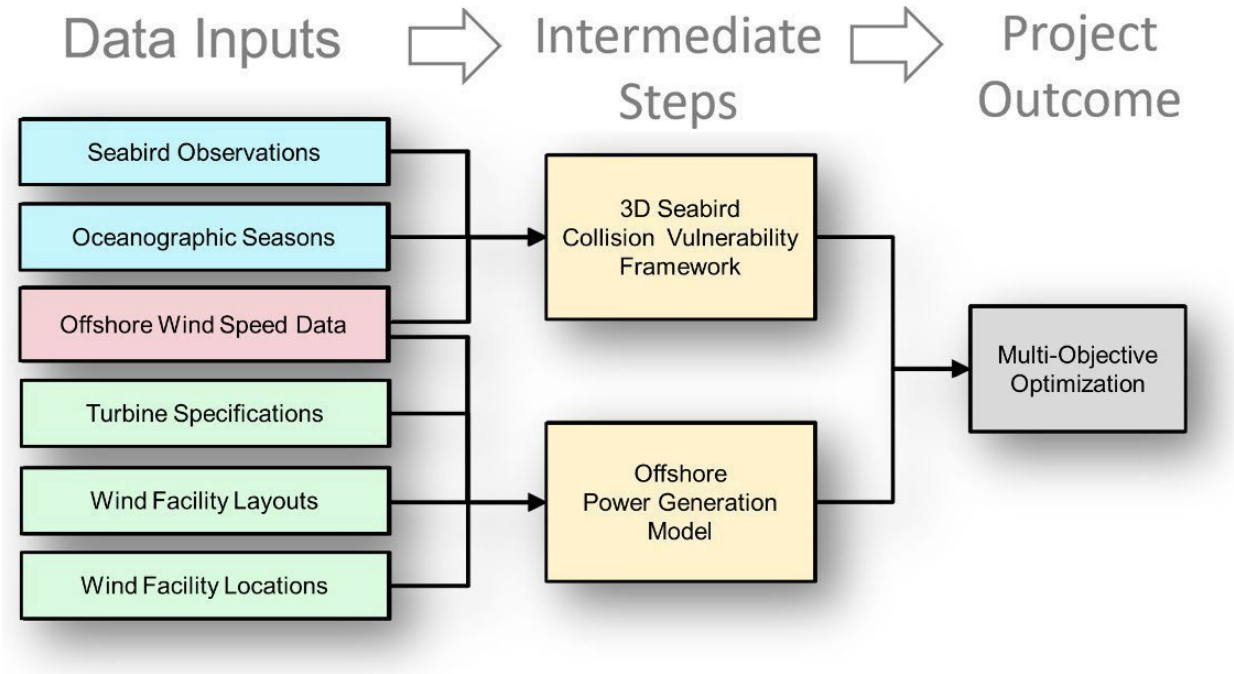

Figure 1. Diagram of the 3D Seabird Collision Vulnerability Framework Integrated into the Broader Multi-Objective Optimization Framework of the 3D Seabird Project

The 3D Seabird Collision Vulnerability Framework (upper yellow box) was just one integral part of the broader Multi-Objective Optimization Framework of this more comprehensive Project, intended to quantitatively evaluate trade-offs between offshore power generation capacity and seabird collision vulnerability (grey box). This overarching objective relied on two intermediate assessments (yellow boxes): the 3D Seabird Collision Vulnerability Framework, the focus of this interim report, and an Offshore Power Generation Model, detailed in a separate interim report. Data inputs supporting these assessments were color-coded as being either specific to the 3D Seabird Collision Vulnerability Framework (blue boxes), the Power Generation Model (green boxes), or both (pink box).

Project Approach

Overview of the 3D Framework

The Project's 3D Framework (Figure 2) integrates various analyses to predict the composition and density of portions of the central and northern CCS seabird community. This includes a subset of dynamic soaring birds, which are suspected to be more vulnerable to turbine blade collisions due to their propensity to fly at heights vertically overlapping RSZs in certain wind conditions. The total assemblage of seabirds modeled represents the seabird 'community' of the study area. By focusing the aggregate community, in addition to individual species, the analyses can explore emergent properties of the species within the Framework—such as the proportional contribution of each species to the overall community and overall density predictions.

The 3D Framework is best conceptualized as a multi-component analysis:

- Component I: Relate Flight Heights to Wind Speed
  The CCS's diverse seabird community was divided into distinct FGs, unified by relatively homogenous taxonomy and morphology, as identified by Ainley et al. (2015; see also Spear and Ainley 1997a, b). FG-specific probability curves, which indicate the chance of a bird overlapping RSZs across the full spectrum of wind speeds typically encountered in the CCS (0 to 30 m/s), were generated via a mixed-effects logistic regression using an extensive seabird flight height behavior dataset.

- Component II: Predict Densities in 2D
  At-sea seabird count data were partitioned into one of three oceanographic seasons recognized to exist in the CCS, each with distinct wind-driven upwelling and temperature regimes: Upwelling, Oceanic, Davidson Current (e.g., Bolin and Abbott 1963, Hickey 1979, Chelton et al. 1982). Traditional 2D density predictions were made at regularly spaced (i.e., gridded) intervals for each species and season using a spatial interpolation algorithm (see Supporting Data Section under Component II Methods for study details). To evaluate the accuracy of the 2D density predictions (birds/km^2), a cross-validation approach was used to assess how effectively the spatial interpolation algorithm captured underlying patterns in the observed data and made predictions for new, unseen data.

- Component III: Convert 2D Densities to 3D
  Using outcomes of Components I and II, the dimensionality of species density predictions was increased to create a 3D representation of the seabird community. This required the following steps: (S1) for each grid location having a 2D density prediction, a comprehensive distributional representation of the windscape (including extremes) was generated for each season; (S2) this gridded windscape was then integrated with the outcome of Component I to derive seasonal-, site-, and FG-specific probabilities of being at collision risk height; and (S3) probabilities from S2 were then applied

to the outcome of Component II to vertically partition overall density estimates and isolate the predicted density at RSZ-height.

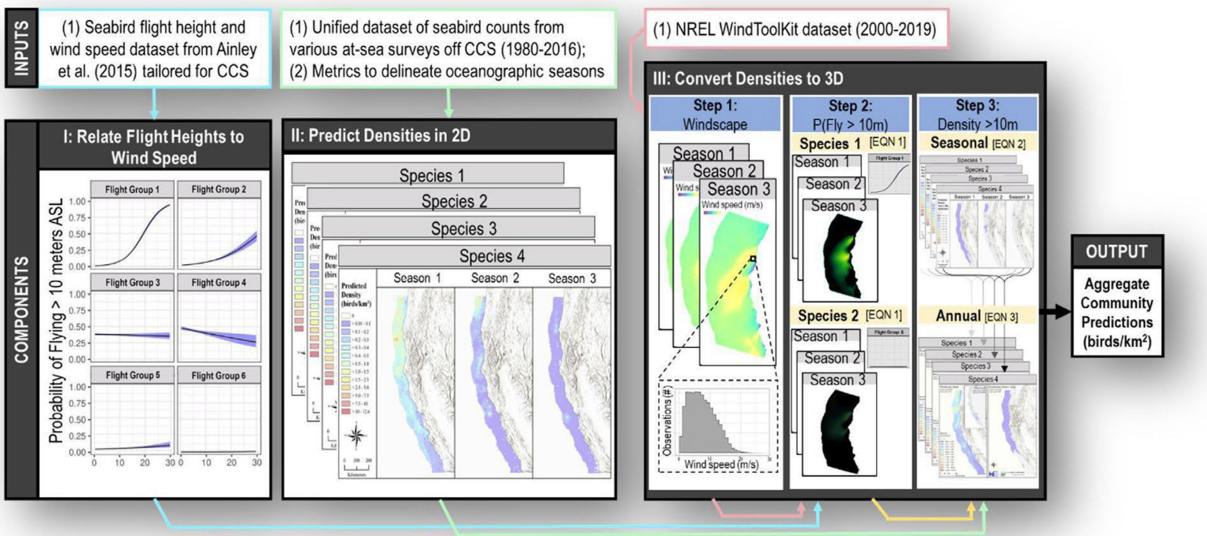

Figure 2. Analysis Components of the 3D Seabird Collision Vulnerability Framework

3D Seabird Collision Vulnerability Framework flowchart illustrates how diverse data were input and integrated across the three analysis components to generate annual predictions of 3D density [birds/km^2] for California's seabird community. Each panel corresponds to a distinct component and colored arrows depict data flow and connections between components, each arrow being colored to match its associated input and/or intermediate step. Definitions: CCS = California Current System; NREL = National Renewable Energy Lab; ASL = above sea level; km = kilometers; m = meters; m/s = meters per second; EQN = equation.

For each seabird type, spatially explicit 2D and 3D density predictions by season were weighted by the length of season to generate an annual perspective of the density of seabirds expected at each prediction location and then visualized using GIS mapping. The annual prediction maps represent what we would expect to see based on a long-term, multi-decadal perspective of the seabird community across the CCS rather than the extremes of abundance exemplified by individual years. While extremes can be important, they are subject to appreciable interannual variation and changing populations (e.g., Veit et al. 1997, Ainley and Hyrenbach 2010, Paleczny et al. 2015, Grémillet et al. 2018), and it is the long-term perspective that will facilitate OSW permitting and siting.

Component I: Flight Heights and Wind Speed

The likelihood of seabirds flying at heights that increase their risk of collision (over 10 m) was calculated for various wind speeds, ranging from calm to strong (0 to 30 m/s). This includes all wind speeds needed to spin wind turbines (3 to 25 m/s) and typical wind conditions in the CCS. The probability estimates were derived from data tailored to seabirds in the CCS, sourced from a comprehensive assessment covering a significant portion of the eastern Pacific Ocean, including the CCS (Ainley et al. 2015). Below, we outline key assumptions and definitions utilized in this analysis.

- The CCS seabird community was simplified into various distinct FGs following Ainley et al. (2015). Results presented here focus on FGs of the CCS species that are abundant enough to offer sufficient information for Components I, II, and III of the 3D Framework.

- Birds vulnerable to collision were defined as those observed to be ***present*** at heights of 10 m or greater, analogous to a 'presence rate'. While 10 m includes airspace below the lower extent of typical OSW RSZs, which is typically at ~25 to 30 m ASL, there was no way to avoid this vertical mismatch due to how the seabird flight height data were originally collected, with observers stationed on vessels where eye-height was ~10-12 m ASL. All birds above 10 m were assigned to the same flight height bin, regardless of whether they were at 10 m or 50 m, etc. Data exist for analogous species outside of the CCS (e.g., Antarctica) in which actual height was recorded to confirm birds in the 10 m category do frequently fly well within RSZs. Until flight height estimates can be improved and made more specific to the CCS (e.g., Matzner et al. 2022, Schneider et al. 2024), this 10 m threshold must serve as a proxy for seabirds achieving heights that make them likely to be present in airspace that will be overlapping RSZs—and are, thus, considered 'vulnerable' to collision.

Supporting Data

To generate probability curves of seabirds flying at RSZ height for various FGs and wind speeds, an extensive dataset collected on a series of cruises between 1976 and 2006 served as the foundation of this analysis. The original database contained relevant information on 131,354 individuals of 271 species across the Pacific Ocean, inclusive of the CCS, the equatorial Pacific off Hawaii, the Humboldt Current off South America, and the Southern Ocean, as detailed in Ainley et al. (2015). To support a CCS-specific analysis, this more extensive database was filtered to retain all observations from the CCS as well as include species known to be present off the coast of CA that were also observed elsewhere (e.g., Laysan albatross in the Equatorial Pacific). For a comprehensive description of the original data collection protocols, refer to Ainley et al. (2015).

A crucial aspect of these data collection initiatives involved categorizing flight heights for all seabird observations into the following predefined categories:

- On the sea surface or foraging, i.e., remaining in one place;
- Flying 0 to 3 m ASL;
- Flying >3 to10 m ASL;
- Flying >10 m ASL.

Including birds present on the sea surface, where flight height equaled 0 m ASL was essential for deriving an overall 2D representation (Component I) because the standardized seabird observation database used to derive 2D density estimates included both flying and stationary birds. As such, accounting for birds on the sea surface was crucial for partitioning 2D densities before converting to 3D.

Logistic Regression

The predicted probability of flying above 10 m for each FG containing a sufficient sample size for further statistical analysis, i.e., 18 FGs, was calculated using a mixed-effect logistic regression. The 'glmer' function in the lme4 package in R (Bates et al. 2015) was used, with wind speed as a fixed effect and FG as a random effect. FG was treated as a random effect to account for correlated structures (Midway 2022), given that the species modeled are part of a larger seabird population (Li et al. 2011). Final plots with wind speed as a predictor versus the probability of the binary response were generated for each FG using the outcome of this analysis, with confidence intervals around each probability curve generated via non-parametric bootstrapping.

Component II: Seabird Densities in 2D

The primary goal of this assessment was to apply the 3D Framework to a large marine region inclusive of areas that could support future OSW facilities. Consequently, our study area included CA's Humboldt and Morro Bay Wind Energy Areas (WEAs), which have already been leased to floating OSW developers (BOEM 2022). We also included seabird observations from central and southern OR due to the extension of the avifauna farther north in the CCS increasing sample size and thereby enhancing predictions about northern CA's seabird community. Other WEAs are being considered, but have not been finalized, within this larger area.

Area of Interest

Seabird observations supporting Component II of the 3D Framework encompassed all continental shelf waters from Point Conception, CA, to Newport, OR, in the South-North direction (34.40°N to 44.74°N) and out to 370 km from the coastline (essentially the U.S. Exclusive Economic Zone) in the East-West direction (-120.40°W to -131.0°W) (Figure 3). Predictions were generated in 2D and 3D for a specific subset of this area, extending out 80 km perpendicular from the coastline (Figure 3). This focused prediction region was inclusive of all waters shallow enough to support the current state-of-the-art OSW mooring infrastructure defined by BOEM and NREL (i.e., the upper OCS, no more than 1,300 m deep). The depth of 200 m represents the continental shelf break along the West Coast, with waters rapidly deepening to 3,000 m west of the continental shelf break, i.e. the OCS. It is the upper portion of the slope (shallower than 1,300 m) that will be leased to support OSW developments. The seabird prediction space was divided into a uniform grid of 1,806 cells, each with a 2D dimension of 5-minute latitude by 5-minute longitude (5' x 5') (ranging in area from 61.1 to 70.5 km^2), and seabird density predictions were made for each grid cell.

To assess differences in the composition of California's seabird community between 2D ('all elevations') and 3D ('above 10 meters') perspectives, the study area was divided into six regions, with Cape Mendocino (40.44°N) serving as the boundary between north-south and east-west divisions determined by distance from the coastline. These divisions considered offshore wind facility jurisdiction, resulting in three main categories: 'nearshore', representing waters under state jurisdiction that extend out to 4.8 kilometers (km) (i.e., 3 miles [mi]); 'intermediate', representing waters out to 32 km [20 mi] and in federal jurisdiction but nut currently being leased; and 'offshore', representing all waters from 32 km out to the western extent of the prediction boundary.

Collectively, these six regions encompassed most waters off California physically capable of supporting offshore wind mooring infrastructure (i.e., waters shallower than 1,300 m; 32 to 80 km [20 to 50 mi] offshore) and inclusive of all currently leased Wind Energy Areas (WEAs). Taxa were grouped broadly for clarity, with average annual density estimates (birds/km^2) provided above each column.

Supporting Data

At-Sea Seabird Studies

Seabird observations were amassed to facilitate Component II's 2D density predictions across the CCS. The dataset for Component II was collected from nine systematic aerial and vessel-based strip-transect surveys conducted in waters off CA and OR between 1980 and 2016 (Table 1 and Table A-1 in Appendix A). Effort associated with these studies varied in terms of annual and seasonal coverage (Table 1), spatial coverage (Figure 4), and total survey effort across the study area (Figure 5).

Data Standardization Across Studies

Although the various surveys employed a range of methodologies, they all adhered to continuous strip-transects typical for at-sea surveys of seabirds (Spear et al. 1992, 2004). At least one but, most often, two observers recorded all birds detected while on a moving platform at sea. Identifications were made to the lowest taxon feasible, and associated counts were noted. Additional details on survey protocols are available through the references listed in Table A-1.

One important difference in survey protocols was the width and segment length of census strips, with the most pronounced difference being the strip-width associated with aerial surveys (50 to 75 m) versus vessel surveys (300 m) (Table A-1). That difference was a result of platform speed and the ability of observers to count every bird within the strip. On aircraft moving ~50 m/s, only 50 to 75 m could be accommodated compared to 300 m on vessels moving 6 to 8 m/s. To account for this difference in effort per length of transect traveled, continuous strip-transect results were standardized to a common format. Each transect line was divided into 1 km^2 units of equal areas of transect effort. These 1 km^2 segments could be better accommodated in the 5' x 5' grid cells, and this standardization ensured that spatial efforts associated with counts were approximately equal, allowing observations from multiple surveys to be combined.

Once all the datasets were harmonized and results were expressed in terms of equitable amounts of effort, these counts were then corrected to account for flux related to the direction and speed of seabirds relative to the direction and speed of observers. Methods explicitly detailed by Spear et al. (1992) and validated by studies that were able to compare estimates from flux-corrected counts of seabirds to adjacent, well-censused seabird colonies were used (e.g., Clarke et al. 2003, Ford et al. 2021, Russell et al. 2023). For counts of birds that were moving too slowly for the possibility of double-counting to be an issue, including stationary birds (e.g., birds resting on the water, foraging, diving, etc.), flux would be negligible and observed counts would match the flux-corrected counts.

Oceanographic Seasons

Seabirds exhibit strong responses to changes in productivity and food availability (Ainley et al. 2005), driven by seasonally variable oceanographic conditions not captured in conventional calendar-based seasons. In recognition of this, the 3D Framework generates species-specific predictions for each oceanographic season in the CCS defined by winds and productivity: Upwelling, Oceanic, and Davidson Current. By partitioning seabird observations to better align with shifts in the seasonal productivity of the CCS, the intention was for 3D Framework predictions to be sensitive to and capture resulting shifts in seabird distribution and density across the region over a typical annual cycle. For each of the three CCS-specific oceanographic seasons (Figure 6), a description of key characteristics and the methods used to identify approximate start and end dates are detailed in the following subsections. The start and end dates were determined by averaging across multi-decadal ocean climate records.

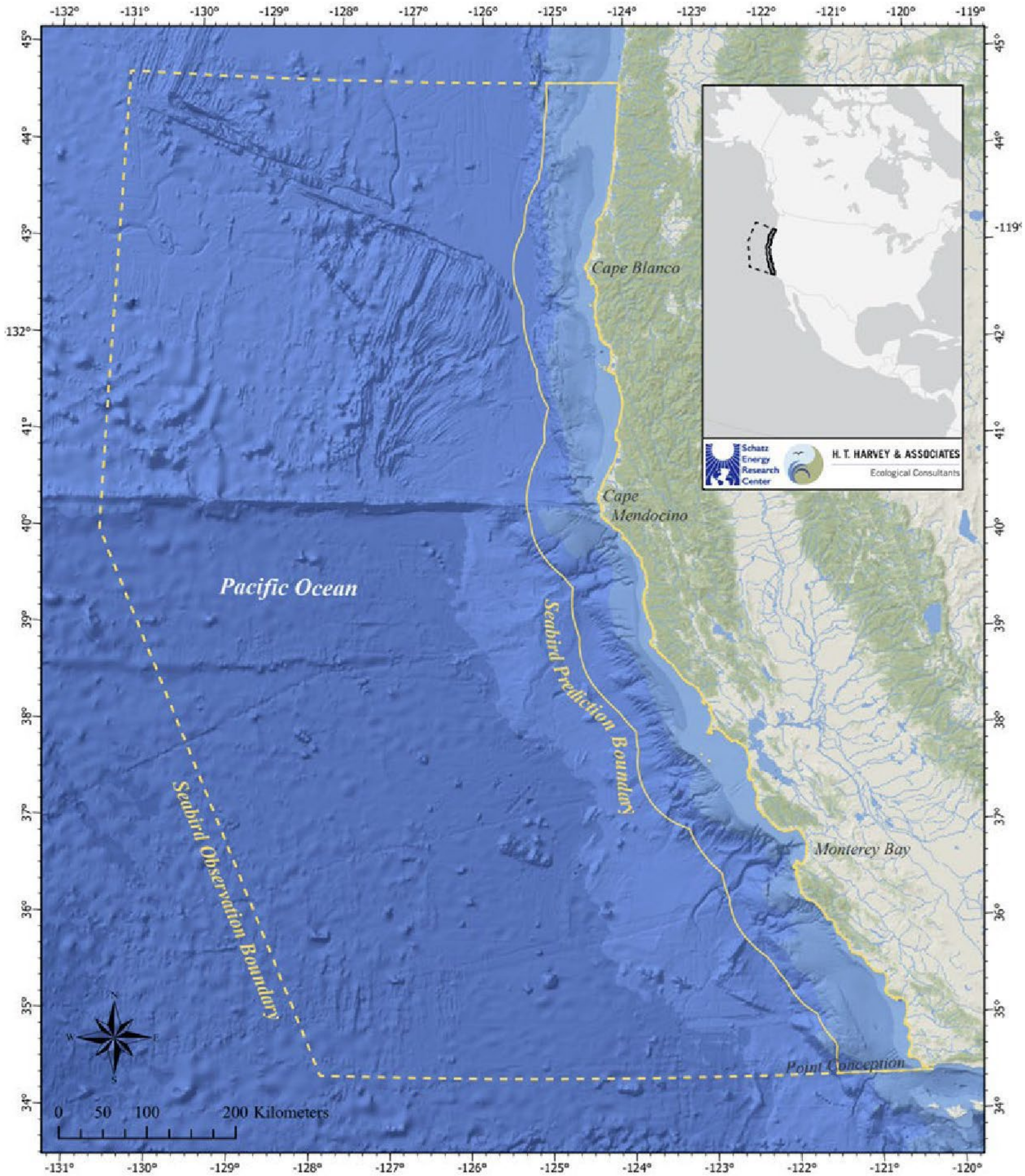

Figure 3. Seabird Observation and Prediction Boundaries

The seabird observation boundary (dashed yellow line) delineates the entire area for which seabird observations were amassed and standardized to support development of 2D predictions via the 3D Seabird Collision Vulnerability Framework. This observation boundary extended as far as the U.S. Exclusive Economic Zone. In contrast, the seabird prediction boundary (solid yellow line) delineates the more focused spatial extent of 2D and 3D density predictions, with this more focused area inclusive of all areas being considered for offshore wind development off California.

Table 1. At-Sea Surveys Supporting Component II of the 3D Seabird Collision Vulnerability Framework

					Area Surveyed (km^2)			
Survey Name	**Code**	**Type**	**State**	**Years**	**Upwelling**	**Oceanic**	**Davidson**	**Annual**
Marine Mammals and Seabirds of Central and Northern CA Aerial Survey, BLM OCSEAP	CNCA	Aerial	CA	1980 – 1983	2,015	1,456	930	4,401
Office of Spill Prevention and Response, CA Department of Fish and Wildlife	OSPR	Aerial	CA	1994 – 1997 2001 – 2012 2014 – 2016	2,920	2,525	1,594	7,039
Pacific Continental Shelf Environmental Assessment, USGS	PSEA	Aerial	OR	2011 – 2012	641	657	661	1,959
San Francisco Deep Ocean Disposal Site, U.S. Army Corps of Engineers	DODS	Vessel	CA	1995 – 2001	1,634	990	381	3,005
Equatorial Pacific Ocean Climate Studies, NOAA PMEL	EPOC	Vessel	CA	1983 1985 – 1986 1988 – 1992 1994 – 1995	118	55	207	380
Global Ocean Ecosystem Dynamics, NSF Ocean Sciences	GOEO	Vessel	OR	2000 2002	1,989	147	0	2,136
Rockfish Recruitment and Ecosystem Survey, NOAA-NMFA	JVRK	Vessel	CA	1997 – 2006	2,712	0	0	2,712
OR, CA, Washington Line-Transect Expeditions, National Marine Fisheries Service SWFSC	OCWA	Vessel	CA/OR	2001 2005 2008 2014	901	3,407	300	4,608
Wecoma Navy Acoustic Work	RVWE	Vessel	OR	2005	79	0	0	79
All Surveys	ALL	Both	CA/OR	1980 – 2016	13,009	9,237	4,073	26,319

Table Notes: Nine independent aerial- and vessel-based studies used continuous strip-transects surveys to identify and make counts of all observable seabirds. Raw data were amassed into a single analysis database by stratifying transect lines of various widths and lengths into uniform 1 km^2 units of effort such that counts could be tallied in an equitable way across the various efforts and served as the foundation for all 2D density estimates. Pertinent details provided included: the survey name, code, type (platform), location, duration, and area surveyed (km^2) both seasonally and overall. Definitions: CA = California; OR = Oregon; USGS = U.S. Geological Survey.

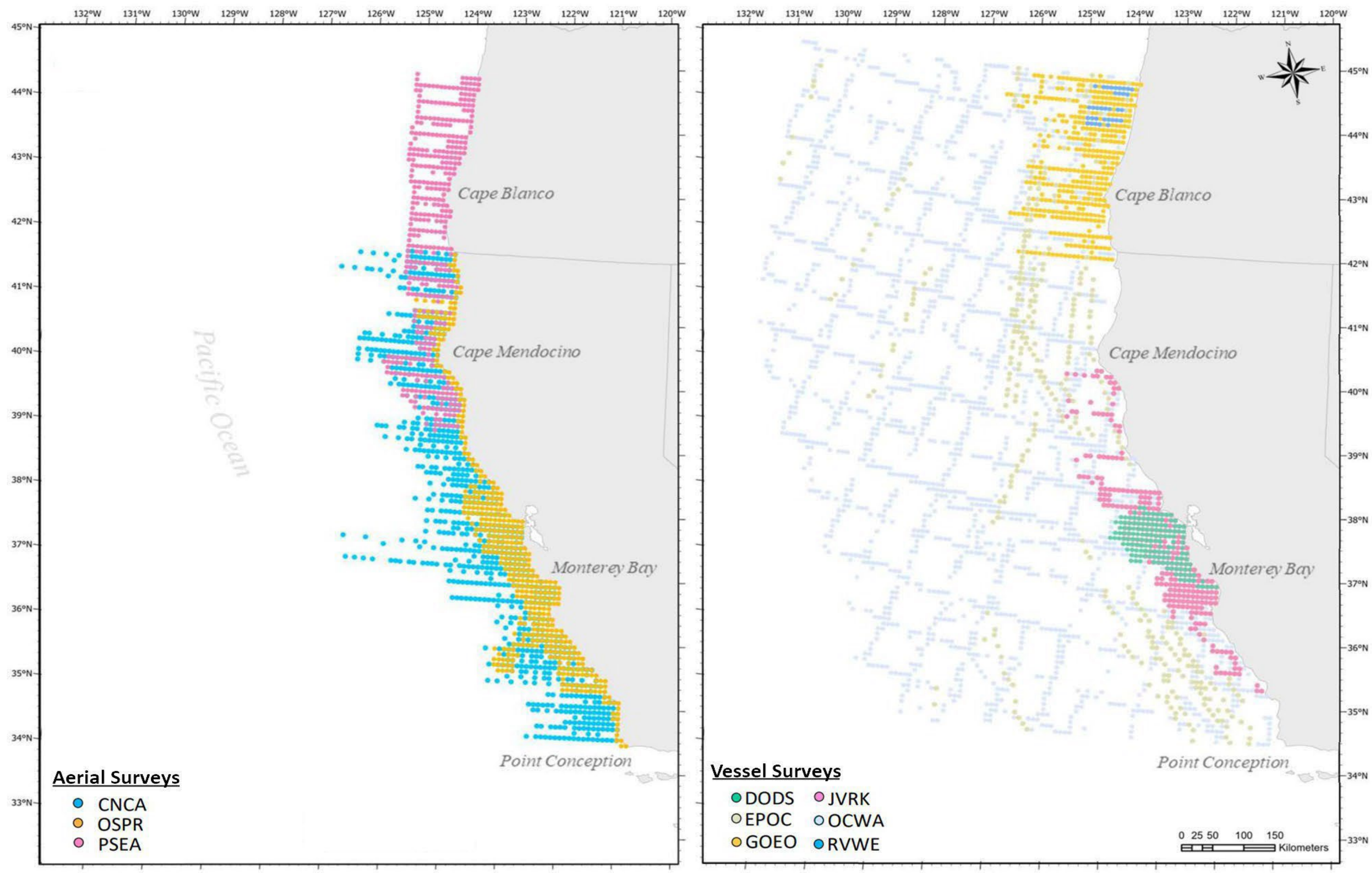

Figure 4. Center Point of each 1 km² Survey Effort Unit for Seabird Studies Supporting Component II of the 3D Seabird Collision Vulnerability Framework

Spatial extent of the three aerial (left panel) and six vessel (right panel) at-sea studies serving as sources of 2D density predictions made by the 3D Seabird Collision Vulnerability Framework. Each point along the various transect lines represented the centroid of each 1 km² survey effort unit. Information on specific surveys, including full survey names, are provided in Table 1.

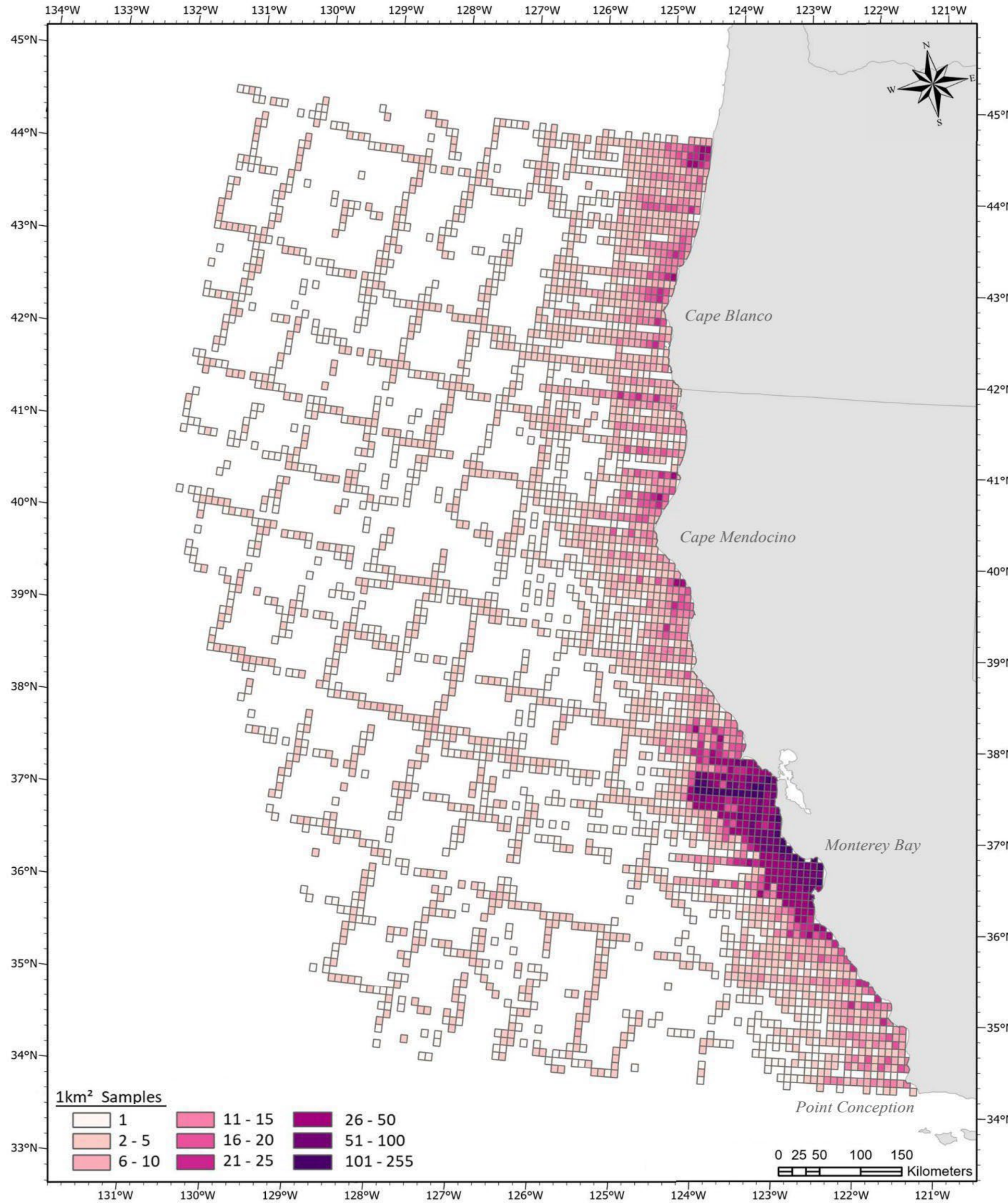

Figure 5. Spatial Variability in Survey Effort Associated with Seabird Studies Supporting Component II of the 3D Seabird Collision Vulnerability Framework

This figure illustrates the distribution of survey effort across the full seabird observation areas. Survey effort was quantified by summing the total number of 1 km² units of at-sea survey effort, aligned with the resolution of the 2D and 3D prediction grid (5'x5' cells). The intensity of survey effort at each location was depicted using a color gradient, with darker shades indicating areas of greater survey coverage.

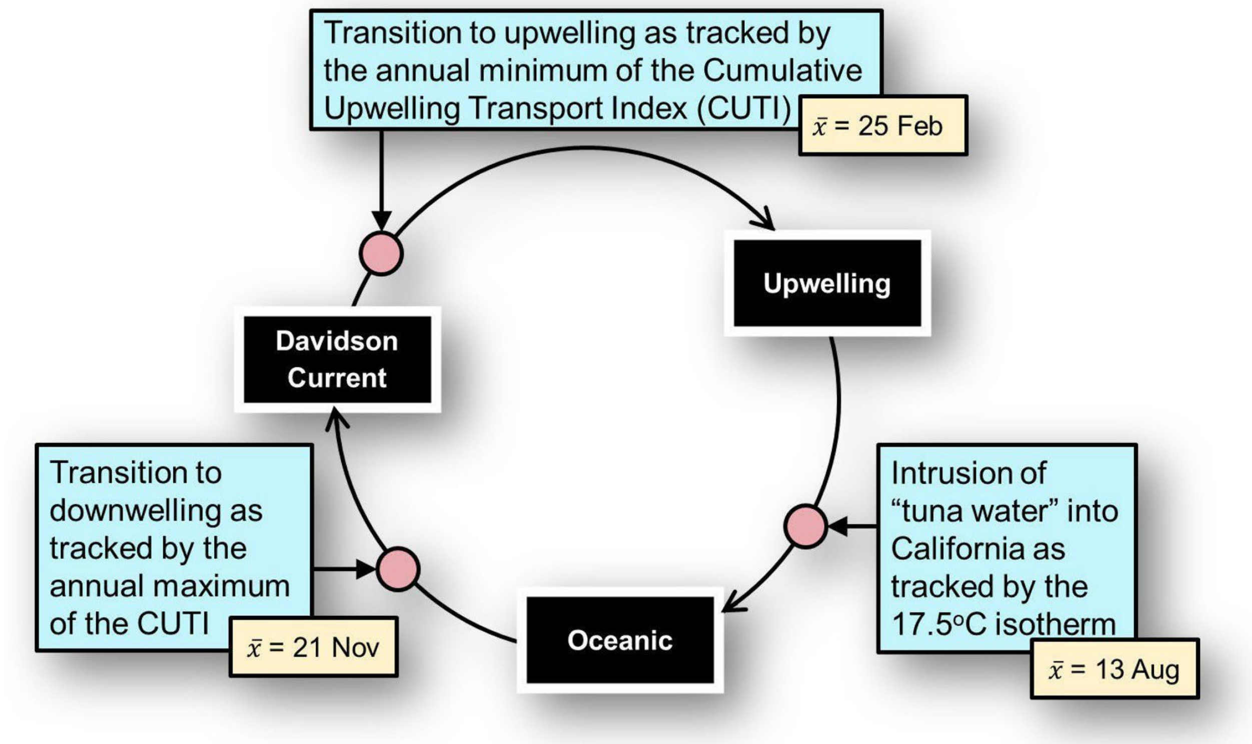

Figure 6. Oceanographic Seasons of the California Current System
The 3D Seabird Collision Vulnerability Framework partitioned the annual cycle into three oceanographic seasons with distinct water circulation patterns that are associated with changes in seabird community composition and behavior: Upwelling, Oceanic, and Davidson Current (see Bolin and Abbott 1963, Hickey 1979, and Chelton et al. 1982 for ocean processes associated with each season). Yellow boxes indicate the initiation dates for each season, while blue boxes represent the commencement criteria. For the Upwelling season, the diagram indicates its onset on February 25th, determined by the annual minimum of the Cumulative Upwelling Transport Index curve observed over recent decades, as described in Bograd et al. (2009).

Upwelling Season

- The upwelling season is characterized by the upward transport of cold, nutrient-rich water to the sea surface, which supports phytoplankton blooms (Bolin and Abbott 1963, Checkley and Barth 2009). The increased availability of phytoplankton fuels development of the entire food web and helps synchronize the initiation of nesting by seabirds along the CA coast (Ainley and Boekelheide 1990, Ainley et al. 2005, Nur et al. 2011).

- The commencement of the upwelling season in the CCS is marked by the 'Spring Transition', a period after winter when prevailing winds shift from the south to the northwest, leading to upwelling and coolers sea surface temperatures along the coast (e.g., <12°C). The along-shore winds and Coriolis force shift surface waters from downwelling-dominant to upwelling-dominant. This transition can be identified by the shape of the Cumulative Upwelling Transport Index (CUTI) curve, specifically at the inflection point indicating that upward transport of deep water has become predominant. Timing can vary over two months with repercussions to the food web and the seabird community (Ainley and Boekelheide 1990, Ainley and Hyrenbach 2010). While the Spring Transition occurs earliest in the south, and shows a northward shift, we used the average date of this CUTI inflection point for latitudes between 33 and 45° N over a 40-year period (1967-2007), as determined by Bograd et al. (2009), for the entire study area.

- Based on the last few decades, the Upwelling season extends from February 25th to August 13th, totaling 170.25 days (the 0.25 represents extra day added to February every fourth year).

Oceanic Season

- This season is characterized by the weakening of northwesterly winds, reducing the upwelling of cold, dense water to the surface, allowing warmer, subtropical waters to intrude from the west. Intrusion of these warmer waters, sometimes called 'tuna water,' was tracked using the position of the 17.5°C isotherm, the ocean boundary along which the Albacore (*Thunnus alalunga*) troll fishery operates.
- The commencement of this season was determined by tracking the seasonal progression of the 17.5°C isotherm using NASA's State Of The Ocean Worldview visualizer over a 19-year period (2002-2021). The isotherm maintained a consistent position far offshore during the Upwelling season, then shifted eastward to varying degrees depending on year into a relatively nearshore position, marking the beginning of the Oceanic season.
- This season extends from August 14th to November 20th, totaling 99 days.

Davidson Current Season

- This season can be characterized by the surfacing of the Davidson Current, an undercurrent flowing counter to the California Current. Southerly winds, especially from winter storms, allow this warmer, low productivity current to surface
- The commencement of this season was based on the 40-year average of CUTI's deflection point, contrasting with the inflection point used for the Upwelling season (Bograd et al. 2009).
- This season extends from November 21st to February 24th, totaling 96 days.

Inverse Distance Weighting

The 2D density predictions were derived using an interpolation technique known as Inverse Distance Weighting (IDW). Geographic weights assigned by IDW are inversely proportional to the distance between the observed point and the prediction point, hence the name 'Inverse Distance Weighting.' Using the IDW algorithm, density estimates (birds/km^2) for each species-season combination were generated across the seabird prediction area (Figure 3) for each of 1,814 5'x5' cells. Once estimates were generated, 2D density observations and predictions could be visualized for all seabird taxa as maps matching the resolution of this seabird prediction grid. The general process for estimating the density of seabirds using IDW involved:

1. **Create IDW Input Database:** Details regarding the extensive seabird dataset amassed were summarized for each species included in the 3D Framework (see Table A-2). To make targeted predictions of 2D seabird density into regions with significant effort and potential for OSW development using IDW, these extensive observation datasets were truncated to only include observations up to 83 km [50 mi] from the coastline. These observations were further segmented by oceanographic season, with each iteration of the IDW algorithm processing a single species-season combination.

2. **Calculate Observed Densities for Each Species-Season Combination:** Observed density datasets created in step 1 were averaged into the highest-resolution grid possible given the resolution of the input data (i.e., a 1 km by 1 km grid that was equivalent in area to the standardized unit of effort for the input data). Each cell in this high-resolution grid was populated with a single density value, representing the average density of all survey points falling within each cell. Cells with zero bird densities in any season-species combination, were treated as true zeros (i.e., no birds detected) if surveys had occurred and were valid to support the IDW algorithm. In contrast, cells with zero bird densities resulting from not being surveyed were treated as missing data rather than valid count data and therefore required an interpolated density estimate.

3. **Apply IDW Algorithm:** Due to the reliance on distance metrics for IDW interpolation, input data were treated as point estimates, as opposed to polygons, to make the necessary distance calculations. Using the average observations for each IDW grid cell centroid and the distances to cell centroids for which density estimates were computed, seabird density was estimated for each species and season. These estimates were used to populate the 5'x5' grid associated with the seabird prediction area using the IDW algorithm described by EQN 1.

$$B(x,y) = \frac{\sum_{obs} b_{obs} \times \left(\frac{1}{d_{obs}}\right)^{IDP}}{\sum_{obs}\left(\frac{1}{d_{obs}}\right)^{IDP}}$$

(EQN 1)

Where:

- *B(x, y):* estimated bird density at the prediction point located at coordinates (*x, y*)
- *obs*: represents the observed points within the 1x1 km grid cell
- b_{obs}: observed bird density at each observed
- d_{obs}: distance from each observed point to the prediction point (*x, y*), and
- *IDP*: IDW Power, a parameter that determines the influence of distance on the weights assigned to observed points

For distances between observation and prediction points equal to zero, the IDW algorithm applied an infinite weight, meaning that if the location (*x, y*) of a prediction coincided with the location of an observation then prediction density would be identical to the observation density.

Generate IDW Predictions: The IDW approach for generating seabird density predictions was implemented using the *Gstat* package (Pebesma and Wesseling 1998, Pebesma 2004) in R (R Core

Team 2016). To determine the optimal IDW power for each species and season, we conducted leave-one-out cross validation (LOO-CV) using additional functions within the *Gstat* package. Maps of all LOO-CV results for each species and season are provided in Appendix D. LOO-CV involved iteratively removing a single prediction location from the IDW algorithm, generating a density estimate for that location using EQN 1, and comparing it with the withheld data. This process was repeated for each location with observations, and the error was calculated as the difference between the prediction and the withheld data. The root mean squared error was then calculated using these errors, providing a robust measure of the uncertainty and model performance.

We used LOO-CV to tune the IDW power parameter separately for each season and bird species. Optimal IDW powers were determined using a Limited Memory Broyden-Fletcher-Goldfarb-Shanno optimization algorithm, implemented by the stats package in R. Limited Memory Broyden-Fletcher-Goldfarb-Shanno optimization involved bounding constraints; in our case, we constrained the IDW power to be between 1 and 3. The optimal power for each season and species was defined as the power that minimized the root mean squared error calculated through LOO-CV.

4. **Finalize Seabird Density Predictions and Optimization:** Once the optimal IDW power was determined, final seabird density predictions were made on the 5'x5' seabird prediction grid. Except for cells along the shoreline, the prediction grid largely matched the seabird grid shapefile. We converted this raster of predictions into a shapefile format by sampling the centers of each polygon within the shapefile from the raster grid. Although we explored other tuning parameters, such as max distance and max points, these parameters did not meaningfully improve model fit and were not included in the IDW expression provided earlier.

Component III: Converting 2D Densities to 3D

The final component (3D assessment) provides species-specific estimates of seabird density at heights ASL of at least 10 m. This 3D conversion integrated three sets of information:

1. Response curves (logistic regressions) for each FG that describe the log odds of a binary behavior: the predicted probability of flying above versus below 10 m based on wind speed (Component I);
2. The 2D density estimates for 44 species (Component II); and
3. The probability of a seabird species flying above 10 m given the windscape for a specific 5'x5' grid cell (Component III).

Supporting Data

Windscape

The windscape analysis, i.e. the strength of winds by location, relied on data from the CA-20 and Northwest Pacific modeled wind speed assessment provided by NREL (2023). The raw data encompassed a 20-year period (2000 and 2019) and had a temporal resolution of 5-minute timesteps. These were down-sampled to derive a 15-minute timestep to balance the benefits of increased granularity with practical considerations such as data volume, computational burden, statistical robustness, and resource allocation. For our purposes, a 15-minute interval balanced the need to capture important variations in wind speed while managing the complexity and resources associated with incorporating such a large dataset into the 3D Framework. The raw data are also at a 2 km by 2 km spatial resolution and were trimmed to match the extent of the seabird prediction space.

Component Integration

The 2D density estimates were converted into 3D densities with flight height in three steps.

Step 1: Quantifying the Windscape

For each grid cell having a 2D density prediction, the high-resolution wind speed measures were grouped into bins of 0.5 m/s covering the full range of typically observed wind speeds at 10 m elevation from 0 to over 30 meters per second (m/s) and tallied to generate a histogram of the frequency of all observed wind speeds across encompassed by the data. Then, using the midpoint wind speed of each bin, the FG-specific flight height and wind speed logits (Component I) were used to estimate the overall probability of exceeding 10 m ASL given the distribution of all observed wind speeds.

Step 2: Calculate the Probability of Each Species Flying Over 10 m

The probability of each species exceeding 10 m ASL in each season per grid cell was calculated using EQN 2.

$$FPA(S, FG, GC) = \sum_{ws(GC)} P(ws, S) * FP(ws, FG) \quad \textbf{(EQN 2)}$$

Where:

- FPA: overall average probability of a seabird species flying over 10 m (unitless);
- S: season;
- FG: flight-style grouping that the species belongs to;
- GC: grid cell (native to the 2D density estimate);
- WS: wind speed bin (in 0.5 m/s intervals);
- P: probability of being in a specific wind speed bin (i.e., the count of timesteps in bin/total count of timesteps; unitless); and
- FP: probability of a seabird flying over 10 m, as estimated by the logistic regression model in Component I for a given wind speed and flight group (unitless).

Step 3: Calculate the Seasonal Density of Each Seabird Species at Heights > 10 m ASL

Part A: Seasonal Estimates

With these season and FG specific estimated probabilities of flying above 10 m, the density of each seabird species exceeding 10 m was then calculated using the 2D density estimates and EQN 3.

$$SA10(S, SB, GC) = SA(S, SB, GC) * FPA(S, FG, GC) \textbf{ (EQN 3)}$$

Where:

- SA10: the seabird density > 10 m ASL (seabird counts per km^2);
- SB: is the seabird species; and SA is the seabird density (seabird counts per km^2); and
- The remaining components of the formula have been defined under EQN 2.

Part B: Annual Estimates

The annual estimates of seabirds flying above 10 m were calculated by combining seasonal estimates using EQN 4.

$$SA10(SB, GC) = \sum_S PS(S) * SA10(S, SB, GC) \textbf{ (EQN 4)}$$

Where:

- PS: probability of being in a specific season; and
- The remaining components of the formula have been defined under EQN 2.

Results

We begin by presenting the flight height and wind speed probability curves for each of the 18 FGs included in the 3D Framework (Component I, Figure 7), which are fundamental for increasing dimensionality of predictions from 2D to 3D (Components II and III). We then shift focus to the substantial proportion of the CCS seabird community included in the 3D Framework (Figure 8, Table A-2, Appendix B) by presenting intermediate results and ultimate outcomes of Components II and III in the following order:

- Windscape results relevant to converting 2D predictions to 3D (Figures 9-10);
- Aggregate community predictions in both 2D and 3D (Figures 11-12);
- Four case studies (Figures 13-18) spotlighting two species that together constitute ~50% of CA's seabird population, the sooty shearwater and the common murre, as well as two species of conservation interest: the marbled murrelet (endangered in CA and federally threatened) and the ashy storm-petrel (a CA Species of Special Concern and listed as endangered by the International Union for Conservation of Nature);
- Annual density prediction maps for all 44 taxa included in the 3D Framework (Appendix B);
    - Final predictions are available online as spatial data files as well (Wallach et al. 2024):
- Seasonal density prediction maps for a subset of migratory species that move in and out of the CCS over the annual cycle (Appendix C);
- Prediction quality metrics, determined through LOO-CV, for each species and season summarized in both tabular (Table D-1) and visual (Appendix D) formats;
- Fundamental background information on the ecology, morphology, and flight behavior of seabirds included in the 3D Framework (Appendix E).

Flying at RSZ-Height

A logistic mixed-effects model was fitted to 74,802 observations across 18 FGs (Table A-4) to predict the probability of seabirds that could be flying above 10 m and in RSZs [Figure 7]). Across all observations, the likelihood of a bird flying above 10 m increased by a factor of 1.08 for every one-unit change in wind speed (Logistic Regression, $P < 0.001$, df = 76,367). When examined by FG, the odds of a bird flying above 10 m was more variable (Figure 7), with some FG's more likely to fly above 10 m, others less likely, others unlikely, and some whose flight heights showed no relationship to wind speed.

One FG that exhibits an extreme response to wind is that of larger diving shearwaters. Owing to their morphology and dynamic soaring flight-style, their flight height and chance of entering the RSZ increased steeply with wind speed (Appendix E). Small albatrosses and surface-feeding shearwaters also show this response, though to a lesser extent. Pelican flight height also increases with wind speed despite pelicans not flying by dynamic soaring. The contrast is exhibited by storm-petrels, phalaropes, cormorants, and alcids, for which the probability of flying above 10 m ASL is minimal, regardless of wind speed. Due to their flapping flight style, wind can actually be an impediment. (Appendix E). Finally, some FGs, including medium gulls, small gulls, and terns show a decline in the probability of entering the RSZ as wind speed increases. The exact coefficients associated with the FG-specific flight height regressions presented here (Figure 7) are available in Table A-4.

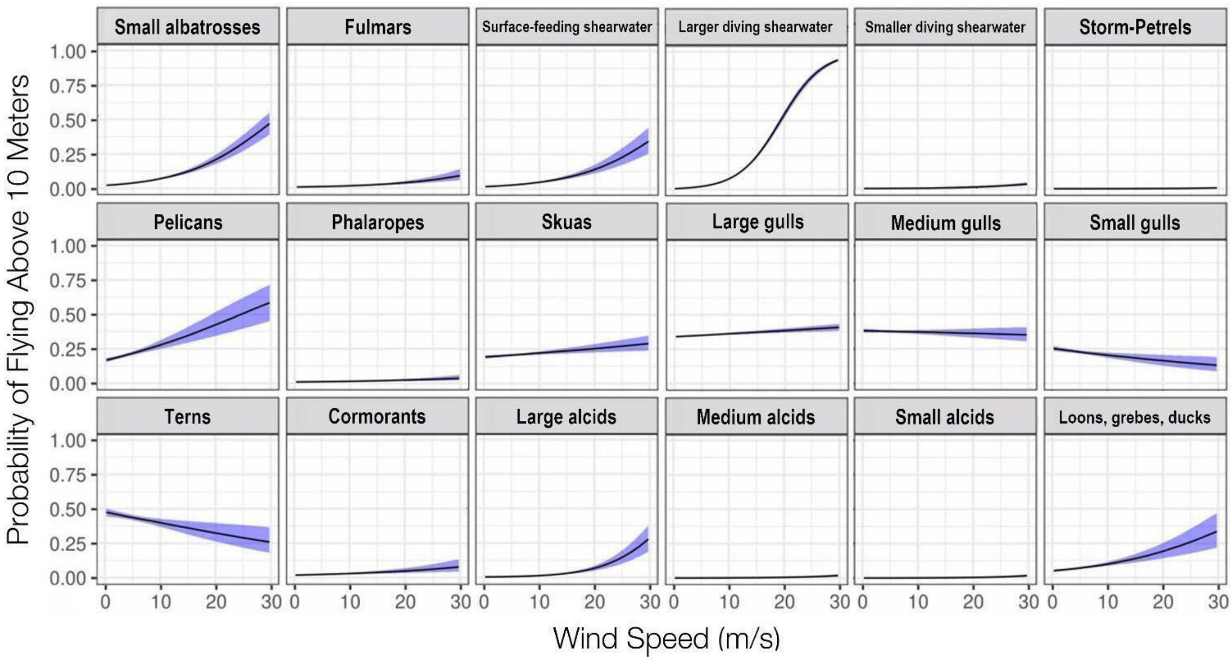

Figure 7. Probability of Flying At Least 10 Meters Above the Sea Surface as a Function of Wind Speed
Predicted probability of seabirds flying above 10 m above sea level at varying wind speeds (m/s) for each flight-style grouping. Data and predictions encompass the full range of wind speeds needed for turbine rotation (3 to 25 m/s). Purple shaded regions about each line depict the bootstrapped 95% confidence intervals.

Seabirds in 3D

Species Included

The seabird community included in Components II and III of the 3D Framework (Figure 8) represented a diverse assemblage of all but the CCS's rarest seabirds. Among the 109 taxa present in the database supporting Component II, 44 met the criterion of being observed within any 100 km² of survey effort. These taxa include both highly abundant species, such as the sooty shearwater and common murre, and relatively rare (though locally abundant) taxa like the marbled murrelets, designated as endangered in California and federally threatened. While there are other endangered/threatened seabird species that occur within the study area besides the marbled and the *Synthliboramphus* spp. (Scripps's, Guadalupe, and Xantus's murrelet species complex), not in numbers sufficient to be included in this Framework.

At-sea counts of the 44 taxa included in the 3D Framework revealed the a few noteworthy patterns: (1) Two species, the sooty shearwater and common murre, accounted for a substantial portion of all individuals present, approximately 55.7% of the total counts per unit effort; (2) the additional 9 species of gull accounted for another sizable proportion of the bird community; (3) the 17 rarest taxa included in the Framework only contributed to less than 1% of the total counts per unit effort or, conversely, most of the community was accounted for by just 27 of the 44 included species (see Table A-2). While most density predictions were species-specific, three of the 44 taxa were grouped due to challenges in distinguishing sympatric species during aerial surveys: red and red-necked phalaropes (*Phalaropus* spp.); western and Clark's grebes (*Aechmophorus* spp.); and Scripps's, Guadalupe, and Xantus's murrelet (*Synthliboramphus* spp.).

An additional 65 species were observed in CCS waters but too infrequently to be included (Table A-3). While one species, Cook's petrel (*Pterodroma cookii*), technically met the inclusion criteria, it was only observed in an area 17 km² larger than the 100 km² threshold. Due to the rarity of this species, resulting predictions were so small that they did not alter the outcome of aggregate community predictions. Additional species worth noting that could not be included due to rarity were Hawaiian petrel (*Pterodroma sandwichensis*) and short-tailed albatross (*Phoebastria albatrus*), which are federally endangered and species of conservation concern. All three are dynamic soaring species and have been increased in the CCS during recent decades because of successful conservation measures, and may qualify for inclusion in the model in future analyses.

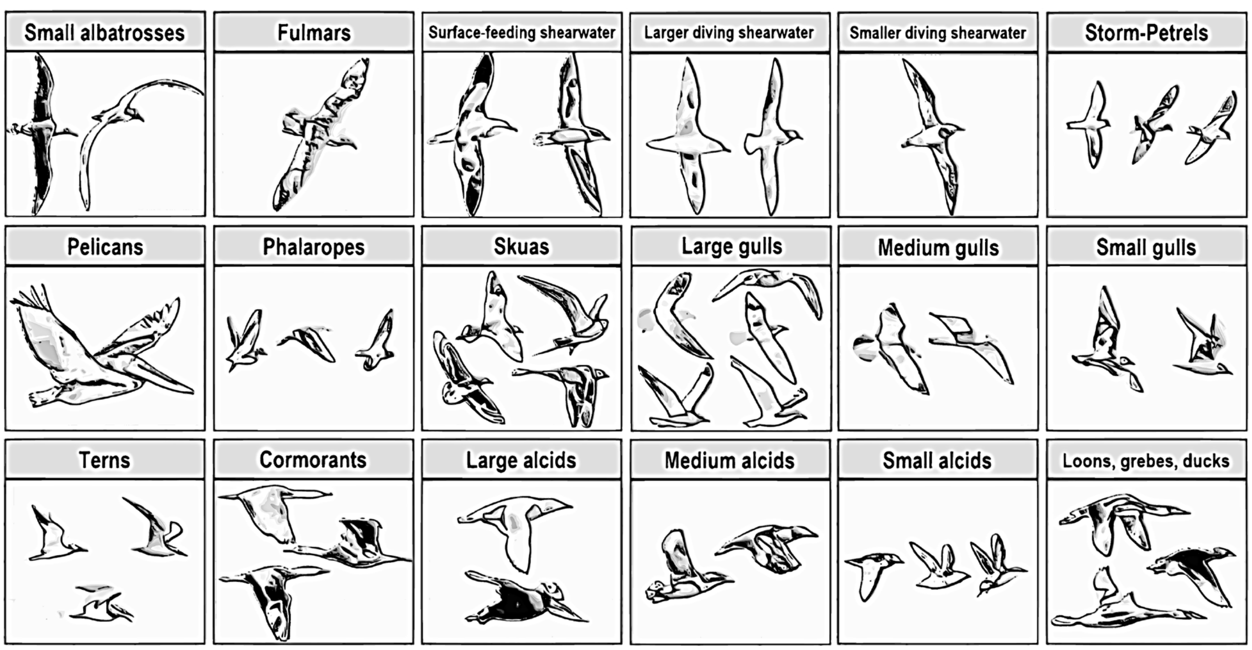

Figure 8. All Seabird Types Included in the 3D Seabird Collision Vulnerability Framework
All taxa included in the 3D Framework, organized by flight-style group. Please note that bird images and sizes have been adjusted for ease of comparing wing and body morphology, rather than representing their actual body sizes.

Converting 2D to 3D

Seasonal Windscape Off CA

The seasonal windscape in the CCS over the previous two decades has exhibited distinct wind-strength patterns unique to each of the oceanographic seasons (Figure 9). Except for winter storms, the strongest winds occur during the upwelling season, predominantly from the northwest. In contrast, the Davidson Current season is characterized by slower average wind speeds, but wind speeds are not uniform across the broad offshore region and winds are perceptibly stronger in offshore and northern portions of the study area. These seasonal differences in the windscape have significant implications for seabird behavior, particularly the probability of birds flying above 10 m ASL. In addition to seasonal changes in the windscape, there are also longer-term (i.e., decadal) changes in the composition and abundance of species and FGs present in the CCS, as noted above, a pattern that also would influence the collective vulnerability of the seabird community. While long-term average wind speeds offer valuable insights into spatial and temporal patterns within the windscape, seabird flight heights can vary in response to site-specific wind conditions (Spear and Ainley 1997a, b; Ainley et al. 2015). In the Humboldt WEA for instance, maximum wind speeds typically remain below 20 m/s for most days of the year, but there are recurring periods during the Upwelling season and during the winter Davidson Current season when wind pulses greatly exceed this threshold (Figure 10). While extreme wind events above 20 m/s are rare in any given year (Figure 10), they represent critical periods when seabirds in specific FGs (e.g., larger diving shearwater, gulls) are likely to fly at heights facilitating overlap with RSZs. During these periods, dynamic soarers like larger diving shearwaters and small albatrosses, are likely to regularly soar to heights far exceeding 10 m ASL.

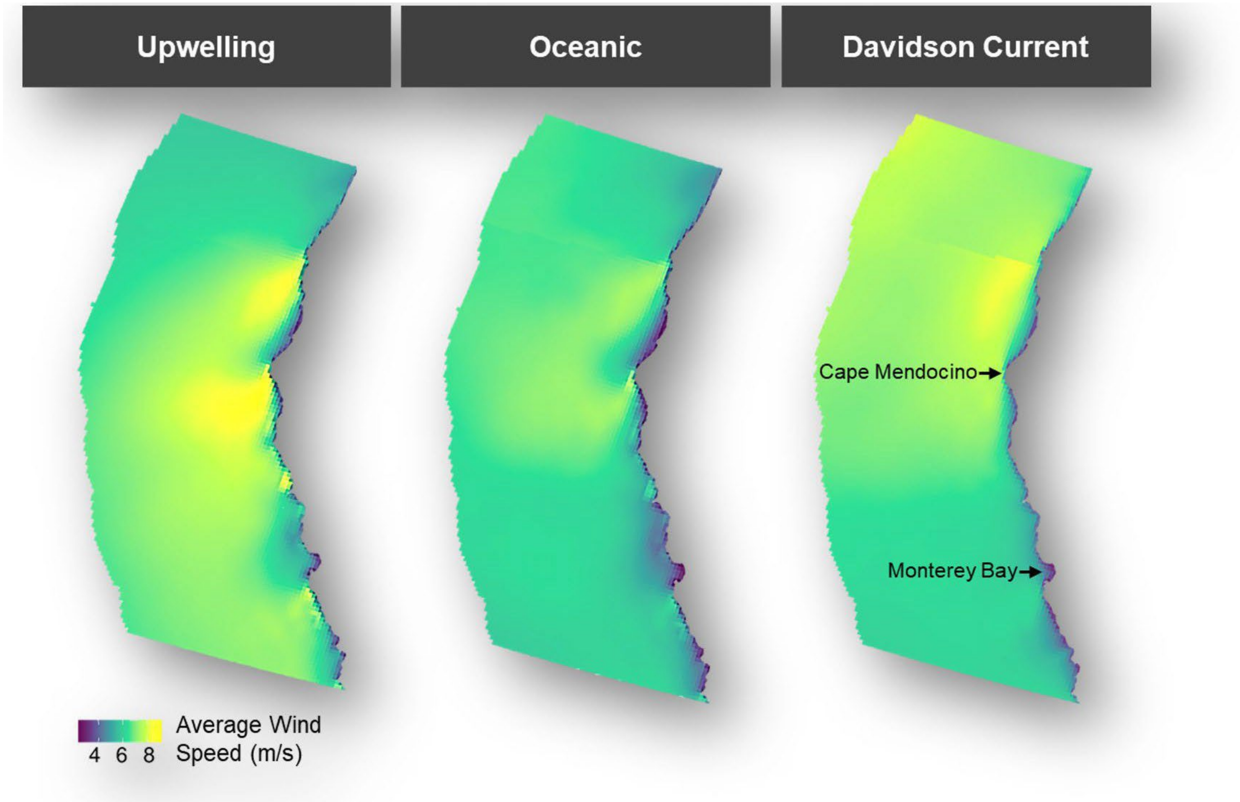

Figure 9. Offshore Windscape for Each Oceanographic Season
Twenty-year (2000-2019) wind speeds averages (m/s) off California as derived from CA-20 and Northwest Pacific wind speed models provided by National Renewable Energy Lab. Seasonal averages were calculated based on wind speeds at 10 m above sea level. Data source: National Renewable Energy Lab (2023) Wind Toolkit Data Downloads for Offshore CA <https://developer.nrel.gov/docs/wind/wind-toolkit/offshore-ca-download/>).

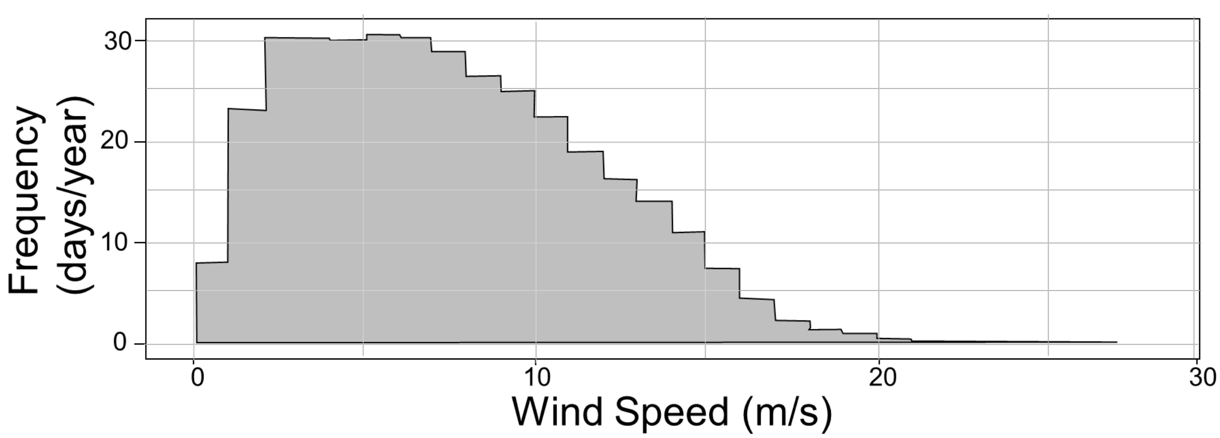

Figure 10. Annual Frequency Distribution of Wind Speeds from the Humboldt Wind Energy Area
Histogram depicting the annual frequency distribution of all wind speeds estimated at the center point of the Humboldt Wind Energy Area. Data sourced from CA-20 wind speed data provided by the National Renewable Energy Lab. Wind speeds were averaged at 10m above sea level) into 15-minute intervals and binned into 0.5 m/s intervals for frequency analysis. Data source: National Renewable Energy Lab (2023) Wind Toolkit Data Downloads for Offshore CA <https://developer.nrel.gov/docs/wind/wind-toolkit/offshore-ca-download/>).

Community-Level Predictions

The composition (Figure 11) and density (Figure 12) of the CCS seabird community exhibits broad-scale patterns of variability north to south, and east to west, showing different species composition above 10 m ASL relative to the overall community and across seasons. Various spatial and temporal investigations of the CCS seabird community could be made using the predictions from the 3D Framework, several of which will be briefly explored in the next two sections.

Differences in Composition

When considered in aggregate, the composition of the seabird community varied most notably in the vertical dimension (Figure 11). Some seabird types that dominated the community when evaluated from a 2D perspective, constituted only a small portion of the community above 10 m ASL (for example, few alcids flew at that height), while the dominance of gulls above this threshold was much greater than calculated in 2D analysis. Above 10 m, the seabird community in all areas was primarily comprised of gulls and shearwaters, collectively accounting for at least 80% of the individuals, with a diverse collection of other taxa forming the remainder of the community.

All six geographic regions considered were dominated by alcids (primarily common murre) and collectively, just three groups—alcids, shearwaters, and gulls—accounted for 70% or more of individuals present (Figure 11). The remaining ~30% of individuals in the community showed the following variations by region: a greater proportion of alcids north of Cape Mendocino and within 20 miles of the coast, a robust presence of storm-petrels offshore north of Cape Mendocino, and a concentration of loons, grebes, and ducks in state waters (0 to 3 miles from the coast).

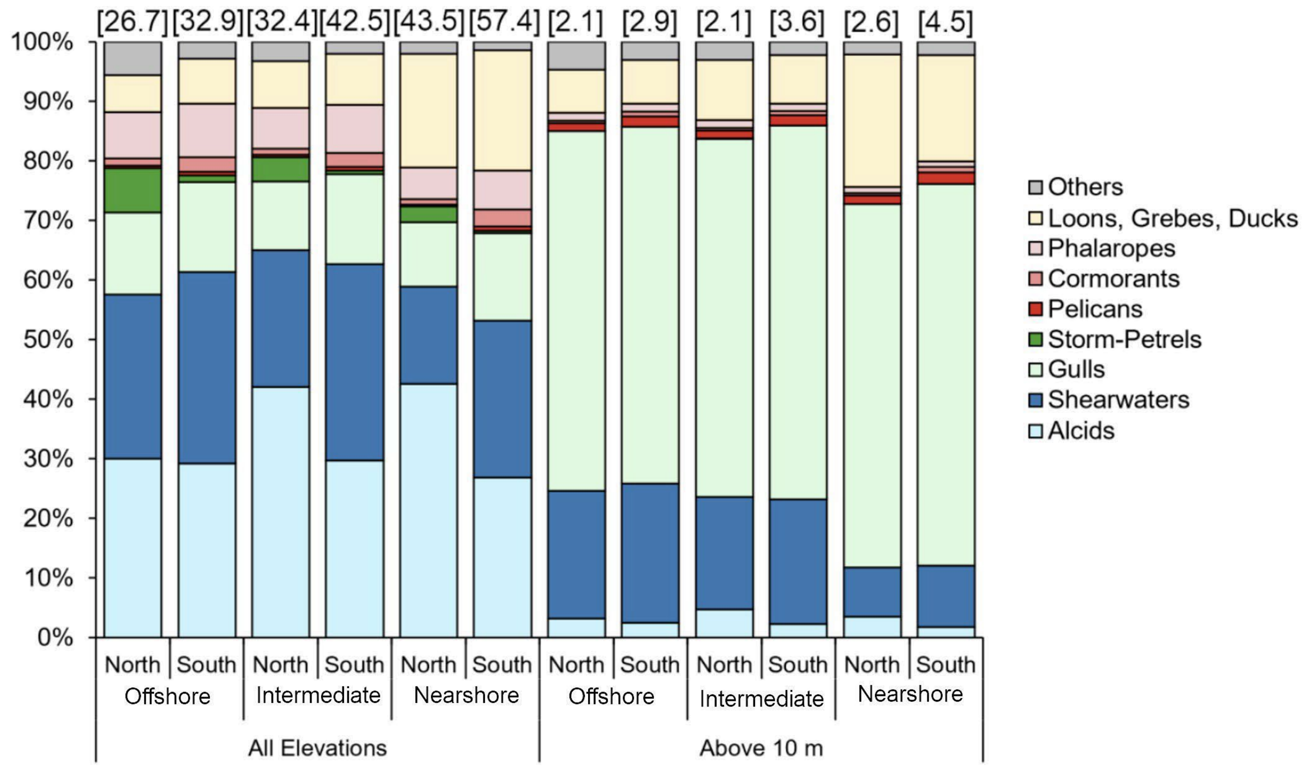

Figure 11. Comparing 2D and 3D Predictions of California Seabird Community Composition Across Geographic Regions

To assess differences in the composition of California's seabird community from 2D ('all elevations') and 3D ('above 10 meters') perspectives, the study area was divided into six regions defined by latitude (north and south of Cape Mendocino at 40.44°N) and distance from coastline (offshore [20+ miles], intermediate [3-20 miles], and nearshore [0-3 miles]). Taxa were grouped broadly for clarity, with average annual density estimates (birds/km^2) provided above each column.

Differences in Density

The predicted densities of all 44 seabird taxa included in the 3D Framework annually averaged 35 birds/km^2, with a maximum site-specific average density of 127 birds/km^2 (Figure 12). However, when considering birds flying at least 10 m ASL, the predicted densities were lower, averaging 2.8 birds/km^2 with the maximum site-specific average density prediction equaling 17.8 birds/km^2 (Figure 12). Two broad region-wide patterns were easily discerned from the density distribution maps presented here for all species: (1) densities were greatest in waters over the inner shelf and decreased as distance from shore increased, and (2) densities were greater in the southern portion of the study area and tapered off with increasing latitude (Figure 12). Notable concentrations of seabirds were found in association with inner shelf areas from Point Conception, extending north beyond Morro Bay, as well as Monterey Bay extending north to encompass the Gulf of the Farallones (Figure 12).

It is crucial to provide context for the instantaneous 2D and 3D density estimates presented for the overall seabird community, as well as for each individual species discussed in subsequent sections of this report. These values offer estimates of bird densities at any given point in time, denoted as 'birds/km^2' but without a temporal component. Derived from data spanning several decades, these 'collision vulnerability estimates' provide instantaneous expectations of seabird densities at and below RSZs as a function of these multi-decadal seasonal and annual conditions. For instance, an average density of 35 birds/km^2 for all seabirds included in the 3D Framework across the entire prediction region can be interpreted as follows: on average, approximately 35 birds (or a similar order-of-magnitude density) could be expected to be present within each square kilometer across the entirety of the prediction area at any given moment throughout the year (or season when considering seasonal predictions), assuming wind speed and bird densities similar to long-term historical conditions.

The estimates of instantaneous collision vulnerability offer several benefits. Firstly, they are derived from comprehensive data spanning multiple decades, providing a more representative range of environmental conditions and extremes than approaches focused on higher-resolution (i.e., shorter) temporal scales. By incorporating data from various periods, including multi-decadal extremes, these estimates offer a robust representation of long-term historical averages. Secondly, these estimates provide an order-of-magnitude expectation of bird presence at a given area, considering bird distributions across different heights that may expose them to rotor swept zones. This nuanced understanding enhances our comprehension of seabird abundance and distribution, particularly in identifying potential areas of increased collision risk. Thirdly, they serve as a valuable tool for comparing species, sites, and vertical strata. This facilitates assessments of region-wide collision vulnerability and supports targeted conservation efforts.

While there are clear benefits to generating these instantaneous collision vulnerability estimates, it is important to also recognize their limitations. Despite being based on long-term averages, they do not capture rapid or temporally sensitive changes resulting from single events or anomalous conditions that may impact the windscape, seabird community, or both (e.g., mortality events).

Furthermore, it is essential to acknowledge that these instantaneous density estimates primarily reflect the community vulnerability to collision with RSZs by providing a metric similar to what might be expected in terms of seabird passage rates occurring at the heights of RSZs. An important distinction between the instantaneous vulnerability estimates quantified here and the passage rates input into collision risk models to generate collision rates is that passage rates (and the resulting collision rates) have an explicit time component, measured in units of birds/km^2 per year. Further, while passage rates and collision rates are related, one does not directly equate to the other because actualized collision between seabirds and RSZs will be influenced by a multitude of factors beyond vulnerability and passage rates (e.g., bird behaviors that affect their ability to detect and avoid rotor swept zones at all relevant spatial scales (near, intermediate, far). Therefore, while the instantaneous 2D and 3D density estimates presented throughout this report offer insights into seabird distributions and potential vulnerability to collision risk, they should be interpreted mindfully and in conjunction with other relevant metrics and considerations.

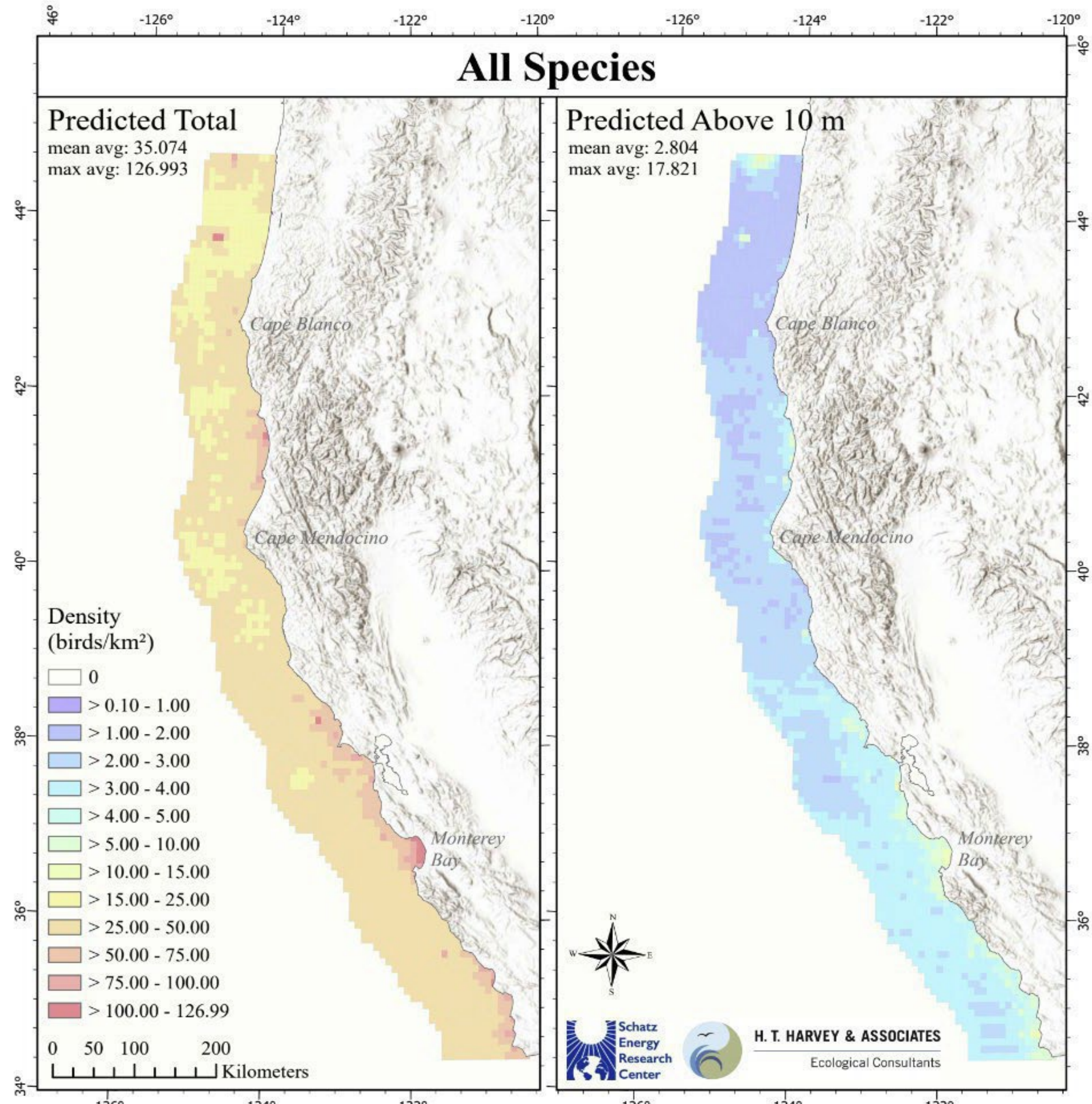

Figure 12. Annual 2D and 3D Predictions for California's Seabird Community

Predicted densities for all 44 seabird taxa included in the 3D Framework from a 2D perspective of the total community (left) as well as a 3D perspective of individuals flying at least 10 m above the sea surface (right). The mean average and maximum average values, shown at the top of the panels, are measured in birds/km². These values represent the average expected density across all cells and the highest density predicted within a single cell in the area, respectively.

Species-Level Predictions

Map Overview

Graphical representation of various 2D and 3D species-level density predictions for the 44 seabird types included in the 3D Framework have been generated and are shown below both annually and by season. The following summary is organized to aid in the interpretation of these species-specific maps, with details presented first for all 2D and 3D maps, followed by information specific to annual maps, and finally, details specific to seasonal maps.

We illustrated these points, relevant to all density maps, by reviewing a few species, following this summary:

- Prior to examining the details of the 2D and 3D prediction maps, we advise reviewing the guidance provided in the 'Community-Level Predictions' section for interpreting the density estimates. While this guidance was tailored for the 'All Species' map (Figure 12), it is equally applicable to interpreting the species-level prediction maps.
- 3D predictions of bird densities at and above 10 m can never exceed those of the corresponding overall 2D bird density predictions, as the birds above 10 m are inherently a subset of the overall population. Typically, densities predicted above 10 m are an order of magnitude lower than overall densities due to most of the broader seabird community concentrating their activity in the first 10 m ASL (Schneider et al. 2024).
- Any grid cells visibly outlined on these maps, but lacking fill color, represent observations and/or predictions that were either equal to zero or extremely small.

Information specific to annual density maps:

- These maps have two panels and four main pieces of information:
    - <u>Predicted Total (left main panel):</u> This panel displays the annual 2D density predictions generated using a spatial interpolation approach, providing insights into seabird densities across unobserved areas based on adjacent observations from at-sea surveys.
    - <u>Observed (left inset panel):</u> Visualizing the underlying at-sea seabird count data, this panel illustrates cells where surveys were conducted but no individuals were observed, outlined in grey and lacking color.
    - <u>Predicted Above 10 m (right main panel):</u> Here, the annual 3D density prediction of birds flying in the rotor swept zone (>10 m) is showcased, a key output of the 3D Framework.
    - <u>Flight Height Probability Curve (right inset panel):</u> For each species, this inset illustrates the relationship between the probability of flying above 10 m and wind speed.
- Mean average and maximum average densities (birds/km^2) are displayed at the top of each main panel. These values represent the average expected density across all cells and the highest density predicted

within a single cell in the area, respectively. Further exploration of these metrics is conducted within the context of the four species-specific case studies featured in the 'Differences Across Species' section.

Information specific to seasonal density maps:

- Seasonal predictions were generated for all 44 seabird species encompassed in the 3D Framework.
- Given the seasonal variability in distribution and density observed in many seabird populations, efforts were concentrated on illustrating this variation for 15 migratory species that reside elsewhere for a portion of the year.
- Each seasonal prediction map for a migratory species consists of six panels:
    - Three columns dedicated to specific seasons—Upwelling, Oceanic, and Davidson Current.
    - Two rows representing 2D and 3D predictions, respectively.

Sooty Shearwater

Sooty shearwaters have been the most widely observed and numerous seabirds in the CCS since at-sea surveys began, despite their numbers decreasing in recent decades (Veit et al. 1997, Ainley and Hyrenbach 2010) and, despite them being a migratory species that is only present in the CCS during Upwelling and Oceanic seasons. The greatest 2D densities of sooty shearwater were observed in Monterey Bay, with the observed maximum average density reaching 778 birds/km² (Figure 13, left panels). Notably, the observed maximum annual average density was 7.1 times greater than the corresponding prediction (778.3 versus 95.7 birds/km², respectively; Figure 13, left panels). Meanwhile, the mean annual average densities showed an opposing pattern, with predictions being 2.2 times greater than observations (3.0 versus 9.6 birds/km², respectively; Figure 13, left panels). This discrepancy stemmed from this species' extreme flocking behavior and resulting patchy distribution; flocks exceeding 10,000 birds/km² were documented on two occasions, once in 1980 and once in 2002, but smaller flocks are more typical (see below). Importantly, during at-sea surveys when sooty shearwater presence in the CCS was greatest (i.e., during Upwelling; see Figure 14), more often than not sooty shearwaters were not observed (i.e., 64.6% of the 22,246 km² of survey effort reported a count of zero sooty shearwater) likely due to their flocking (Figure 13, left inset panel). For the remainder of sooty shearwater observations during these Upwelling and Oceanic Seasons, flock sizes reported across the 22,246 km² of survey effort equaled or exceeded 1,000 individuals 0.02% of the time, 100 individuals 1.9% of the time, 10 individuals 9.1%of the time, and 1 individual 35.4% of the time. This means the predicted mean average densities balance out the extremes of individual observations, yielding a more accurate representation of the expected density of sooty shearwaters across the prediction area over longer time periods (e.g., years) rather than being representative of anomalous and/or more extreme conditions. The seasonal distribution of sooty shearwaters has been visualized (Figure 14) to show that this species is present during Upwelling and Oceanic seasons, albeit less so during the Oceanic season. They are scarce during the Davidson Current season, typically having returned to the Southern Hemisphere. Note that in all annual and seasonal prediction maps presented here and in Appendices B and C, cells that have been outlined, but are lacking color, represent observations and/or predictions that are extremely small or equal to zero. As part of the larger diving shearwater FG, sooty shearwater morphology allows them to travel great distances by dynamic soaring, which results in the flight altitude of this species being very responsive to wind speed; specifically, the probability of flying above 10 m escalates rapidly with increased wind speeds, especially winds faster than ~15 m/s (Figure 13, right inset panel), during which virtually all traveling sooty shearwaters are reaching heights of the RSZs.

Because of their responsiveness to the wind and their significant contribution to the overall CCS seabird community, sooty shearwaters were one of the species warranting a more extensive walkthrough of the 3D Framework, aiming to be more explicit in interpreting and gaining insights into collision vulnerability for this species. Using the Humboldt WEA as an example for this walkthrough, Figure 15 was generated to support this in-depth explanation. We will begin with the probability curve representing the propensity of sooty shearwaters to fly at altitudes overlapping RSZs (see Figure 7 and also right panel of Figure 15). Their probability curve indicates that individuals exposed to winds of 18 to 27 m/s (i.e., 40 to 60 mph) will likely be maneuvering above 10 m ASL between 50 and 85% of the time. Even in the wind-rich Humboldt WEA, winds exceeding 18 m/s have been and are expected to remain episodic (Figure 15, left panel; also see Figure 10 for an alternative presentation of these data). Vulnerability is predicted to be greatest for sooty shearwaters and other species in this FG during these elevated wind events, which are expected to be most frequent during the Upwelling, and to a lesser degree, Oceanic seasons when this species is most abundant.

While considering the extremes to be insightful, that perspective cannot accurately represent the day-in and day-out expectations of vulnerability. To get a better sense of what exposure level might be expected in the Humboldt WEA across a longer duration of time requires considering the full range of possible bird density and wind speed conditions, not just the episodic conditions of strong winds. The 3D Framework relies on capturing the conditions over decadal time periods, which is important for understanding and properly interpreting the 3D Framework vulnerability predictions.

Returning to the Humboldt WEA example, the 3D Framework predicted an annual average density of sooty shearwaters above 10 m ASL to be 0.48 birds/km² (Figure 15, left panel). This metric of vulnerability can be interpreted as follows: given the multi-decadal observations of the 2D densities of sooty shearwaters and the 20-year windscape in the Humboldt WEA, if one were to go to the Humboldt WEA and make an observation of the sooty shearwaters above 10 m with wind conditions relatively similar to the long-term average, one would expect to see approximately 0.48 birds/km² flying at risk-heights at any given moment during daylight hours (to date, no comparable species-specific observations have been made in darkness). This 0.48 birds/km² is equivalent to ~8% of the sooty shearwaters predicted to be present in any 1 km² area of this WEA (Figure 15, left panel). The right panel in Figure 15 presents the same information as in the left panel except the width of the columns in the right panel changes based on the relative duration of each wind speed bin in the Humboldt WEA. In the right panel, these columns were plotted with a uniform width to improve visibility of density and percentage predictions across all available wind speeds, even rare ones.

Overall, the long-term prediction indicates a persistent vulnerability of sooty shearwaters to collision with RSZs due to their dynamic soaring and tendency to maneuver at heights of RSZs. As noted, wind conditions conducive to maximizing this vulnerability are most prevalent during the Upwelling season (Figure 9), coinciding with the highest densities of sooty shearwaters in the CCS (Figure 14).

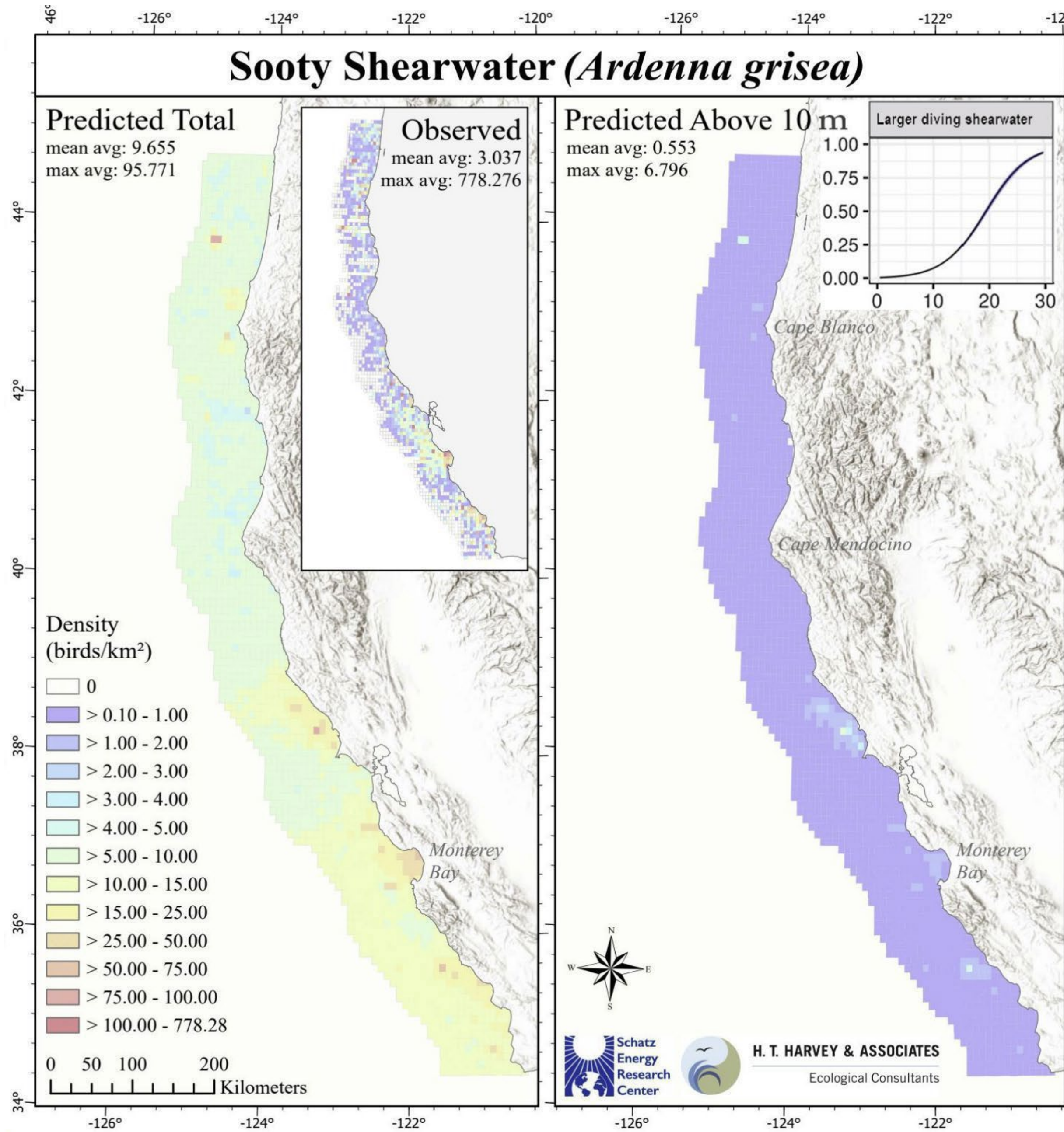

Figure 13. Annual 2D and 3D Predictions for Sooty Shearwater, an Abundant and Widespread Species Likely to Fly at Rotor Swept Heights

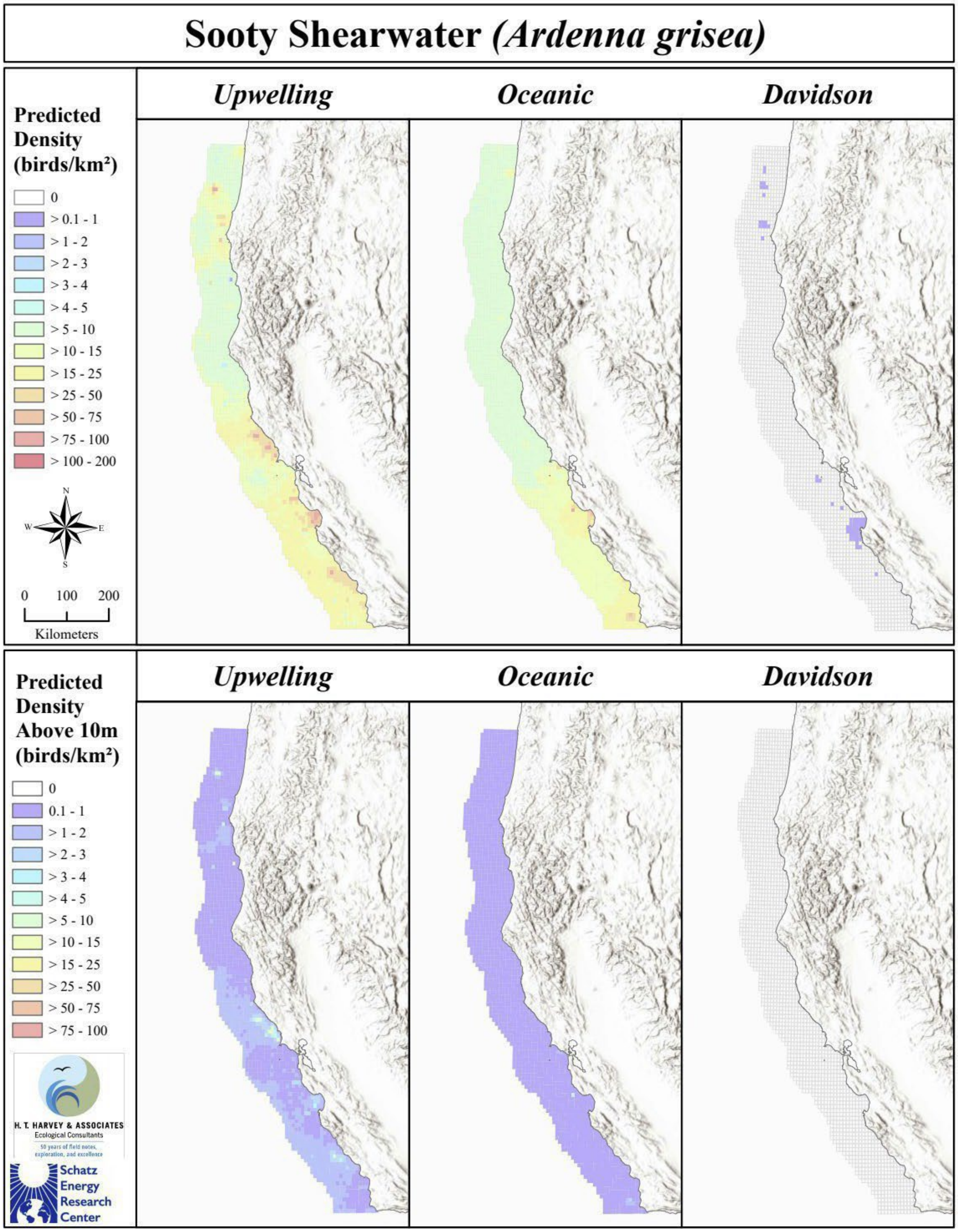

Figure 14. Seasonal 2D and 3D Predictions for Sooty Shearwater
The cells lacking color in the Davidson Current season result from an absence of this species during that time as they are nesting in the southern hemisphere at that time.

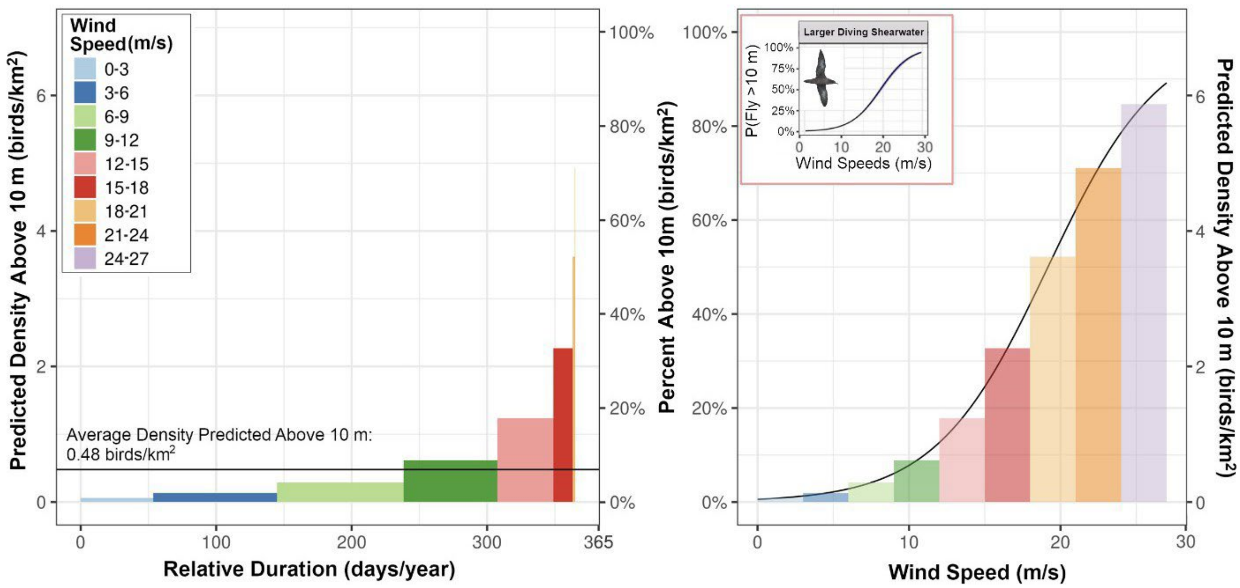

Figure 15. Integrating the Windscape into Site-specific Predictions of Sooty Shearwater Densities at Rotor Swept Zone Heights

This figure demonstrates how wind speed data were used to predict seabird densities at the heights at which they could encounter wind turbine rotor-swept zones (Component III of the 3D Framework; see Figure 2), using calculations for Sooty Shearwater in the Humboldt WEA as an example. Wind speeds were hindcast at each prediction site for each 5-minute interval over a 20-year period (2000-2019). These measurements were grouped into 0.5 m/s increments to capture the full range of wind conditions. These detailed wind data were then applied to models predicting the likelihood of seabirds flying above 10 m. For example, in the Humboldt WEA, it is predicted that, based on long-term historical data, an average of 0.48 Sooty Shearwaters/km^2 would be flying above 10 m in this WEA, or approximately 7-8% of the predicted population at this location (range: >0% to <85%). The left panel indicates an average density of 0.48 birds/km^2 expected to be flying at altitudes exceeding 10 m, presuming wind speed and bird densities similar to long-term historical conditions. This single point estimate was derived from the underlying range of density estimates resulting from the windscape, rather than a single average wind speed. Both the left and right panels display this information in terms of absolute density (birds/km^2) and proportional (%) to the larger 2D density estimate. Finally, regarding wind speed, the left panel visualized the proportional dominance of each wind-speed bin with variable-width columns (wider columns representing greater prevalence), while the right panel used fixed-width columns to visualize density estimates for even the rarest and most extreme wind speeds.

Definitions: Wind Energy Area: WEA; kilometers: km; meters: m; meters per second: m/s.

Common Murre

Common murre, a subspecies (*U. a. californica*) endemic to the CCS, is abundant year-round in CCS continental shelf waters, nesting in colonies on rocky islands and headlands for most of the year (Ainley and Boekelheide 1990, Ainley et al. 2021). They are concentrated closer to shore than sooty shearwaters but exhibit similar 2D densities (Figure 16, left panels). However, unlike sooty shearwaters, murres have a lower probability of flying above 10 m as wind speeds increase (Figure 16, right inset panel). Consequently, the density of murres flying above 10 m is predicted to be substantially lower than that of sooty shearwaters (Figure 16, right main panel). It is important to note that, like sooty shearwaters, the observed maximum annual average density of common murres was greater than that of predictions (390.3 versus 60.8 birds/km², respectively) and the mean annual average densities exhibited the opposite pattern, where the predictions were larger than the observations (2.4 versus 8.1 birds/km², respectively) (Figure 16, left panels). As with the sooty shearwater, this discrepancy arises from flocking behavior, as indicated by the potential for large numbers of individuals to be counted within a single km² --- the largest flock of common murre observed across the at-sea survey effort was 2010 birds/km² in 1982. Importantly, over a longer period, the average density balances out between these extremes, resulting in a more accurate representation of the density of common murres expected across the prediction area over a long duration of time (i.e., years to decades). Because common murres were present year-round in the study area, their distribution and density exhibited only some minor local shifts associated with changes in seasonal energetic demands (e.g., more concentrated around colonies while nesting, less concentrated during other seasons when regular attendance of the breeding colony was not required), compared with more drastic changes in densities as was observed with migratory species (e.g., shearwaters, albatross, etc.). Unlike sooty shearwater, populations of common murres in the CCS have been increasing in recent decades, recovering from former decimation (i.e., egging, oil spills; Ainley et al. 2021).

Ashy Storm-Petrel

Ashy storm-petrels are endemic to the CCS, nesting on islands and coastal rocks from northern Baja California, Mexico, to northern central California and are present in the CCS year-round (Ainley et al. 2020). They are most likely to be encountered in waters overlying the outer continental shelf and slope south of Cape Mendocino and are spatially associated with breeding colonies for several months of the year (Figure 17, left panels). Ashy storm-petrels exhibited a 2D density an order of magnitude lower than that of sooty shearwaters and common murres, in line with population estimates (Ford et al. 2021). Regarding their flight altitudes, ashy storm-petrels tended to remain below 10 m across all wind speeds, indicated by the flat probability curve centered near zero for the storm-petrel flight height and wind speed regression (Figure 17, right inset panel). Consequently, the density of ashy storm-petrels predicted to be flying above 10 m was virtually zero (Figure 17, right main panel). Like the other two species highlighted above, ashy storm-petrels also form flocks (especially during the Oceanic season), which explains the discrepancies in observed versus predicted maximum densities. However, due to the relatively low density of this species in general, the magnitude of difference in the observed and predicted mean annual average densities (~0.04 birds/km² greater for predictions) was relatively small in an absolute sense. Seasonal maps of their seasonal density distributions were not provided because these birds remained in the study area year-round, exhibiting only minor local shifts associated with changes in seasons.

Marbled Murrelet

Marbled murrelets, protected under both state and federal Endangered Species Acts (ESA) in CA and OR, are coastal residents found within a few kilometers from shore, typically at low densities across the region (Figure 18, left panels). Unlike the other CCS seabirds which nest on offshore rocks and islands, marbled murrelets nest in old-growth or mature coniferous forests sometimes at appreciable distances inland from the coast (Figure 18, left panels). Similar to the other species discussed here, marbled murrelets may gather at sea near the shore, although not as abundantly as the aforementioned species. During the Upwelling season, they tend to aggregate in coastal areas adjacent to old-growth forests to minimize travel distances to and from nest sites, leading to discrepancies between observed and predicted maximum densities. Due to their generally low density, the differences between observed and predicted mean annual average densities were relatively small (~0.006 birds/km^2 greater for predictions). Their distribution and density show minor local shifts with changing seasons, and as such, seasonal density distributions are not provided.

Similar to ashy storm-petrels, marbled murrelets tend to fly below 10 m across all wind speeds (Figure 18, right inset panel), with a negligible predicted probability of flying above 10 m (Figure 18, right main panel). One caveat is that when murrelets are traveling between inland nest sites and the ocean at dusk and dawn, throughout the Upwelling season, they ascend nearshore to the heights of their nest sites (many 10s of meters ASL). Upon return to the ocean, they quickly descend to sea level (see Figure 18), thereby eliminating the potential to interact with RSZ's.

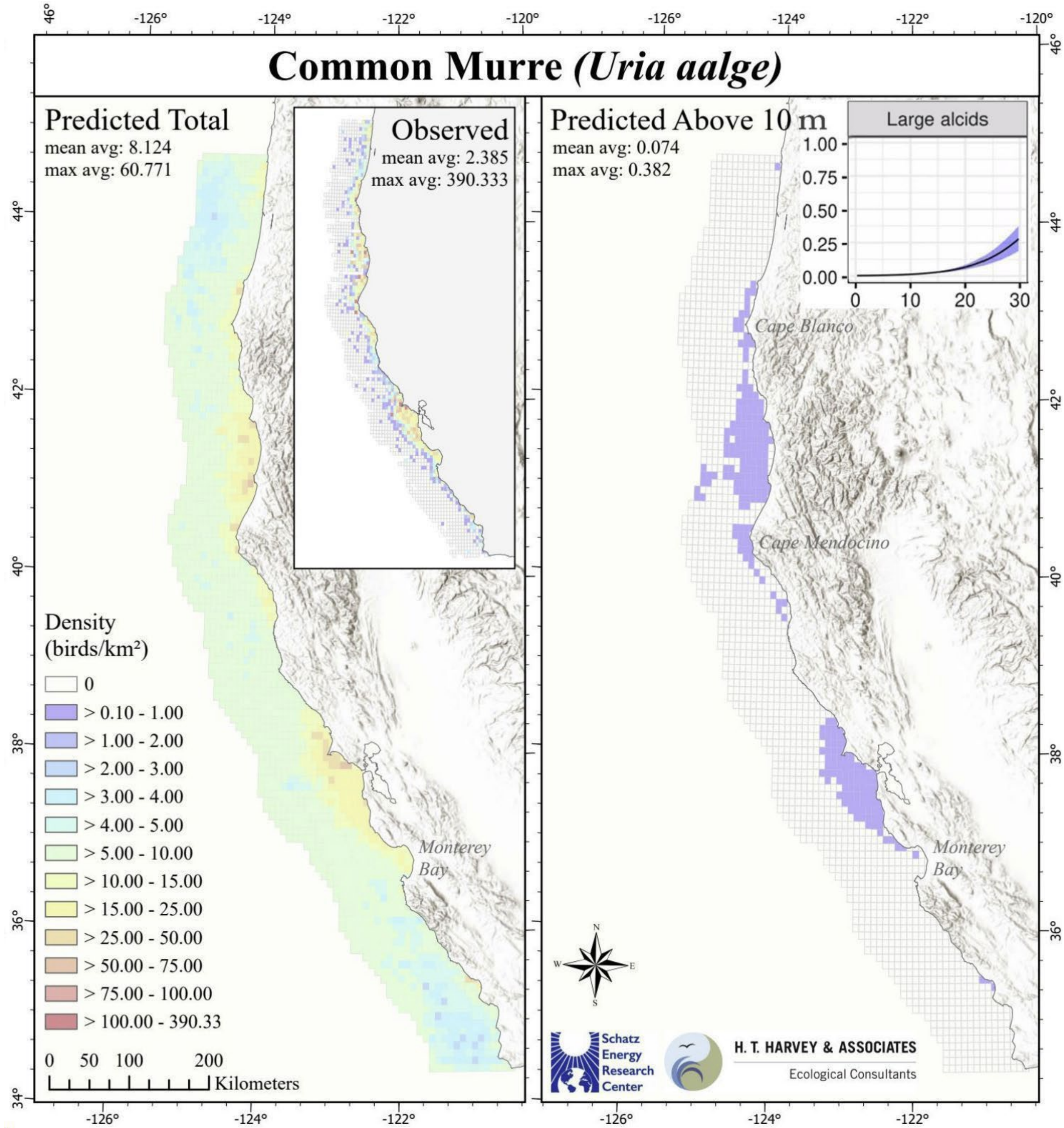

Figure 16. Annual 2D and 3D Predictions for Common Murre, an Abundant and Widespread Species with a Relatively Low Probability of Flying at Rotor Swept Heights

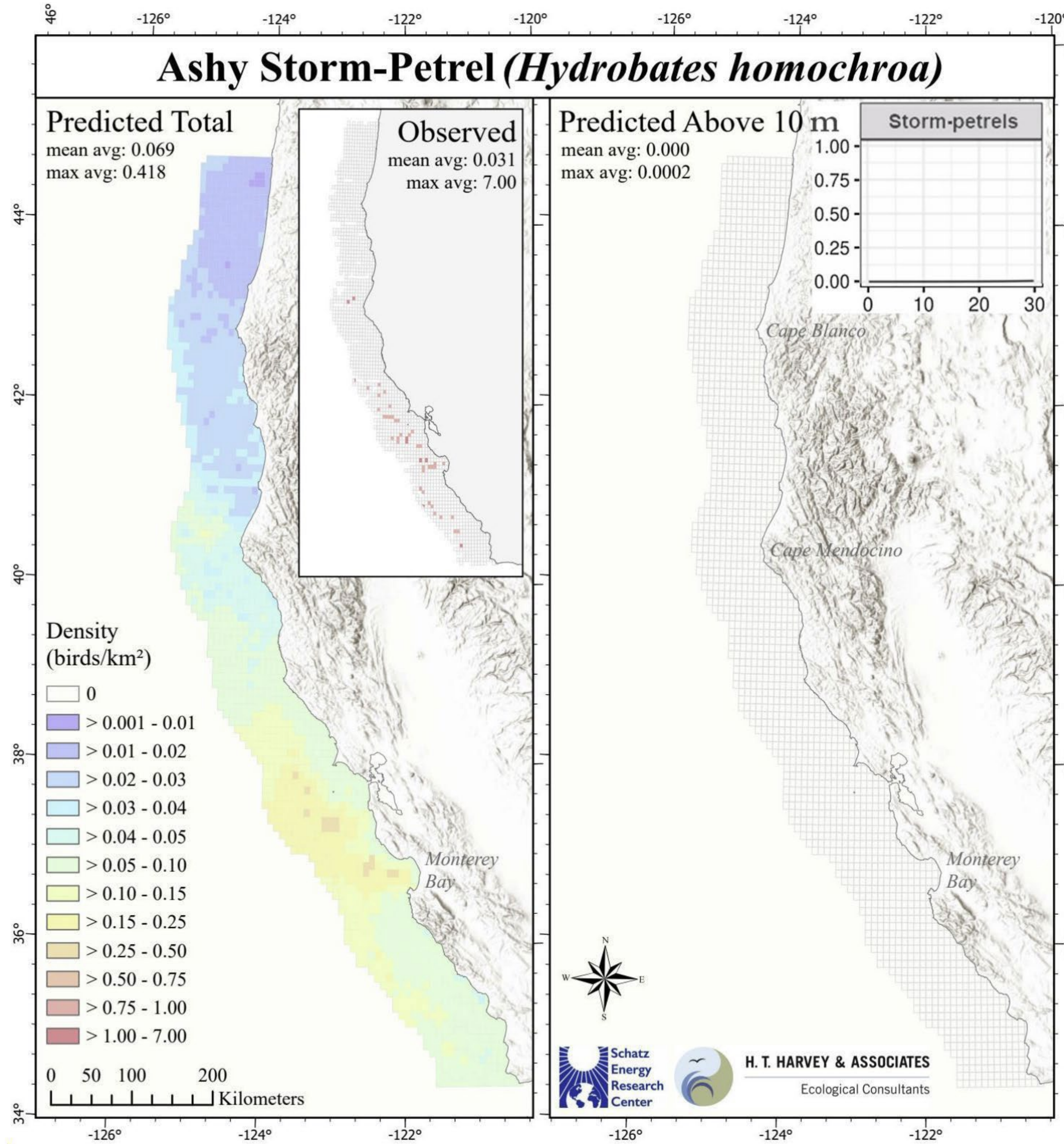

Figure 17. Annual 2D and 3D Predictions for Ashy Storm-Petrel, a Special Status and Range-Restricted Species Unlikely to Fly at Rotor Swept Heights

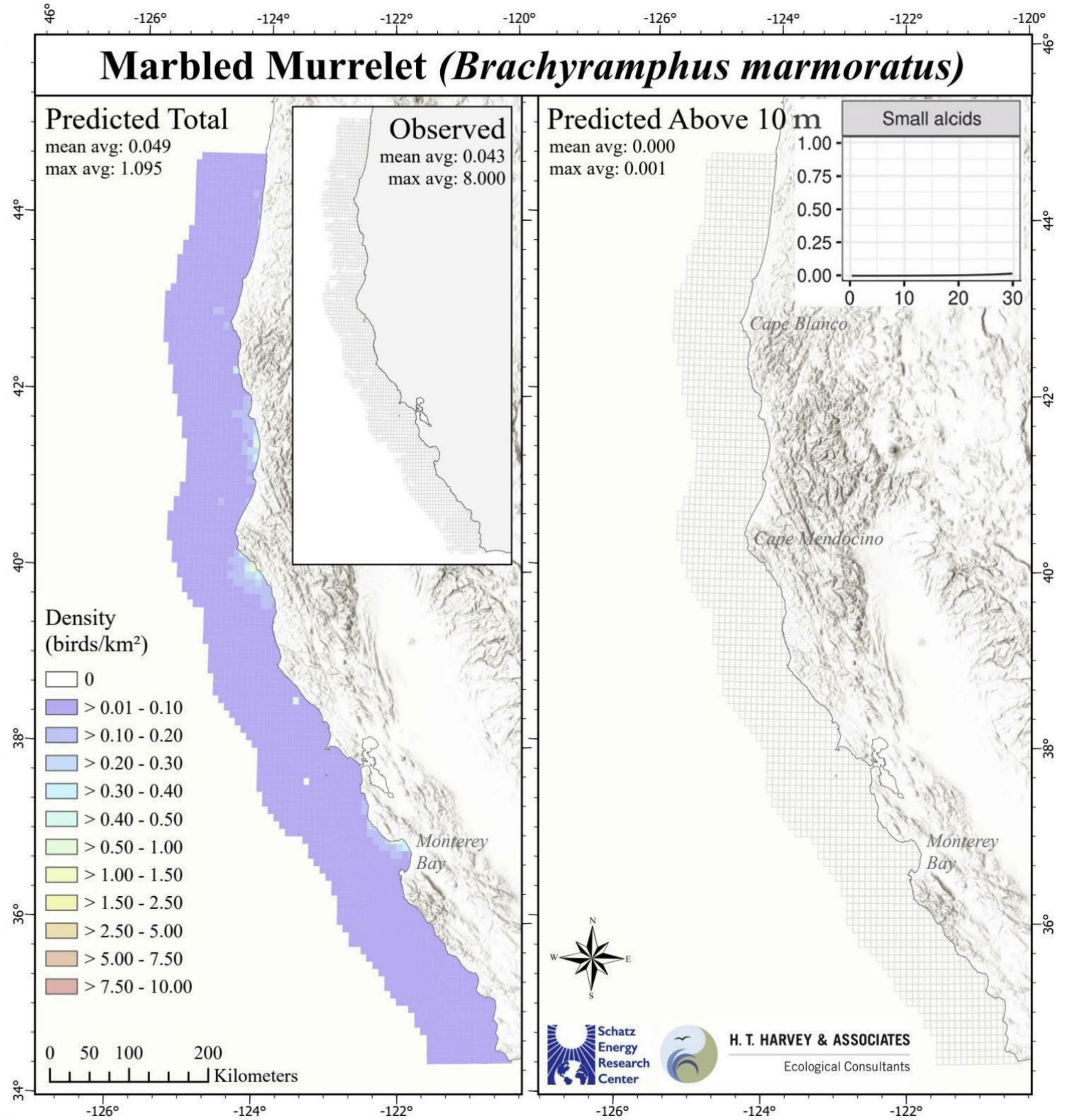

Figure 18. Annual 2D and 3D Predictions for Marbled Murrelet, a Special Status and Extremely Coastal Species Unlikely to Fly at Rotor Swept Heights

Summary and Conclusions

The 3D Framework developed for this project is an innovative effort to better understand the vertical airspace used by seabirds in the CCS. By integrating extensive data on seabird presence, abundance, and flight height in response to wind speed and the windscape off CA and OR, the 3D Framework offers valuable insights into the distribution and behavior of seabirds in three dimensions.

Collision Vulnerability Assessment

The results of this 3D Framework enhance understanding of how seabird distribution may intersect with OSW infrastructure. Previous studies (e.g., Adams et al. 2016, Leirness et al. 2021, Russell et al. 2023) were significant achievements that help to better understand the seabird community of the CCS. However, these studies relied on planar predictions, overlooking the interplay between wind speed, flight height, and windscape, all of which are crucial for assessing vertical distributions of seabirds and collision vulnerability. The 3D Framework represents an initial attempt to enhance the dimensionality of seabird density predictions to include the vertical component and facilitate a more explicit evaluation of seabird overlap with RSZs. A primary outcome of the assessment presented here is that dynamically soaring species are particularly susceptible to overlapping RSZs, highlighting the need to consider them in the OSW permitting and consultation processes.

The development of 2D seabird density estimates in the 3D Framework involved integrating data from multiple long-term observation databases derived from aerial and vessel-based platforms and correcting counts for flux. Establishing relationships between flight height and wind speed required re-analyzing data from Ainley et al. (2015) to generate probabilities of flying at or above 10 m ASL. The 3D Framework presented here included 18 distinct FGs and 44 regularly observed species from CA. Results indicate that most of CA's seabird community remains near the sea surface and close to the coastline. While flying at-sea, most FGs remain below the RSZ-height, but the propensity to enter RSZs can vary considerably for those FGs likely to do so. For instance, larger diving shearwaters may fly at collision risk height anywhere from 0% to 100% of the time depending on wind speed. For all included seabird taxa, the 3D Framework predicted annual and seasonal density flying below and above 10 m ASL. These predictions capture seasonal and site-specific patterns, offering valuable insights into the expected distribution of seabirds in the CCS over longer time periods.

Relevance to Collision Risk Modeling

The 3D Framework is not a Collision Risk Model but rather a broad quantification of the spatial variability in the composition and magnitude of seabirds likely to fly at heights increasing their potential to encounter RSZs and consequently, their vulnerability to turbine-blade collision. The predictions provided by the 3D Framework, akin to passage rates, offer density estimates and flight height information across the CCS, which are critical inputs for generating a formal Collision Risk Model. Such models aim to estimate the probability of a single bird colliding with a turbine blade upon entry into a RSZ and the likely number of collisions over a specific period (Band 2012; Masden and Cook 2016). Understanding flight heights can also be helpful for generating accurate predictions of collision rates using a Collision Risk Model, such as understanding if a bird ever flies at collision risk heights, for example. Thus, the predictions provided by the 3D Framework provide insight into the flight heights of various seabirds off CA as well as an indication of the possible magnitude of passage at collision risk heights and includes predictions for areas that have been previously surveyed.

Small albatrosses, shearwaters (both diving and surface-feeding types), and small and large gadfly petrels (not included in this analysis due to insufficient observations) are known to increase flight height with increased wind speed (Ainley et al. 2015). These species are also known to occur in the shelf break location near existing areas proposed for WEAs. Notably, all currently existing OSW facilities in the U.S., all on the Atlantic coast, are positioned in relatively shallow water where the presence of these dynamic soarers (that are expected to regularly fly above 10 m in certain wind conditions) is negligible. Therefore, assumptions regarding how these types of birds will alter their flight in the presence of turbines in their environment will need to be made based on the best available science from our understanding of other birds until these assumptions can be refined using empirical data (i.e, turbines must exist in areas where these types of birds are present before we can make species-specific measurements of avoidance rate).

It should also be noted that two federally listed species, the Hawaiian petrel and short-tailed albatross, both of which are in dynamic soaring FGs, were extremely rarely encountered in California waters during the time period the surveys providing the data used for this analysis were conducted. However, as a result of conservation efforts at breeding sites, both species have been increasing in the CCS in recent years, especially the Hawaiian petrel, which is now a regular annual visitor in small numbers. It has been observed primarily, but not exclusively, in continental slope waters.

Recommendations and Future Directions

The 3D Framework, while a significant advancement, has certain limitations and areas for improvement that should be addressed in future research endeavors. For instance, the 3D Framework was constrained to seabird species detected within at least 100 km² of at-sea transect effort, resulting in the exclusion of species like the Hawaiian petrel and short-tailed albatross, both listed under state and/or federal ESAs. These species are crucial to consider during permitting processes and should be incorporated into future iterations of the 3D Framework. Other data limitations were that: 1) observations could only be made during daylight even though seabirds do fly at night (Schneider et al. 2024), 2) the timing of surveys may not have captured short-lived migration pulses because surveys provide only 'snapshots' in space and time, and 3) aerial surveys were limited to mild weather conditions. Additionally, it is difficult for human observers to see vertically across the full extent of the RSZ (up to 260 m ASL), and thus the flight height data used in this study were based on conservative thresholds for flight in the RSZ. Although the 10 m ASL threshold may seem conservative, based on findings of new technologies deployed in the Humboldt WEA off CA (Matzer et al. 2022, Schneider et al. 2024) ~ 50% birds do remain within the first 10 m of airspace. However, also noted were birds moving at heights that humans are likely unable to see, let alone assign a precise flight height more detailed than 'above 10 m'. To overcome these challenges, future research should explore the integration of new technologies capable of detecting and identifying seabirds across the RSZ in varied environmental conditions and times of day. Projects funded by organizations like the CEC are actively developing such technologies to address these limitations.

Methodologically, the IDW spatial interpolation algorithm was selected for seabird 2D density estimates because it provided the most stable and reliable predictions across all species and regions, based on the available observational data. While other modeling approaches were considered, including zero-inflated General Additive Models, Occupancy Models, and Kriging, these methods relied on covariates (e.g., sea surface temperature, depth, distance to coast) that did not consistently reflect the ecological drivers of seabird presence and density across the diverse species and locations. In some cases, simpler models like IDW outperform more complex models by avoiding the complications and assumptions that can lead to inaccurate predictions. When environmental factors are not fully understood or are poorly represented in the data, IDW's straightforward interpolation provides more reliable and intuitive results. After carefully evaluating various options, IDW emerged as the most effective approach for achieving the objectives of this Framework.

Future modification and use of the 3D Framework off CA could include incorporating newer at-sea observational data including efforts funded by BOEM and others. Observations from the past 10 or more years, as noted, indicate that some species have significantly changed in abundance (e.g., fewer sooty shearwaters, more common murres and brown pelicans), including historically rare birds that have increased in waters off CA (e.g., sulids). Some of the reasons for these changes include recovery of populations from protective measures at remote nesting sites (such as predator exclusion, in the case of the Hawaiian petrel), reducing commercial fisheries bycatch (for albatross), and changing ocean conditions (for boobies).

Lastly, the applicability of the 3D Framework extends beyond the CCS and can be adapted for use in other regions with sufficient observational data. The relationships between CCS seabird flight behavior and wind speed, particularly above 10 m ASL, offer valuable insights applicable to various seabird species, including those uncommonly observed in the CCS such as the Hawaiian petrel, as they are being increasingly observed and their FG characteristics are well understood. Thus, ongoing efforts to refine and expand the 3D Framework will contribute to its broader utility in informing OSW development and environmental management strategies.

Acknowledgements

The authors would like to acknowledge several individuals that provided technical guidance, including Ryan Terrill (Klamath Bird Observatory) and Jerome Carman (Humboldt Transit Authority). The members of the Technical Advisory Committee provide valuable input: David Pereksta (Bureau of Ocean Energy Management), Chris Potter (formerly of the California Department of Fish and Wildlife), Garry George (National Audubon Society), Dan Barton (Cal Poly Humboldt), Kaus Raghukumar (Integral Consulting), Mike Optis (National Renewable Energy Lab), Yi-Hui Wang (formerly of the Ocean Protection Council), Mark Severy (Pacific Northwest National Laboratory), Tyler Studds (Ocean Winds), and Brita Woeck (Ørsted). We thank the California Energy Commission for funding and support.

References

Adams, J., E. C. Kelsey, J. J. Felis, and D. M. Pereksta. 2016. Collision and Displacement Vulnerability among Marine Birds of the California Current System Associated with Offshore Wind Energy Infrastructure. Open-File Report 2016-1154. U.S. Geological Survey, Reston, Virginia. Prepared in cooperation with Bureau of Ocean Energy Management (OCS Study, BOEM 2016-043).

Ainley, D. G., L. B. Spear, C. T. Tynan, J. A. Barth, S. D. Pierce, G. R. Ford, and T. J. Cowles. 2005. Physical and biological variables affecting seabird distributions during the upwelling season of the northern California Current. Deep-Sea Research II 52(1-2):123-143.

Ainley, D. G., E. Porzig, D. Zajanc, and L. B. Spear. 2015. Seabird flight behavior and height in response to altered wind strength and direction. Marine Ornithology 43:25-36.

Band, B. 2012. Using a Collision Risk Model to Assess Bird Collision Risks for Offshore Wind Farms. SOSS-02. Prepared for Strategic Ornithological Support Services Programme.

Bates D., M. Machler, B. Bolker, and S. Walker. 2015. Fitting linear mixed-effects models using lme4. Journal of Statistical Software 67(1):1-48.

[BOEM] Bureau of Ocean Energy Management. 2022. Pacific wind lease sale 1 (PACW-1) for commercial leasing for wind power in the Outer Continental Shelf in California - Proposed sale notice. Federal Register 87(104):32443-32458.

Bograd, S. J., I. Schroeder, N. Sarkar, X. Qiu, W. J. Sydeman, and F. B. Schwing. 2009. Phenology of coastal upwelling in the California Current. Geophysical Research Letters 36:1-5.

Bolin, R. L., and D. P. Abbott. 1963. Studies on the marine climate and phytoplankton of the coast of California 1954-1960. California Cooperative Oceanic Fisheries Investigations Reports 9:23-45.

Checkley, D. M., and J. A. Barth. 2009. Patterns and processes in the California Current System. Progress in Oceanography 83(1-4):49-64.

Clarke, E. D., L. B. Spear, M. L. McCracken, F. F. C. Marques, D. L. Borchers, S. T. Buckland, and D. G. Ainley. 2003. Validating the use of generalized additive models and at-sea surveys to estimate size and temporal trends of seabird populations. Journal of Applied Ecology 40(2):278-292.

Cook, A. S. C. P., R. M. Ward, W. S. Hansen, and L. Larsen. 2018. Estimating seabird flight height using LiDAR. Scottish Marine and Freshwater Science 9(14).

Flint, S., R. deMesa, P. Doughman, and E. Huber. 2022. Offshore Wind Development Off the California Coast: Maximum Feasible Capacity and Megawatt Planning Goals for 2030 and 2045. August. CEC-8002022-001-REV. Prepared for California Energy Commission.

Ford, G. R., S. Terrill, J. Casey, D. Shearwater, S. R. Schneider, S. R. Ballance, L. Terrill, et al. 2021. Distribution patterns and population size of the ashy storm petrel *Oceanodroma homochroa*. Marine Ornithology 49(2):193-204.

Harwood, A. J., M. R. Perrow, and R. J. Berridge. 2018. Use of an optical rangefinder to assess the reliability of seabird flight heights from boat-based surveyors: Implications for collision risk at offshore wind farms. Journal of Field Ornithology 0(0):1-12.

Largey, N., A. S. C. P. Cook, C. B. Thaxter, A. McCluskie, B. G. Stokke, B. Wilson, and E. A. Masden. 2021. Methods to quantify avian airspace use in relation to wind energy development. Ibis 163(3):747-764.

Leirness, J. B., J. Adams, L. T. Ballance, M. Coyne, J. J. Felis, T. Joyce, D. M. Pereksta, et al. 2021. Modeling At-Sea Density of Marine Birds to Support Renewable Energy Planning on the Pacific Outer Continental Shelf of the Contiguous United States. August. OCS Study BOEM 2021-014. Camarillo, California. Prepared for U.S. Department of the Interior, Bureau of Ocean Energy Management, Pacific OCS Region. Prepared by U.S. Department of Commerce, National Oceanic and Atmospheric Administration, and U.S. Department of the Interior, U.S. Geological Survey, Western Ecological Research Center.

Li, B., H. F. Lingsma, E. W. Steyerberg, and E. Lesaffre. 2011. Logistic random effects regression models: A comparison of statistical packages for binary and ordinal outcomes. BMC Medical Research Methodology 11(77):1-11.

Masden, E. A., and A. S. C. P. Cook. 2016. Avian collision risk models for wind energy impact assessments. Environmental Impact Assessment Review 56(43-49).

Matzner, S., T. E. Warfel, R. Hull, and N. Williams. 2022. ThermalTracker-3D Offshore Validation Technical Report. April. Contract DE-AC05-76RL01830. Prepared for U.S. Department of Energy. Prepared by Pacific Northwest National Laboratory.

Midway, S. 2022. Chapter 9 Random Effects. Data Analysis in R. <https://bookdown.org/steve_midway/DAR/random-effects.html>.

[NREL] National Renewable Energy Lab. 2023. Wind Toolkit Data Downloads: Offshore CA Data Download. <https://developer.nrel.gov/docs/wind/wind-toolkit/offshore-ca-download/>.

Nur, N., J. Jahncke, M. P. Herzog, J. Howar, K. D. Hyrenbach, J. E. Zamon, D. G. Ainley, et al. 2011. Where the wild things are: Predicting hotspots of seabird aggregations in the California Current System. Ecological Applications 21:2241-2257.

Pebesma, E. J. 2004. Multivariate geostatistics in S: The gstat package. Computer and Geosciences 30(7):683-691.

Pebesma, E. J., and C. G. Wesseling. 1998. Gstat, a program for geostatistical modelling, prediction and simulation. Computer and Geosciences 24(1):17-31.

Pennycuick, C. J. 1987a. Flight of seabirds. Pages 43-62 *in* J. P. Croxall, Seabirds: Feeding Biology and Role in Marine Ecosystems. Cambridge University Press.

Pennycuick, C. J. 1987b. Flight of auks (Alcidae) and other northern seabirds compared with southern procellariforms: Ornithodolite observations. Journal of Experimental Biology 128:335-347.

R Core Team. 2016. Package 'stats.' R Package Version 3.3.1.

Rose, A., D. Wei, and A. Einbinder. 2022. The co-benefits of California offshore wind electricity. The Electricity Journal 35(7):107167.

Russell, T. M., A. R. Szesciorka, T. Joyce, D. G. Ainley, and L. T. Ballance. 2023. National Marine Sanctuaries capture enhanced abundance and diversity of the California Current Ecosystem avifauna. Journal of Marine Systems 240(1038887):1-16.

Schneider, S. R., S. H. Kramer, S. B. Bernstein, S. B. Terrill, D. G. Ainley, and S. Matzner. 2024. Autonomous thermal tracking technology reveals spatiotemporal patterns of seabird activity relevant to interactions with future floating offshore wind facilities. Frontiers in Marine Science. Frontiers in Marine Science 11:1346758.

Severy, M., C. Ortega, C. Chamberlin, and A. Jacobson. 2020. Wind Speed Resource and Power Generation Profile. September. California North Coast Offshore Wind Studies. Prepared for U.S. Department of the Interior, Bureau of Ocean Energy Management. Prepared by Schatz Energy Research Center, Humboldt, California.

Spear, L. B., and D. G. Ainley. 1997a. Flight speed of seabirds in relation to wind speed and direction. Ibis 139:234-251.

Spear, L. B., and D. G. Ainley. 1997b. Flight behaviour of seabirds in relation to wind direction and wing morphology. Ibis 139:221-233.

Spear, L. B., N. Nur, and D. G. Ainley. 1992. Estimating absolute densities of flying seabirds using analyses of relative movement. The Auk 109(2):385-389.

Spear, L. B., D. G. Ainley, S. N. G. Howell, B. D. Hardesty, and S. G. Webb. 2004. Reducing biases affecting at-sea surveys of seabirds: Use of multiple observer teams. Marine Ornithology 32:147-157.

Wallach, E., Schneider, S., Ainley, D., Terrill, S., Ford, G., Santora, J., Kramer, S., Casey, J., Chamberlin, C., & Jacobson, A. 2024. 3D seabird density estimates [Data set]. Zenodo. https://doi.org/10.5281/zenodo.11620539.

Webb, A., and G. Nehls. 2019. Surveying seabirds. Pages 60-96 *in* D. M. Pereksta, Wildlife and Wind Farms, Conflicts and Solutions. Volume 4 Offshore: Monitoring and Mitigation. Pelagic Publishing, Exeter, United Kingdom.

Appendix A. Additional Information Regarding Seabird Observations and Predictions

Table A-1. Additional Information About At-Sea Surveys that were Foundational to Predictions made by the 3D Seabird Collision Vulnerability Framework

Survey Name	Type	Transect Width (meters)	References
[CNCA] Marine Mammal and Seabird Surveys of Central and Northern California Aerial survey, BLM OCSEAP	Aerial	50	Halpin et al. 2009, Ford et al. 2021
[OSPR] Office of Spill Prevention and Response, California Department of Fish and Wildlife	Aerial	50 or 75	Ford et al. 2021
[PSEA] Pacific Continental Shelf Environmental Assessment, U.S. Geological Survey	Aerial	75	Adams et al. 2014, 2016
[DODS] San Francisco Deep Ocean Disposal Site, U.S. Army Corps of Engineers	Vessel	300	Ford et al. 2021
[EPOC] Equatorial Pacific Ocean Climate Studies, NOAA PMEL	Vessel	300	Spear et al. 1995
[GOEO] Global Ocean Ecosystem Dynamics, NSF Ocean Sciences	Vessel	300	Ainley et al. 2005, 2009
[JVRK] Rockfish Recruitment and Ecosystem Survey, NOAA-NMFA	Vessel	300	Sakuma et al. 2006; Santora et al. 2011, 2012; Wells et al. 2017
[OCWA] Oregon, California, Washington Line-Transect Expeditions, NMFS SWFSC	Vessel	300	Philbrick et al. 2003, Appler et al. 2004
[RVWE] *Wecoma* Navy Acoustic Work	Vessel	300	D. Ainley, pers. obs. during naval cruise, July 2005

Table Notes: Seabird observations derived from nine continuous strip-transect surveys were used to support density estimates made by the 3D Seabird Collision Vulnerability Framework. For each survey, 4-letter codes and names have been provided along with an indication of if seabirds were counted from aircraft (aerial) or ship (vessel) and the width of the transect in which seabirds were counted. The references point to sources with additional information on each survey.

Table A-2. Detection and Count Details for Each Seabird Included in the 3D Seabird Collision Vulnerability Framework

Flight Group, Common and Latin Name	Species Code	Effort with Presence (km²)	Total Flux Corrected Counts[1]			
			Annual	Upwelling	Oceanic	Davidson
Small Albatrosses						
Black-footed Albatross, *Phoebastria nigripes*	ALBF	2,489	5,882	4,644 (79.0%)	1,068 (18.2%)	170 (2.9%)
Laysan Albatross, *Phoebastria immutabilis*	ALLA	183	276	60 (21.7%)	93 (33.7%)	123 (44.6%)
Fulmars						
Northern Fulmar, *Fulmarus glacialis*	FUNO	3,674	11,208	3,183 (28.4%)	4,152 (37.0%)	3,873 (34.6%)
Surface-Feeding Shearwaters						
Buller's Shearwater, *Ardenna bulleri*	SHBU	951	4,657	138 (3.0%)	4,495 (96.5%)	24 (0.5%)
Pink-footed Shearwater, *Ardenna creatopus*	SHPF	2,074	8,249	4,297 (52.1%)	3,907 (47.4%)	45 (0.6%)
Larger Diving Shearwaters						
Sooty Shearwater, *Ardenna grisea*	SHSO	8,001	347,262	220,998 (63.6%)	125,979 (36.3%)	285 (0.1%)
Short-tailed Shearwater, *Ardenna tenuirostris*	SHST	108	246	45 (18.3%)	118 (48.0%)	83 (33.7%)
Smaller Diving Shearwaters						
Black-vented Shearwater, *Puffinus opisthomelas*	SHBV	199	2,040	11 (0.5%)	693 (34.0%)	1,336 (65.5%)
Storm-Petrels						
Fork-tailed Storm-Petrel **, *Hydrobates furcatus*	STFT	789	10,022	8,548 (85.3%)	1,327 (13.2%)	147 (1.5%)
Leach's Storm-Petrel, *Hydrobates leucorhous*	STLA	2,289	8,367	4,310 (51.5%)	3,778 (45.2%)	279 (3.3%)
Ashy Storm-Petrel, *Hydrobates homochroa*	STAS	695	2,253	678 (30.1%)	1,419 (63.0%)	156 (6.9%)
Pelicans						
Brown Pelican *, *Pelecanus occidentalis*	PELB	1,580	5,501	1,198 (21.8%)	2,808 (51.1%)	1,495 (27.2%)
Phalaropes						
Phalaropes, *Phalaropus* spp.	PHAL	4,185	79,180	30,853 (39.0%)	45,476 (57.4%)	2,851 (3.6%)
Skuas						
Long-tailed Jaeger, *Stercorarius longicaudus*	JALT	368	796	155 (19.5%)	638 (80.2%)	3 (0.4%)
Parasitic Jaeger, *Stercorarius parasiticus*	JAPA	363	495	124 (25.1%)	360 (72.7%)	11 (2.2%)

Flight Group, Common and Latin Name	Species Code	Effort with Presence (km^2)	Total Flux Corrected Counts[1]			
			Annual	Upwelling	Oceanic	Davidson
Pomarine Jaeger, *Stercorarius pomarinus*	JAPO	727	912	175 (19.2%)	600 (65.8%)	137 (15.0%)
South Polar Skua, *Stercorarius maccormicki*	SKMA	145	159	35 (22.0%)	123 (77.4%)	1 (0.6%)
Large Gulls						
California Gull, *Larus californicus*	GUCA	4,601	56,432	7,899 (14.0%)	26,092 (46.2%)	22,441 (39.8%)
Herring Gull, *Larus argentatus*	GUHR	1,789	7,866	1,323 (16.8%)	1,701 (21.6%)	4,842 (61.6%)
Western Gull, *Larus occidentalis*	GUWE	8,400	38,189	17,509 (45.9%)	13,346 (35.0%)	7,334 (19.2%)
Glaucous-winged Gull, *Larus glaucescens*	GUGW	1,200	2,844	438 (15.4%)	530 (18.6%)	1,867 (66.0%)
Heermann's Gull, *Larus heermanni*	GUHE	1,008	3,412	610 (17.9%)	1,928 (56.5%)	874 (25.6%)
Medium Gulls						
Black-legged Kittiwake, *Rissa tridactyla*	KWBL	1,508	10,283	6,546 (63.7%)	190 (1.9%)	3,547 (34.5%)
Short-billed Gull, *Larus brachyrhynchus*	GUME	111	237	24 (10.1%)	60 (25.3%)	153 (64.6%)
Small Gulls						
Bonaparte's Gull, *Chroicocephalus philadelphia*	GUBO	524	5,879	2,599 (44.2%)	2,610 (44.4%)	670 (11.4%)
Sabine's Gull, *Xema sabini*	GUSA	645	2,850	1,590 (55.8%)	1,253 (44.0%)	7 (0.3%)
Terns						
Arctic Tern, *Sterna paradisaea*	TEAR	520	3,266	323 (9.9%)	2,943 (90.1%)	0 (0.0%)
Caspian Tern, *Hydroprogne caspia*	TECA	167	254	209 (82.3%)	41 (16.1%)	4 (1.6%)
Elegant Tern, *Thalasseus elegans*	TEEL	307	1,729	349 (20.2%)	1,380 (79.8%)	0 (0.0%)
Cormorants						
Brandt's Cormorant, *Urile penicillatus*	COBR	2,399	19,012	9,688 (51.0%)	5,922 (31.2%)	3,402 (17. 9%)
Double-crested Cormorant, *Nannopterum auritum*	CODC	150	327	140 (42.8%)	55 (16.8%)	132 (40.4%)
Pelagic Cormorant, *Urile pelagicus*	COPE	272	398	247 (62.1%)	54 (13.6%)	97 (24.4%)
Large Alcids						
Common Murre, *Uria aalge*	MUCO	8,725	215,044	100,286 (46.6%)	71,068 (33.1%)	43,690 (20.3%)
Tufted Puffin **, *Fratercula cirrhata*	PUTU	110	153	126 (82.4%)	24 (15.7%)	3 (2.0%)

Flight Group, Common and Latin Name	Species Code	Effort with Presence (km²)	Total Flux Corrected Counts[1]			
			Annual	Upwelling	Oceanic	Davidson
Medium Alcids						
Rhinoceros Auklet, *Cerorhinca monocerata*	AKRH	3,833	20,435	7,338 (35.9%)	5,165 (25.3%)	7,932 (38.8%)
Pigeon Guillemot, *Cepphus columba*	GUPI	281	730	525 (71.9%)	47 (6.4%)	158 (21.6%)
Small Alcids						
Cassin's Auklet **, *Ptychoramphus aleuticus*	AKCA	4,282	44,631	24,342 (54.5%)	13,734 (30.8%)	6,555 (14.7%)
Marbled Murrelet*, *Brachyramphus marmoratus*	MRMA	346	1,333	283 (21.2%)	323 (24.2%)	727 (54.5%)
Scripps's, Guadalupe, Craveri's Murrelet *, *Synthliboramphus* spp.	MRXA	108	193	82 (42.5%)	93 (48.2%)	18 (9.3%)
Loons, Grebes, Ducks						
Western & Clark's Grebes, *Aechmophorus* spp.	GREB	2,150	69,665	21,057 (30.2%)	17,013 (24.4%)	31,595 (45.4%)
Surf Scoter, *Melanitta perspicillata*	SCSU	904	27,581	3,314 (12.0%)	3,626 (13.2%)	20,641 (74.9%)
Pacific Loon, *Gavia pacifica*	LOPA	1,301	6,570	3,741 (56.9%)	1,207 (18.4%)	1,622 (24.7%)
Common Loon **, *Gavia immer*	LOCO	562	1,327	436 (32.9%)	241 (18.2%)	650 (49.0%)
Red-throated Loon, *Gavia stellata*	LORT	400	750	209 (27.9%)	82 (10.9%)	459 (61.2%)

Notes: Detailed presence and count information for the 44 seabird taxa included in the 3D Seabird Framework. For inclusion, at least one individual for each taxa had to be observed in at least 100 km² units of effort) across the full 26,319 km² of standardized at-sea survey effort supporting this assessment. All taxa have been organized according to their flight-style grouping (indicated in bold) and the January 2024 nomenclature recommended by the American Ornithologists Union was used to maximize interpretability of species included in the future despite ongoing name changes. To help with organizing the data inputs and model outputs, consistent 4-letter codes assigned to each seabird type: the first two letters were related to a broader common identity of the taxa (e.g., all loons were assigned 'LO') and the second two letters were related to the specific identity of each taxon (e.g., the Pacific Loon was assigned 'PA').

[1] The summation of individuals counted, after correcting for flux, for the full extent of at-sea survey effort in total (Annual) and by season (Upwelling, Oceanic and Davidson Current). Percent of counts per season for each taxon provided in parentheses after seasonal flux corrected counts.

* Indicates species that have additional protections and may be of regulatory concern. MRXA are threatened under the CA Endangered Species Act (ESA). MRMA are endangered under CA ESA and threatened under the federal ESA.

** Indicates that species are designated by the CA Department of Fish and Wildlife as State Species of Special Concern. These species have less regulatory constraints compared to species listed under the CA or federal ESA

Table A-3. Seabird Species Excluded from 3D Framework Due to Insufficient Observations (Less Than 100 km² of 26,319 km² Survey Effort with Presence)

Flight-Style Grouping	Common and Latin Name	Effort with Presence (km^2)	Total Flux Corrected Count
Large Albatrosses	Wandering Albatross (*Diomedea exulans*)	1	1
	Chatham Albatross (*Thalassarche eremita*)	1	1
	Short-tailed Albatross (*Phoebastria albatrus*)	1	1
Fulmars	Parkinson's Petrel (*Procellaria parkinsoni*)	2	2
Large Gadfly Petrels	Murphy's Petrel *(Pterodroma ultima)*	28	28
	Hawaiian Petrel *(Pterodroma sandwichensis)*	15	15
	Juan Fernandez Petrel *(Pterodroma externa)*	10	12
	White-necked Petrel *(Pterodroma cervicalis)*	4	6
	Tahiti Petrel *(Pseudobulweria rostrata)*	2	2
	Kermadec Petrel *(Pterodroma neglecta)*	1	1
	Phoenix Petrel *(Pterodroma alba)*	1	1
Small Gadfly Petrels	Cook's Petrel *(Pterodroma cooki)*	117	193
	Mottled Petrel *(Pterodroma inexpectata)*	54	61
	Bulwer's Petrel *(Bulweria bulwerii)*	11	13
	Black-winged Petrel *(Pterodroma nigripennis)*	11	11
	Collared Petrel *(Pterodroma brevipes)*	1	1
	Stejneger's Petrel *(Pterodroma longirostris)*	1	1
Surface-Feeding Shearwaters	Wedge-tailed Shearwater *(Ardenna pacifica)*	79	159
	Flesh-footed Shearwater *(Puffinus carneipes)*	23	23
	Streaked Shearwater *(Calonectris leucomelas)*	2	23
Small Diving Shearwaters	Manx Shearwater *(Puffinus puffinus)*	20	23
	Christmas Shearwater *(Puffinus navitatus)*	4	4
	Newell's Shearwater *(Puffinus newelli)*	1	1
Storm-Petrels	Black Storm-Petrel *(Hydrobates melania)*	93	155
	Least Storm-Petrel *(Hydrobates microsoma)*	18	130
	Band-rumped Storm-Petrel *(Hydrobates castro)*	1	1
Oceanites	Wilson's Storm-Petrel *(Oceanites oceanicus)*	2	2
Tropicbirds	Tropicbirds *(Phaethon* spp.)	54	62
Pelicans	American White Pelican *(Pelecanus erythrorhynchos)*	3	76
Boobies	Brown Booby *(Sula leucogaster)*	13	30
	Masked Booby *(Sula dactylatra)*	7	8
	Red-footed Booby *(Sula sula)*	7	41
Large Gulls	Thayer's Gull *(Larus glaucoides thayeri)*	41	41

Flight-Style Grouping	Common and Latin Name	Effort with Presence (km²)	Total Flux Corrected Count
	Glaucous Gull *(Larus hyperboreus)*	10	12
Medium Gulls	Ring-billed Gull *(Larus delawarensis)*	17	19
	Red-legged Kittiwake *(Rissa brevirostris)*	1	1
Terns	Forster's Tern *(Sterna forsteri)*	98	342
	Common Tern *(Sterna hirundo)*	61	213
	Royal Tern *(Thalasseus maximus)*	45	65
	Sooty Tern *(Onychoprion fuscatus)*	27	100
	White Tern *(Gygis alba)*	7	18
	Brown Noddy *(Anous stolidus)*	6	25
	Noddy spp. (*Anous* spp.)	2	7
	Least Tern *(Sternula antillarum)*	1	1
Large Alcids	Horned Puffin *(Fraterula corniculata)*	28	40
Medium Alcids	Parakeet Auklet *(Aethia psittacula)*	26	29
Small Alcids	Ancient Murrelet *(Synthliboramphus antiquum)*	86	302
	Kittlitz's Murrelet *(Brachyramphus brevirostris)*	1	2
Loons, Grebes, Ducks	Eared Grebe *(Podiceps nigricollis)*	69	328
	Horned Grebe *(Podiceps auritus)*	21	33
	Red-necked Grebe *(Podiceps grisegena)*	3	6
	Yellow-billed Loon *(Gavia adamsii)*	2	2
	White-winged Scoter *(Melanitta deglandi)*	67	280
	Black Brandt *(Branta bernicla)*	53	868
	Red-breasted Merganser *(Mergus serrator)*	9	9
	Black Scoter *(Melanitta americana)*	7	48
	Scaup spp. (*Aythya* spp.)	6	41
	Bufflehead (*Bucephala albeola)*	3	5
	Long-tailed Duck *(Clangula hyemalis)*	3	7
	Common Merganser *(Mergus merganser)*	2	10
	Canada Goose *(Branta canadensis)*	1	1
	Snow Goose *(Anser caerulescens)*	1	1
	Northern Pintail *(Anas acuta)*	1	20
Frigatebirds	Magnificent Frigatebird *(Fregata magnificens)*	1	1

Table A-4. Logistic Regression Parameters Defining Probability of Flying At Least 10 Meters Above the Sea Surface as a Function of Wind Speed for Each Seabird Flight-Style Group

Flight-Style Group	Species Included in Logistic Regression	Observations by Flight-Style Grouping (#)	Intercept (Log Odds When Wind Speed is Zero)	Coefficient for Wind Speed Parameter
Small Albatrosses	Laysan and Black-footed Albatrosses	2,085	-3.87	0.130
Fulmars	Northern Fulmars	2,757	-5.04	0.091
Surface-feeding Shearwaters	Buller's and Pink-footed Shearwaters	2,409	-4.23	0.126
Larger Diving Shearwaters	Sooty and Short-tailed Shearwaters	15,840	-5.16	0.269
Smaller Diving Shearwaters	Black-vented Shearwaters	156	-6.74	0.093
Storm-Petrels	Ashy, Fork-tailed, Leach's and Black Storm-Petrels	10,586	-8.62	0.066
Pelicans	Brown Pelicans	490	-1.65	0.079
Phalaropes	Unidentified Phalaropes	2,596	-4.60	0.025
Skuas	South Polar Skua and Unidentified Jaegers	1,054	-1.43	0.018
Large Gulls	California, Western, Herring, and Glaucous-winged Gulls	10,487	-0.66	0.010
Medium Gulls	Black-legged Kittiwakes	1,177	-0.48	-0.005
Small Gulls	Bonaparte's and Sabine's Gulls	597	-1.02	-0.039
Terns	Arctic Terns	323	-0.05	-0.040
Cormorants	Double-crested, Pelagic, and Brandt's Cormorants	1,527	-3.87	0.023
Large Alcids	Common Murre, Tufted Puffin	5,783	-6.21	0.186
Medium Alcids	Rhinoceros Auklets, Pigeon Guillemots	3,303	-7.61	0.095
Small Alcids	Cassin's Auklets, Unidentified Murrelets	5,783	-7.78	0.087
Loons, Grebes, Ducks	Common and Red-throated Loons, Western Grebes	465	-3.00	0.084

Notes: This table offers detailed information about the species contributing to each Flight-style Group, along with the total number of observations in each group. These observations support a mixed-effects logistic regression aimed at quantifying probability curves that link the windscape to the likelihood of flying above 10 m above sea level. The provided intercept corresponds to the predicted probability and log odds of a given flight group exceeding 10 m above sea level when wind speeds are zero meters per second. In this model, wind speed serves to indicate the rate of change by which the log odds of a flight group exceeding 10 m varies with wind speed. Positive coefficients for wind speed suggest an increased probability of a flight group exceeding 10 m as wind speeds increase.

Appendix A References

Adams, J., J. J. Felis, J. W. Mason, and J. Y. Takekawa. 2014. Pacific Continental Shelf Environmental Assessment (PaCSEA): Aerial Seabird and Marine Mammal Surveys Off Northern California, Oregon, and Washington, 2011-2012. March. OCS Study BOEM 2014-003. Santa Cruz and Vallejo, California. Prepared for U.S. Department of the Interior, Bureau of Ocean Energy Management. Prepared by U.S. Department of the Interior, U.S. Geological Survey, Western Ecological Research Center.

Adams, J., J. J. Felis, J. W. Mason, and J. Y. Takekawa. 2016. Pacific Continental Shelf Environmental Assessment (PaCSEA) GIS Resource Database: aerial Seabird and Marine Mammal Surveys Off Northern California, Oregon, and Washington, 2011-2012. GIS Resource Database: U.S. Geological Survey, <https://www.sciencebase.gov/catalog/item/54d54b8ce4b0f7b2dc9f2ecc>.

Appler, J., J. Barlow, and S. Rankin. 2004. Marine Mammal Data Collected during the Oregon, California and Washington Line-Transect Expeditions (ORCAWALE) Conducted Aboard the NOAA Ships McArthur and David Starr Jordan, July-December 2001. March. NOAA-TM-NMFS-SWFSC-359. La Jolla, California. Prepared for U.S. Department of Commerce, National Oceanic and Atmospheric Administration, National Marine Fisheries Service, Southwest Fisheries Science Center.

Ford, G. R., S. Terrill, J. Casey, D. Shearwater, S. R. Schneider, S. R. Ballance, L. Terrill, et al. 2021. Distribution patterns and population size of the Ashy Storm Petrel *Oceanodroma homochroa*. Marine Ornithology 49(2):193-204.

Halpin, P. N., A. J. Read, E. Fujioka, B. D. Best, B. Donnelly, L. J. Hazen, C. Kot et al. 2009. OBIS-SEAMAP: The world data center for marine mammal, sea bird, and sea turtle distributions. Oceanography 22(2):104-115.

Philbrick, V. A., P. C. Fielder, L. T. Ballance, and D. A. Demer. 2003. Report of Ecosystems Conducted during the 2001 Oregon, California, and Washington (ORCAWALE) Marine Mammal Survey on the Research Vessels David Starr Jordan and McArthur. January. NOAA-TM-NMFS-SWFSC-349. Prepared By U.S. Department of Commerce, National Oceanic and Atmospheric Administration, National Marine Fisheries Services, Southwest Fisheries Science Center.

Sakuma, K. M., S. Ralston, and V. G. Wespestad. 2006. Interannual and spatial variation in the distribution of young-of-the-year rockfish (Sebastes spp.): Expanding and coordinating a survey sampling frame. California Cooperative Oceanic Fisheries Investigations Reports 56:127-139.

Santora, J. A., S. Ralston, and W. J. Sydeman. 2011. Spatial organization of krill and seabirds in the central California Current. ICES Journal of Marine Science 68(7):1391-1402.

Santora, J. A., J. C. Field, I. Schroeder, K. M. Sakuma, B. K. Wells, and W. J. Sydeman. 2012. Spatial ecology of krill, micronekton and top predators in the central California Current: Implications for defining ecologically important areas. Progress in Oceanography 106:154-174.

Spear, L., D. G. Ainley, N. Nur, and S. N. G. Howell. 1995. Population size and factors affecting at-sea distributions of four endangered procellarids in the Tropical Pacific. The Condor 97(3):613-638.

U.S. National Science Foundation. 2024. Biological and Chemical Oceanography Data Management Office. Project: U.S. GLOBEC Northeast Pacific. <https://www.bco-dmo.org/project/2038>.

Wells, B. K., J. A. Santora, M. J. Henderson, P. Warzybok, J. Jahncke, R. W. Bradley, D. D. Huff et al. 2017. Environmental conditions and prey-switching by a seabird predator impact juvenile salmon survival. Journal of Marine Systems 174:54-73.

Appendix B. Annual Predictions for All Seabirds Included in the 3D Seabird Collision Vulnerability Framework

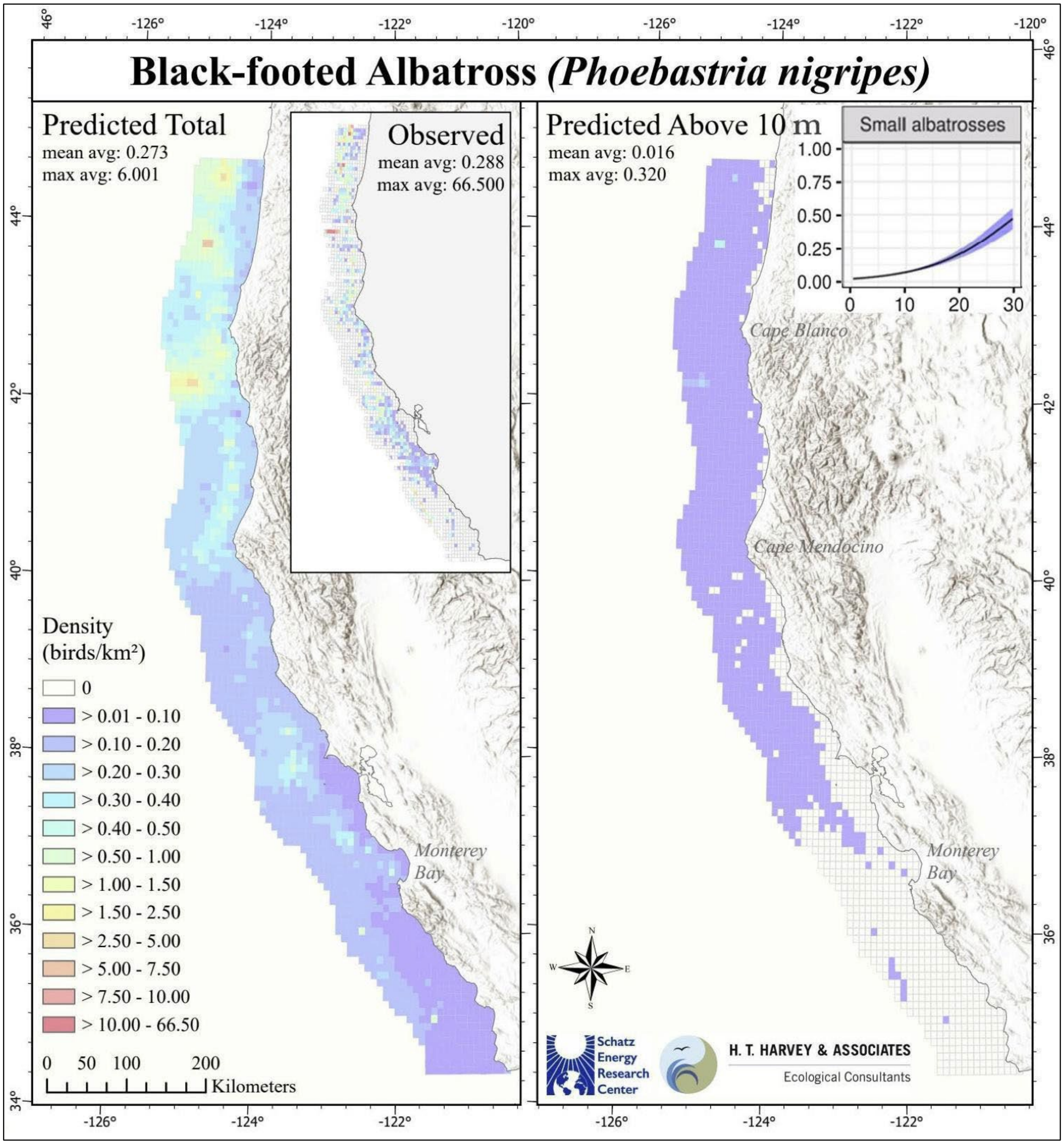

Figure B-1. Black-footed Albatross (*Phoebastria nigripes*)

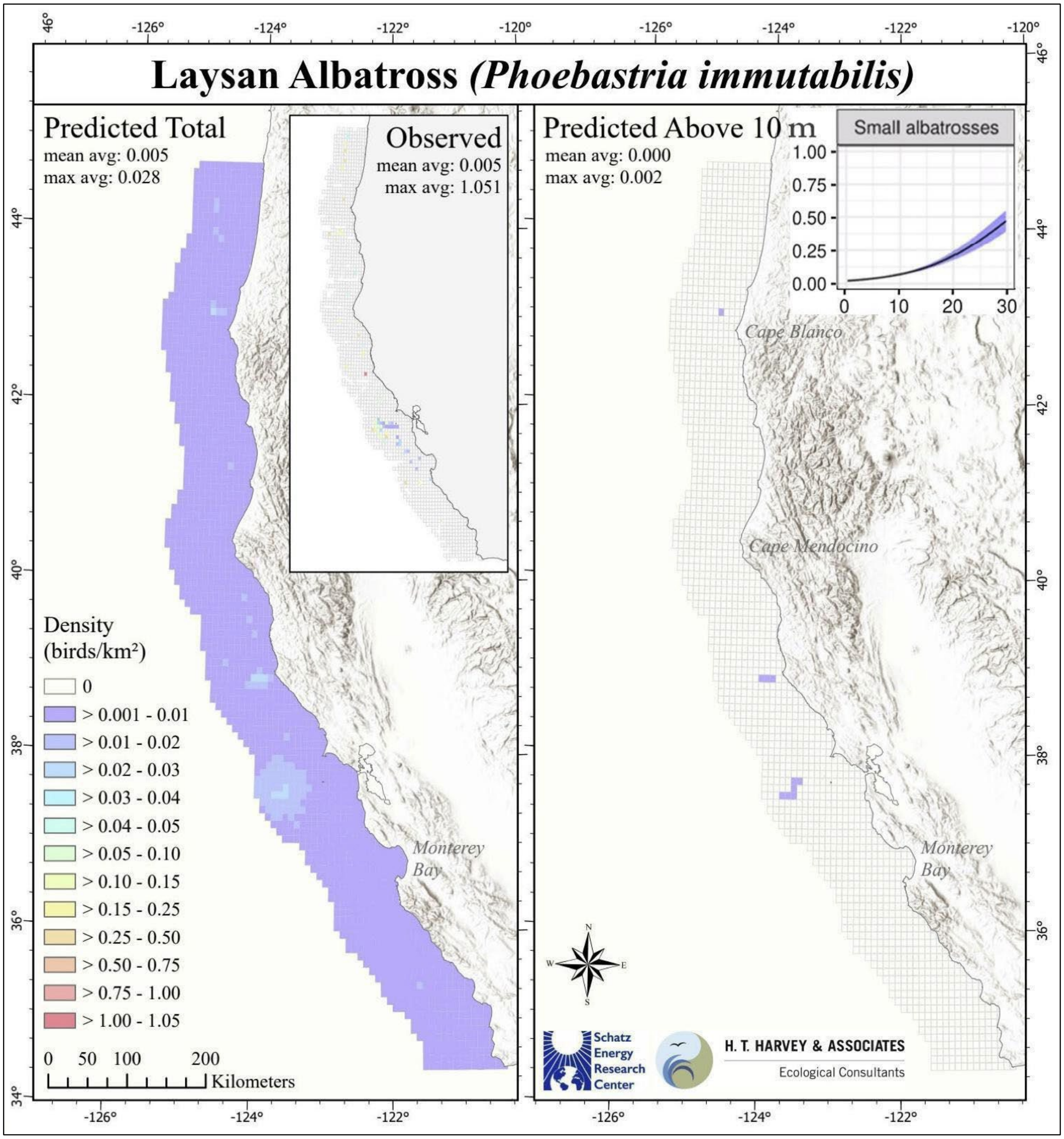

Figure B-2. Laysan Albatross (*Phoebastria immutabilis*)

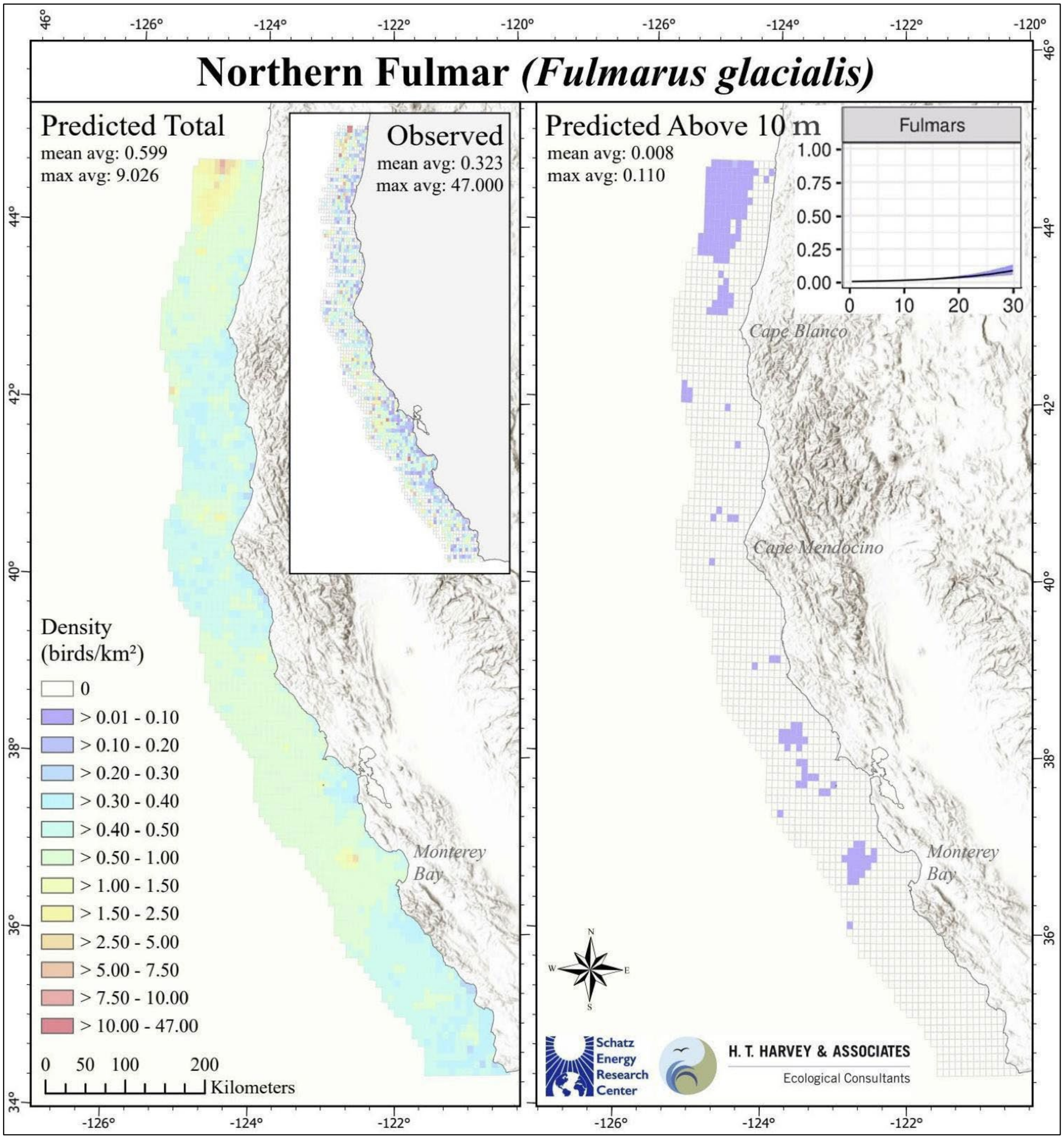

Figure B-3. Northern Fulmar (*Fulmarus glacialis*)

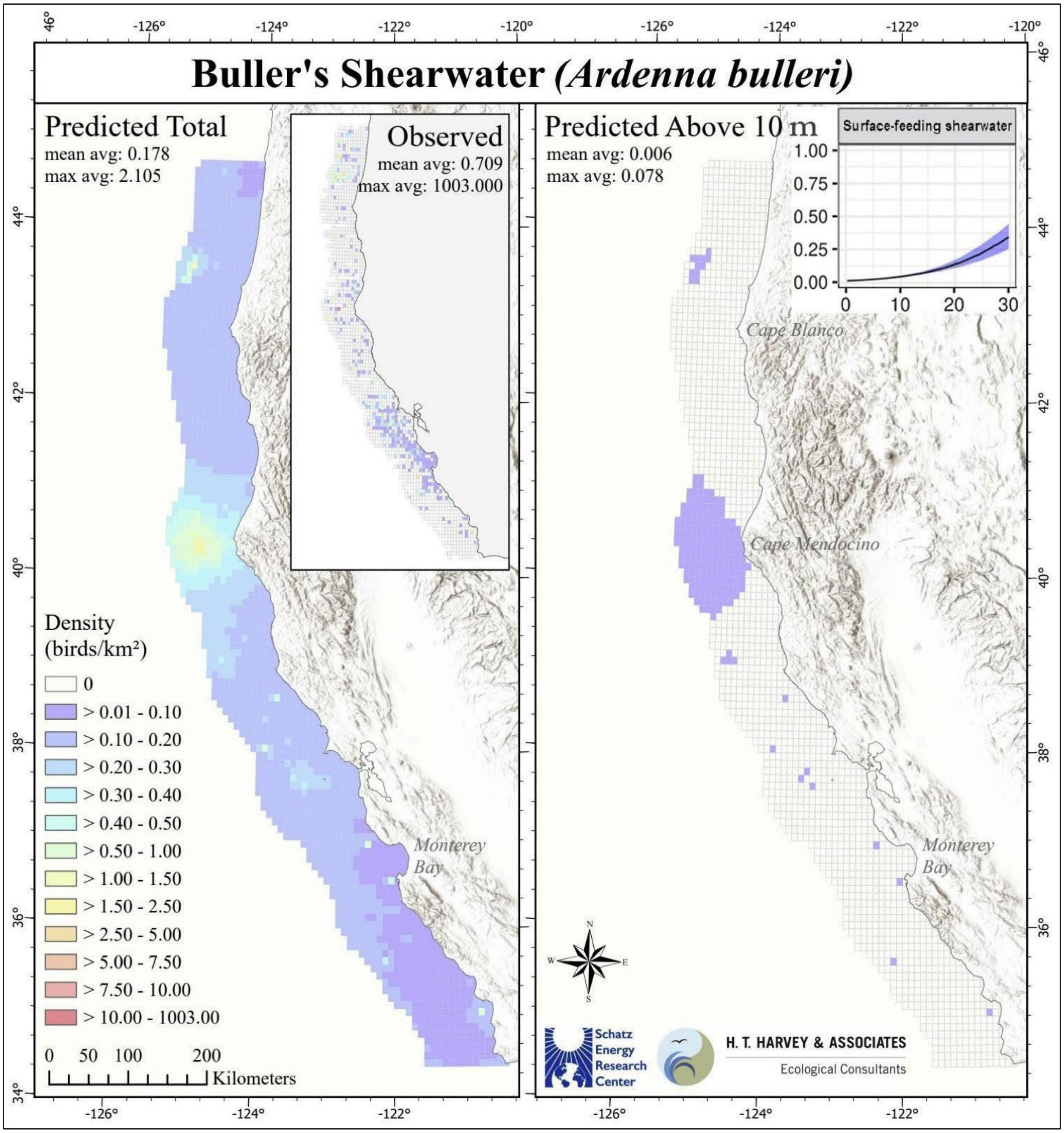

Figure B-4. Buller's Shearwater (*Ardenna bulleri*)

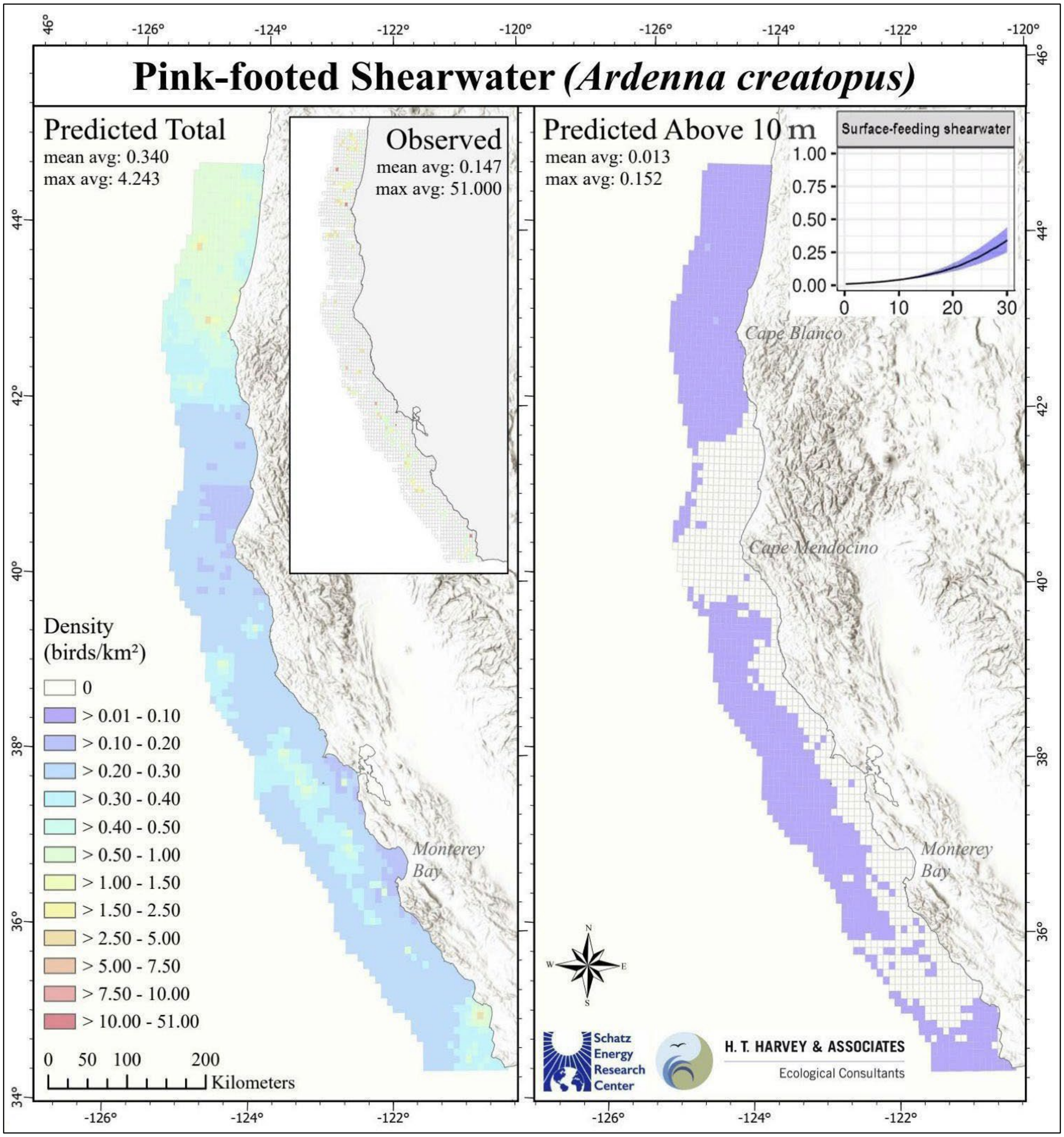

Figure B-5. Pink-footed Shearwater (*Ardenna creatopus*)

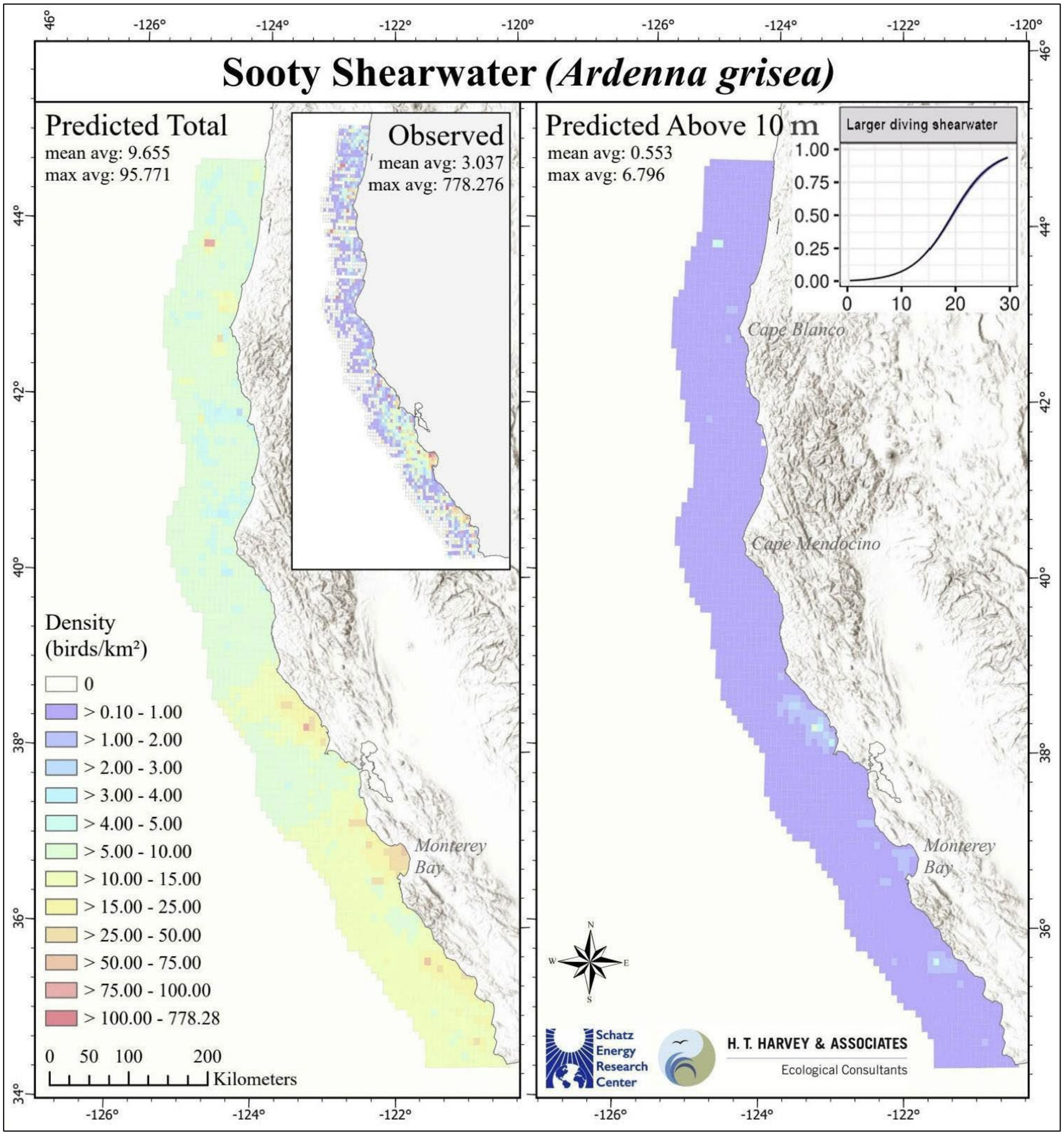

Figure B-6. Sooty Shearwater (*Ardenna grisea*)

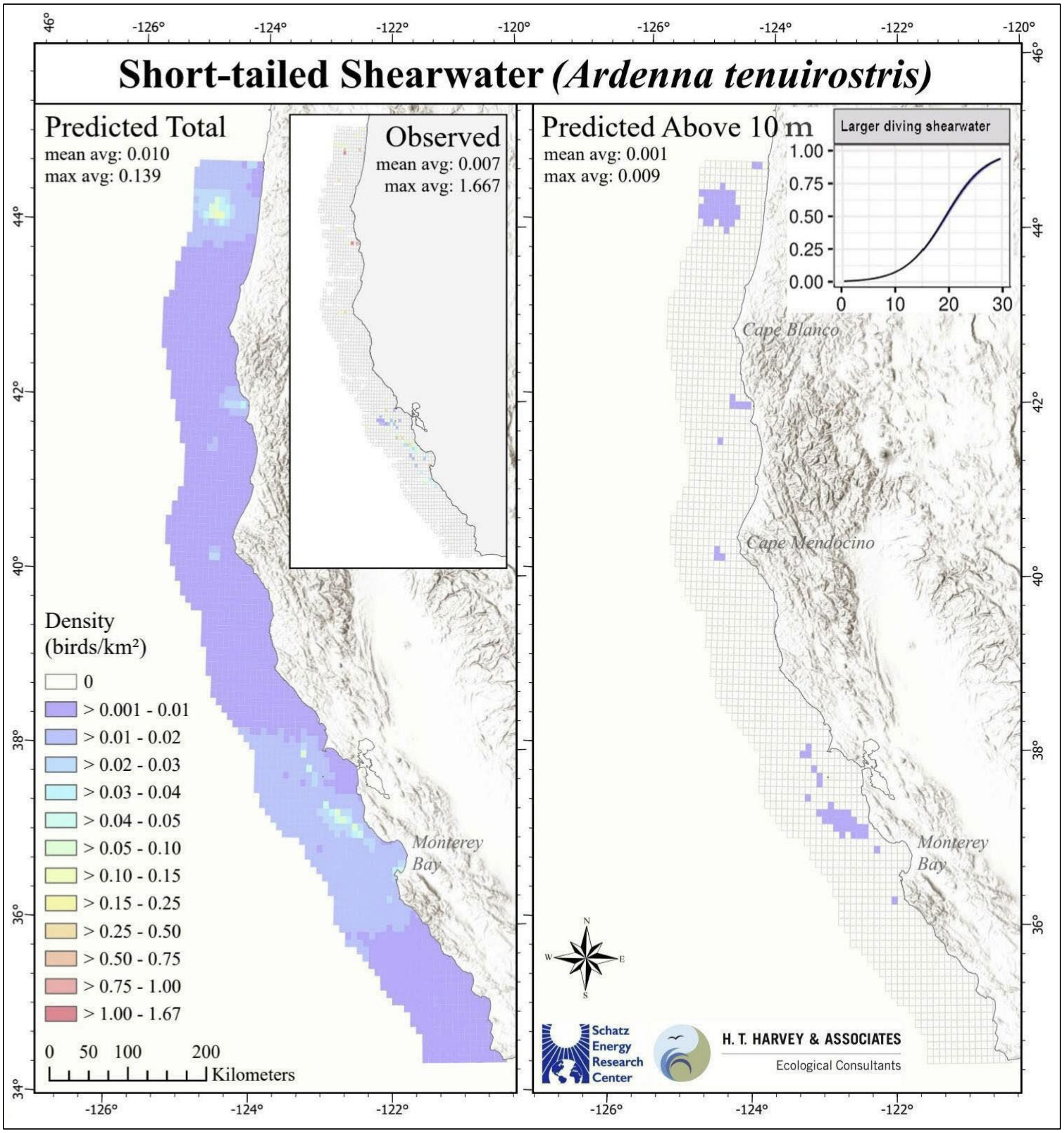

Figure B-7. Short-tailed Shearwater (*Ardenna tenuirostris*)

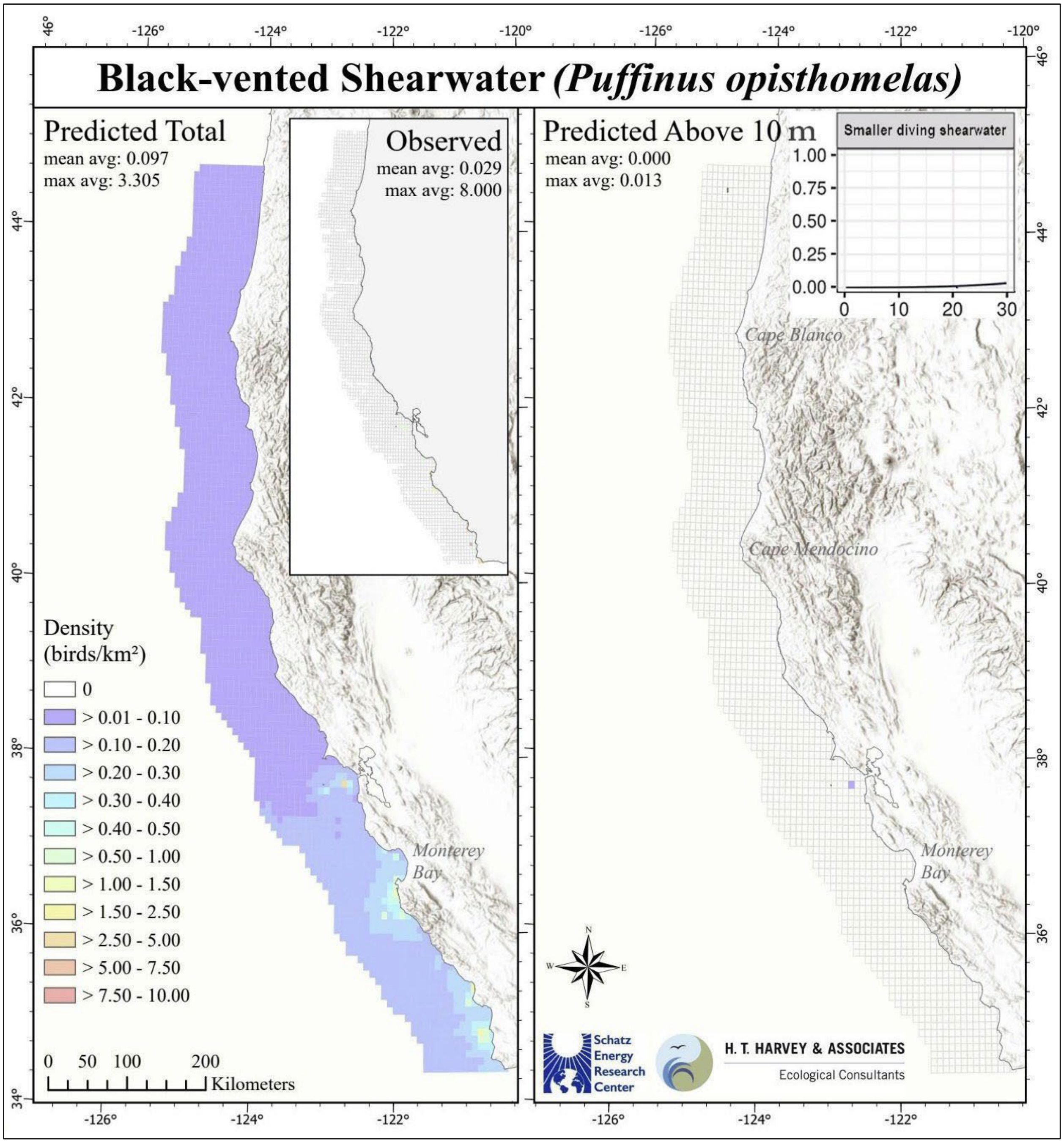

Figure B-8. Black-vented Shearwater (*Puffinus opisthomelas*)

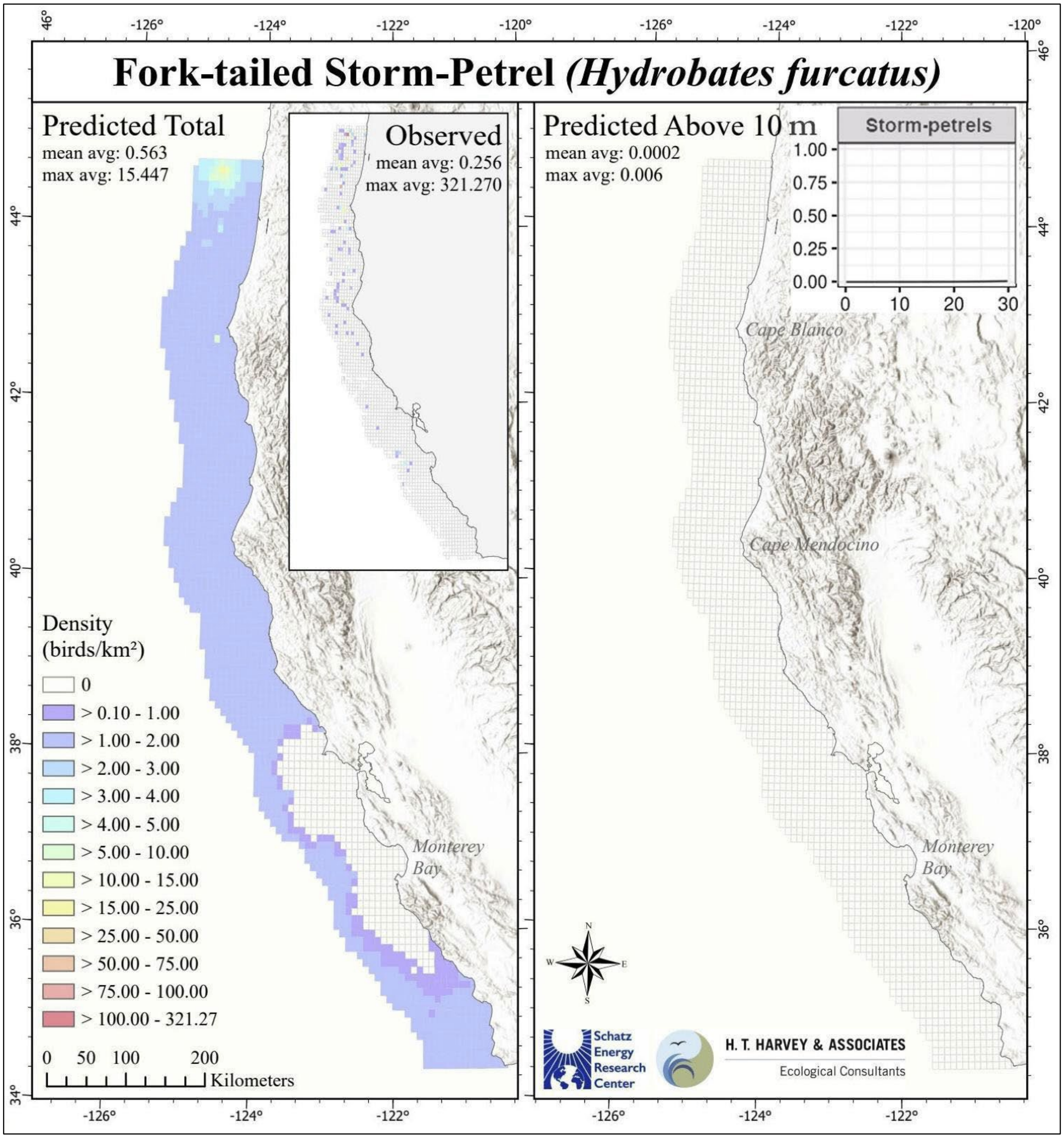

Figure B-9. Fork-tailed Storm-Petrel (*Hydrobates furcatus*)

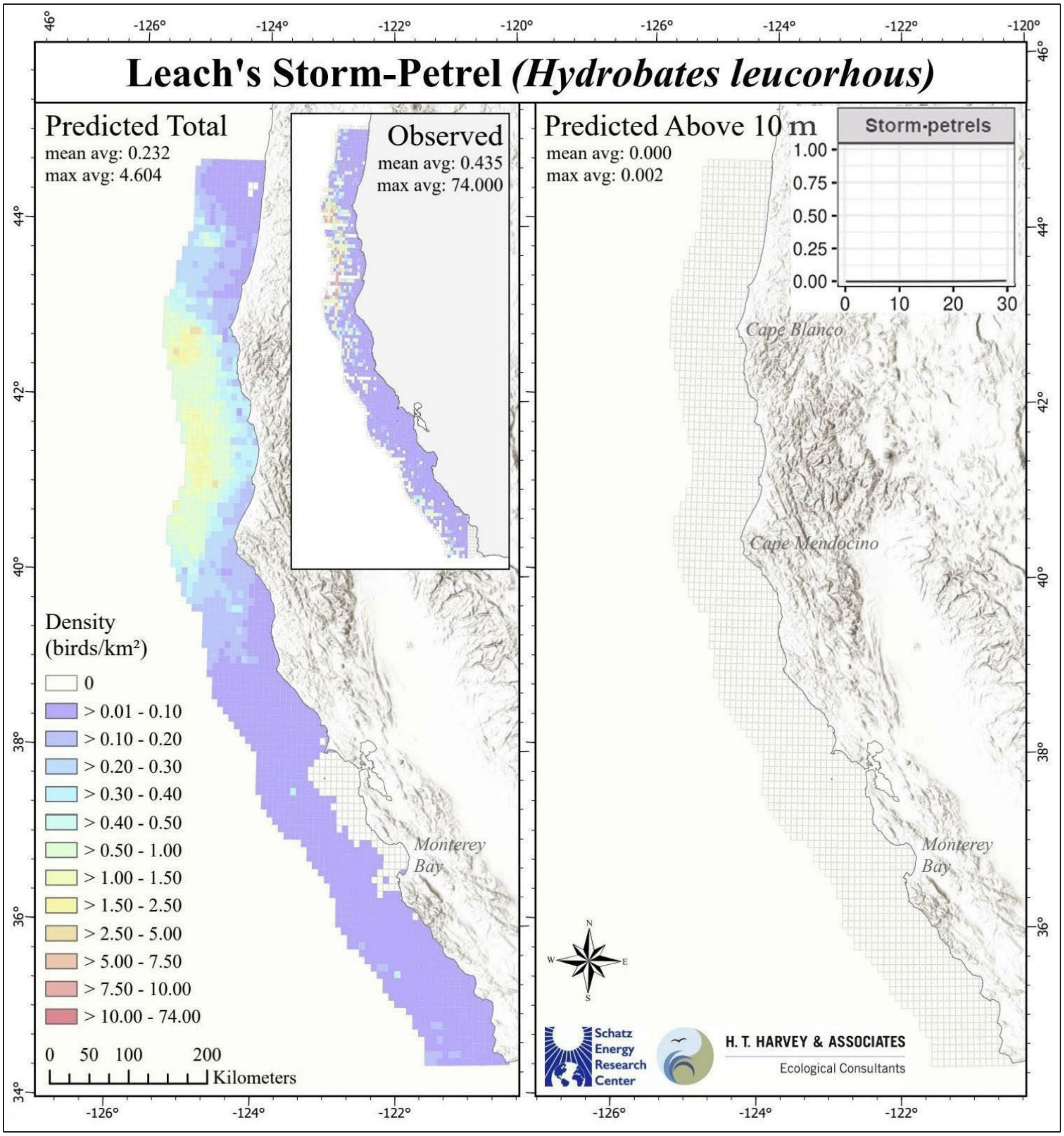

Figure B-10. Leach's Storm-Petrel (*Hydrobates leucorhous*)

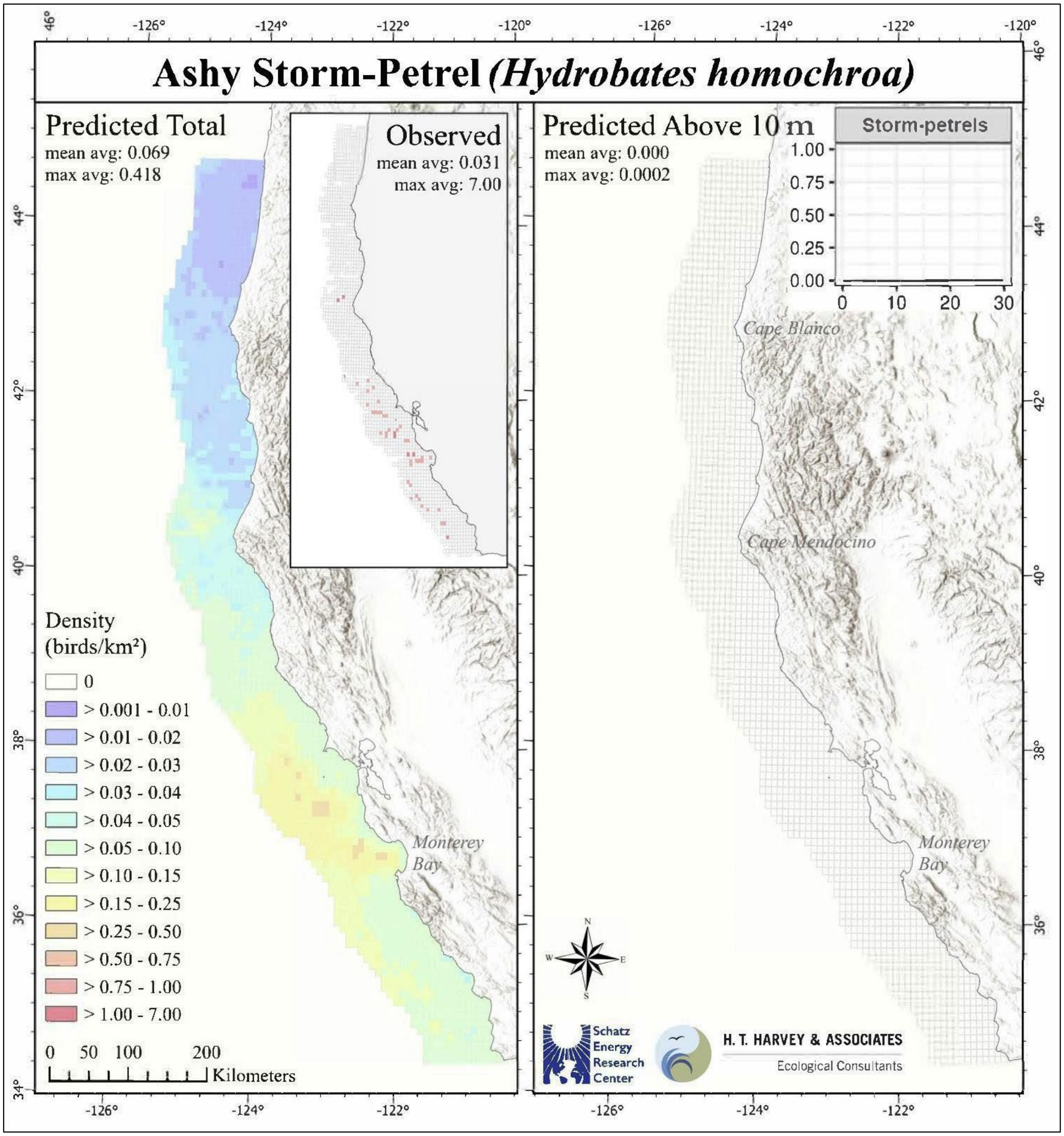

Figure B-11. Ashy Storm-Petrel (*Hydrobates homochroa*)

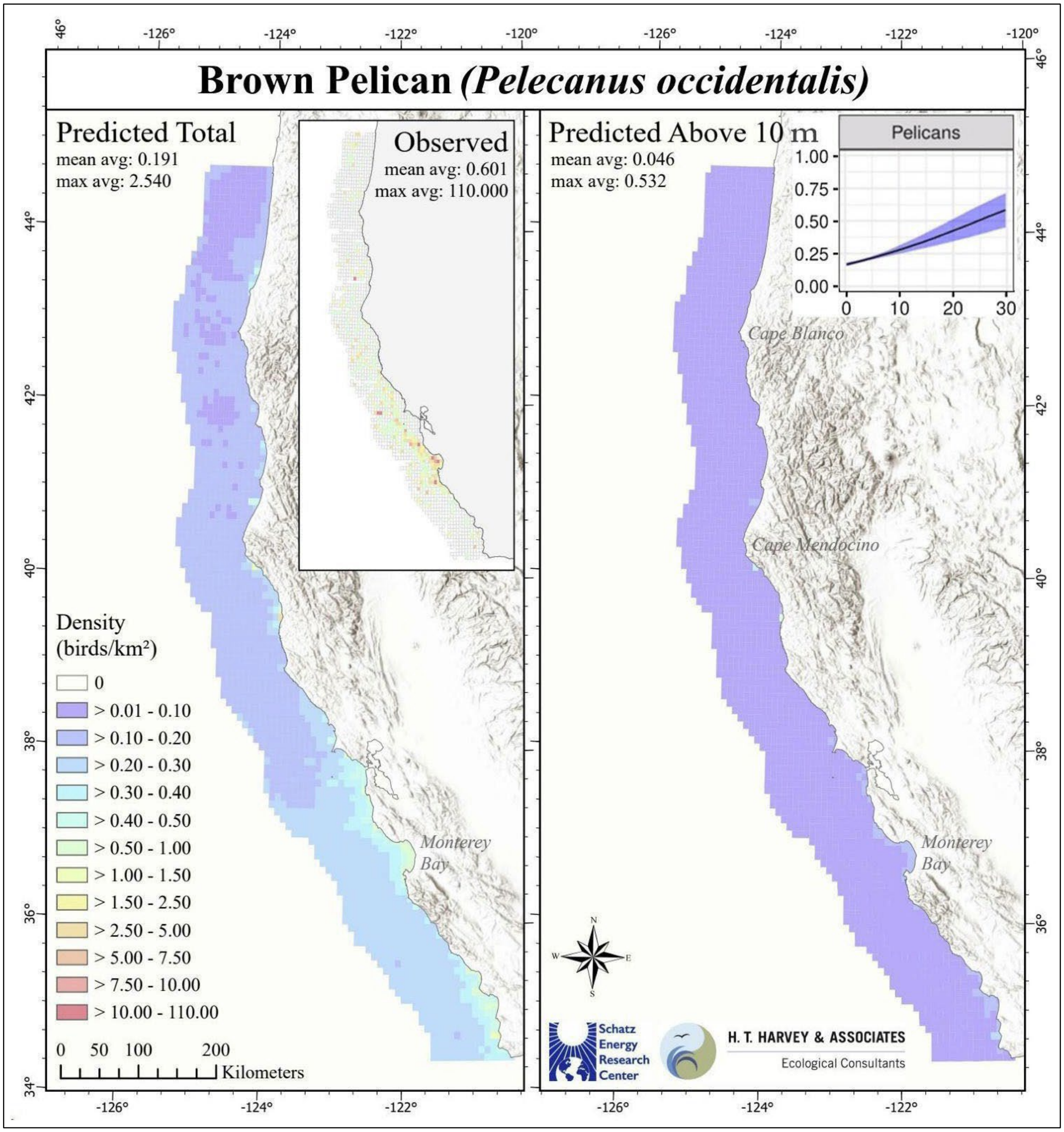

Figure B-12. Brown Pelican (*Pelecanus occidentalis*)

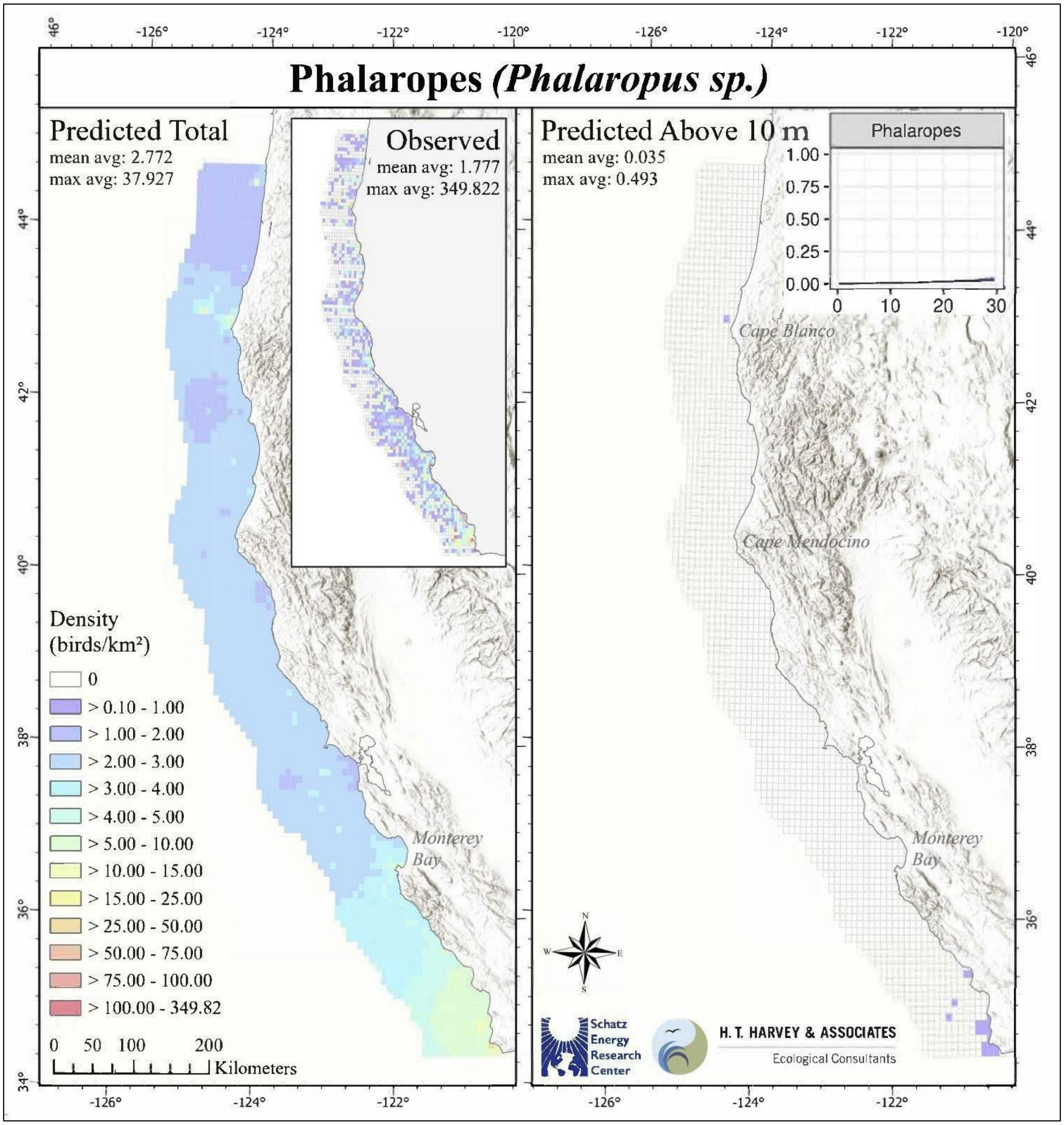

Figure B-13. Phalaropes (*Phalaropus* spp.)

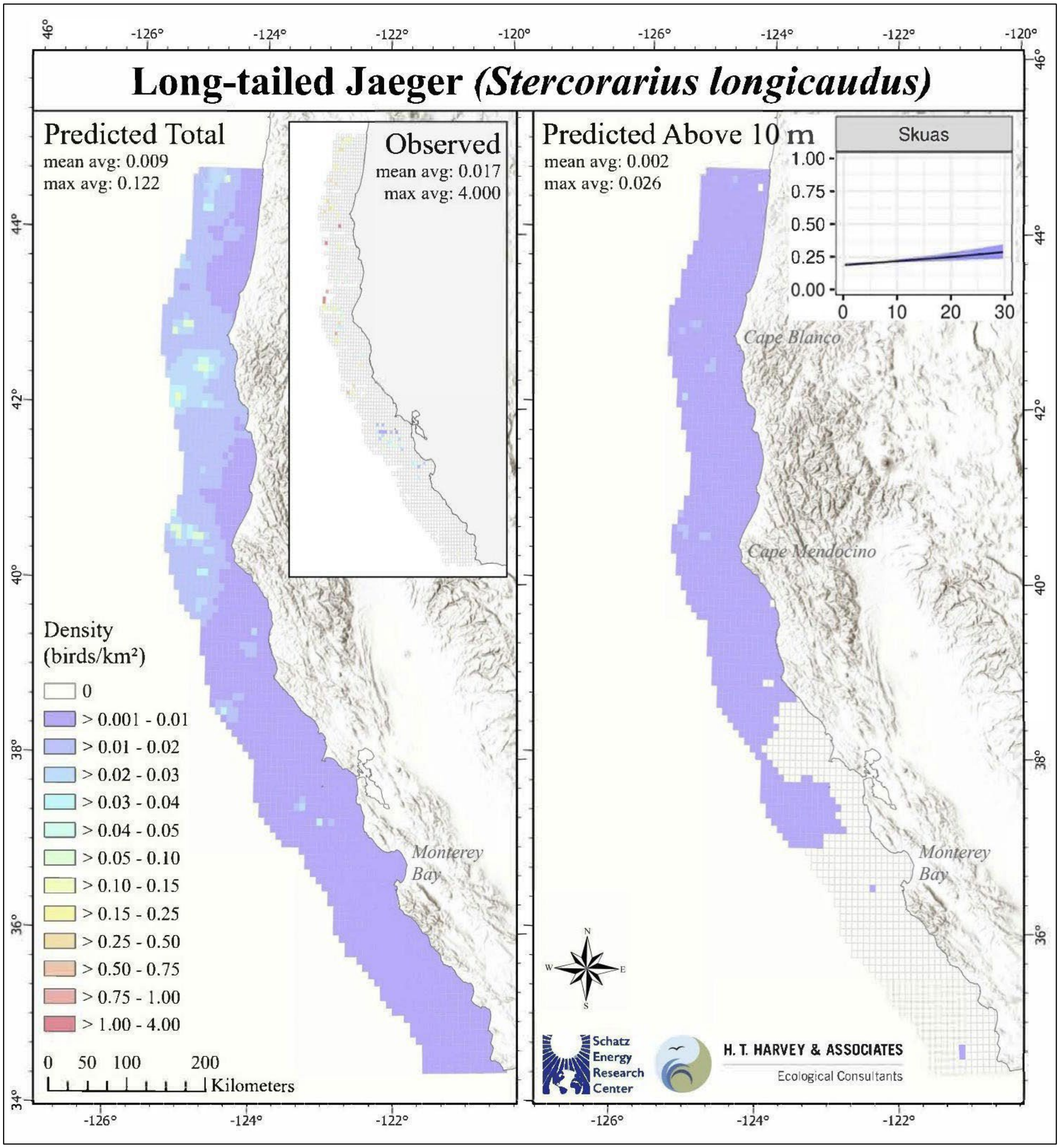

Figure B-14. Long-tailed Jaeger (*Stercorarius longicaudus*)

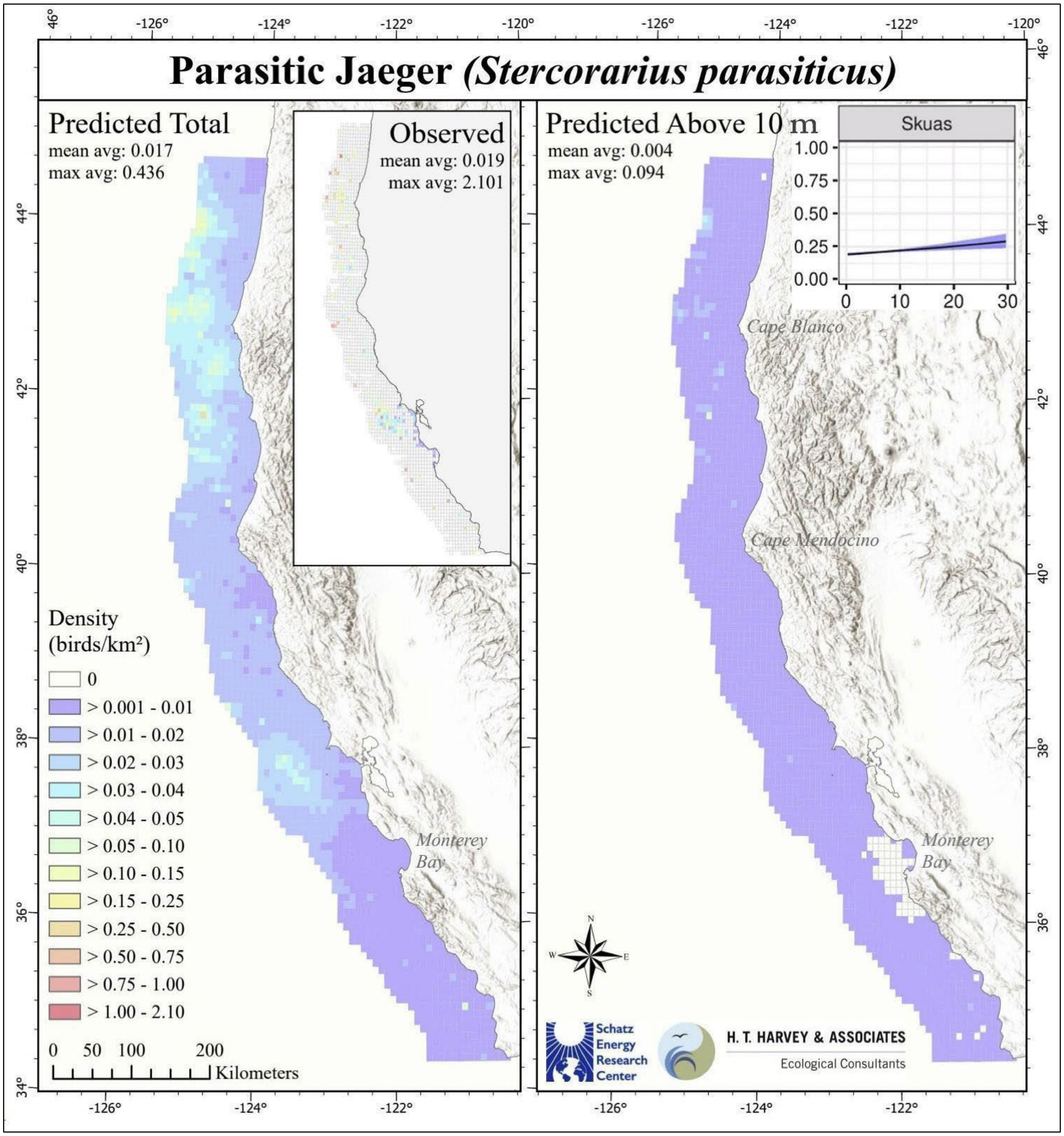

Figure B-15. Parasitic Jaeger (*Stercorarius parasiticus*)

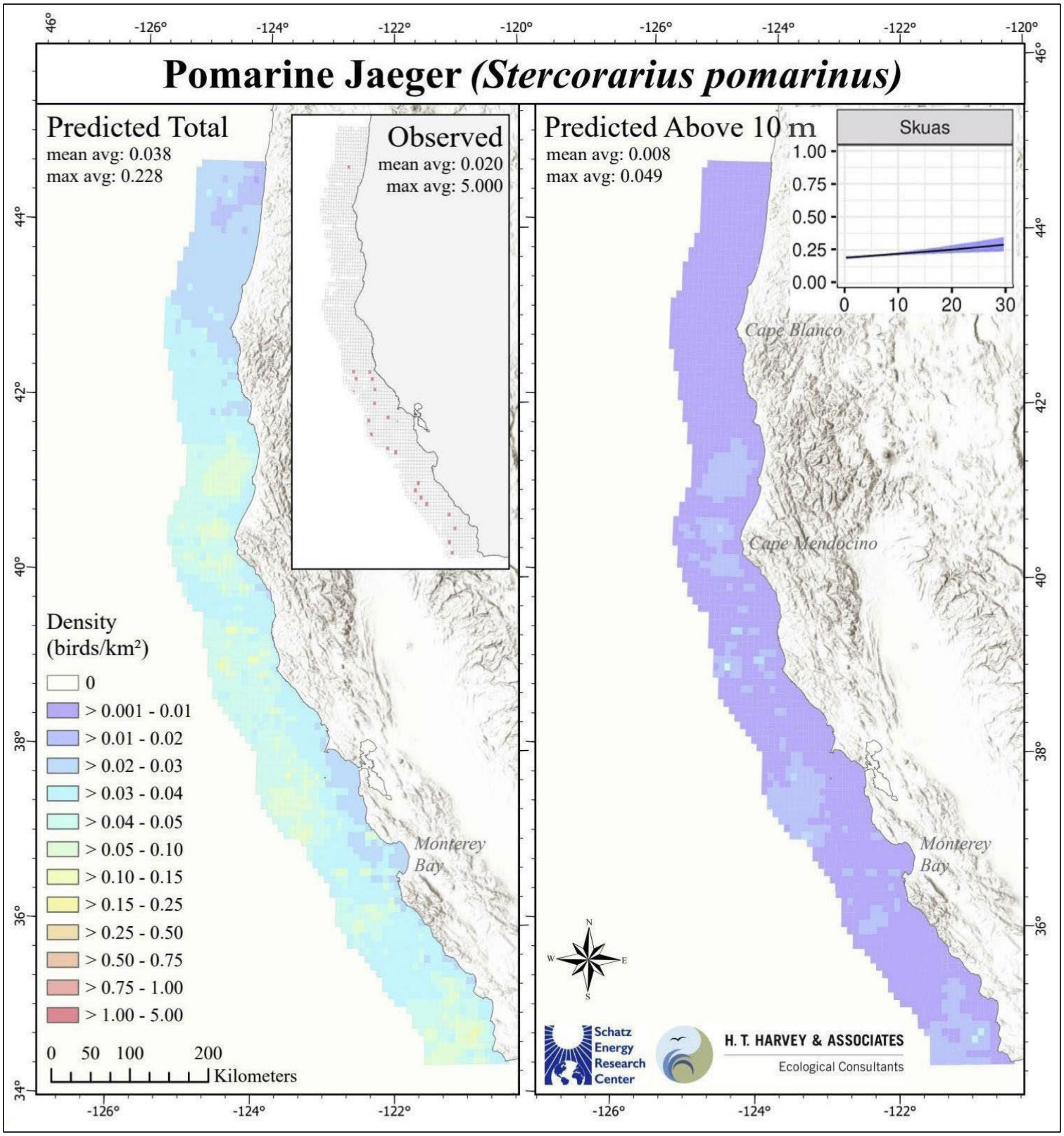

Figure B-16. Pomarine Jaeger (*Stercorarius pomarinus*)

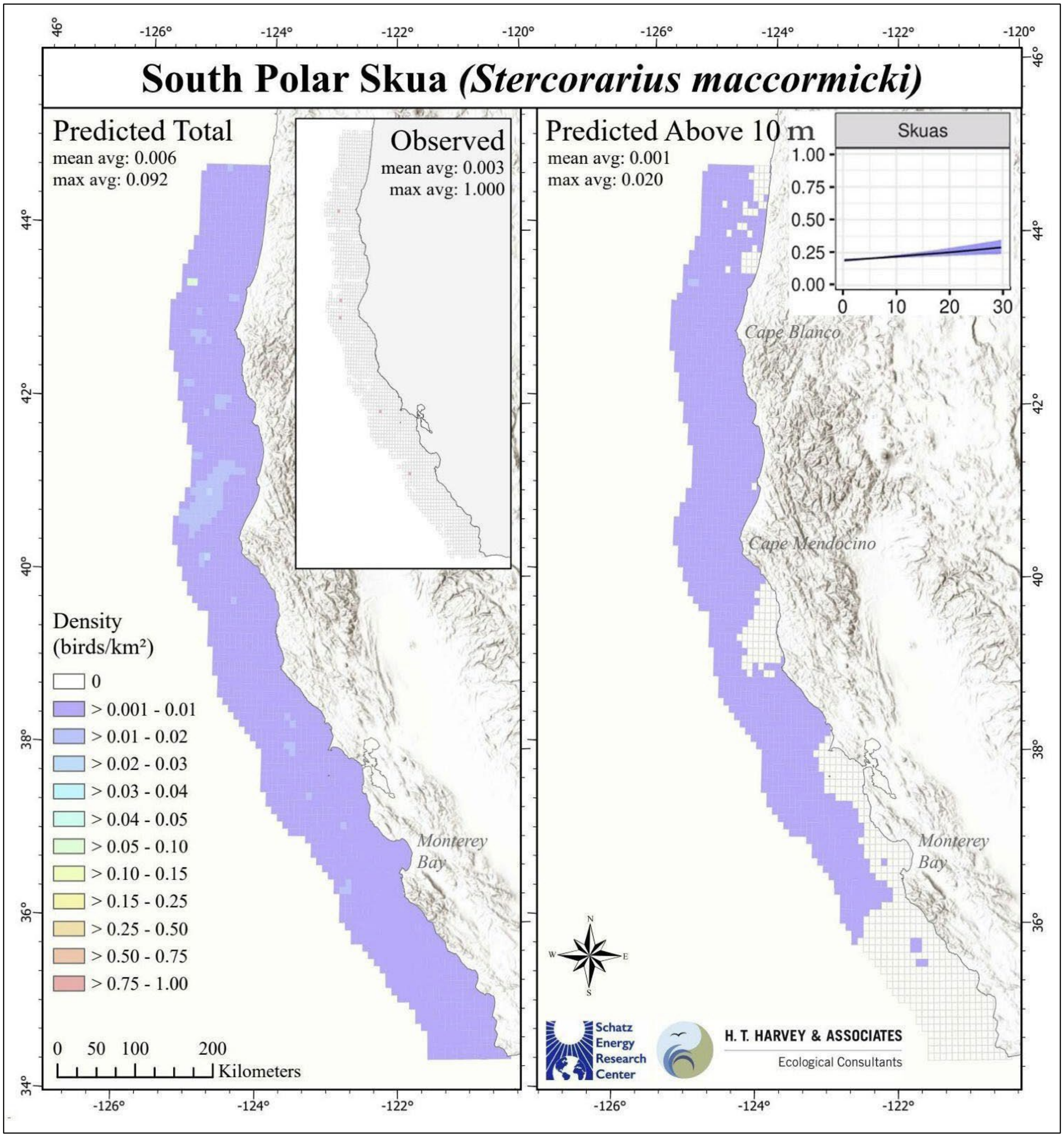

Figure B-17. South Polar Skua (*Stercorarius maccormicki*)

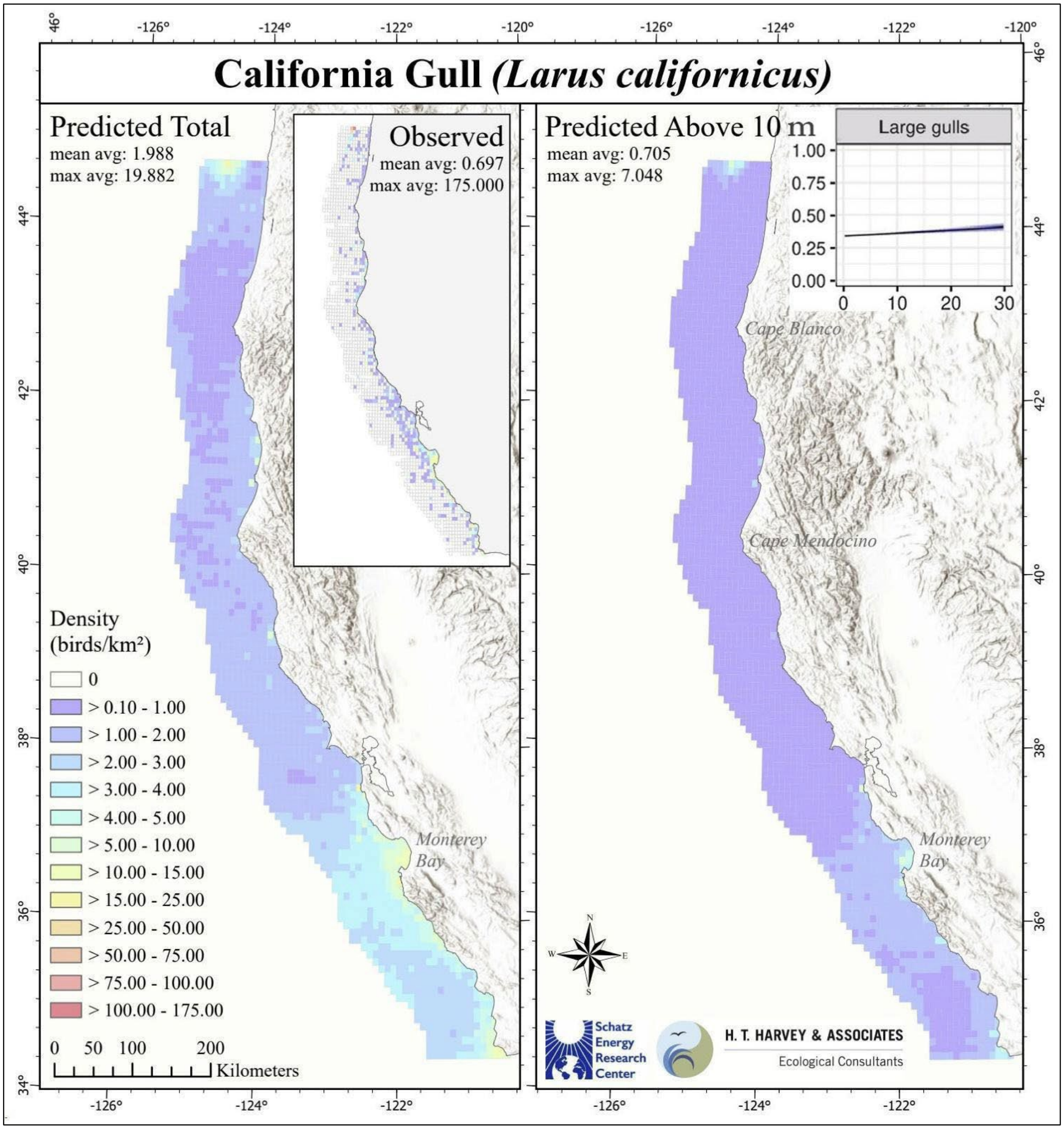

Figure B-18. California Gull (*Larus californicus*)

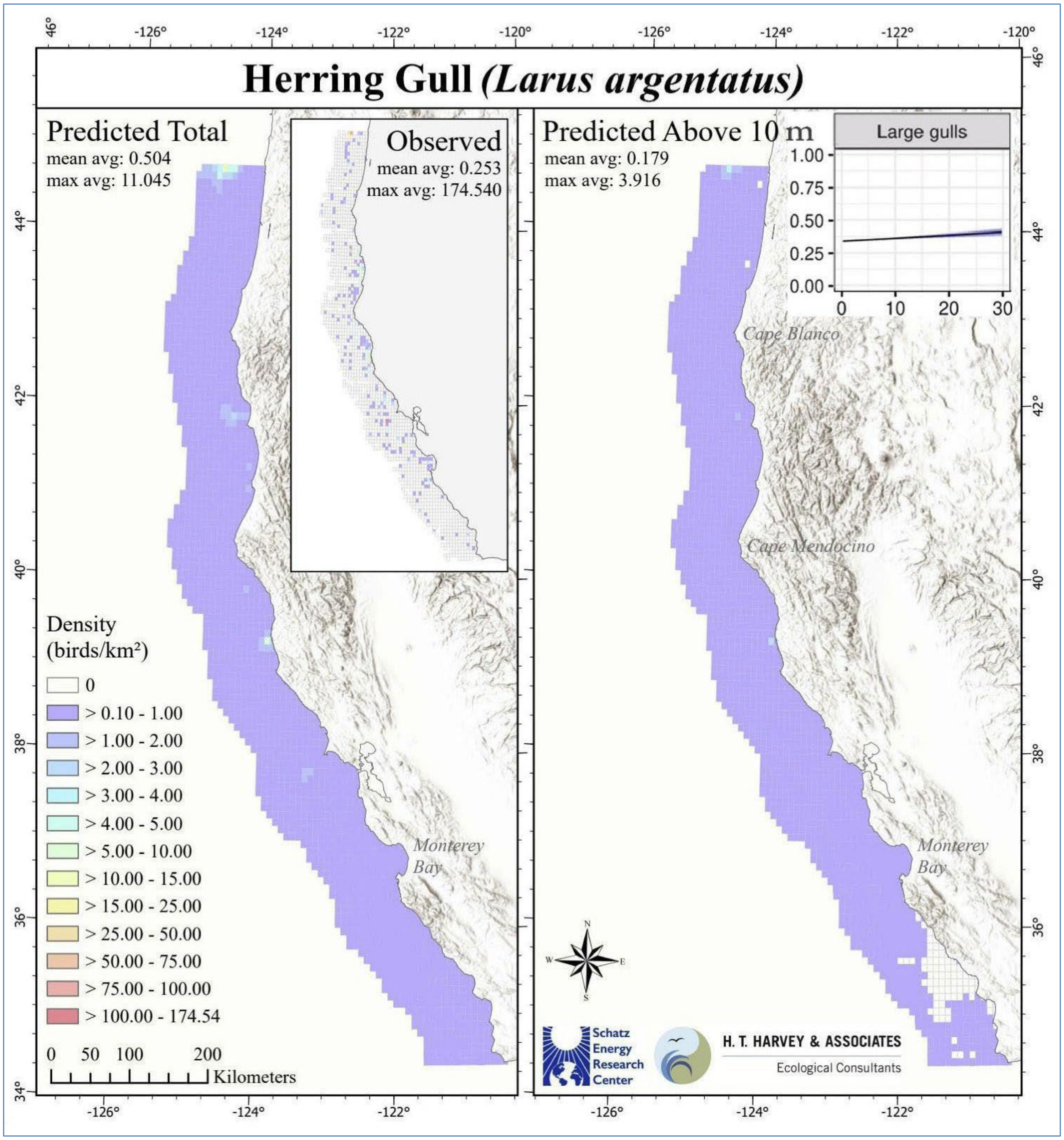

Figure B-19. Herring Gull (*Larus argentatus*)

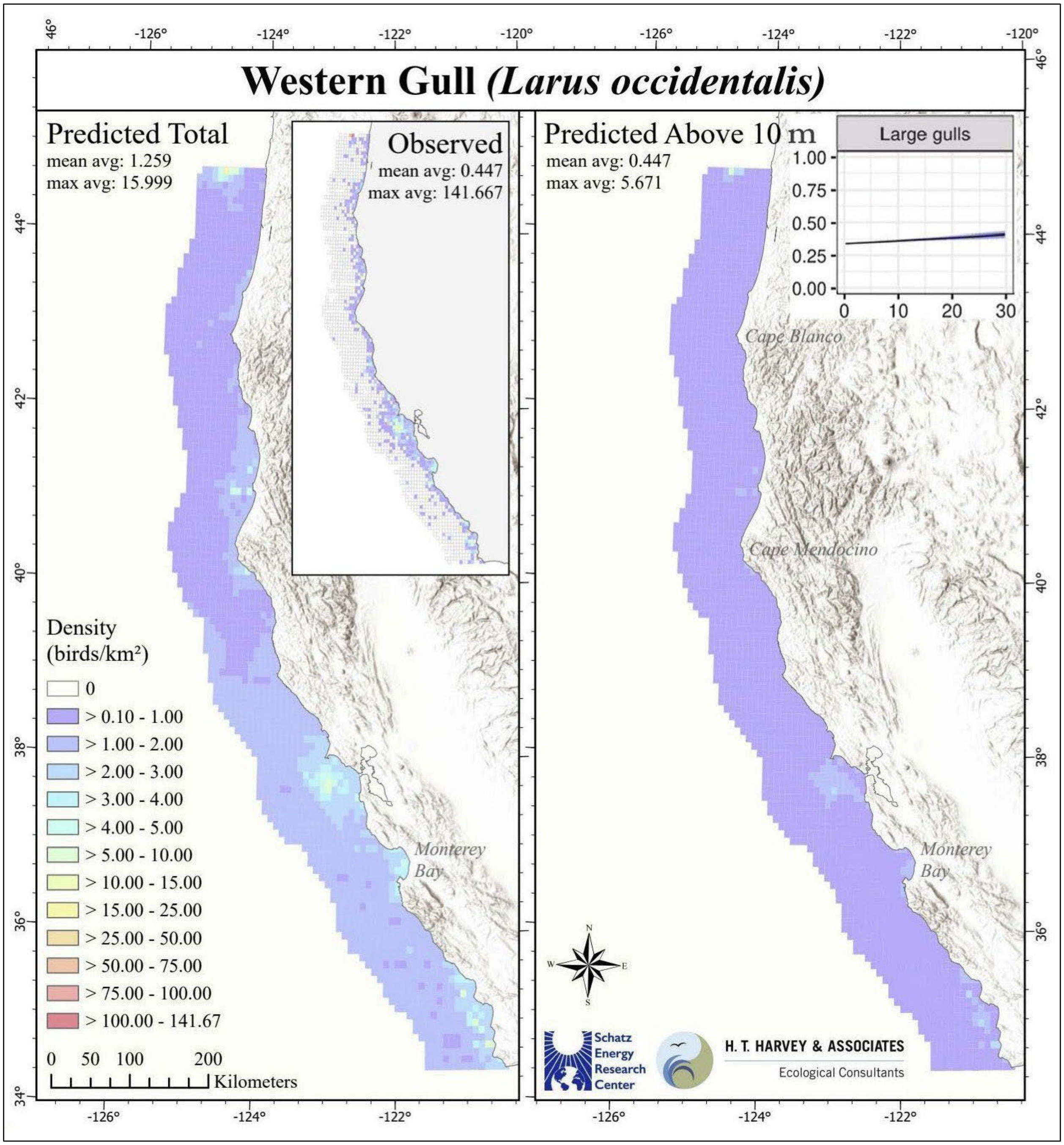

Figure B-20. Western Gull (*Larus occidentalis*)

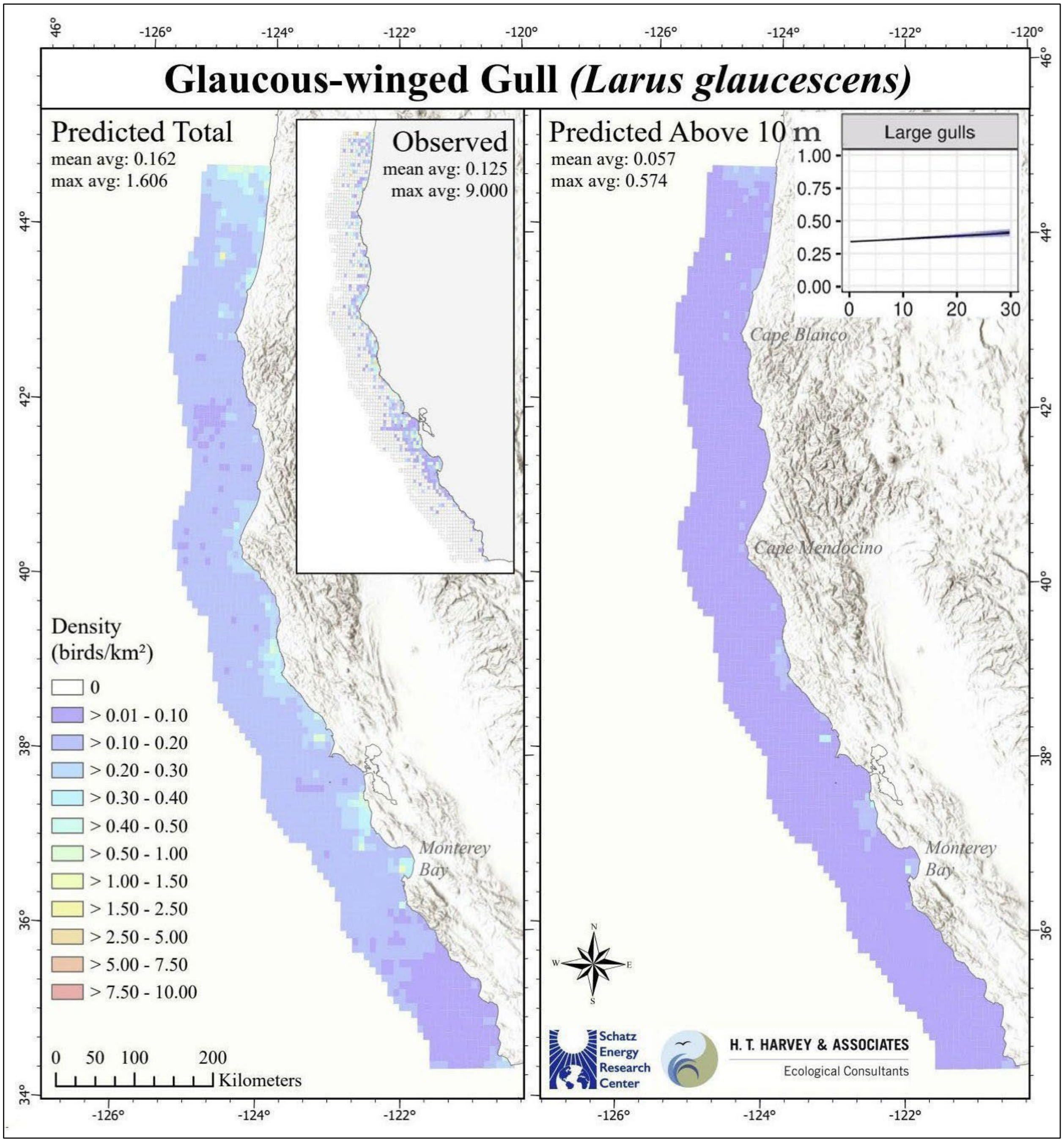

Figure B-21. Glaucous-winged Gull (*Larus glaucescens*)

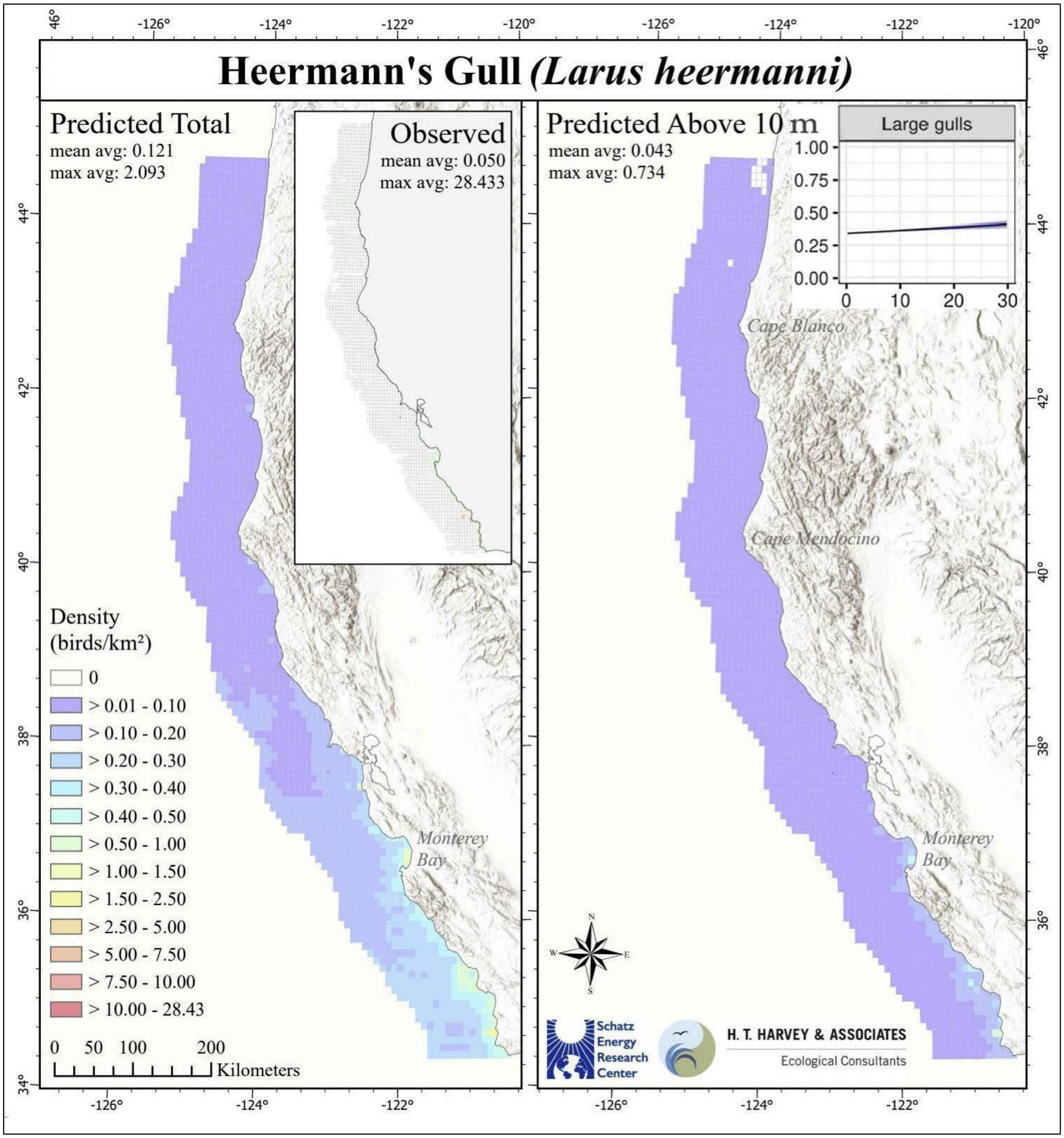

Figure B-22. Heermann's Gull (*Larus heermanni*)

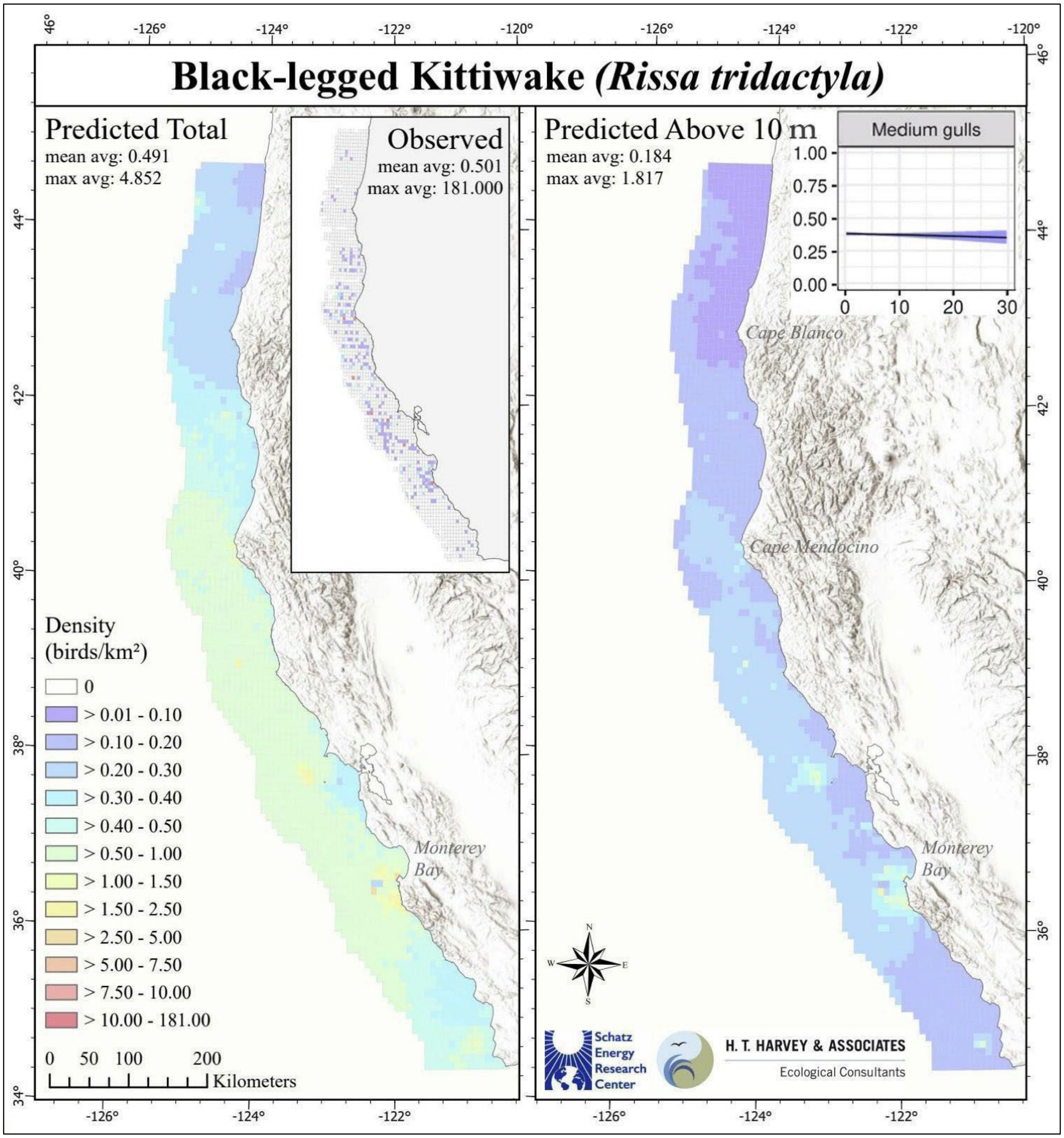

Figure B-23. Black-legged Kittiwake (*Rissa tridactyla*)

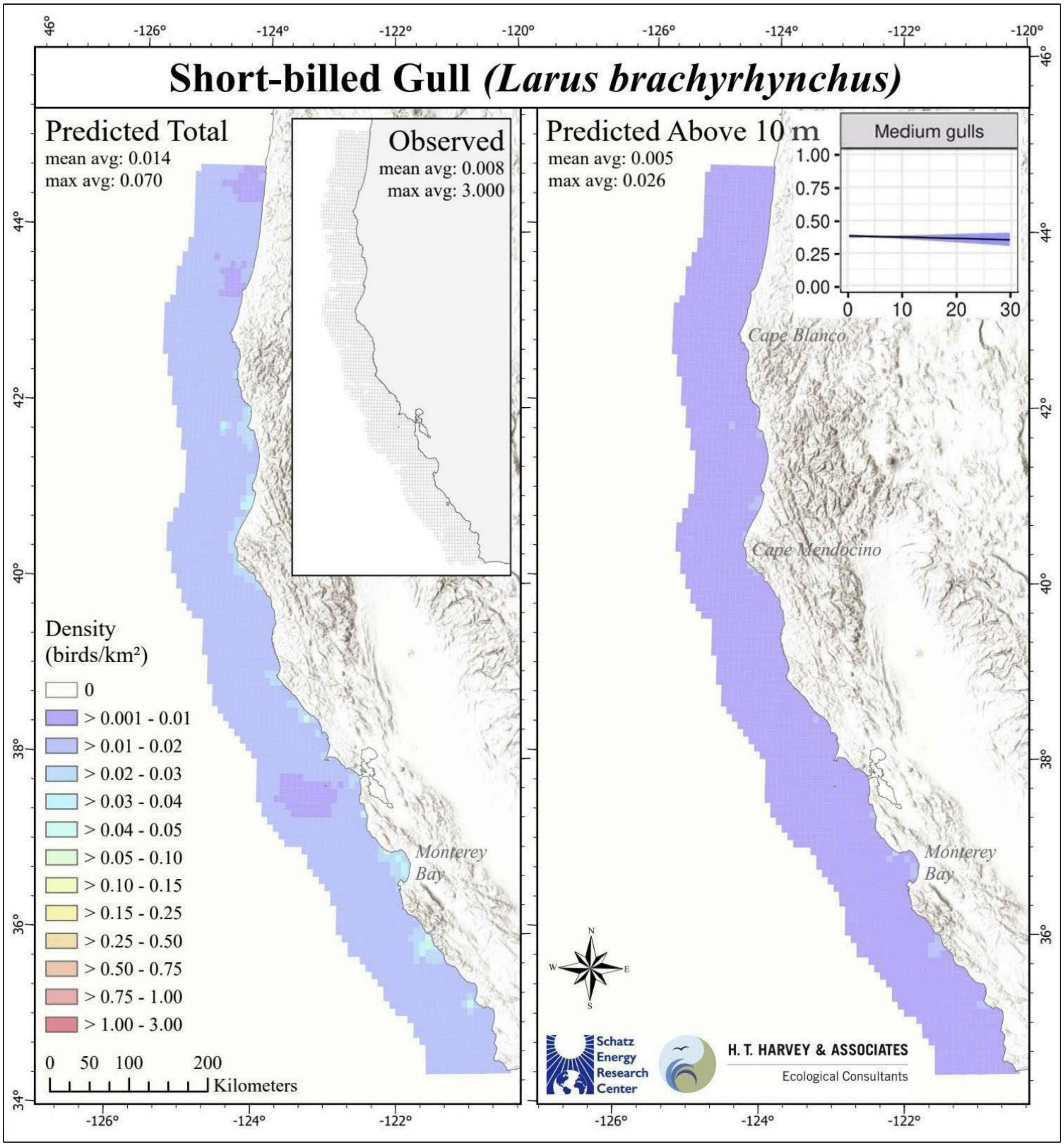

Figure B-24. Short-billed Gull (*Larus brachyrhynchus*)

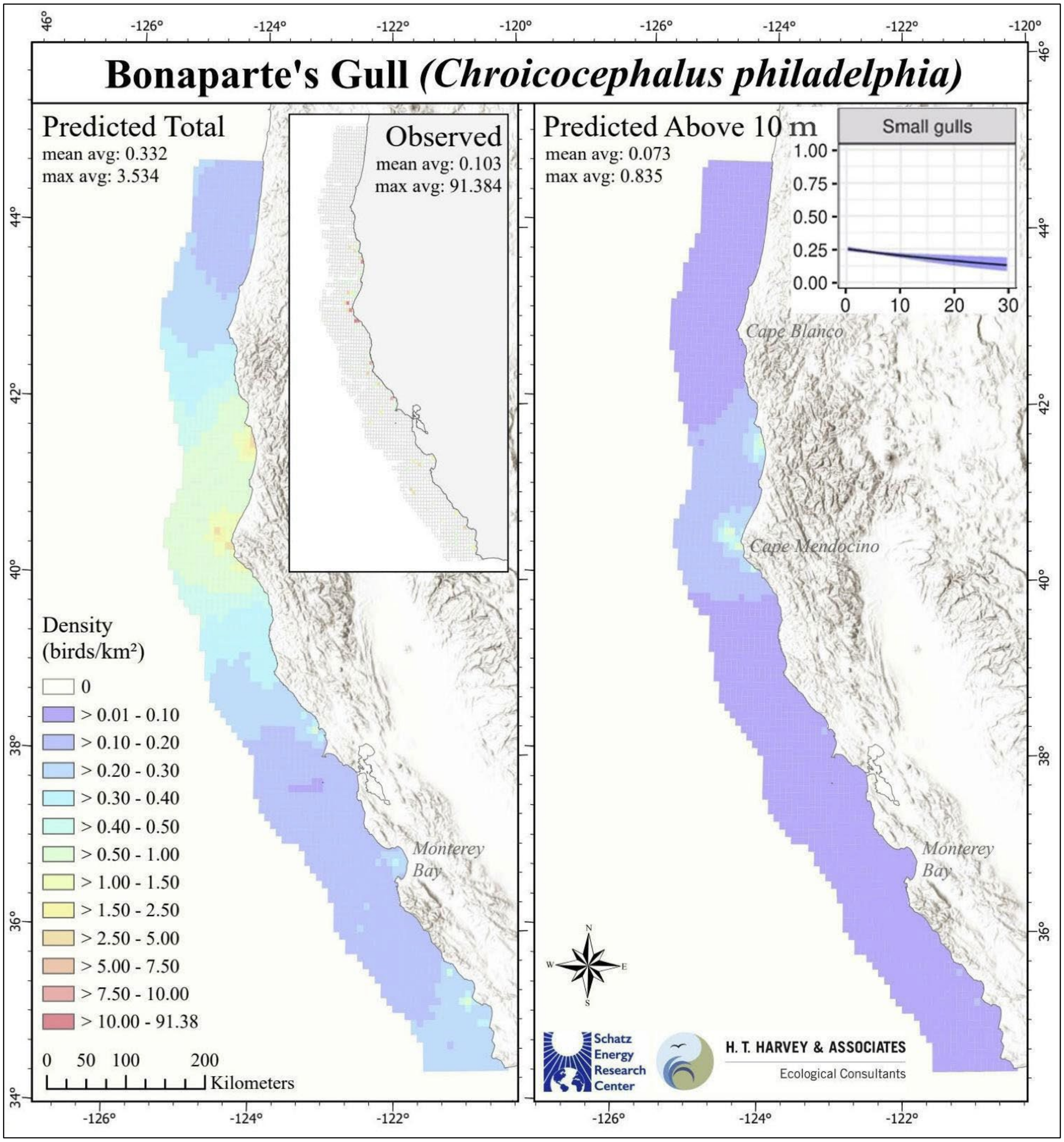

Figure B-25. Bonaparte's Gull (*Chroicocephalus philadelphia*)

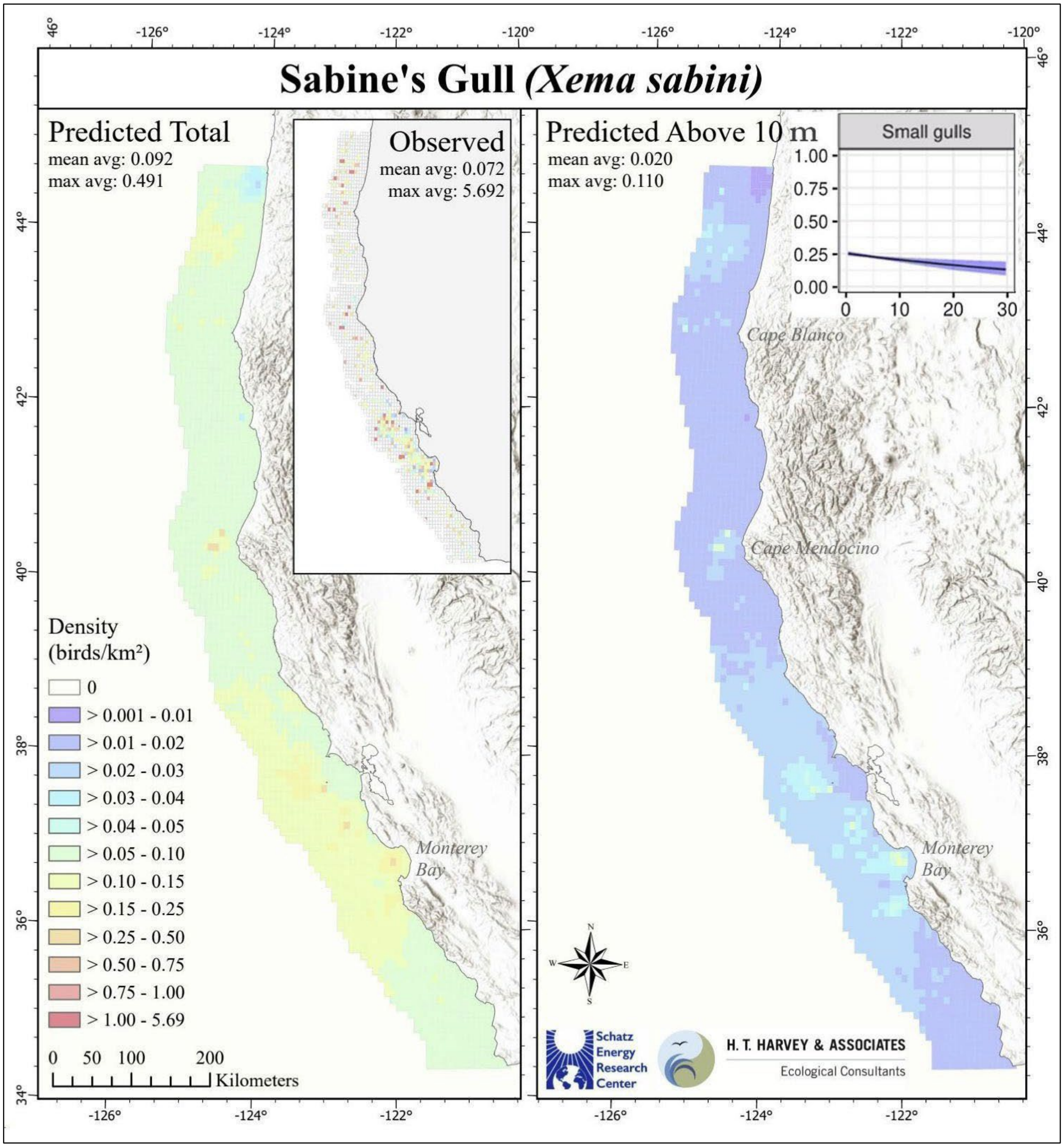

Figure B-26. Sabine's Gull (*Xema sabini*)

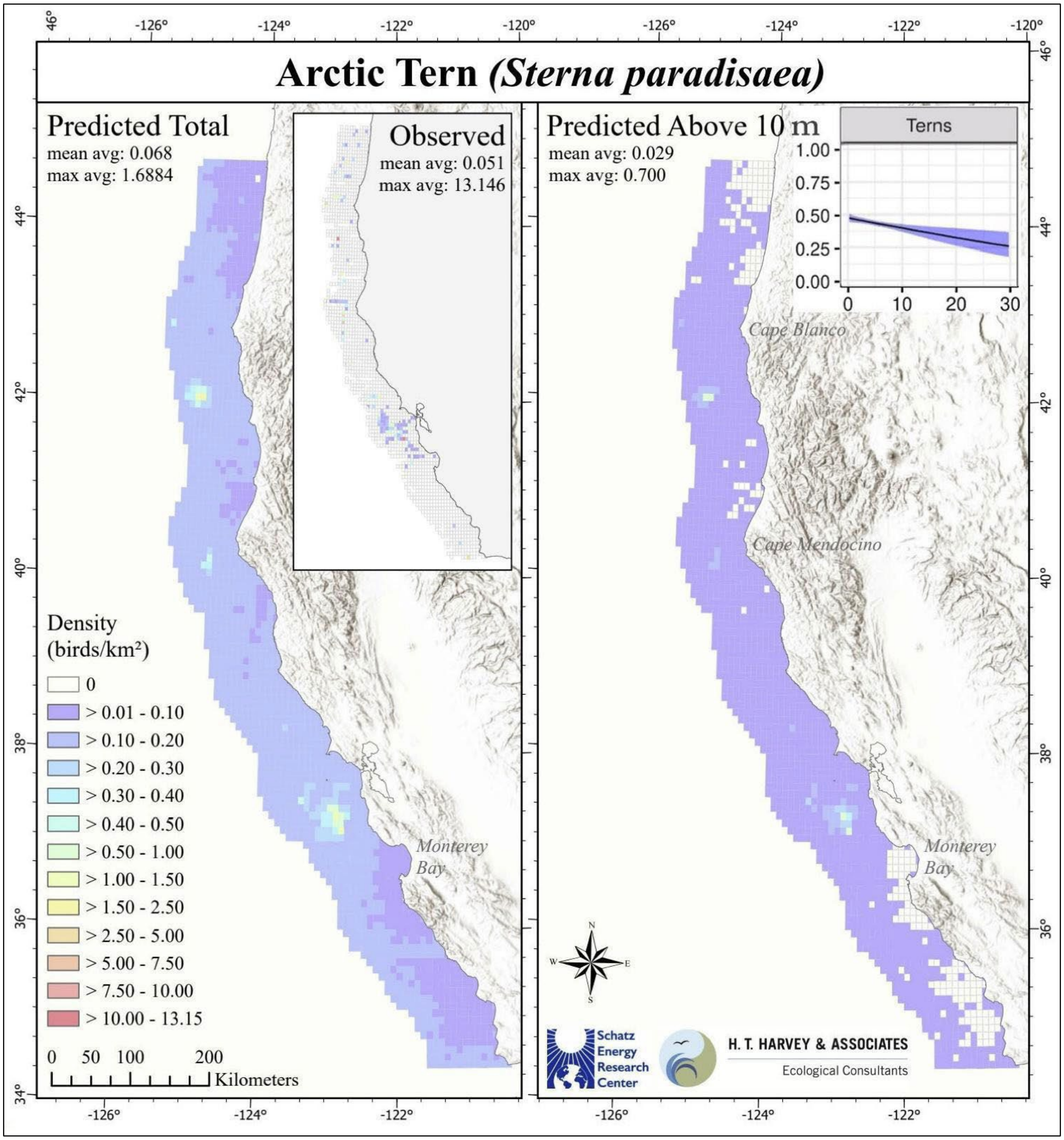

Figure B-27. Arctic Tern (*Sterna paradisaea*)

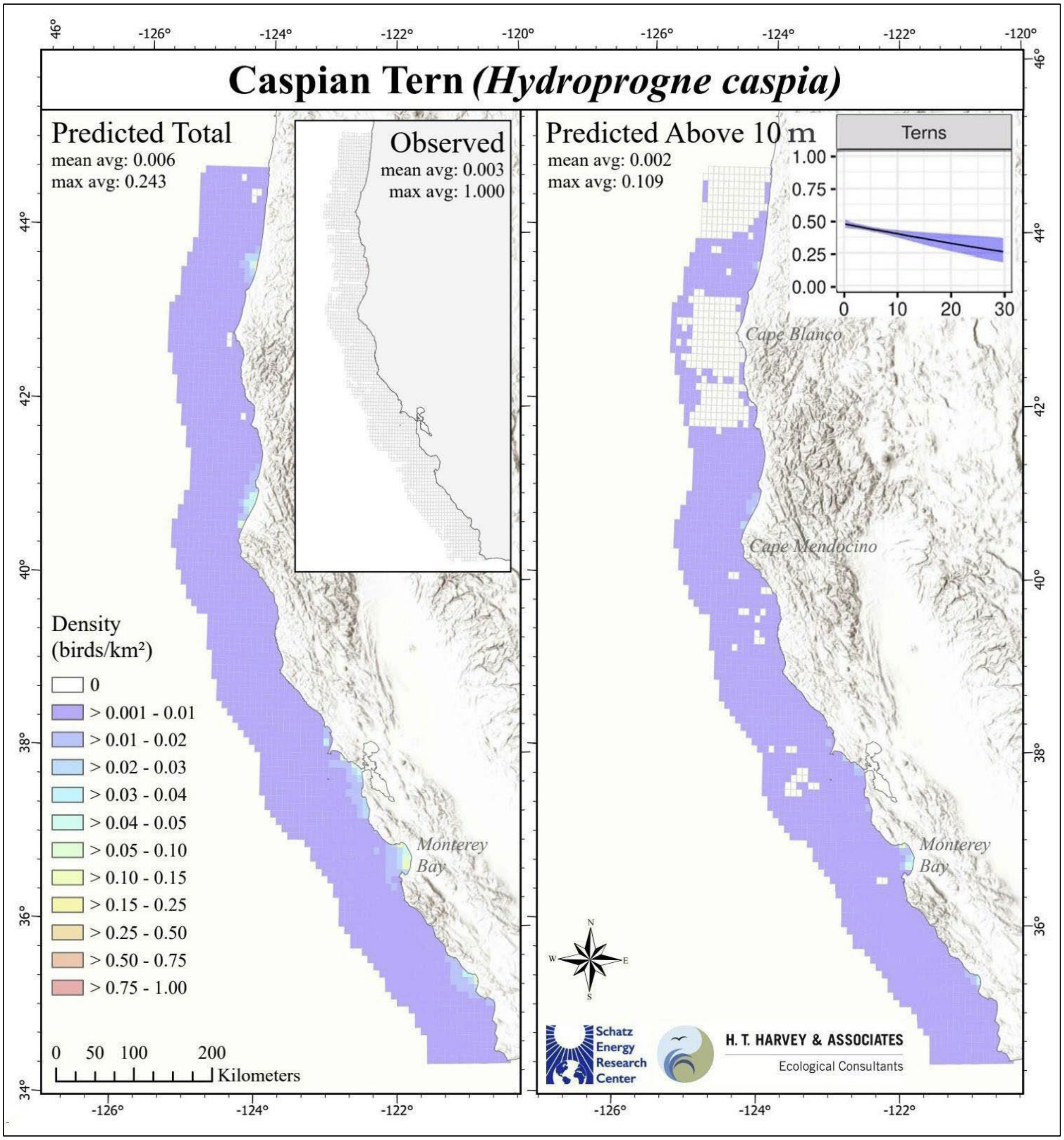

Figure B-28. Caspian Tern (*Hydroprogne caspia*)

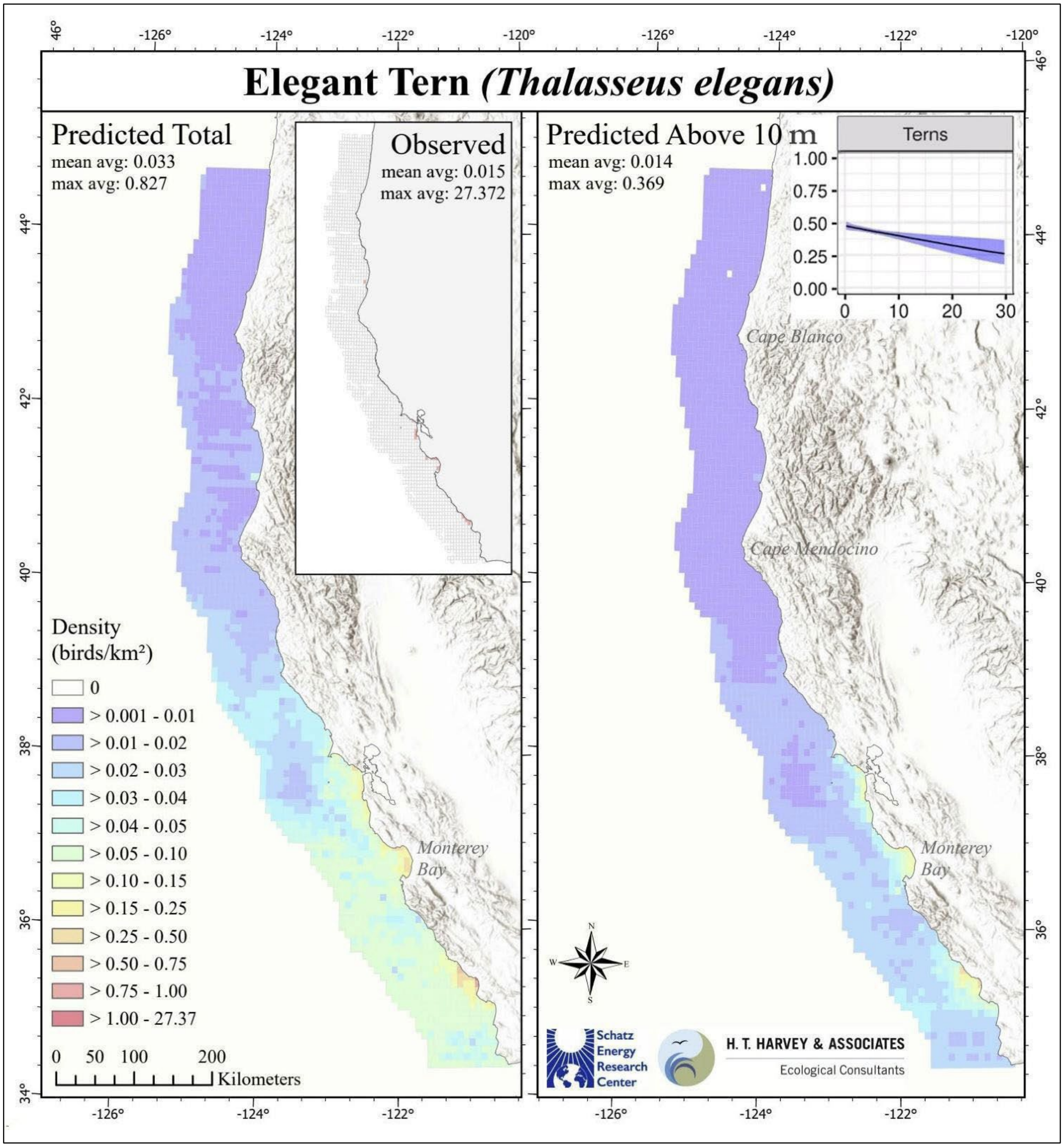

Figure B-29. Elegant Tern (*Thalasseus elegans*)

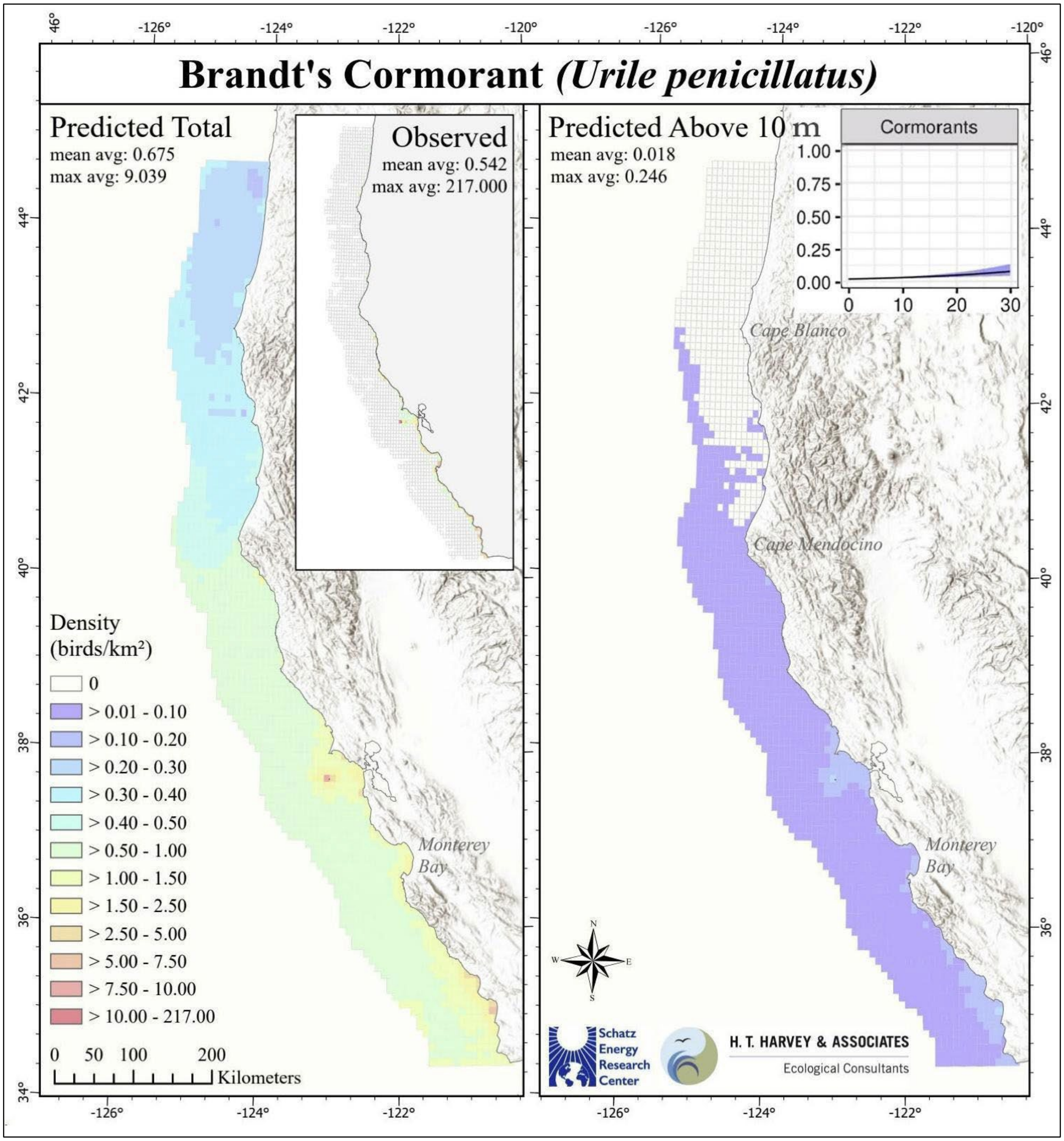

Figure B-30. Brandt's Cormorant (*Urile penicillatus*)

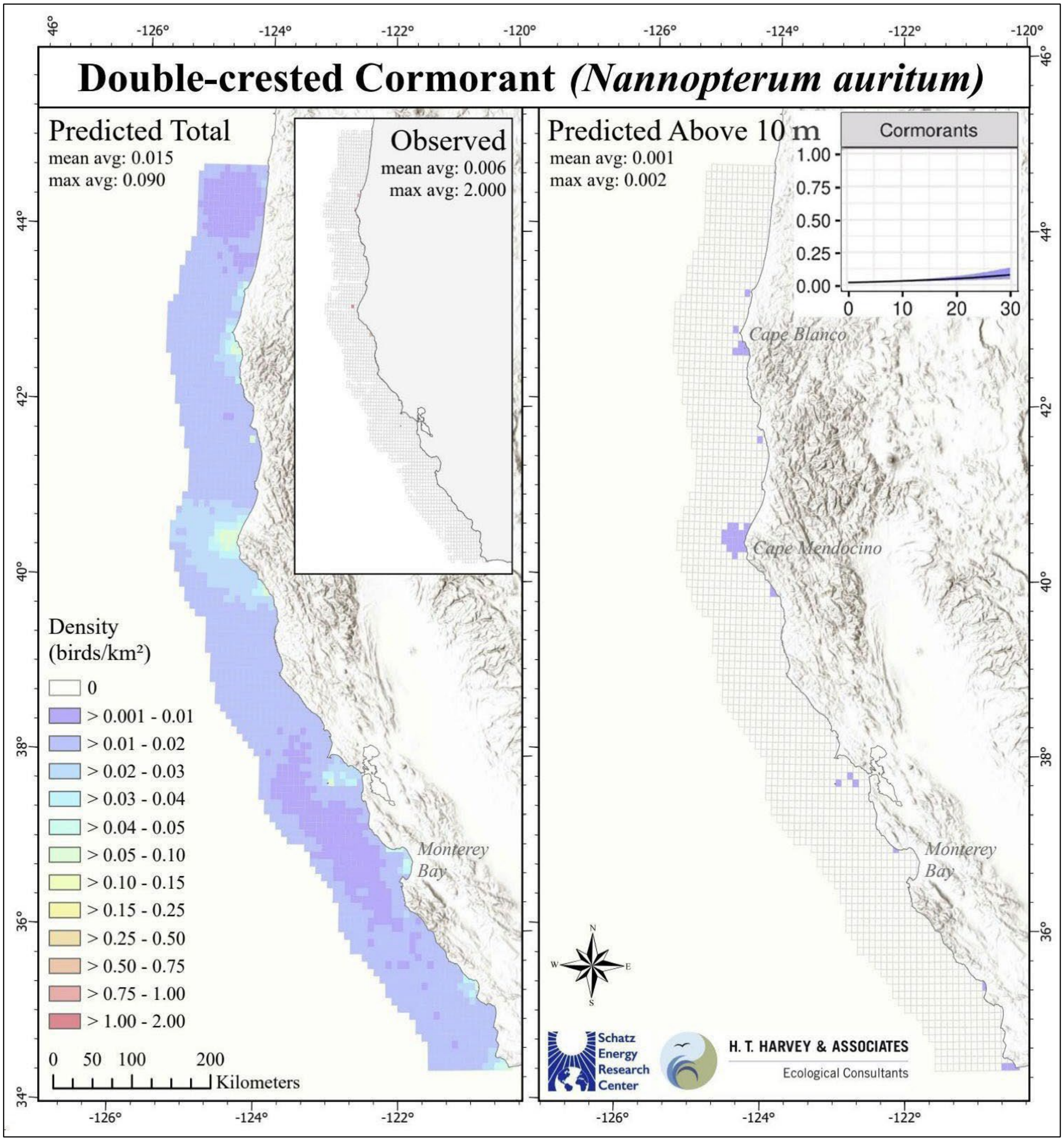

Figure B-31. Double-crested Cormorant (*Nannopterum auritum*)

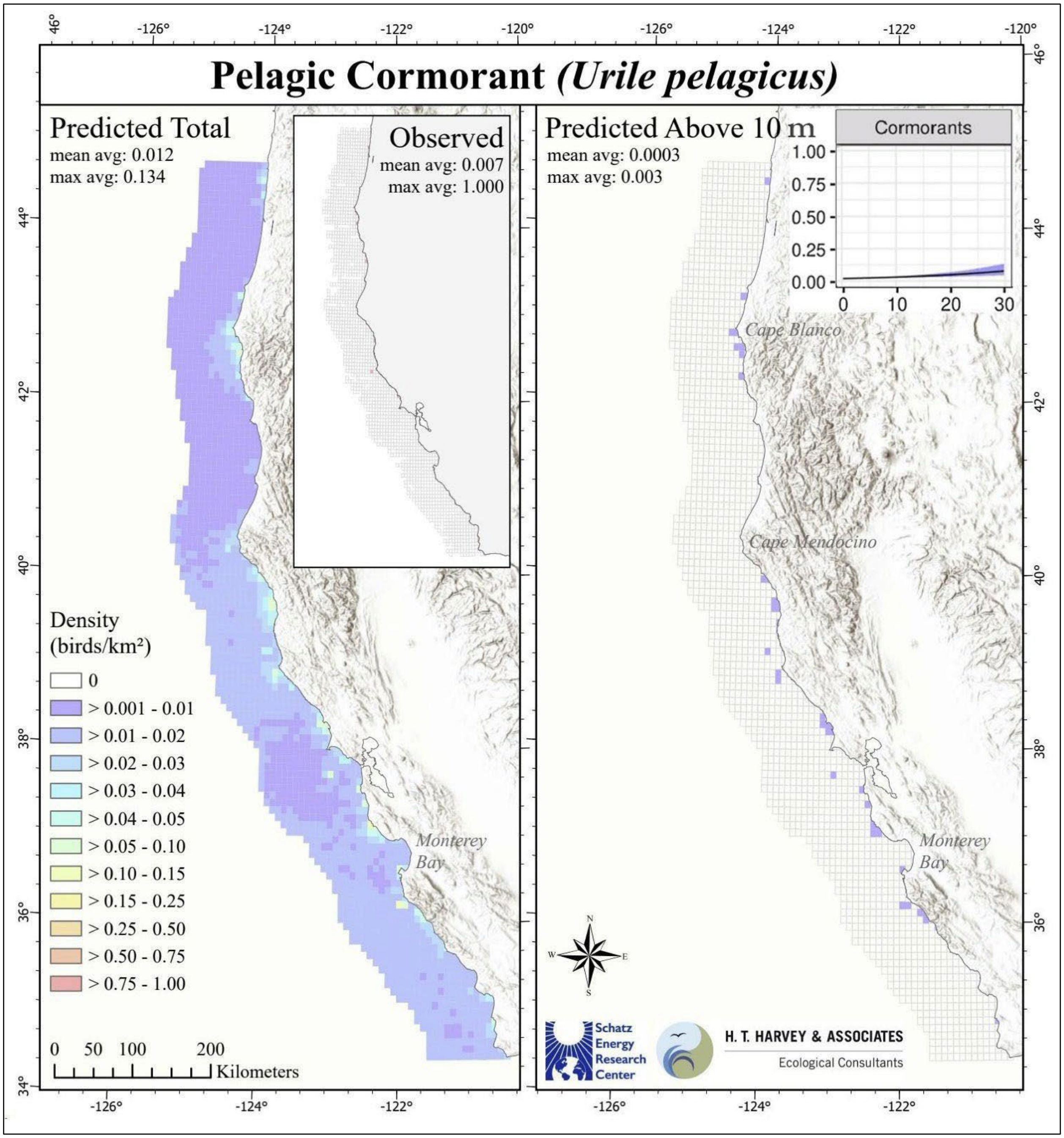

Figure B-32. Pelagic Cormorant (*Urile pelagicus*)

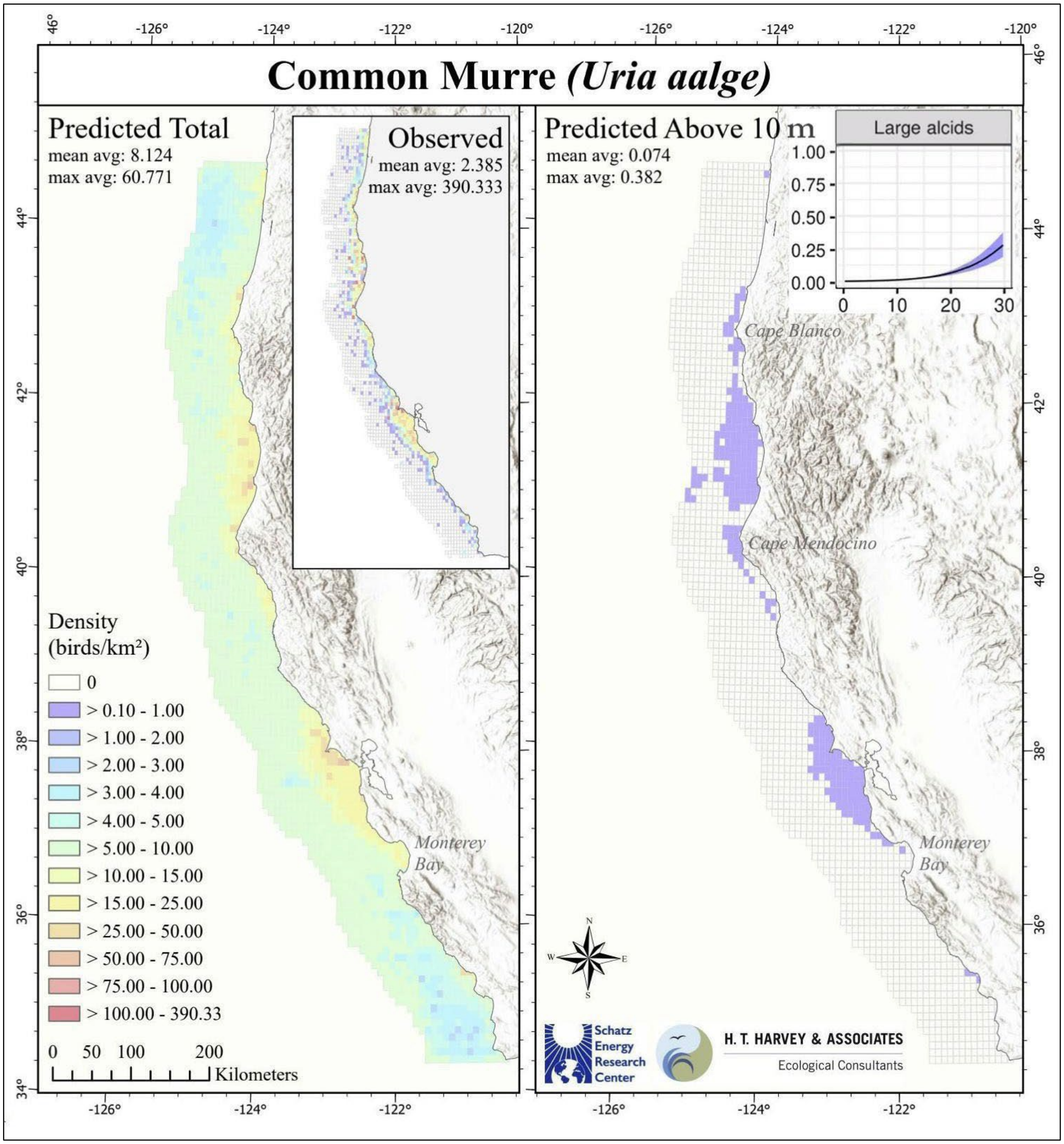

Figure B-33. Common Murre (*Uria aalge*)

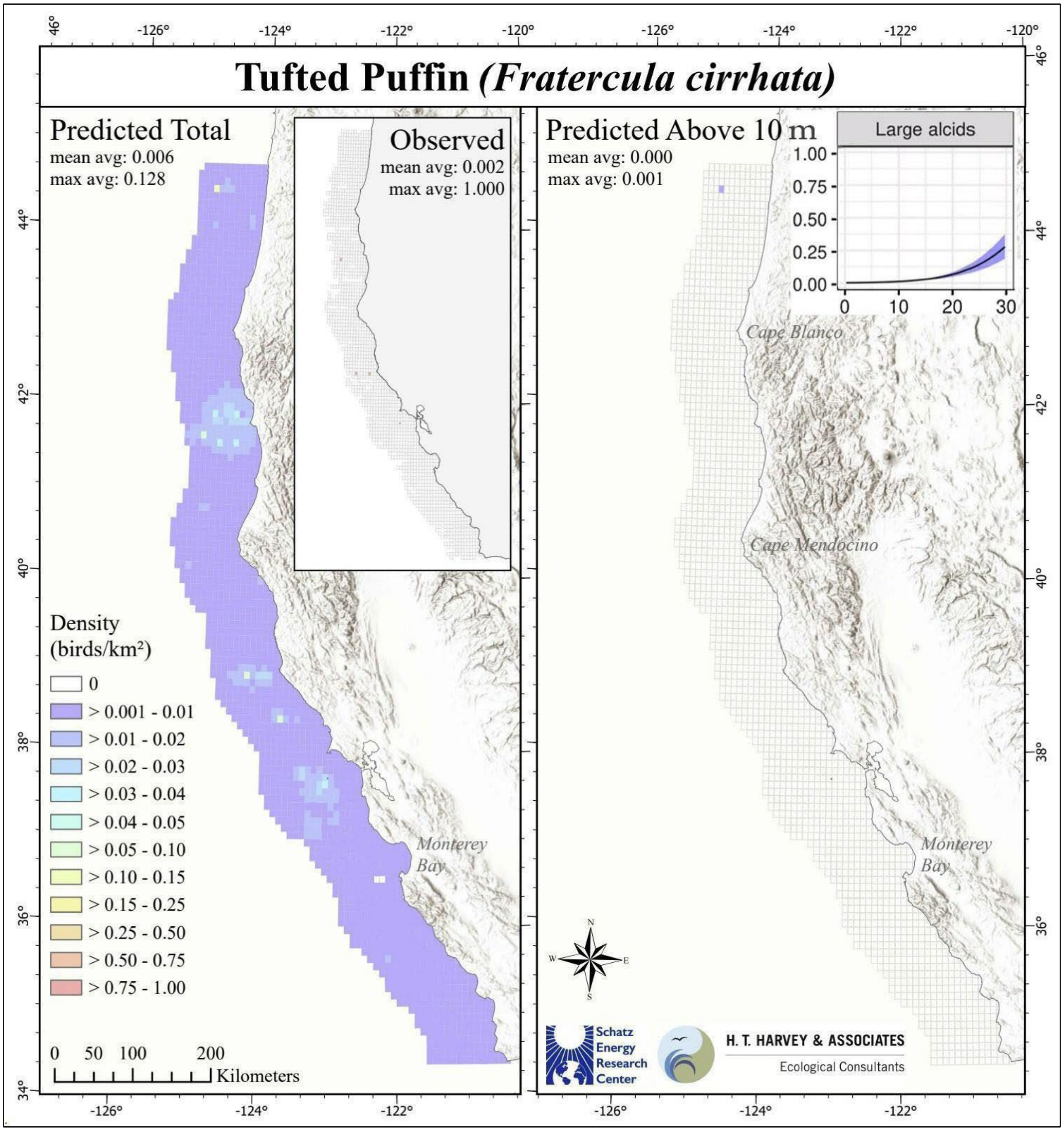

Figure B-34. Tufted Puffin (*Fratercula cirrhata*)

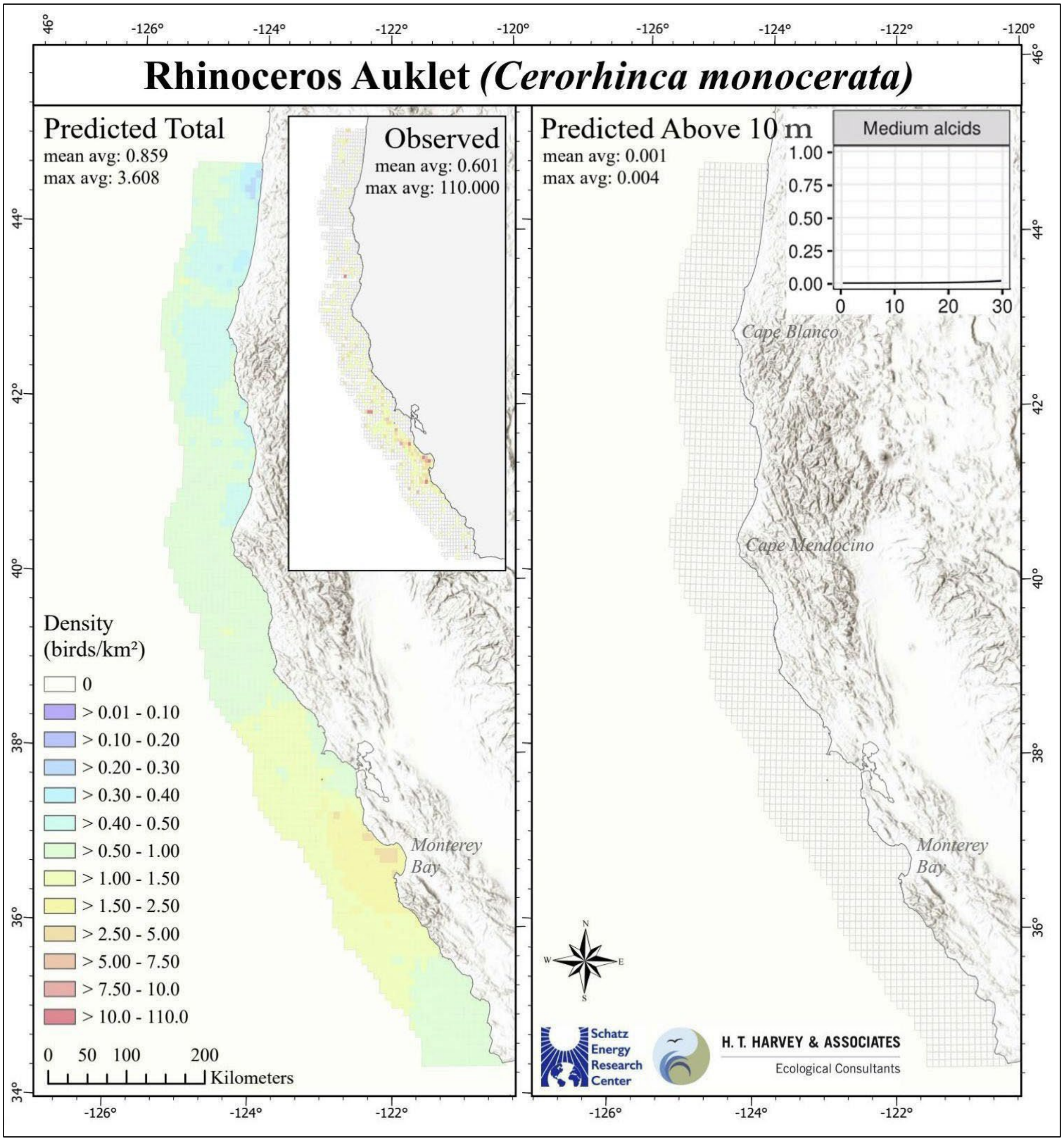

Figure B-35. Rhinoceros Auklet (*Cerorhinca monocerata*)

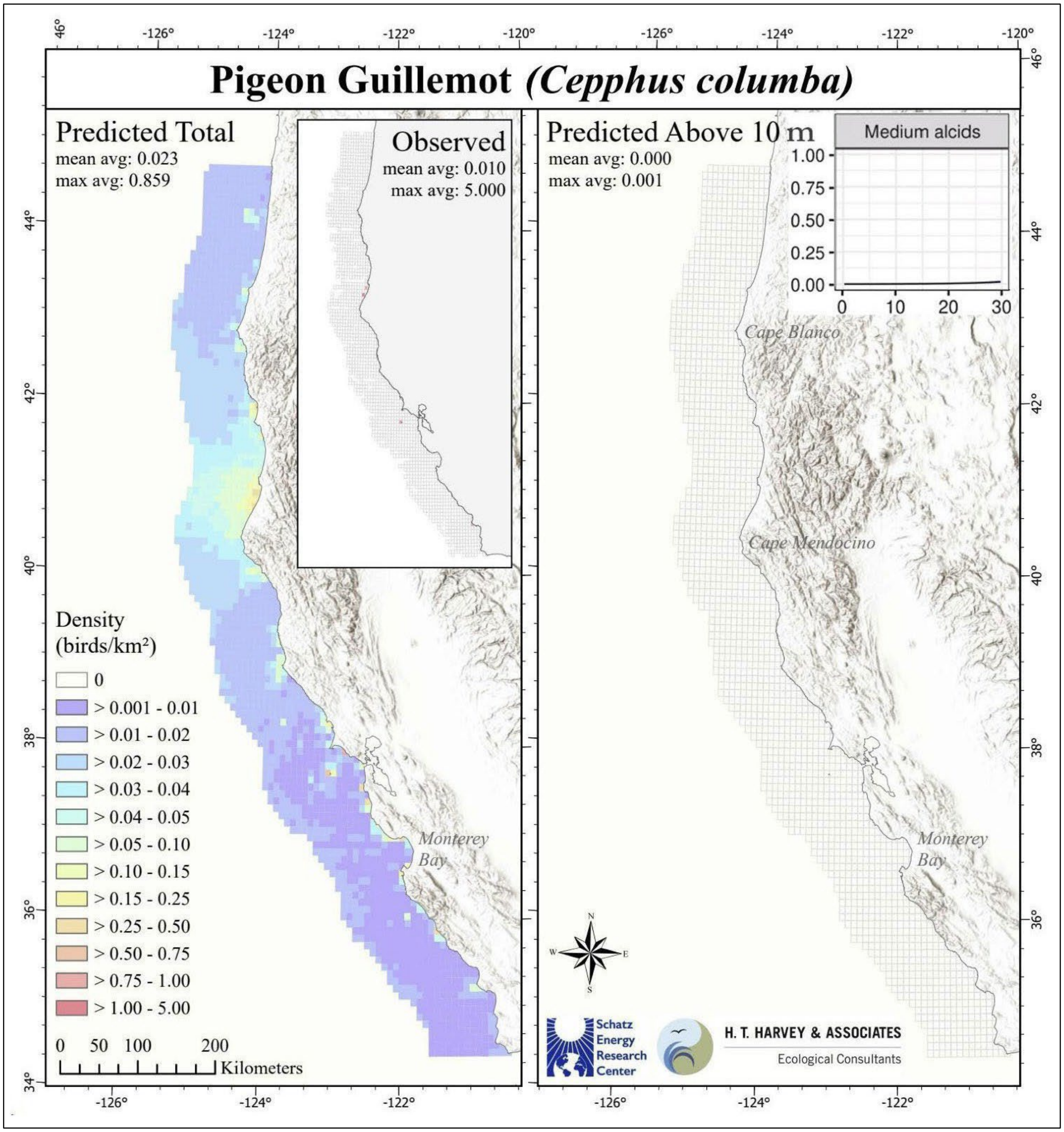

Figure B-36. Pigeon Guillemot (*Cephus columba*)

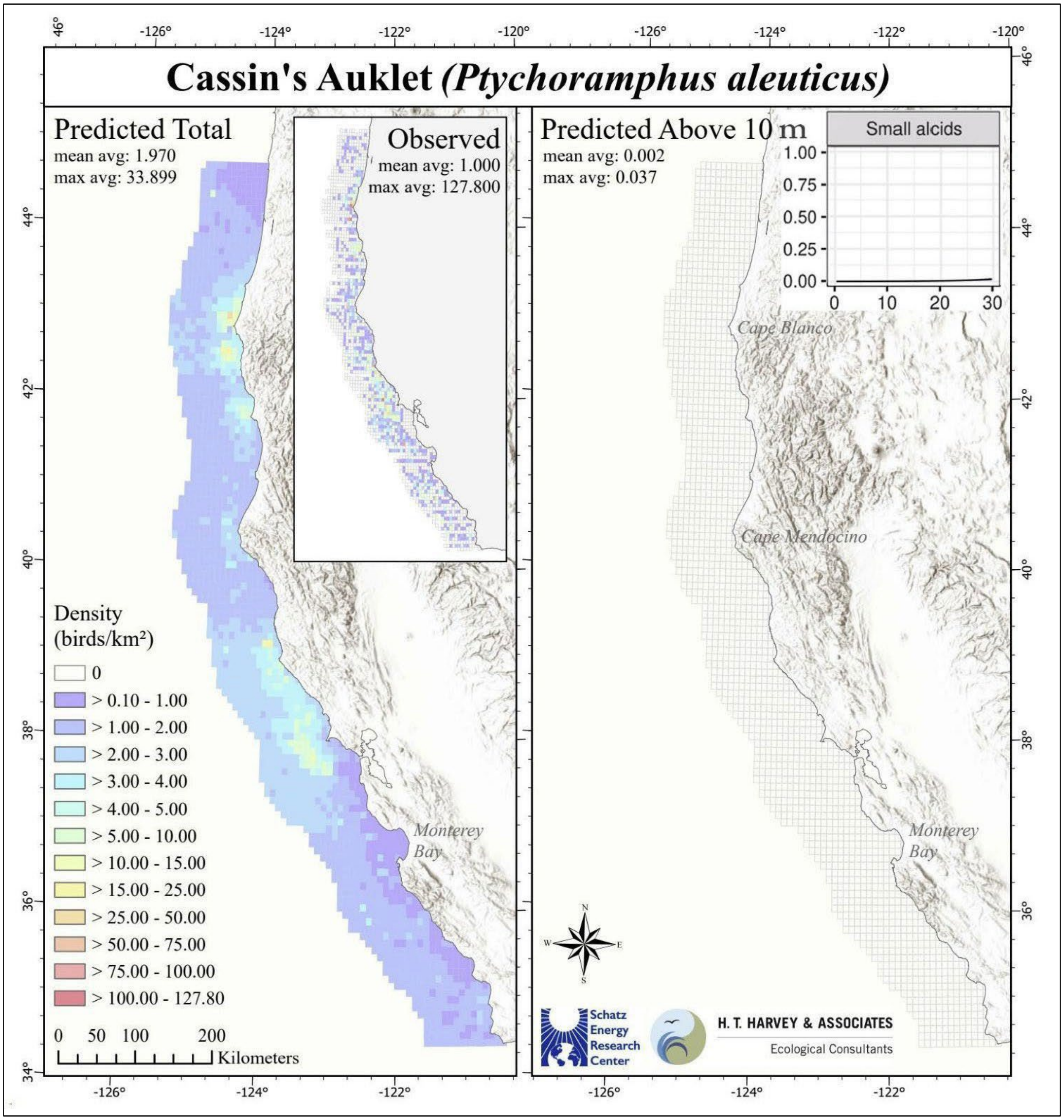

Figure B-37. Cassin's Auklet (*Ptychoramphus aleuticus*)

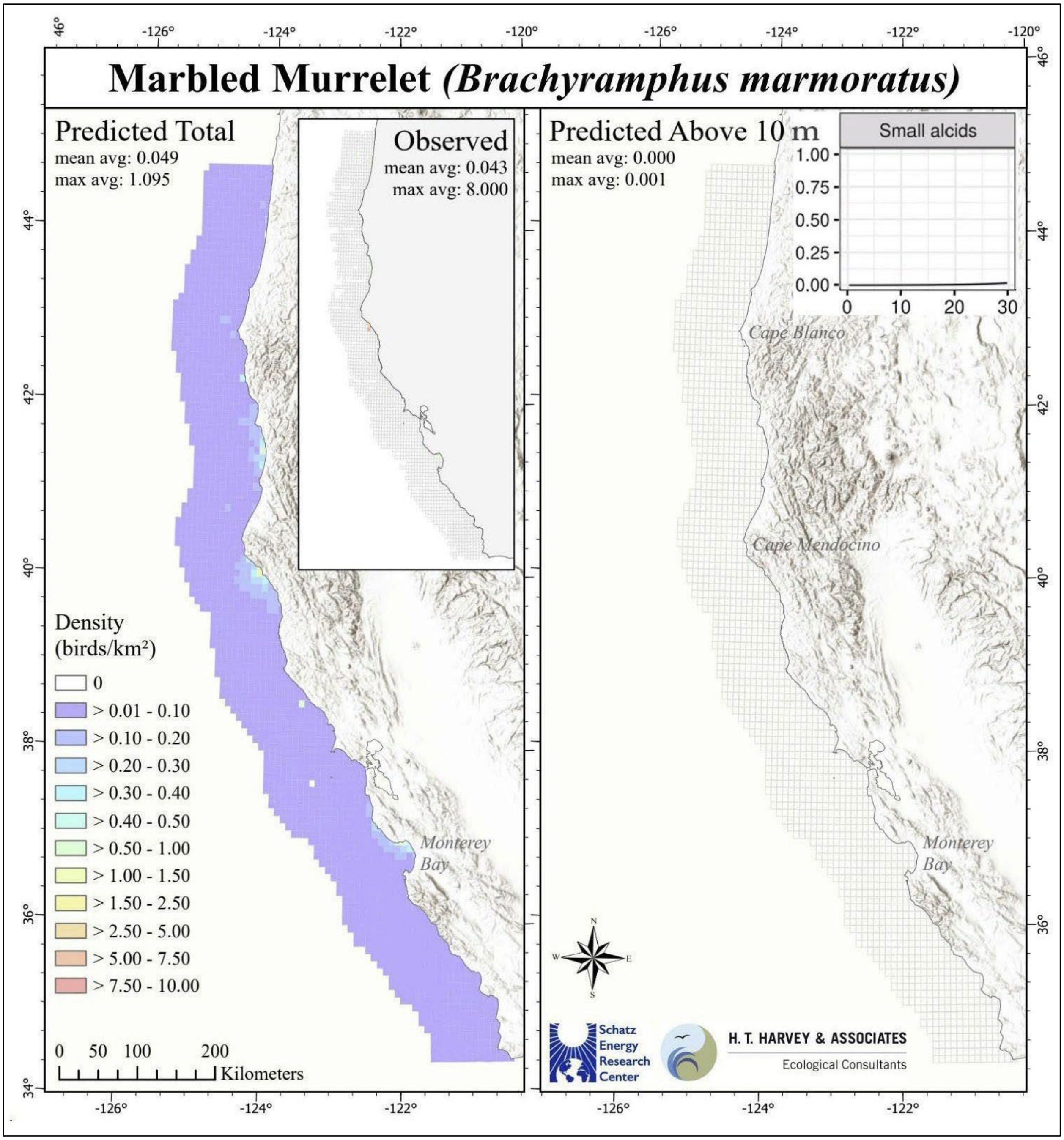

Figure B-38. Marbled Murrelet (*Brachyramphus marmoratus*)

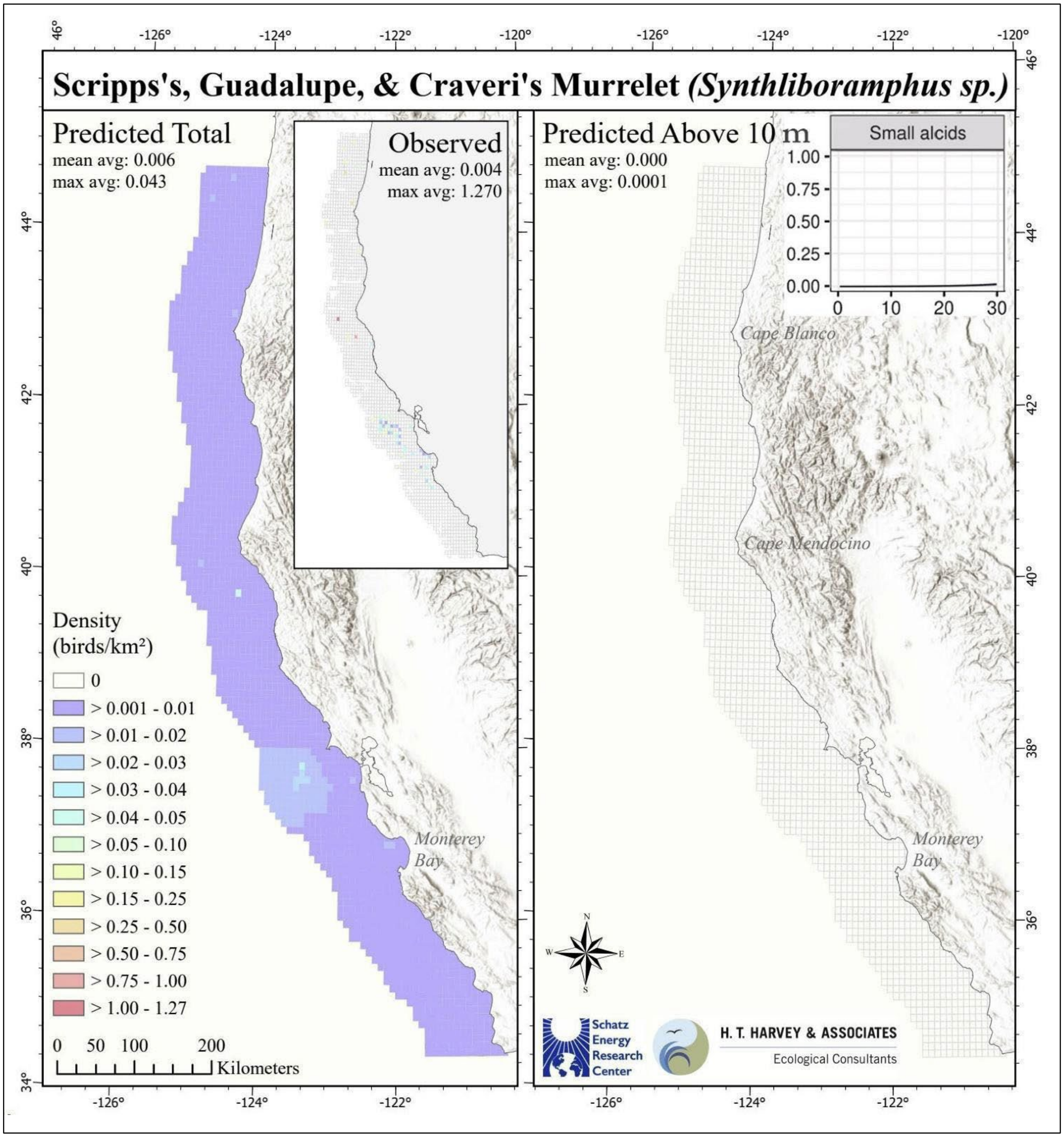

Figure B-39. Scripps's, Guadalupe, and Craveri's Murrelet (*Synthliboramphus* spp.)

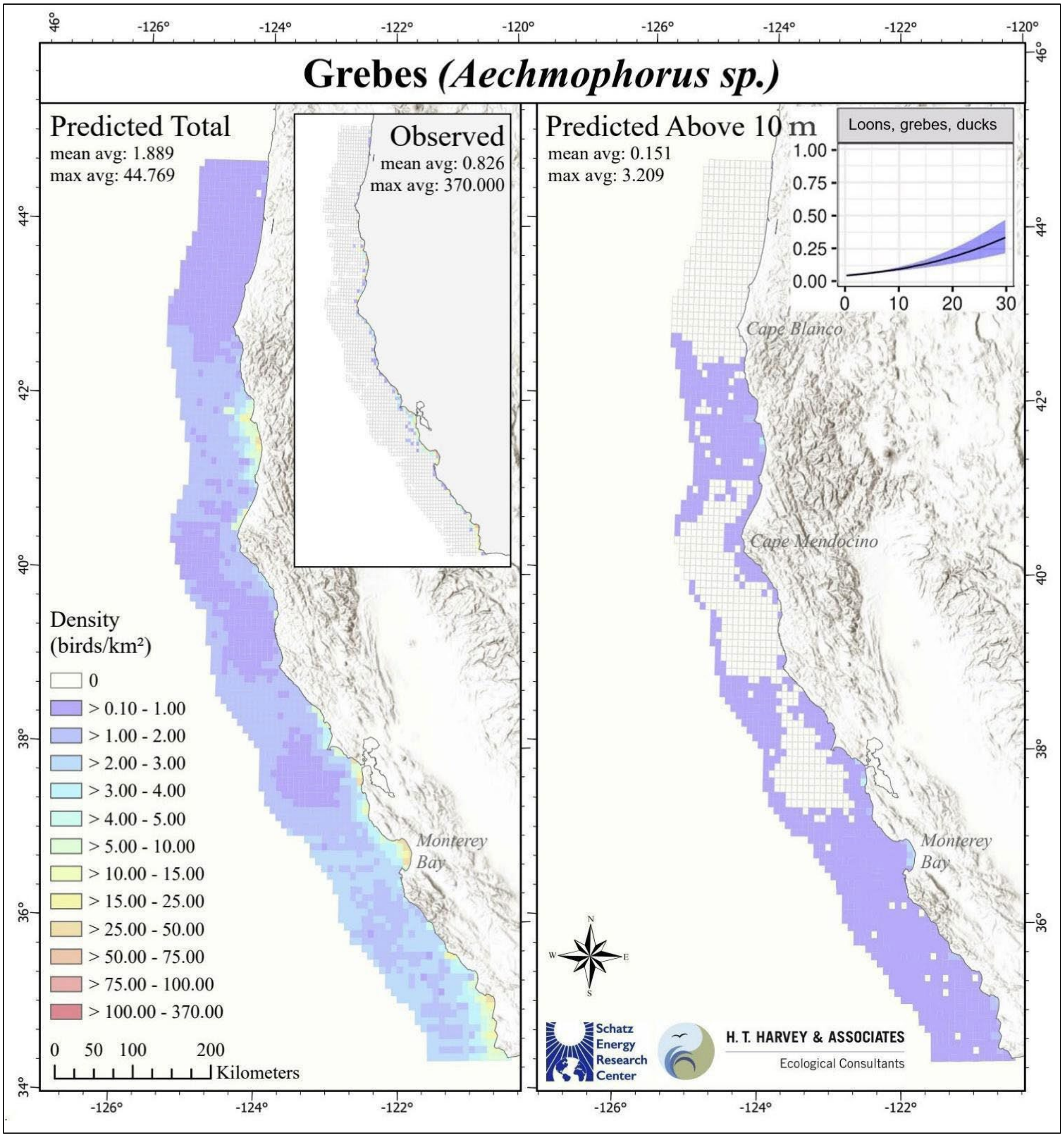

Figure B-40. Western and Clark's Grebes (*Aechmophorus* spp.)

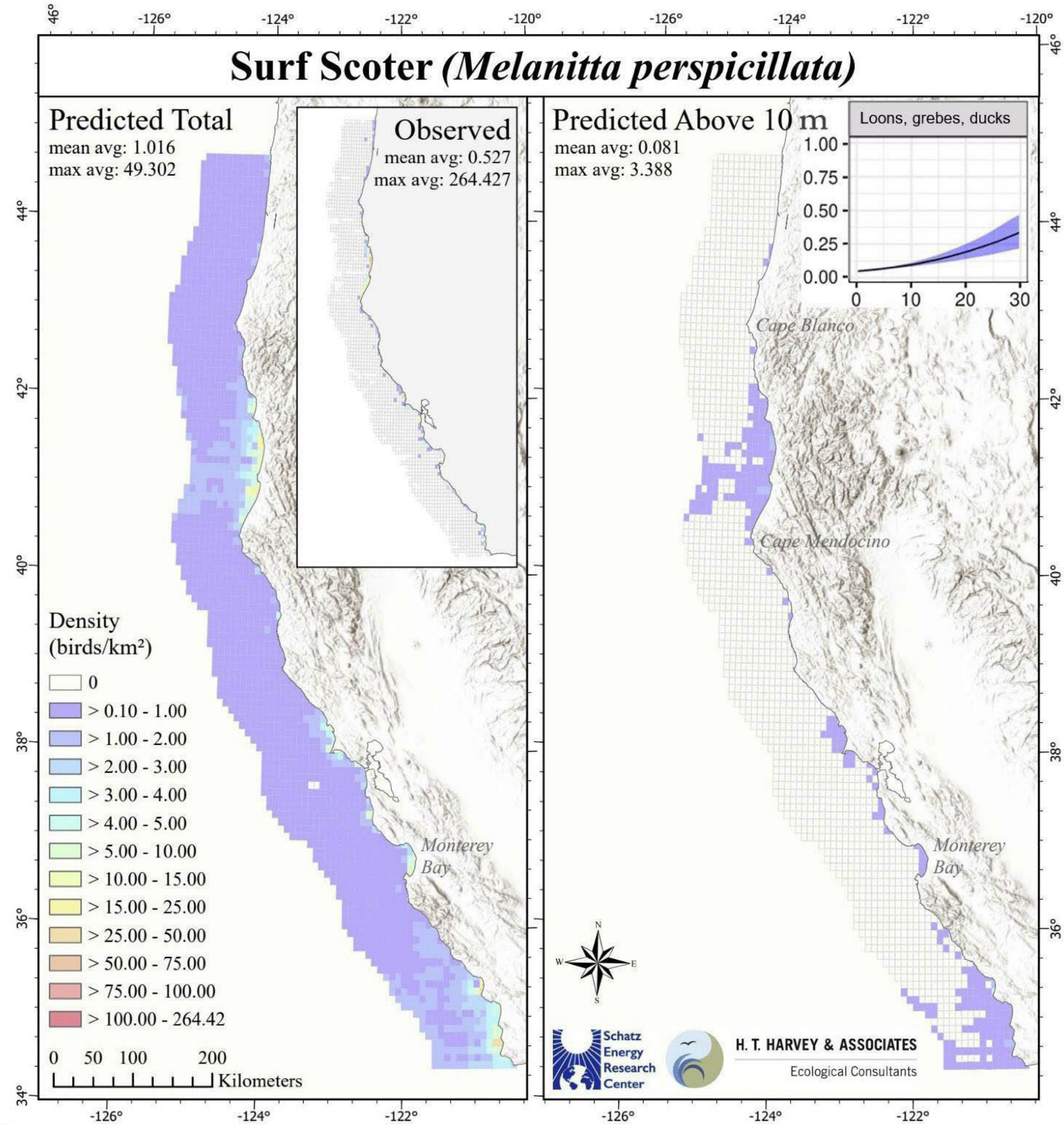

Figure B-41. Surf Scoter (*Melanitta perspicillata*)

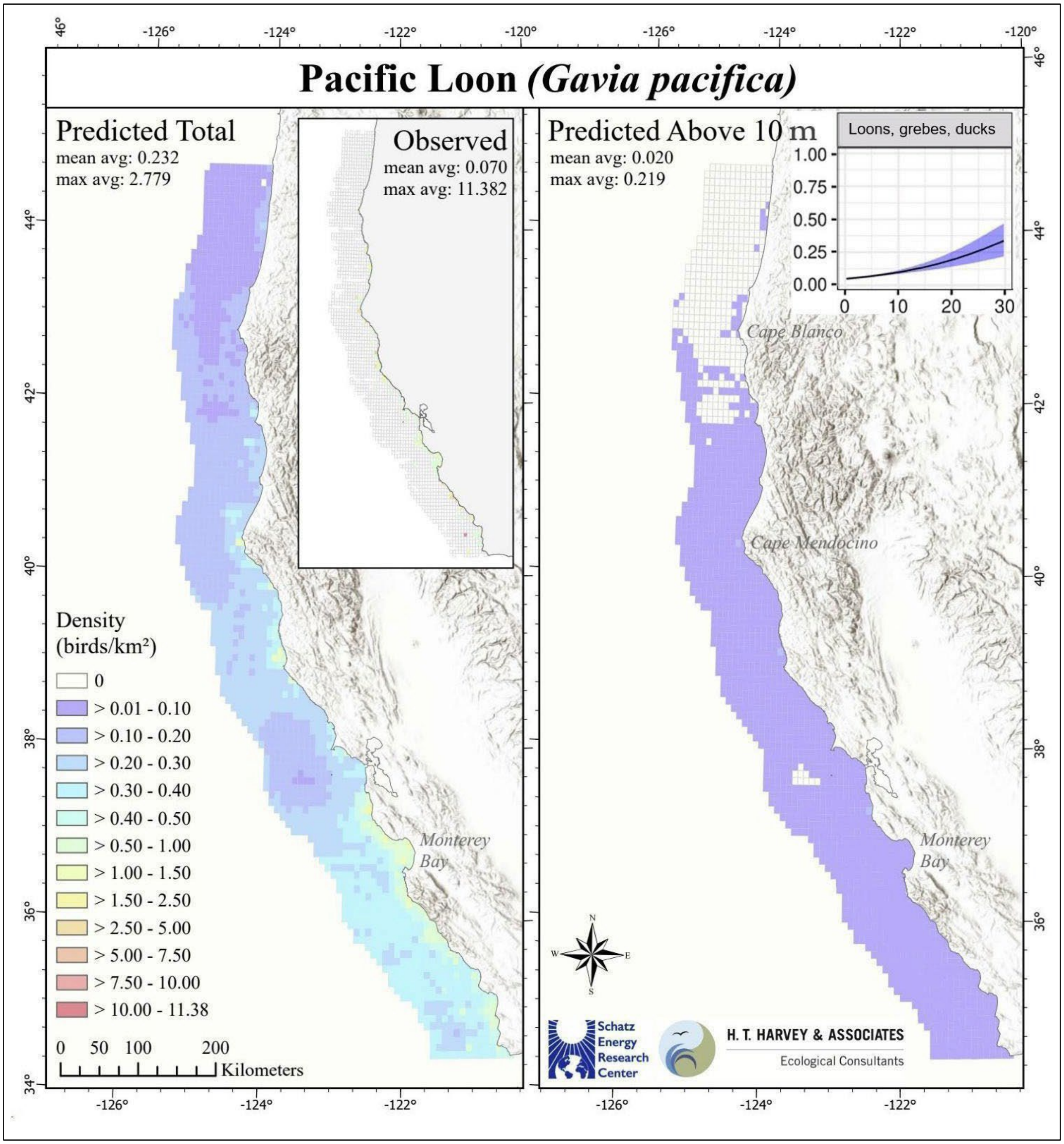

Figure B-42. Pacific Loon (*Gavia pacifica*)

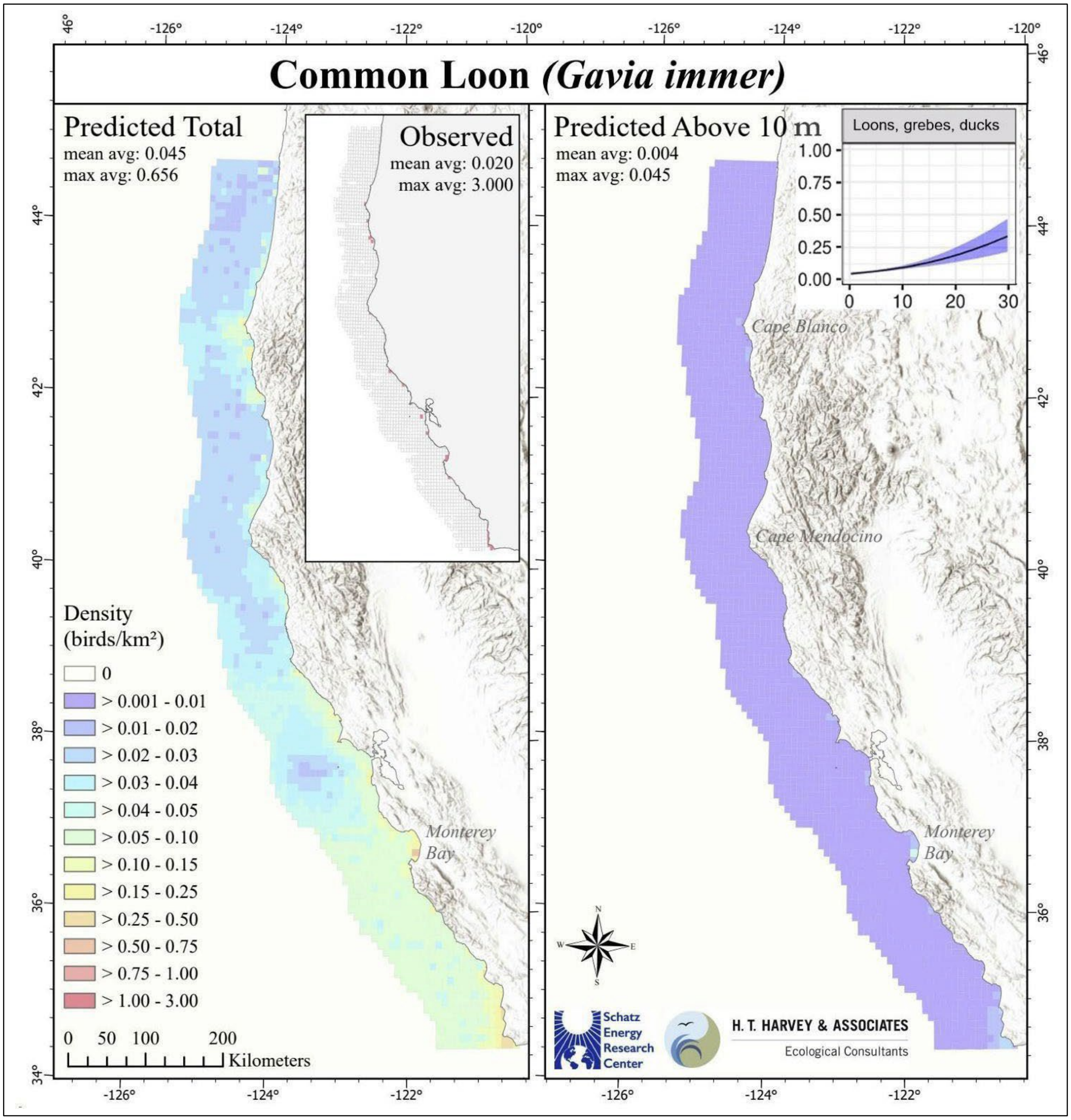

Figure B-43. Common Loon (*Gavia immer*)

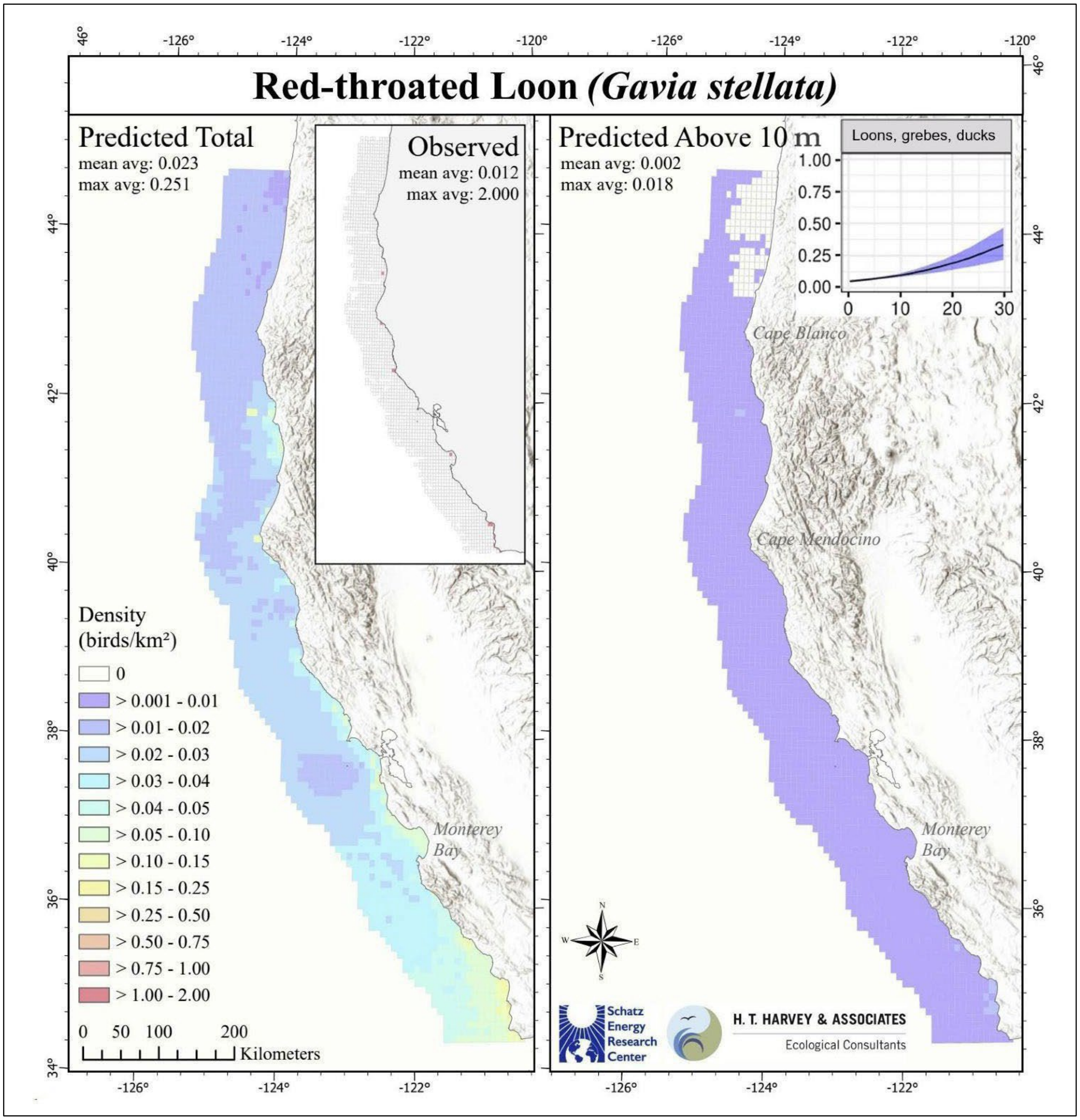

Figure B-44. Red-throated Loon (*Gavia stellata*)

Appendix C. Seasonal Predictions for a Subset of Seabirds Included in the 3D Seabird Collision Vulnerability Framework

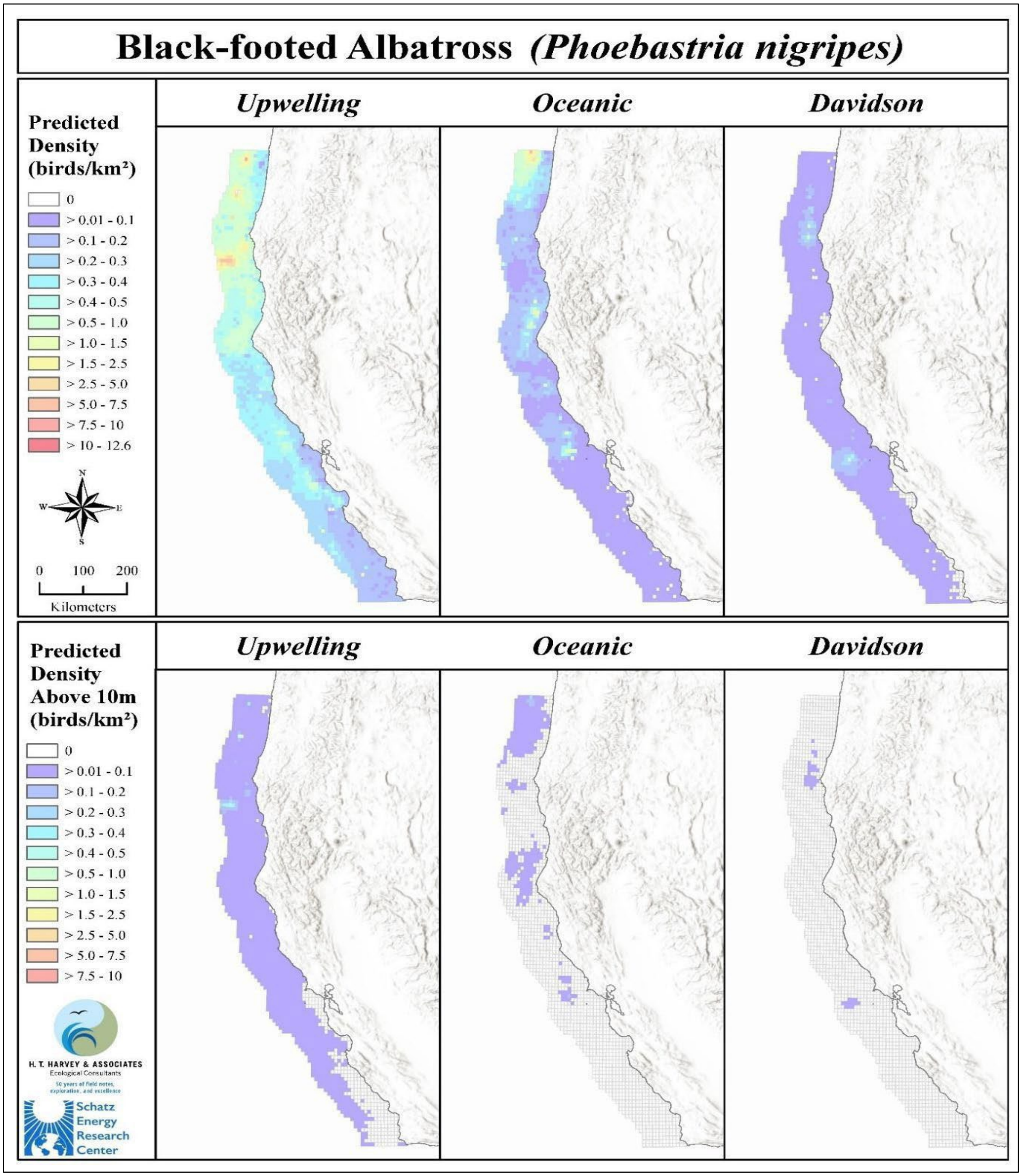

Figure C-1. Black-footed Albatross (*Phoebasatria nigripes*)

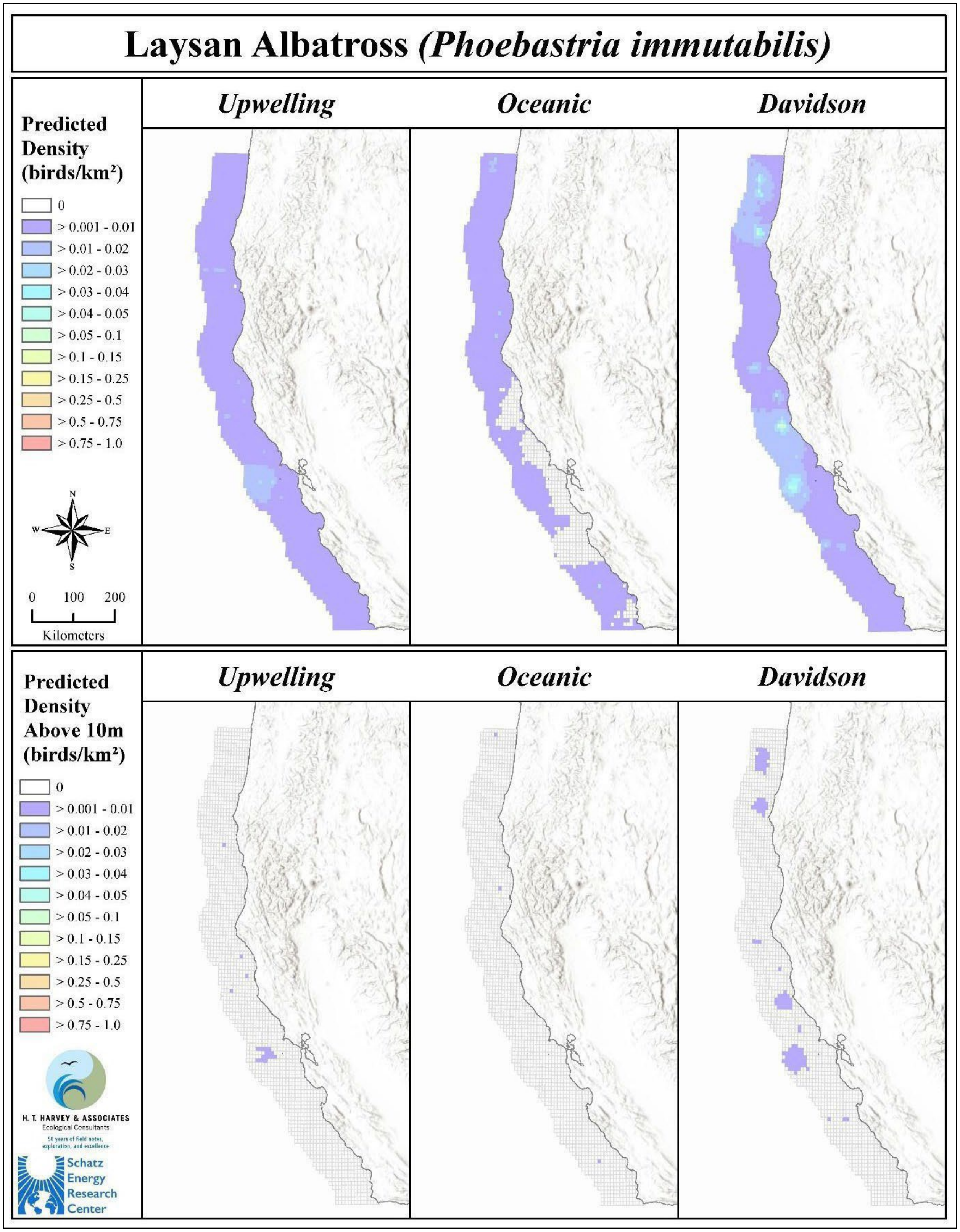

Figure C-2. Laysan Albatross (*Phoebastria immutabilis*)

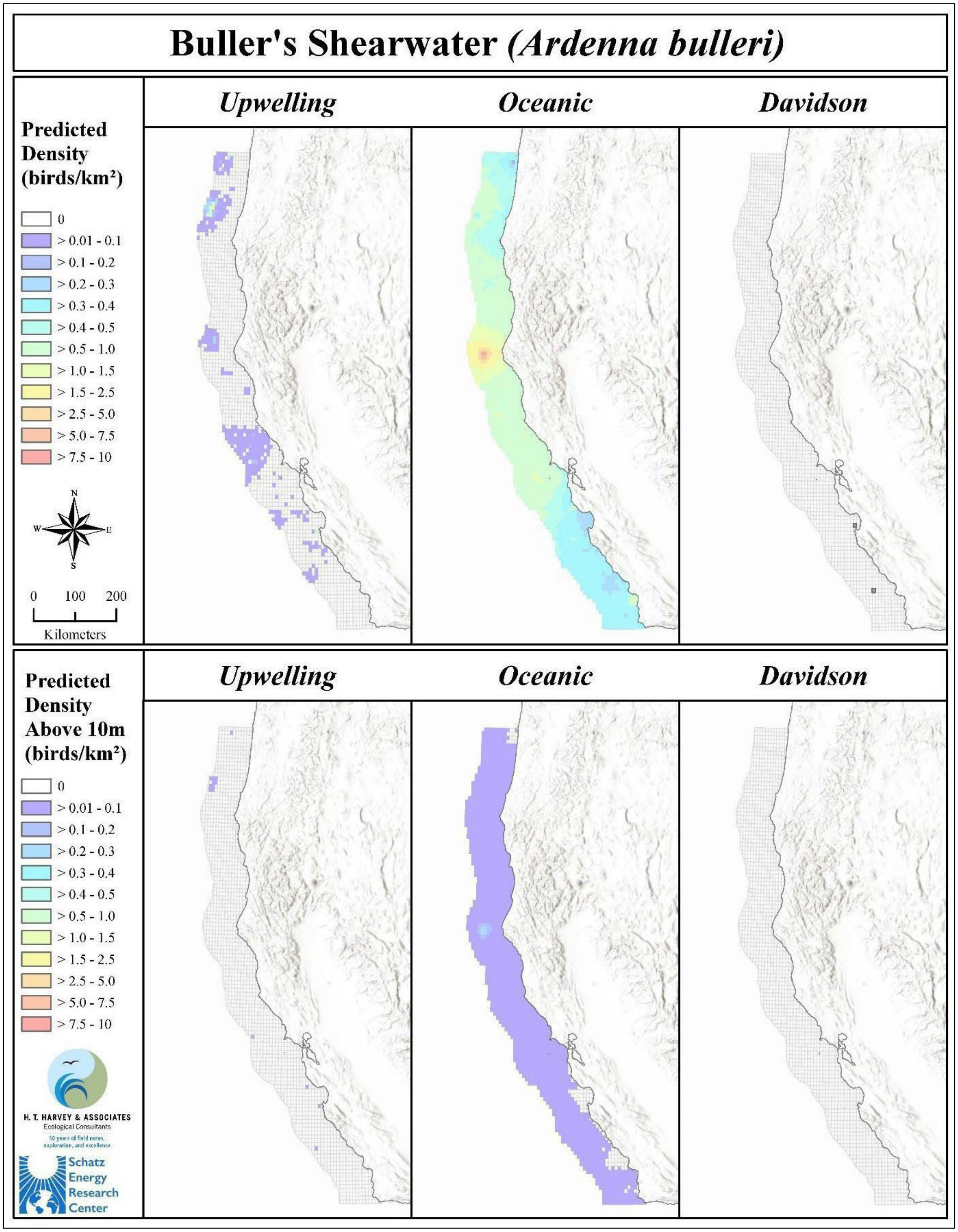

Figure C-3. Buller's Shearwater (*Ardenna bulleri*)

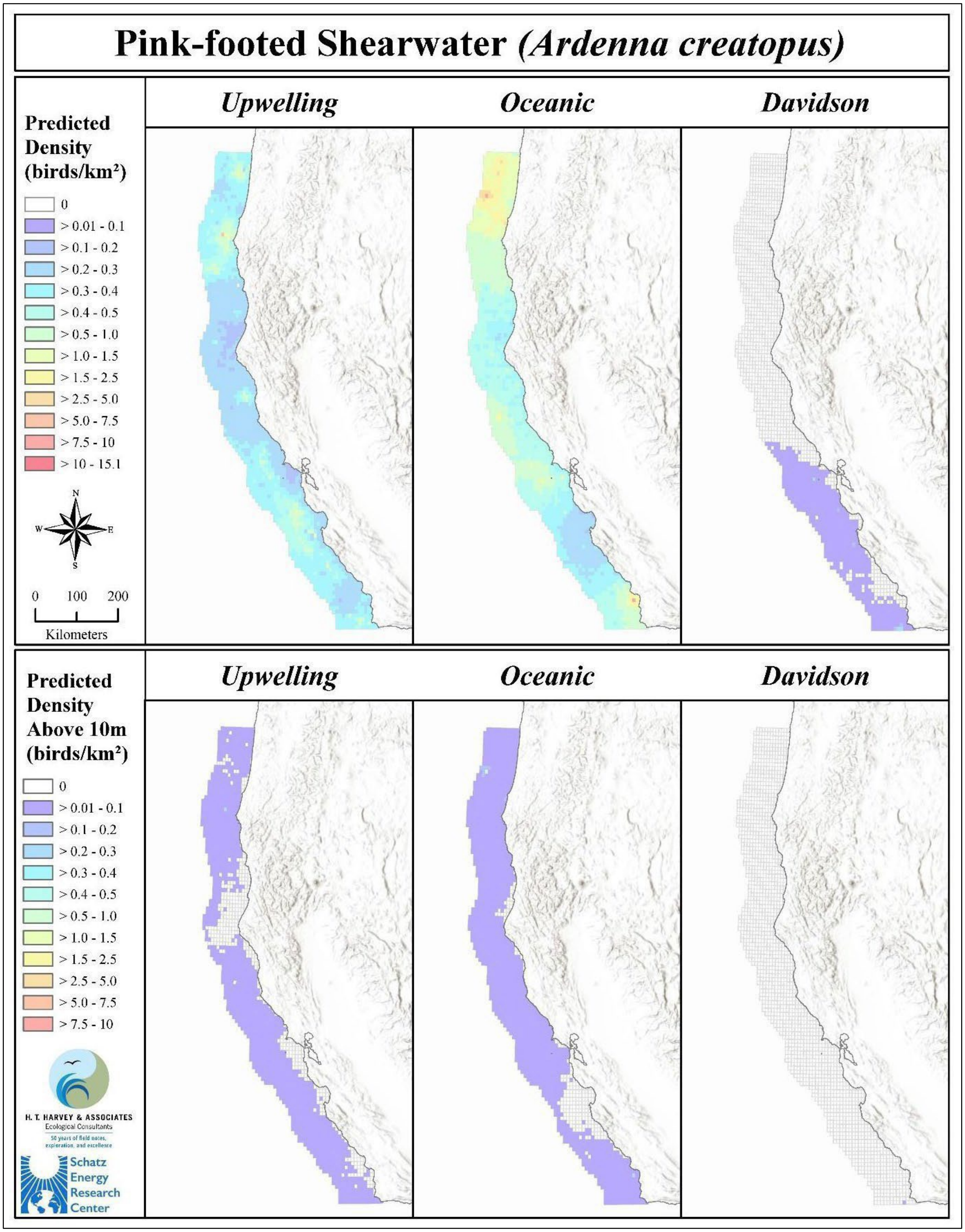

Figure C-4. Pink-footed Shearwater (*Ardenna creatopus*)

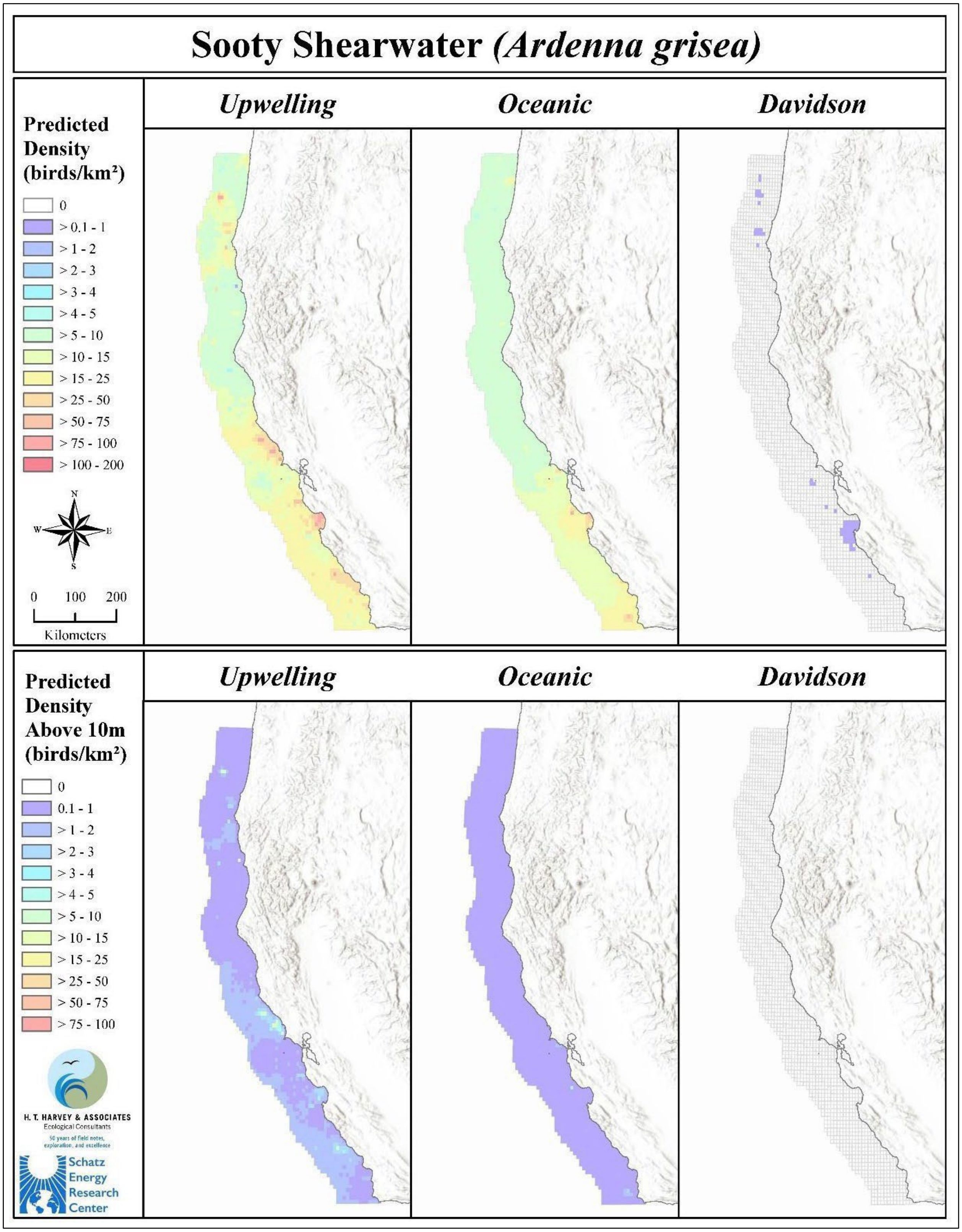

Figure C-5. Sooty Shearwater (*Ardenna grisea*)

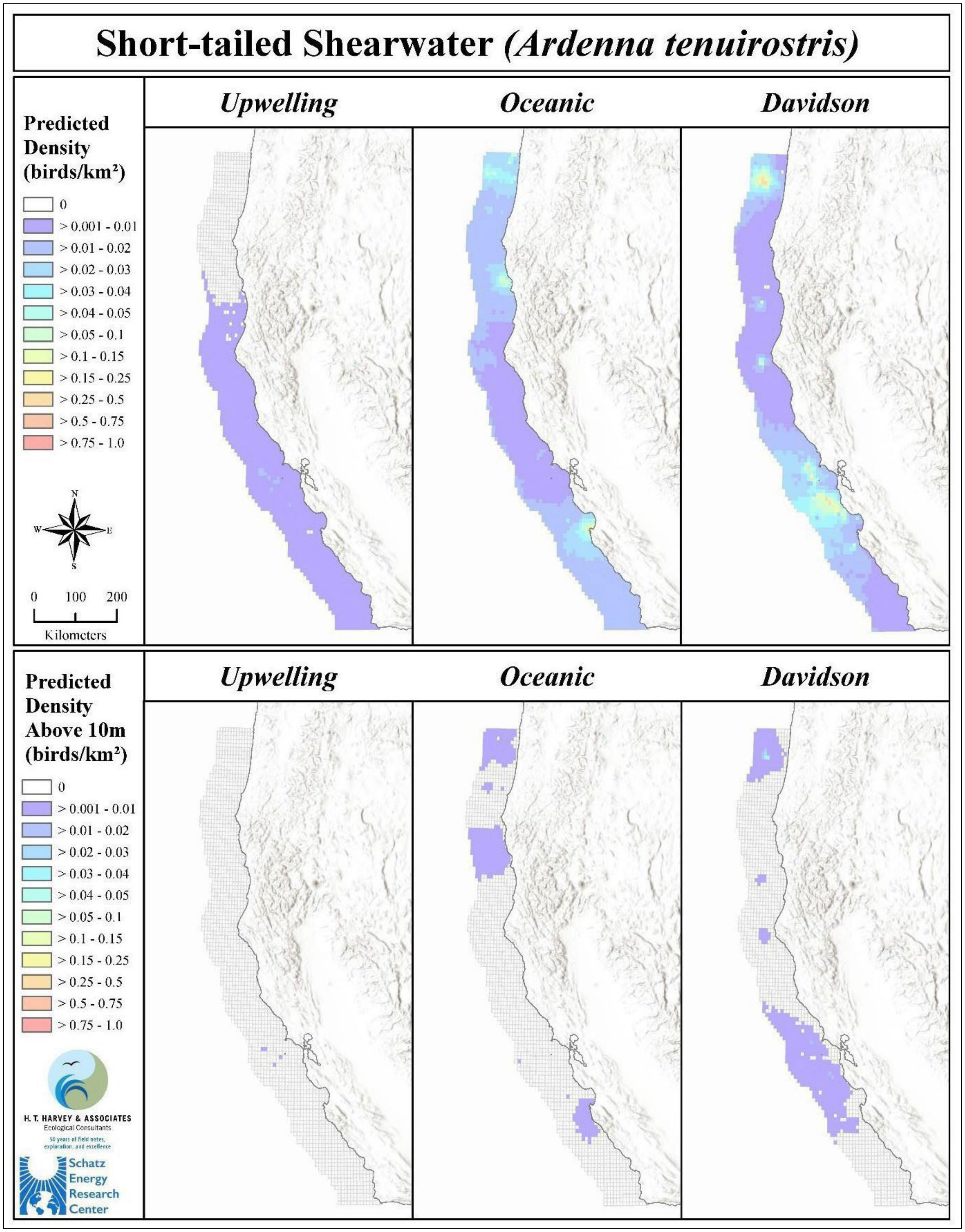

Figure C-6. Short-tailed Shearwater (*Ardenna tenuirostris*)

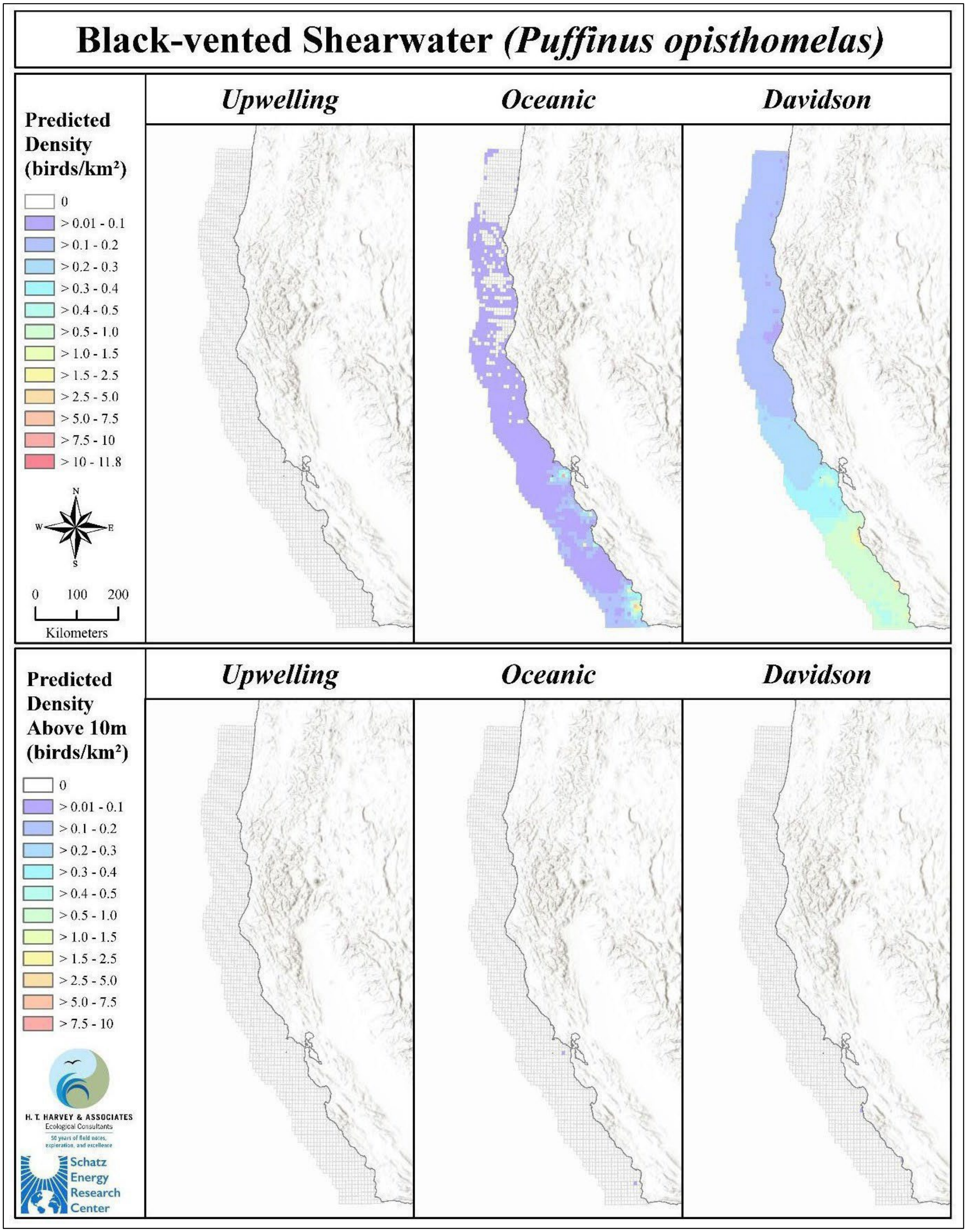

Figure C-7. Black-vented Shearwater (*Puffinus opisthomelas*)

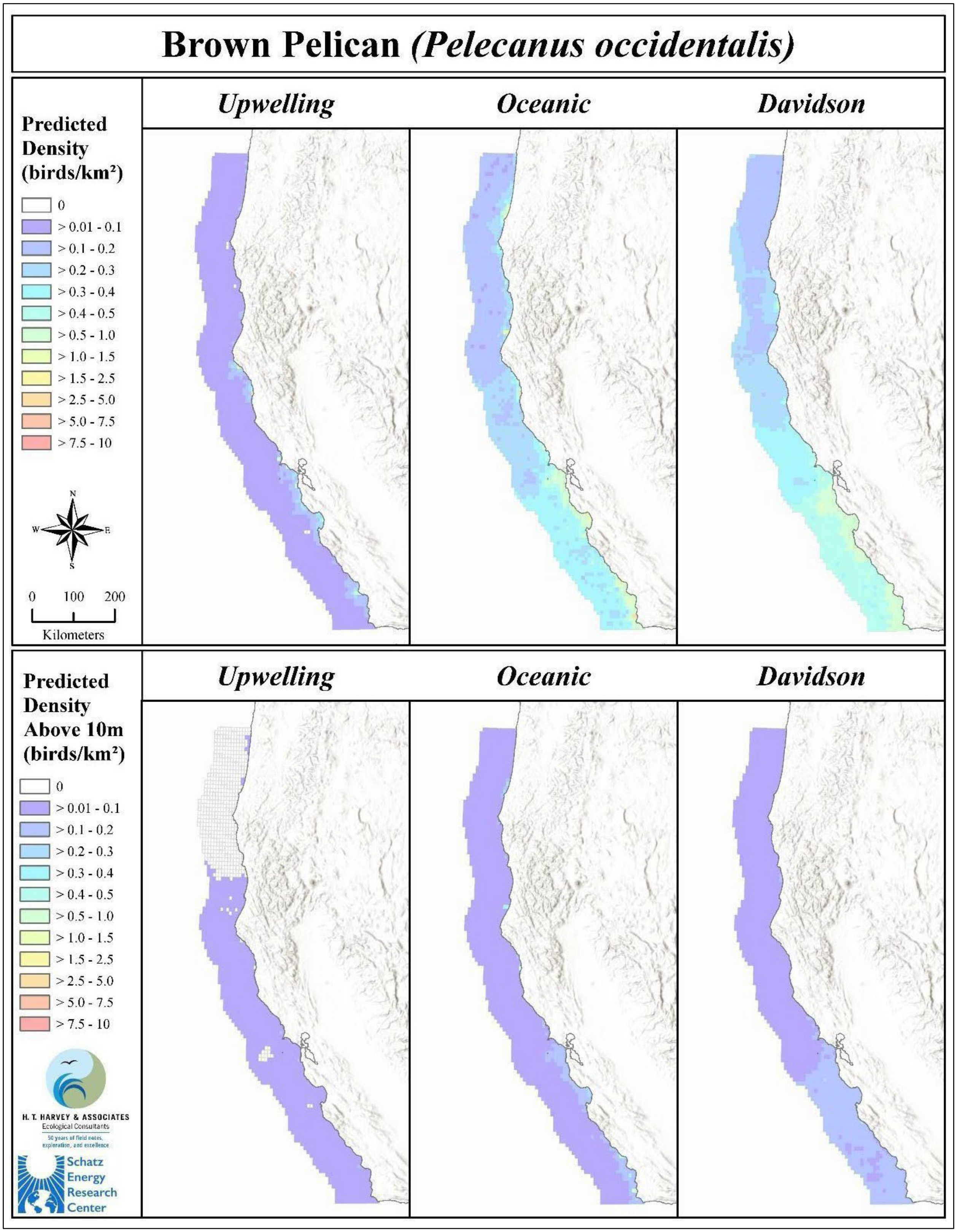

Figure C-8. Brown Pelican (*Pelecanus occidentalis*)

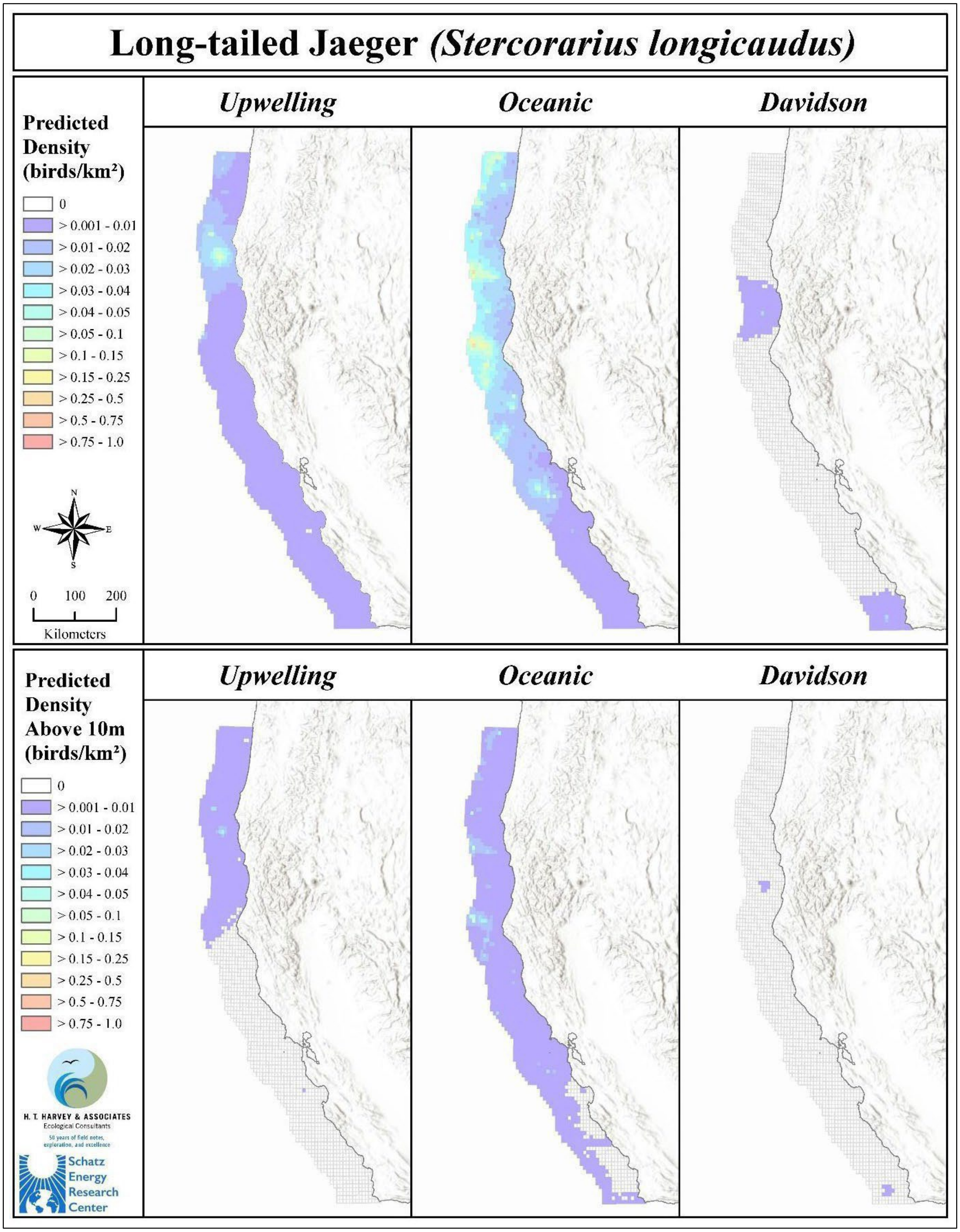

Figure C-9. Long-tailed Jaeger (*Stercorarius longicaudus*)

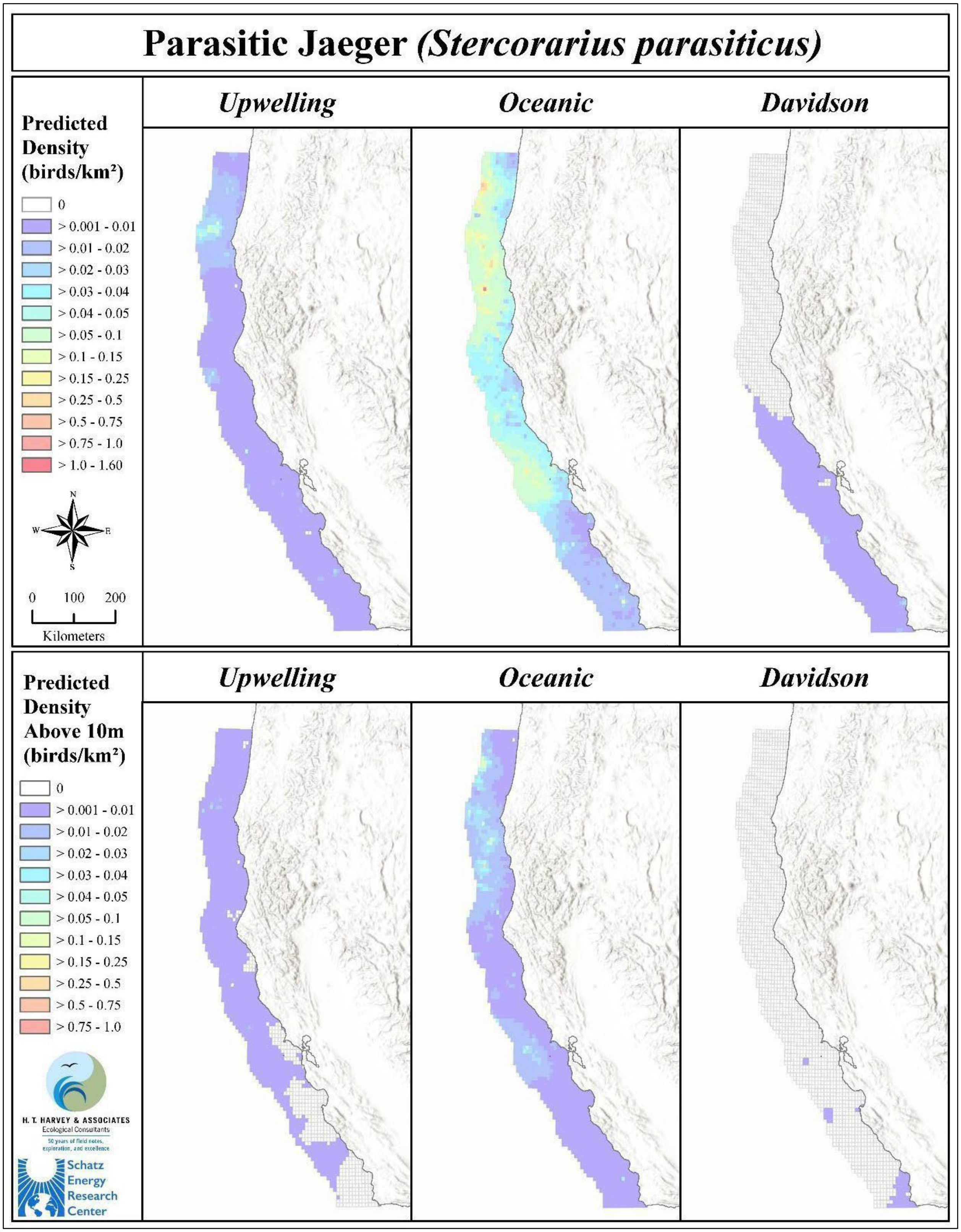

Figure C-10. Parasitic Jaeger (*Stercorarius parasiticus*)

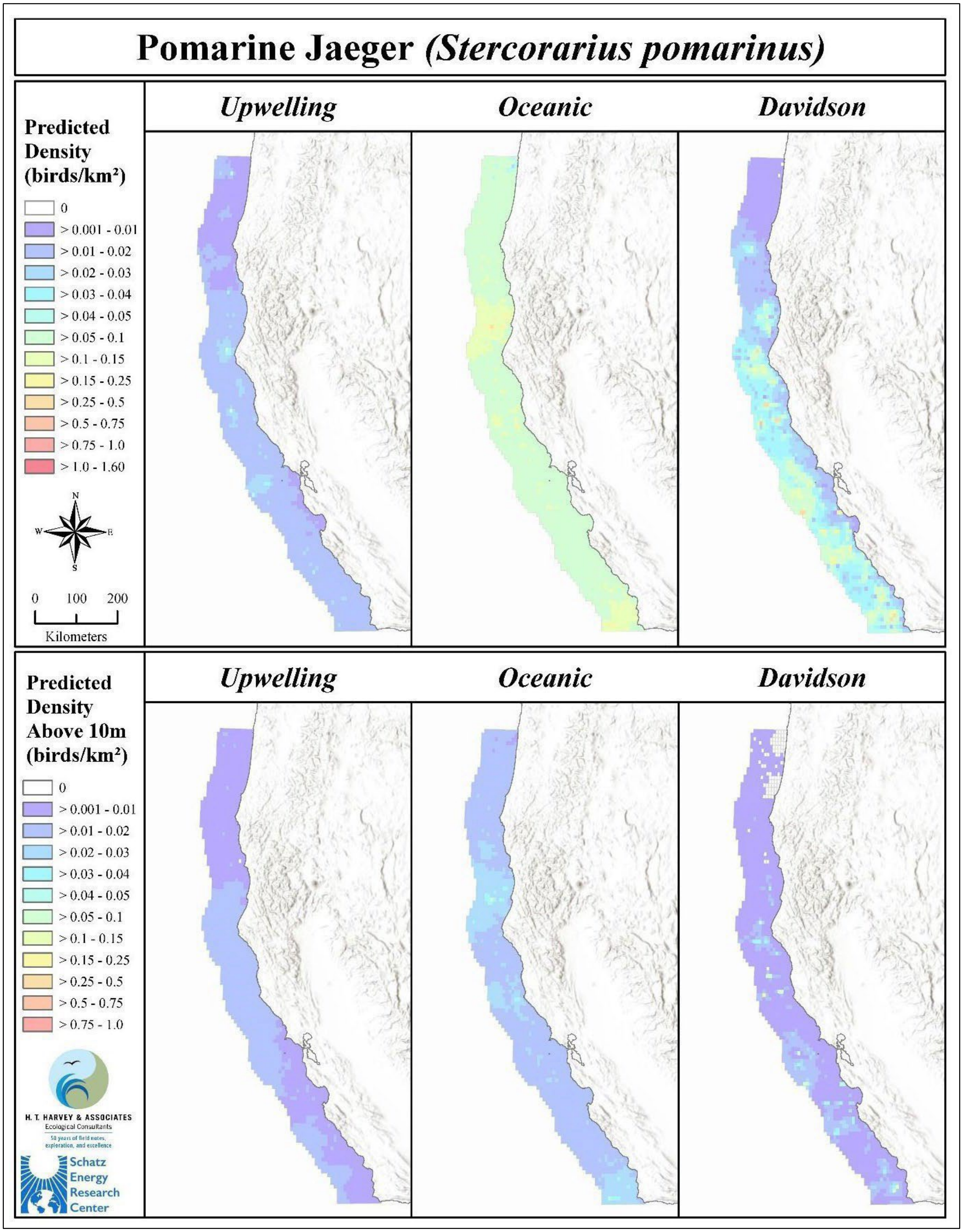

Figure C-11. Pomarine Jaeger (*Stercorarius pomarinus*)

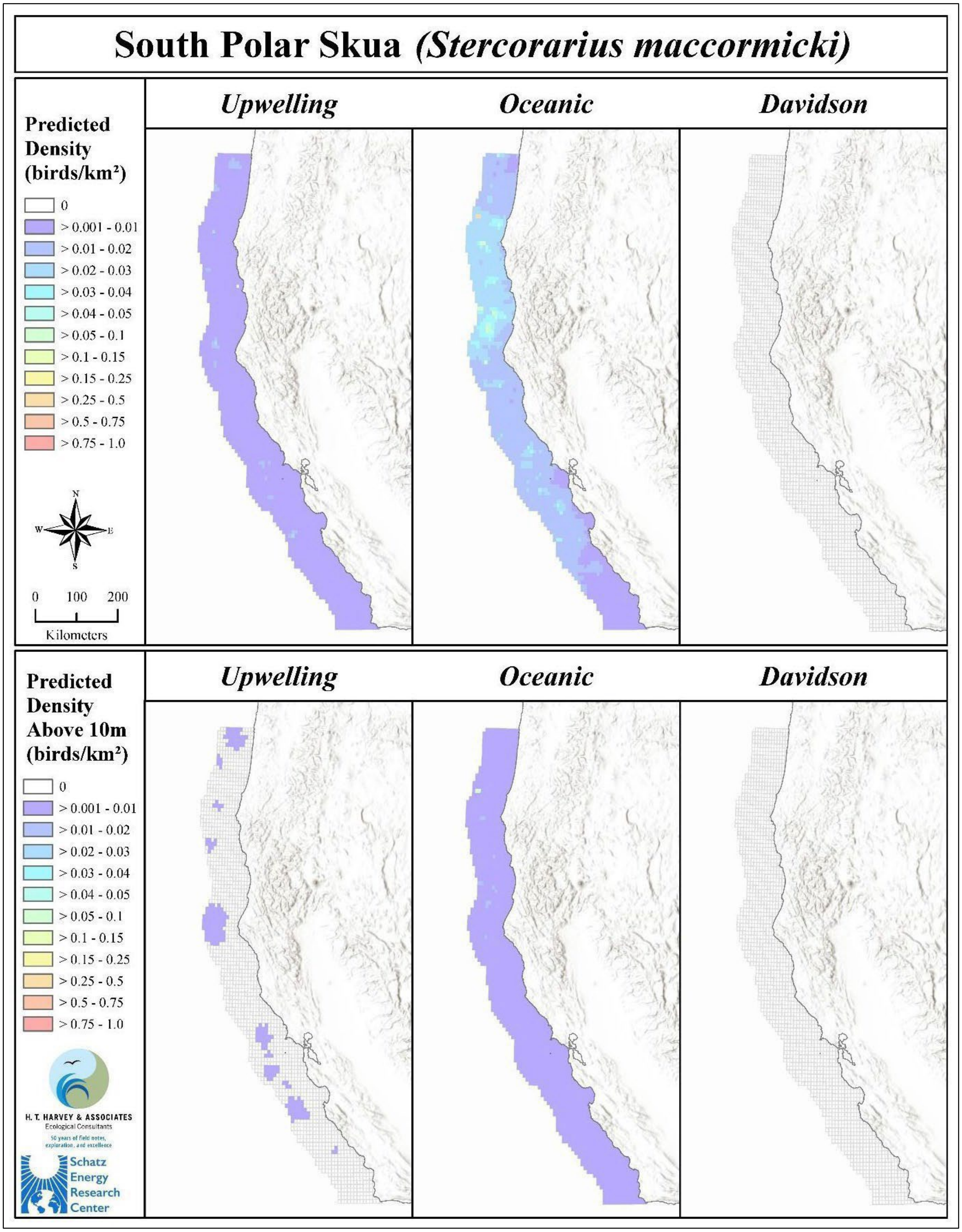

Figure C-12. South Polar Skua (*Stercorarius maccormicki*)

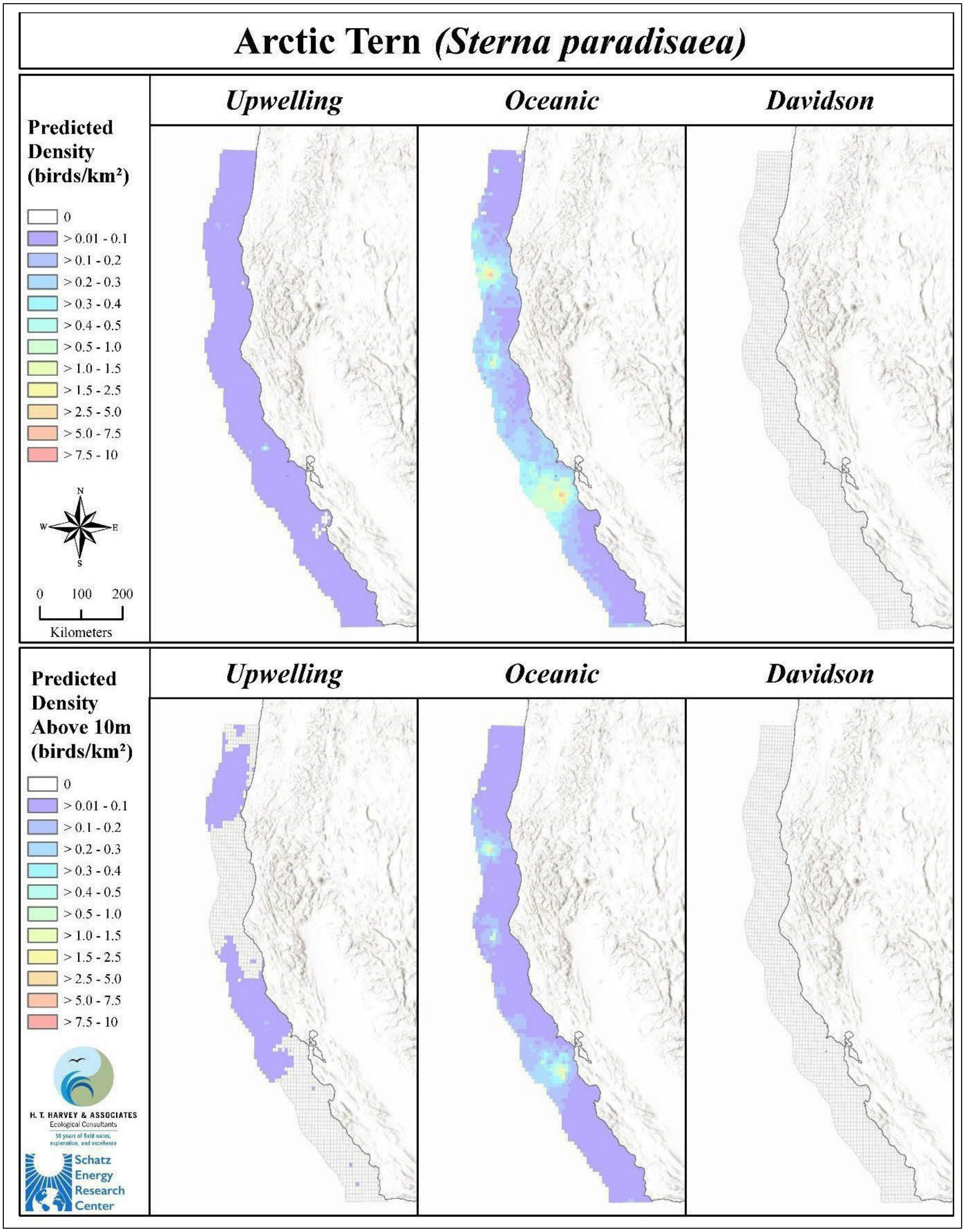

Figure C-13. Arctic Tern (*Sterna paradisaea*)

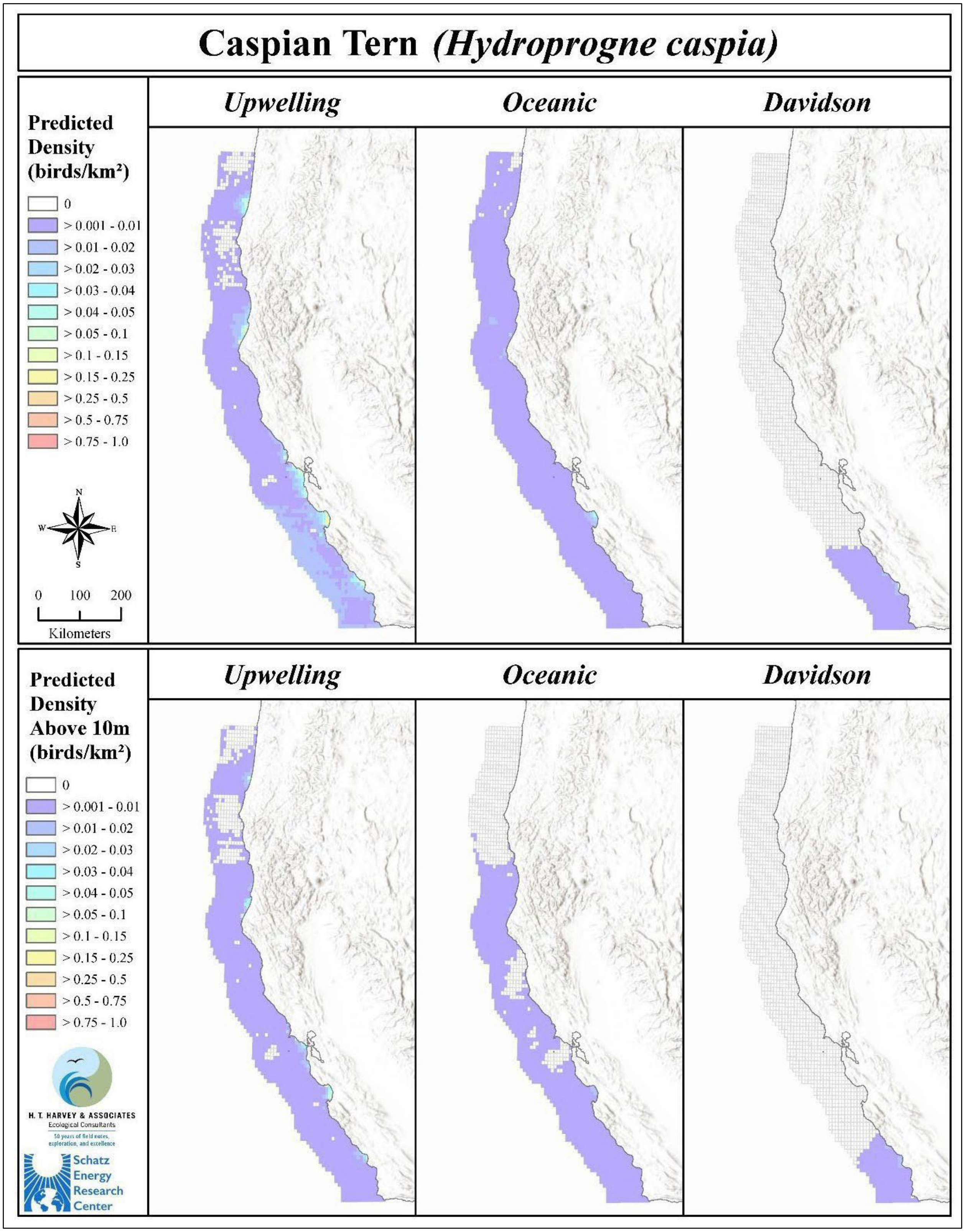

Figure C-14. Caspian Tern (*Hydroprogne caspia*)

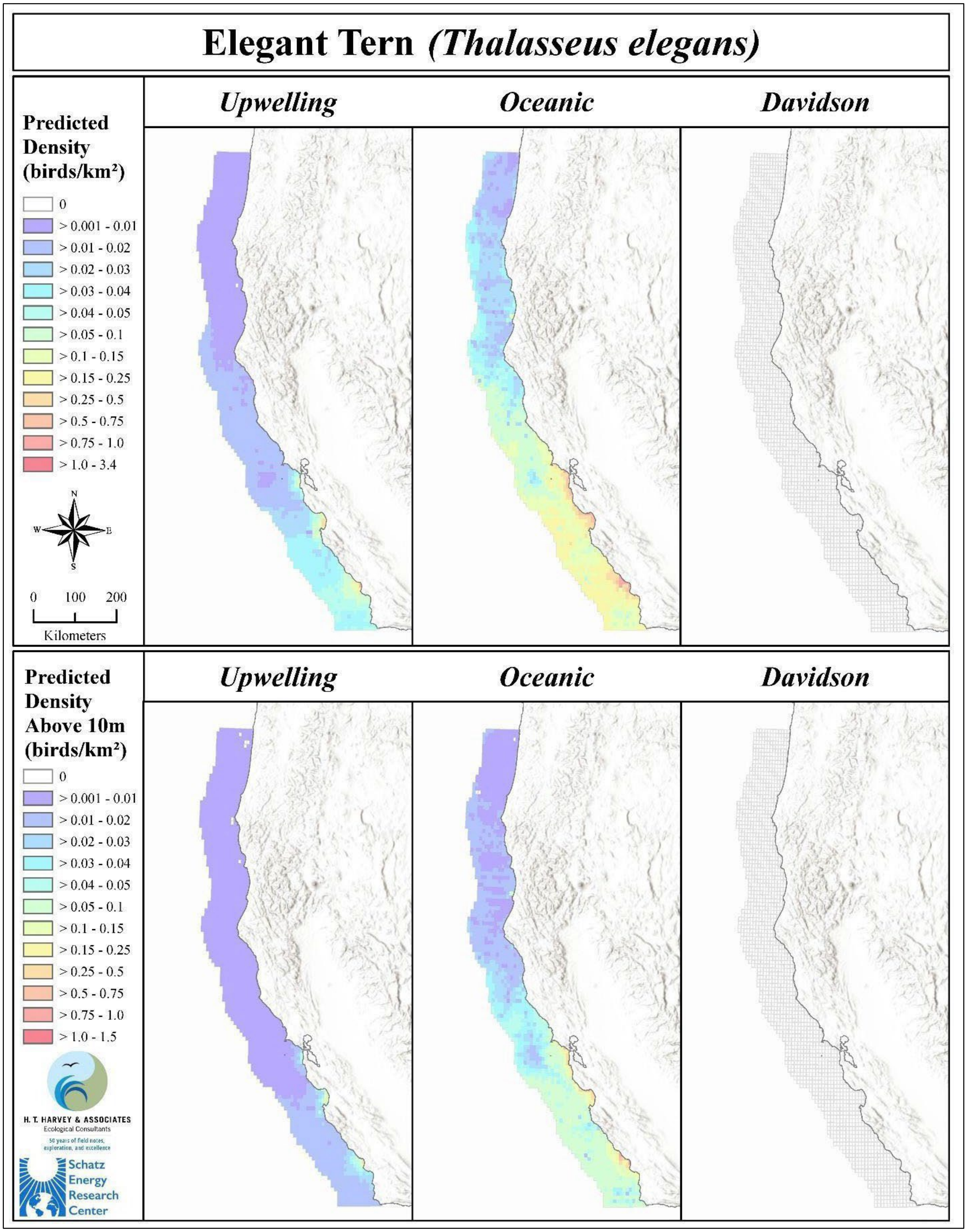

Figure C-15. Elegant Tern (*Thalasseus elegans*)

Appendix D. Leave-One-Out Cross Validation Metrics and Maps for 2D Density Predictions

Table D-1. Leave-One-Out Cross Validation Metrics

Flight Group	Common (Latin) Name	Season	Residual Value (Individuals Observed - Individuals Predicted) Min	2.50%	Mean	Median	97.5%	Max	SD
Small Albatrosses	Black-footed Albatross *(Phoebastria nigripes)*	Upwelling	-15.6	-1	0	-0.2	1.8	149.3	3.2
		Oceanic	-4.5	-0.4	0	0	0.9	37.8	0.9
		Davidson	-1.1	-0.1	0	0	0	11.8	0.4
	Laysan Albatross *(Phoebastria immutabilis)*	Upwelling	-0.1	0	0	0	0	7	0.1
		Oceanic	0	0	0	0	0	1	0
		Davidson	-0.1	0	0	0	0	4	0.1
Fulmars	Northern Fulmar *(Fulmarus glacialis)*	Upwelling	-3.5	-0.6	0	-0.2	1.8	92.6	1.8
		Oceanic	-25.9	-1.8	0	-0.3	3.7	81.9	2.8
		Davidson	-21.1	-1.9	0	-0.8	4	1002.3	18.4
Surface-Feeding Shearwater	Buller's Shearwater *(Ardenna bulleri)*	Upwelling	-0.8	-0.1	0	0	0	10	0.2
		Oceanic	-11.7	-1.4	0	-0.4	2.2	1002.6	14.3
		Davidson	0	0	0	0	0	1	0
	Pink-footed Shearwater *(Ardenna creatopus)*	Upwelling	-5.8	-0.7	0	-0.3	2.4	132.9	2.5
		Oceanic	-14.3	-1.6	0	-0.4	3.2	319.2	5.8
		Davidson	-0.4	-0.1	0	0	0	3.9	0.1
Larger Diving Shearwater	Sooty Shearwater *(Ardenna grisea)*	Upwelling	-311.9	-51.9	-0.4	-11.2	91.6	15254.6	197.9
		Oceanic	-165.5	-31.3	-1.3	-9.7	24.5	9166.3	184.1
		Davidson	-1.7	-0.2	0	0	0	65	1.2
	Short-tailed Shearwater *(Ardenna tenuirostris)*	Upwelling	-0.1	0	0	0	0	2.5	0.1
		Oceanic	-0.8	-0.1	0	0	0	54	0.8
		Davidson	-0.4	-0.1	0	0	0	5	0.2

Flight Group	Common (Latin) Name	Season	Residual Value (Individuals Observed - Individuals Predicted)						
			Min	2.50%	Mean	Median	97.5%	Max	SD
Smaller Diving Shearwater	Black-vented Shearwater (*Puffinus opisthomelas)*	Upwelling	0	0	0	0	0	2	0
		Oceanic	-4.9	-0.5	0	-0.1	0	66.9	1.5
		Davidson	-8.4	-1.3	0	-0.3	0.4	249.4	6.2
Storm-Petrels	Ashy Storm-Petrel (*Hydrobates homochroa)*	Upwelling	-0.7	-0.2	0	0	0.3	30	0.5
		Oceanic	-4.3	-0.7	0	-0.2	1.2	90.4	2.6
		Davidson	-1.1	-0.1	0	0	0	51	1
	Fork-tailed Storm-Petrel * (*Hydrobates furcatus)*	Upwelling	-39.4	-4.4	0.1	-0.2	0.2	3998	43.9
		Oceanic	-23	-1.2	0	0	0	449.6	7.2
		Davidson	0	0	0	0	0	1	0.1
	Leach's Storm-Petrel (*Hydrobates leucorhous)*	Upwelling	-11.6	-1	0	0	1	74.8	2.1
		Oceanic	-1.3	-0.2	0	0	0	19.5	0.4
		Davidson	-0.3	0	0	0	0	6	0.2
Pelicans	Brown Pelican (*Pelecanus occidentalis)*	Upwelling	-3.6	-0.3	0	-0.1	0.7	34.9	1
		Oceanic	-9.9	-1	0	-0.3	2.8	75.5	2
		Davidson	-2.7	-0.8	0	-0.3	2.6	89.6	2.3
Phalaropes	Phalaropes (*Phalaropus* spp.)	Upwelling	-80.2	-5	0.3	-1.8	16.1	1575.1	28.9
		Oceanic	-60.2	-10.2	-0.1	-4.7	30.6	3943.8	63.5
		Davidson	-23.7	-2.2	0.1	-0.5	4.6	621.7	12.6
Skuas	Long-tailed Jaeger (*Stercorarius longicaudus)*	Upwelling	-0.5	0	0	0	0	21	0.2
		Oceanic	-0.4	-0.1	0	0	0	7	0.2
		Davidson	-0.1	0	0	0	0	1	0
	Parasitic Jaeger (*Stercorarius parasiticus)*	Upwelling	-0.2	0	0	0	0	5	0.1
		Oceanic	-1	-0.1	0	0	0.9	8.3	0.3
		Davidson	0	0	0	0	0	1	0
	Pomarine Jaeger	Upwelling	-0.2	0	0	0	0	6	0.1

Flight Group	Common (Latin) Name	Season	Residual Value (Individuals Observed - Individuals Predicted)						
			Min	2.50%	Mean	Median	97.5%	Max	SD
	(Stercorarius pomarinus)	Oceanic	-0.3	-0.1	0	-0.1	0.9	7.9	0.4
		Davidson	-0.5	-0.1	0	0	0.5	5	0.2
	South Polar Skua *(Stercorarius maccormicki)*	Upwelling	-0.1	0	0	0	0	2	0.1
		Oceanic	-0.1	0	0	0	0	3	0.1
		Davidson	0	0	0	0	0	0	0
Large Gulls	California Gull (*Larus californicus)*	Upwelling	-10.7	-1.7	0	-0.4	2.6	303.1	5.5
		Oceanic	-72.4	-12.5	-0.1	-1.5	15.5	592	21.6
		Davidson	-77.1	-15.3	-0.5	-2.8	34.3	706.3	28.5
	Herring Gull (*Larus argentatus)*	Upwelling	-1.1	-0.2	0	-0.1	0.9	114.9	1.5
		Oceanic	-34	-0.8	0	-0.1	0.9	202.9	3.9
		Davidson	-12.7	-2.2	0	-1.1	5.6	663	15.6
	Western Gull (*Larus occidentalis)*	Upwelling	-30.1	-2.9	-0.1	-0.8	5.3	899.8	11.2
		Oceanic	-43.2	-4.5	-0.1	-0.8	8.6	301.2	8.6
		Davidson	-23.2	-3.6	-0.2	-1.2	9.9	252.5	8.2
	Glaucous-winged Gull (*Larus glaucescens)*	Upwelling	-0.2	-0.1	0	0	0.4	6.9	0.2
		Oceanic	-2.4	-0.3	0	0	0.9	20	0.6
		Davidson	-10	-1.2	0	-0.4	3.3	92.4	2.7
	Heermann's Gull *(Larus heermanni)*	Upwelling	-2.6	-0.2	0	0	0.4	60.8	0.8
		Oceanic	-4	-0.9	0	-0.2	1.7	82.6	2.3
		Davidson	-2.8	-0.6	0	-0.2	1.2	61.6	2.1
Medium Gulls	Black-legged Kittiwake Rissa tridactyla)	Upwelling	-12.4	-2	0	-0.4	2.3	338.8	7.2
		Oceanic	-0.2	-0.1	0	0	0	15	0.4
		Davidson	-13.9	-1.9	0	-0.8	4.6	687	13.2
	Short-billed Gull (*Larus brachyramphous)*	Upwelling	-0.2	0	0	0	0	8	0.1
		Oceanic	-0.2	0	0	0	0	12	0.2

Flight Group	Common (Latin) Name	Season	Residual Value (Individuals Observed - Individuals Predicted)						
			Min	2.50%	Mean	Median	97.5%	Max	SD
		Davidson	-0.3	-0.1	0	0	0	17	0.5
Small Gulls	Bonaparte's Gull (*Chroicocephalus* philadelphia)	Upwelling	-22	-0.8	0	-0.1	0	890.7	10.1
		Oceanic	-23.2	-1.1	0.1	-0.3	0.7	1003.7	14.3
		Davidson	-5.8	-0.7	0	-0.1	0	250.8	4.7
	Sabine's Gull (*Xema sabini)*	Upwelling	-1.2	-0.3	0	-0.1	0.8	84.7	1.5
		Oceanic	-1.5	-0.4	0	-0.1	1.4	33.1	1.2
		Davidson	0	0	0	0	0	0.5	0
Terns	Arctic Tern (*Sterna paradisaea)*	Upwelling	-0.6	-0.1	0	0	0	45	0.6
		Oceanic	-15.8	-1.1	0	-0.1	0.5	457.6	6.8
		Davidson	0	0	0	0	0	0	0
	Caspian Tern (*Hydroprogne* caspia)	Upwelling	-0.7	-0.1	0	0	0	5	0.2
		Oceanic	-0.1	0	0	0	0	2	0.1
		Davidson	-0.1	0	0	0	0	2	0
	Elegant Tern (*Thalasseus elegans)*	Upwelling	-1.6	-0.1	0	0	0	50	0.7
		Oceanic	-4.3	-0.8	0	-0.1	0.6	37.8	1.5
		Davidson	0	0	0	0	0	0	0
Cormorants	Brandt's Cormorant (*Urile penicillatus)*	Upwelling	-28.2	-2.8	-0.2	-0.9	1.5	3999.4	43.7
		Oceanic	-33.1	-2	0	-0.4	4.1	549.6	10.3
		Davidson	-16.5	-2	-0.1	-0.6	5.3	160.3	4.8
	Double-crested Cormorant (Nannopterum *auritum)*	Upwelling	-0.4	0	0	0	0	13	0.2
		Oceanic	-0.3	0	0	0	0	8	0.1
		Davidson	-1.9	-0.1	0	0	0	40	0.8
	Pelagic Cormorant (*Urile pelagicus)*	Upwelling	-0.5	-0.1	0	0	0	5.9	0.2
		Oceanic	-0.6	0	0	0	0	3	0.1
		Davidson	-0.5	-0.1	0	0	0	6.9	0.2

Flight Group	Common (Latin) Name	Season	Residual Value (Individuals Observed - Individuals Predicted)						
			Min	2.50%	Mean	Median	97.5%	Max	SD
Large Acids	Common Murre (*Uria aalge)*	Upwelling	-128.3	-19.1	-0.5	-4.2	44.4	1979.8	42.2
		Oceanic	-126.9	-28.2	-0.6	-5.3	65.6	1035.8	42.4
		Davidson	-89.6	-26.9	-1.1	-9.4	82.3	1055.9	56.4
	Tufted Puffin (*Fratercula cirrhata)*	Upwelling	-0.2	0	0	0	0	8	0.1
		Oceanic	-0.1	0	0	0	0	2	0.1
		Davidson	-0.1	0	0	0	0	2	0
Medium Alcids	Rhinoceros Auklet (*Cerorhinca monocerrata)*	Upwelling	-3.6	-1.1	0	-0.6	4.2	173	3.7
		Oceanic	-5.2	-1.7	-0.1	-0.5	5.5	88.5	3.1
		Davidson	-33.5	-5.4	-0.2	-1.4	10.3	1037.4	21.1
	Pigeon Guillemot (*Cepphus columba)*	Upwelling	-1.9	-0.2	0	0	0	7.2	0.2
		Oceanic	-0.2	0	0	0	0	3	0.1
		Davidson	-2.5	-0.3	0	0	0	119.9	2.3
Small Alcids	Cassin's Auklet (*Ptychoramphus*	Upwelling	-92.3	-6.5	-0.1	-0.9	8.4	465.7	14.6
		Oceanic	-37.9	-5.3	-0.1	-1.3	14.4	579.5	13
		Davidson	-21.6	-4.3	0.2	-0.8	11.1	295.7	9.2
	Marbled Murrelet (*Brachyramphus*	Upwelling	-1	-0.1	0	0	0	5.1	0.2
		Oceanic	-2	-0.2	0	0	0	22.9	0.6
		Davidson	-6	-0.7	0	-0.1	1.5	61.6	1.5
	Scripps's, Guadalupe, Craveri's Murrelet (*Synthliboramphus* spp.)	Upwelling	0	0	0	0	0	2	0.1
		Oceanic	-0.2	0	0	0	0	3	0.1
		Davidson	-0.1	0	0	0	0	5	0.1
Loons, Grebes, Ducks	Western and Clark's Grebes (*Aechmophorus sp.)*	Upwelling	-158.6	-7.1	0	-0.1	1.7	566.1	13.8
		Oceanic	-183.6	-8.8	0	-0.3	4.9	915.7	19.5
		Davidson	-133.7	-24.3	-0.9	-3.6	45.8	1076.1	33.6

Flight Group	Common (Latin) Name	Season	Residual Value (Individuals Observed - Individuals Predicted)						
			Min	2.50%	Mean	Median	97.5%	Max	SD
	Surf Scoter (*Melanitta perspicillata)*	Upwelling	-9.3	-1	0	-0.1	0	100.9	3.2
		Oceanic	-36.6	-2.1	0.1	-0.3	-0.1	763.8	12.5
		Davidson	-138.4	-24	-0.6	-1.4	29	647.3	24.9
	Pacific Loon (*Gavia pacifica)*	Upwelling	-3.9	-0.8	0	-0.2	1	124.4	3.2
		Oceanic	-3.6	-0.7	0	-0.1	0.8	106.3	2.2
		Davidson	-3.1	-1.1	0	-0.3	2.8	28.1	1.7
	Common Loon (*Gavia immer)*	Upwelling	-0.6	-0.1	0	0	0	30.5	0.4
		Oceanic	-0.6	-0.1	0	0	0	24.9	0.4
		Davidson	-4	-0.6	0	-0.1	1.3	25.1	0.9
	Red-throated Loon (*Gavia stellata)*	Upwelling	-0.3	0	0	0	0	4	0.1
		Oceanic	-0.1	0	0	0	0	3	0.1
		Davidson	-1.1	-0.3	0	-0.1	0.9	14.9	0.6

Black-footed Albatross *(Phoebastria nigripes)*

Upwelling ***Oceanic*** ***Davidson***

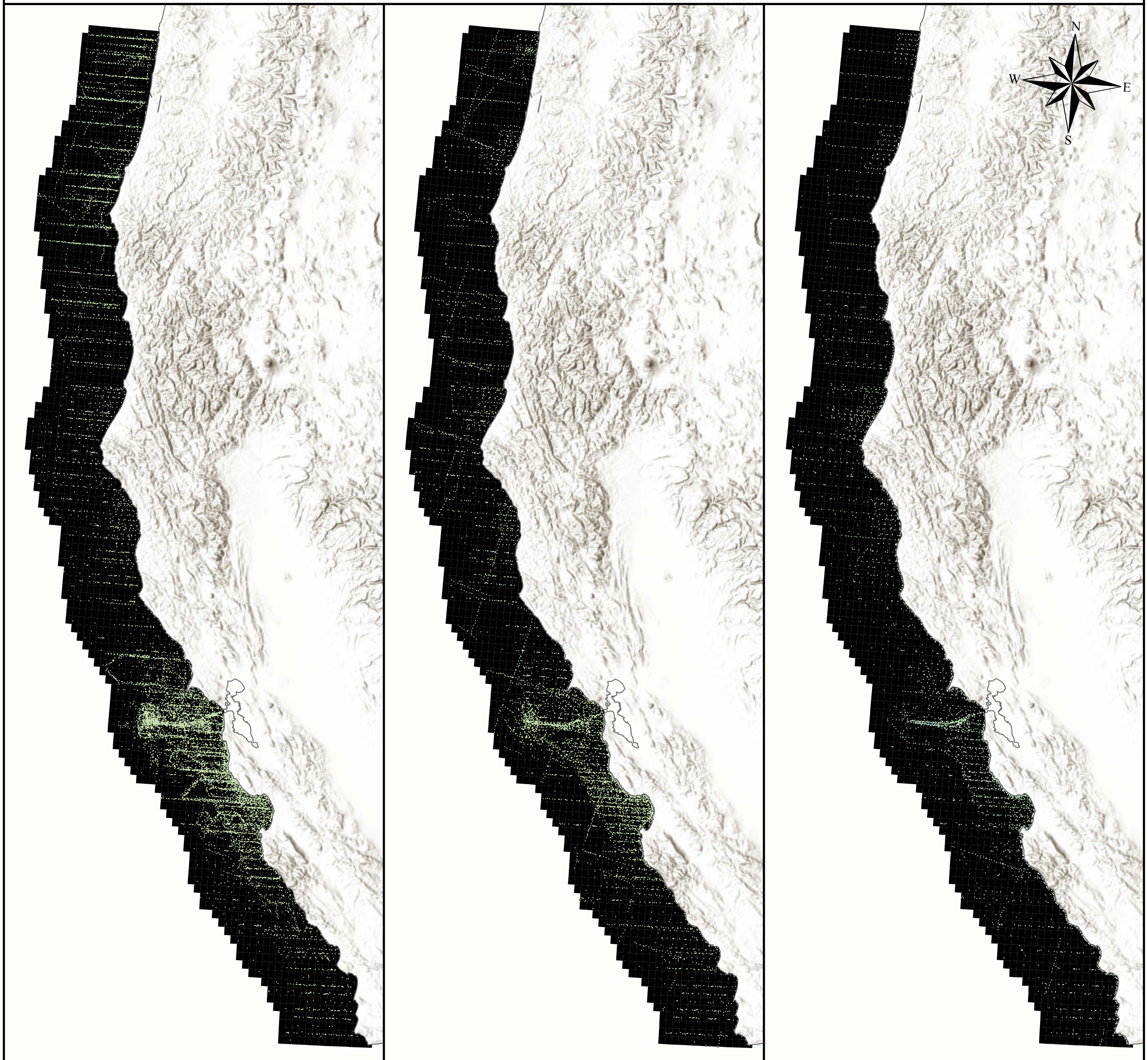

Standardized Residual Value (z-scores)

x < - 2.75	-0.75 < x < -0.25	1.75 < x < 2.25
-2.75 < x < -2.25	-0.25 < x < 0.25	2.25 < x < 2.75
-2.25 < x < -1.75	0.25 < x < 0.75	x > 2.75
-1.75 < x < -1.25	0.75 < x < 1.25	study area
-1.25 < x < -0.75	1.25< x < 1.75	

0 25 50 100
Kilometers

Schatz Energy Research Center

H. T. HARVEY & ASSOCIATES
Ecological Consultants
50 years of field notes, exploration, and excellence

Laysan Albatross *(Phoebastria immutabilis)*

Upwelling | ***Oceanic*** | ***Davidson***

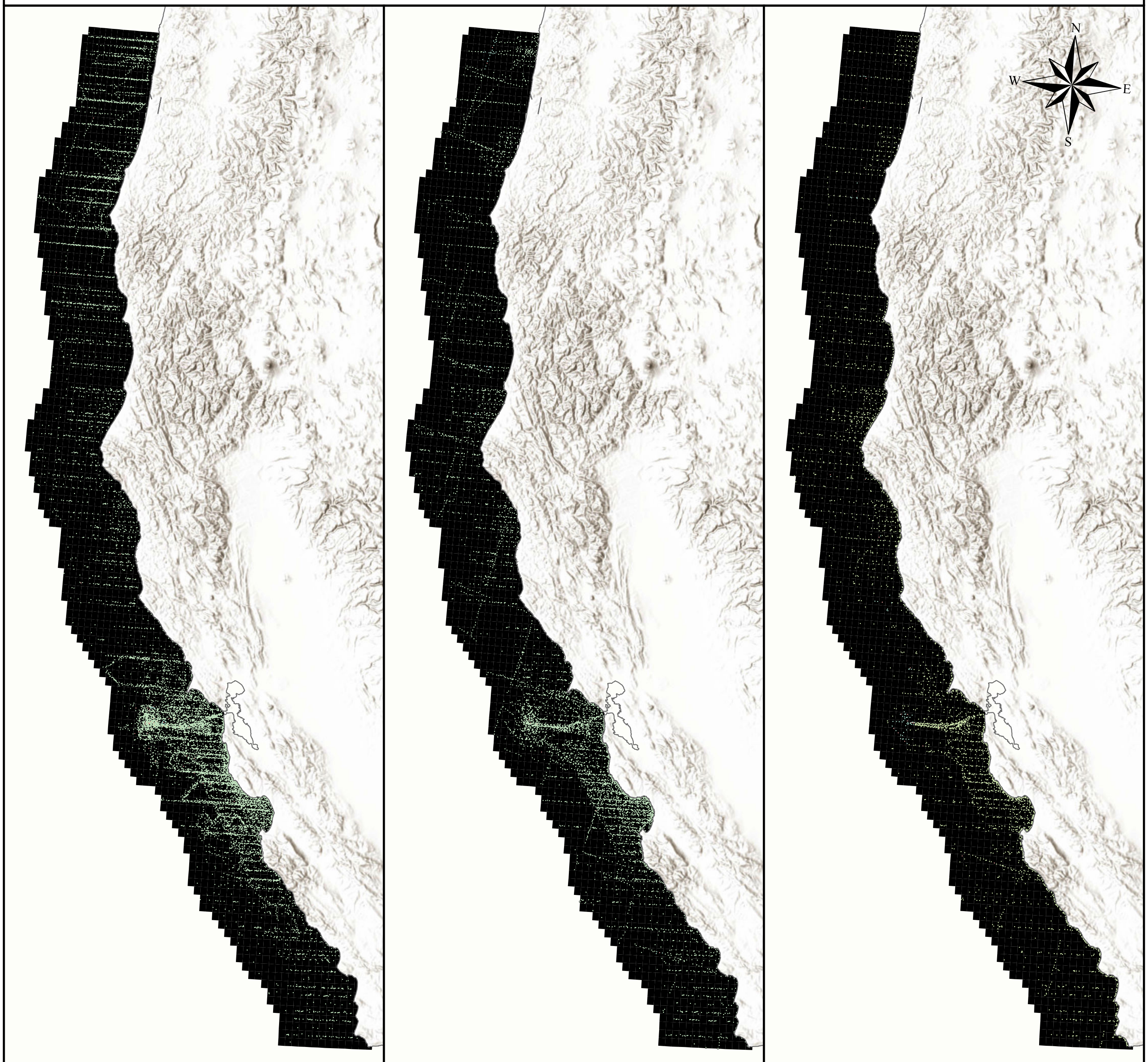

Standardized Residual Value (z-scores)

- x < - 2.75
- -2.75 < x < -2.25
- -2.25 < x < -1.75
- -1.75 < x < -1.25
- -1.25 < x < -0.75
- -0.75 < x < -0.25
- -0.25 < x < 0.25
- 0.25 < x < 0.75
- 0.75 < x < 1.25
- 1.25< x < 1.75
- 1.75 < x < 2.25
- 2.25 < x < 2.75
- x > 2.75
- study area

0 25 50 100 Kilometers

Schatz Energy Research Center

H. T. HARVEY & ASSOCIATES
Ecological Consultants
50 years of field notes, exploration, and excellence

Northern Fulmar *(Fulmarus glacialis)*

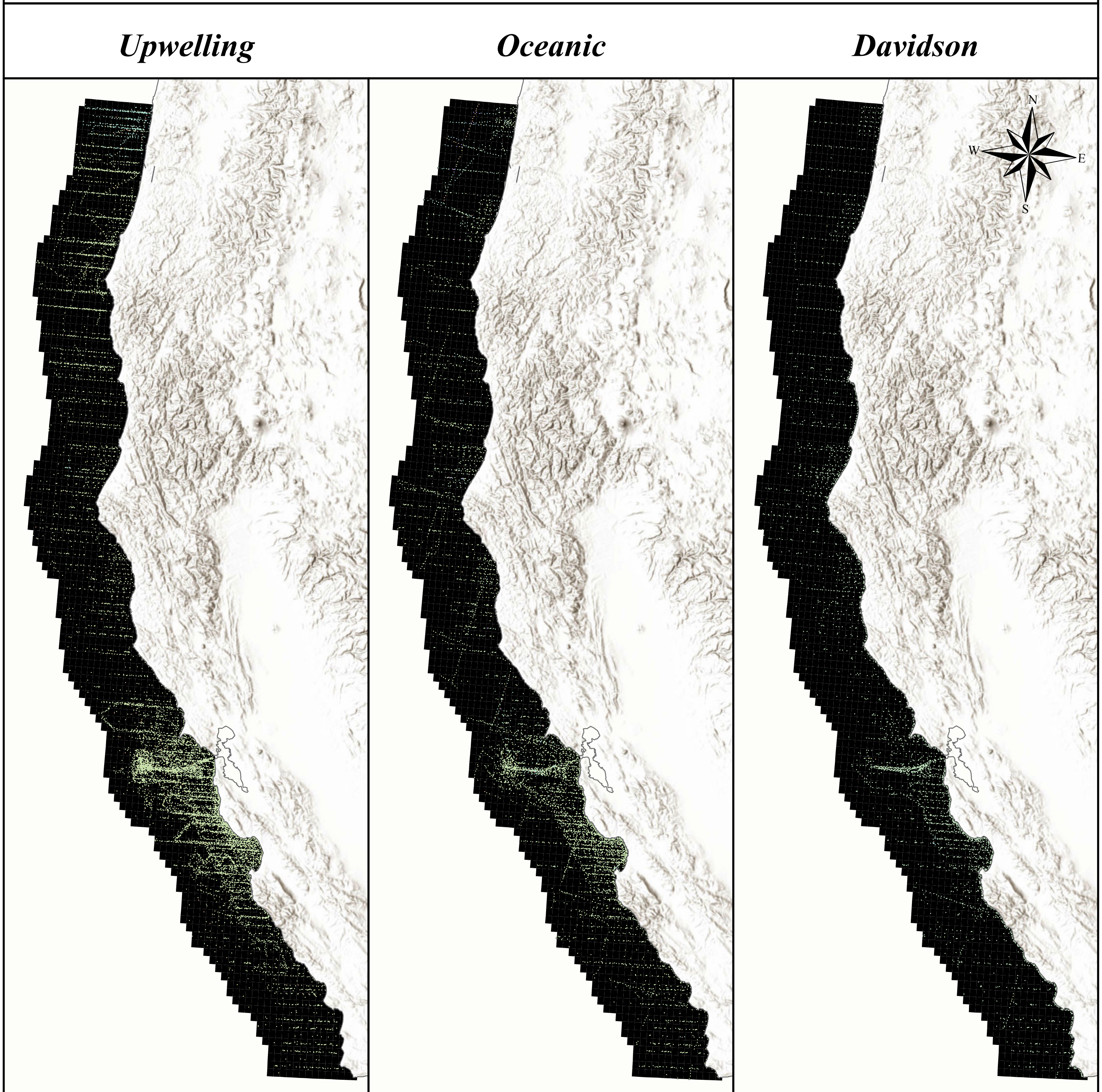

Standardized Residual Value (z-scores)

x < - 2.75	-0.75 < x < -0.25	1.75 < x < 2.25
-2.75 < x < -2.25	-0.25 < x < 0.25	2.25 < x < 2.75
-2.25 < x < -1.75	0.25 < x < 0.75	x > 2.75
-1.75 < x < -1.25	0.75 < x < 1.25	study area
-1.25 < x < -0.75	1.25< x < 1.75	

0 25 50 100 Kilometers

Schatz Energy Research Center

H. T. HARVEY & ASSOCIATES
Ecological Consultants
50 years of field notes, exploration, and excellence

Buller's Shearwater *(Ardenna bulleri)*

Upwelling ***Oceanic*** ***Davidson***

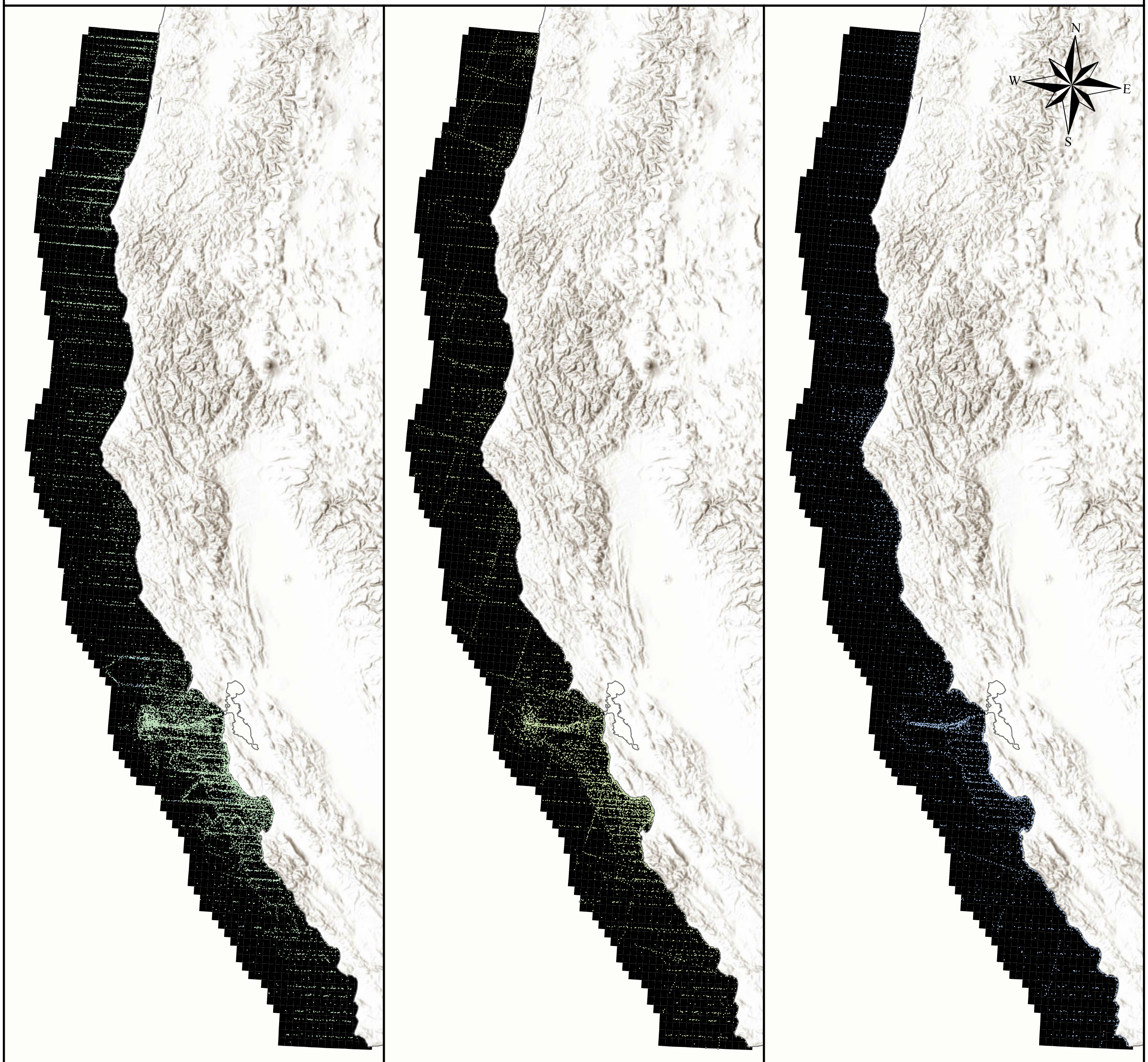

Standardized Residual Value (z-scores)

x < - 2.75	-0.75 < x < -0.25	1.75 < x < 2.25
-2.75 < x < -2.25	-0.25 < x < 0.25	2.25 < x < 2.75
-2.25 < x < -1.75	0.25 < x < 0.75	x > 2.75
-1.75 < x < -1.25	0.75 < x < 1.25	study area
-1.25 < x < -0.75	1.25< x < 1.75	

0 25 50 100
Kilometers

Schatz Energy Research Center

H. T. HARVEY & ASSOCIATES
Ecological Consultants
50 years of field notes, exploration, and excellence

Pink-footed Shearwater *(Ardenna creatopus)*

Upwelling	*Oceanic*	*Davidson*

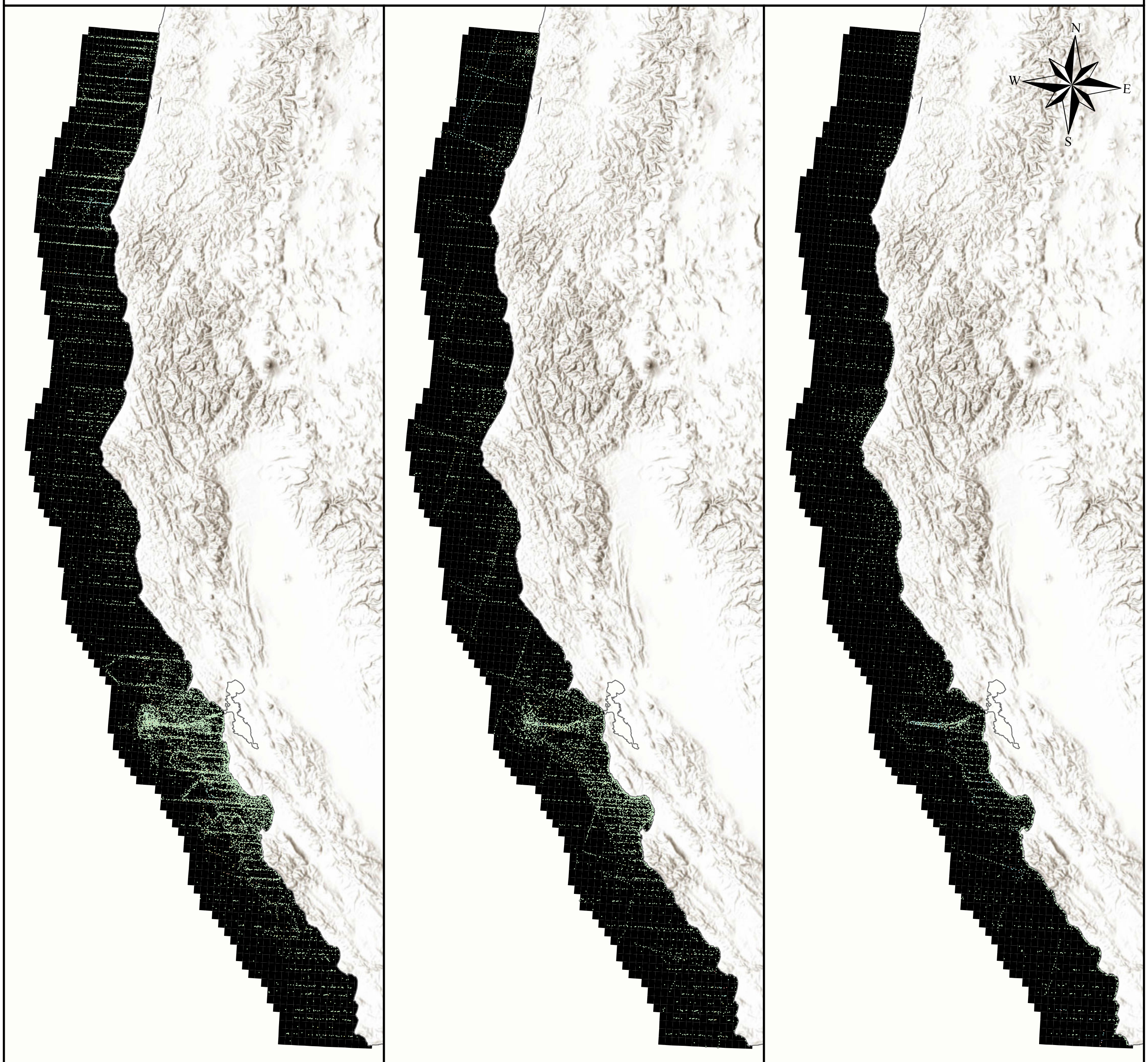

Standardized Residual Value (z-scores)

x < - 2.75	-0.75 < x < -0.25	1.75 < x < 2.25
-2.75 < x < -2.25	-0.25 < x < 0.25	2.25 < x < 2.75
-2.25 < x < -1.75	0.25 < x < 0.75	x > 2.75
-1.75 < x < -1.25	0.75 < x < 1.25	study area
-1.25 < x < -0.75	1.25< x < 1.75	

0 25 50 100
Kilometers

Schatz Energy Research Center

H. T. HARVEY & ASSOCIATES
Ecological Consultants
50 years of field notes, exploration, and excellence

Sooty Shearwater *(Ardenna grisea)*

Upwelling	*Oceanic*	*Davidson*

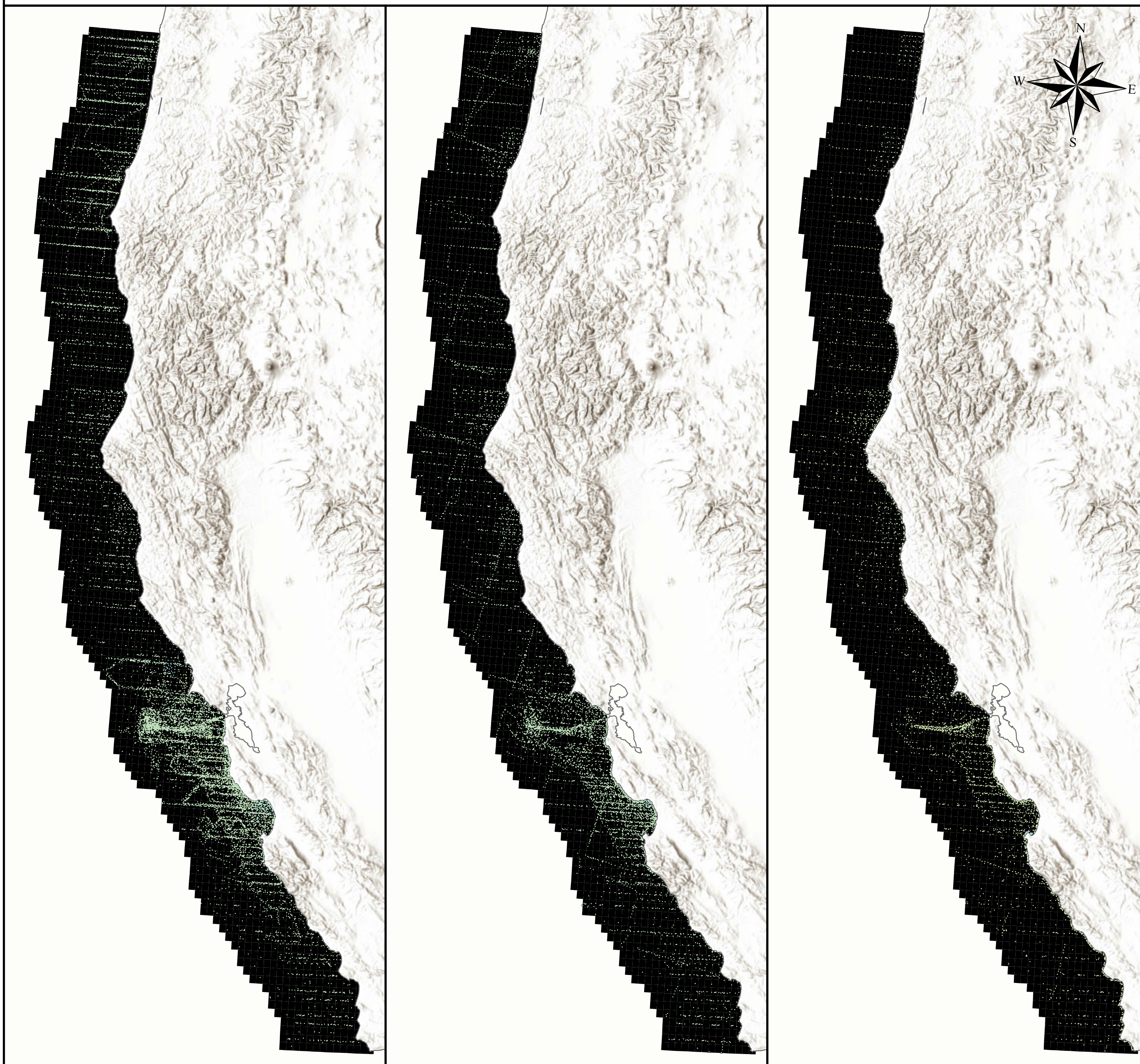

Standardized Residual Value (z-scores)

x < - 2.75	-0.75 < x < -0.25	1.75 < x < 2.25
-2.75 < x < -2.25	-0.25 < x < 0.25	2.25 < x < 2.75
-2.25 < x < -1.75	0.25 < x < 0.75	x > 2.75
-1.75 < x < -1.25	0.75 < x < 1.25	study area
-1.25 < x < -0.75	1.25< x < 1.75	

0 25 50 100
Kilometers

Schatz Energy Research Center

H. T. HARVEY & ASSOCIATES
Ecological Consultants
50 years of field notes, exploration, and excellence

Short-tailed Shearwater *(Ardenna tenuirostris)*

Upwelling | ***Oceanic*** | ***Davidson***

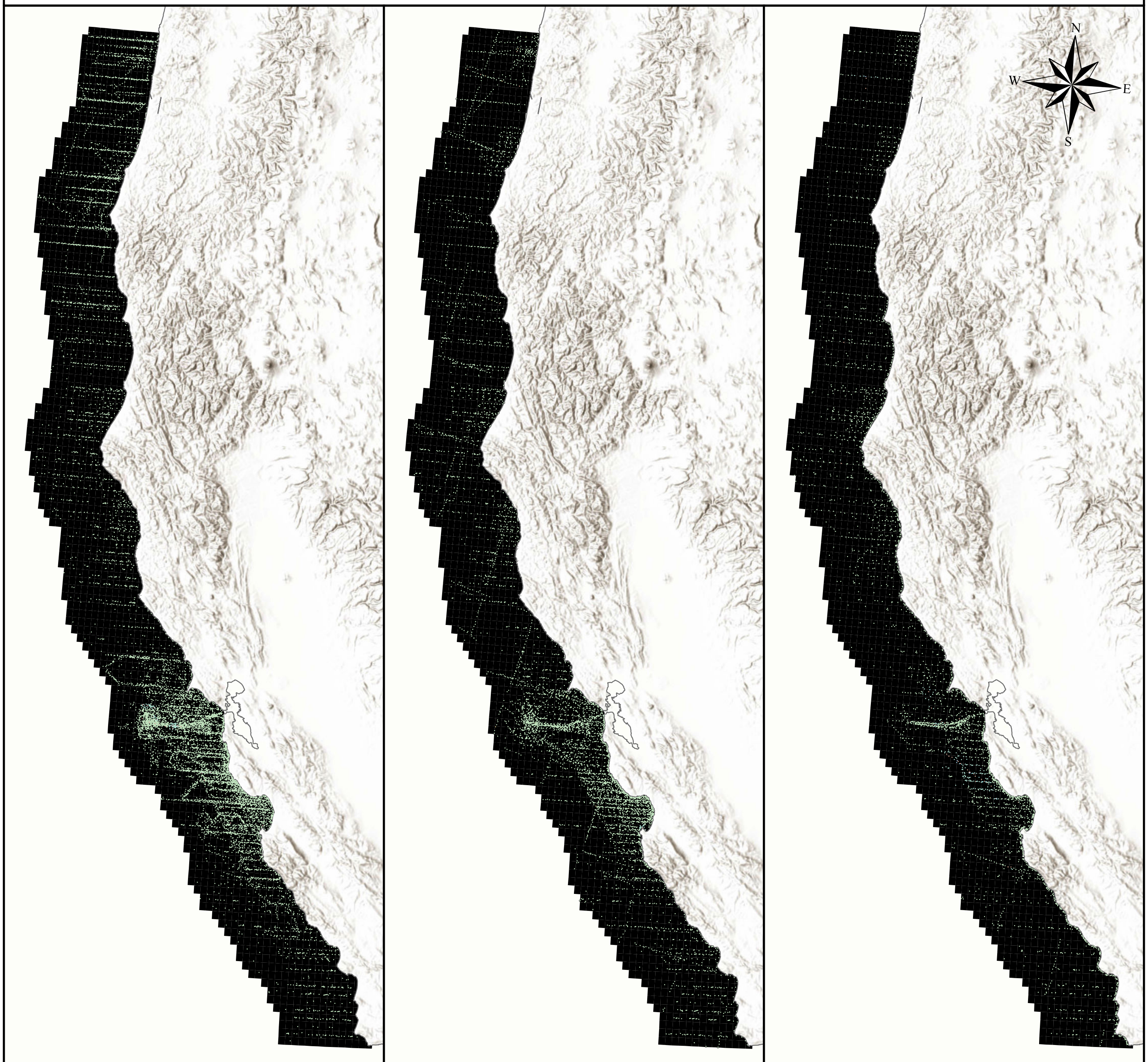

Standardized Residual Value (z-scores)

- x < - 2.75
- -2.75 < x < -2.25
- -2.25 < x < -1.75
- -1.75 < x < -1.25
- -1.25 < x < -0.75
- -0.75 < x < -0.25
- -0.25 < x < 0.25
- 0.25 < x < 0.75
- 0.75 < x < 1.25
- 1.25< x < 1.75
- 1.75 < x < 2.25
- 2.25 < x < 2.75
- x > 2.75
- study area

0 25 50 100
Kilometers

Schatz Energy Research Center

H. T. HARVEY & ASSOCIATES
Ecological Consultants
50 years of field notes, exploration, and excellence

Black-vented Shearwater *(Puffinus opisthomelas)*

Upwelling	*Oceanic*	*Davidson*

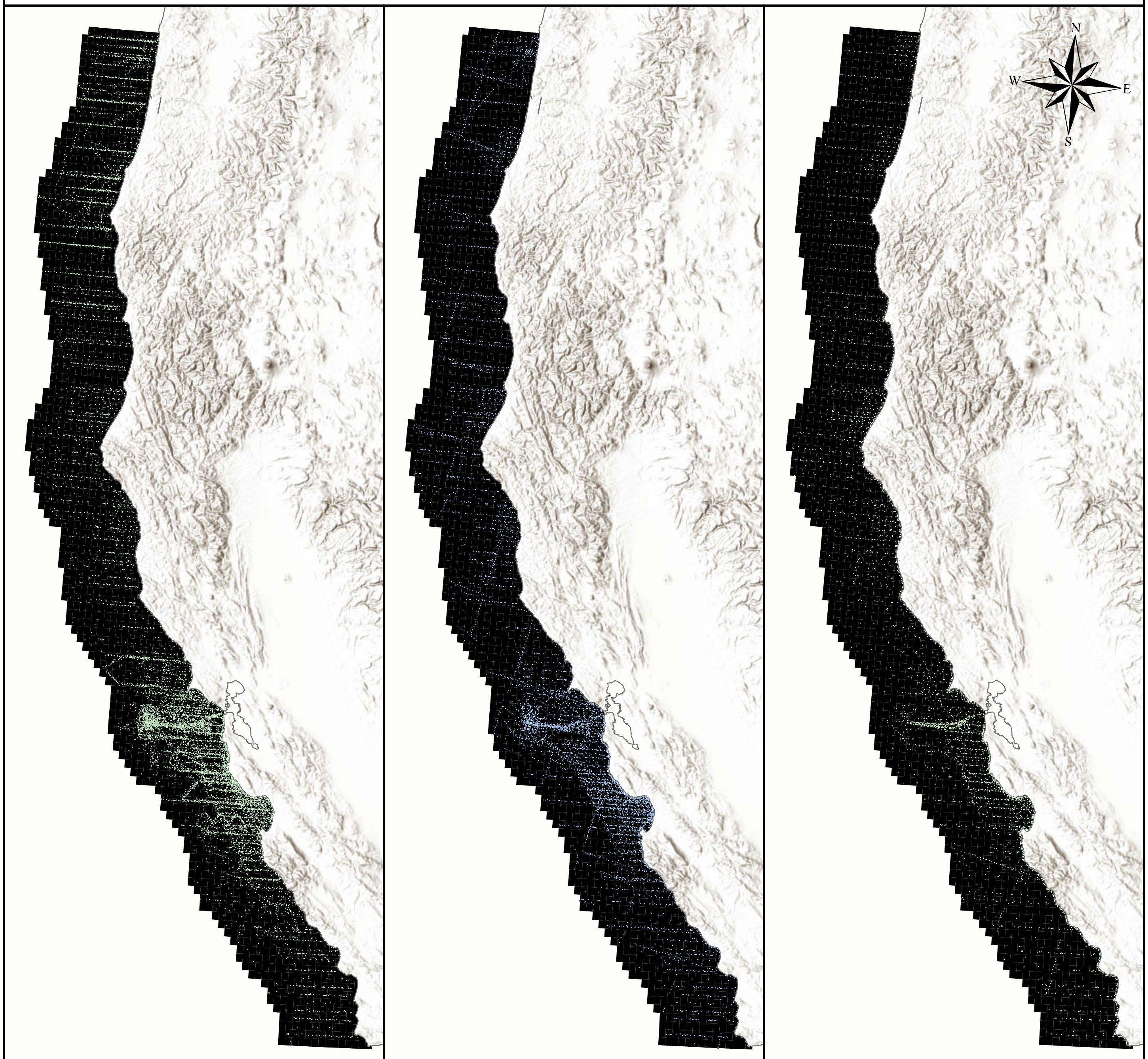

Standardized Residual Value (z-scores)

- x < - 2.75
- -2.75 < x < -2.25
- -2.25 < x < -1.75
- -1.75 < x < -1.25
- -1.25 < x < -0.75
- -0.75 < x < -0.25
- -0.25 < x < 0.25
- 0.25 < x < 0.75
- 0.75 < x < 1.25
- 1.25< x < 1.75
- 1.75 < x < 2.25
- 2.25 < x < 2.75
- x > 2.75
- study area

0 25 50 100
Kilometers

Schatz Energy Research Center

H. T. HARVEY & ASSOCIATES
Ecological Consultants
50 years of field notes, exploration, and excellence

Fork-tailed Storm-Petrel *(Hydrobates furcatus)*

Upwelling | ***Oceanic*** | ***Davidson***

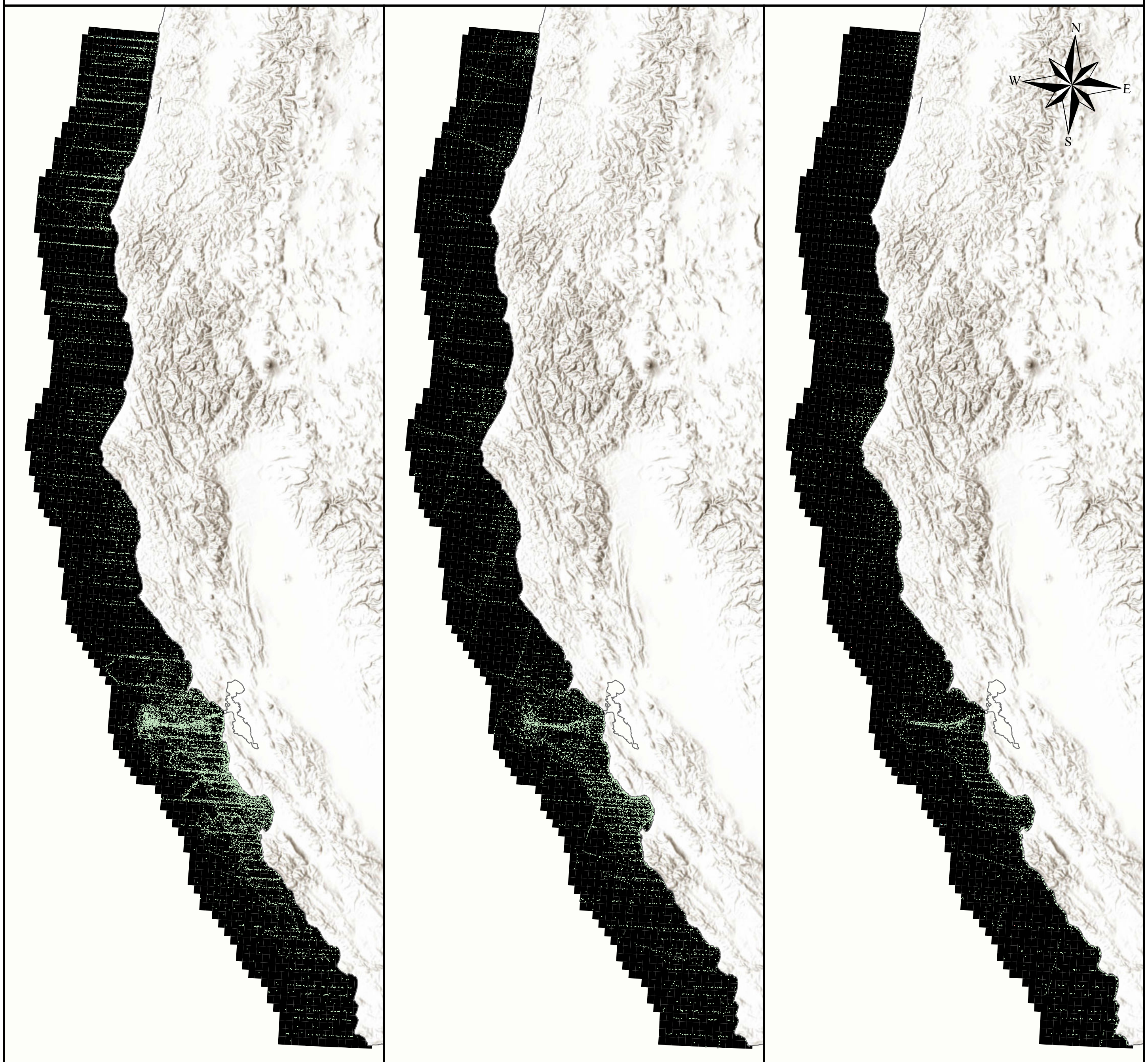

Standardized Residual Value (z-scores)

x < - 2.75	-0.75 < x < -0.25	1.75 < x < 2.25
-2.75 < x < -2.25	-0.25 < x < 0.25	2.25 < x < 2.75
-2.25 < x < -1.75	0.25 < x < 0.75	x > 2.75
-1.75 < x < -1.25	0.75 < x < 1.25	study area
-1.25 < x < -0.75	1.25< x < 1.75	

0 25 50 100
Kilometers

Schatz Energy Research Center

H. T. HARVEY & ASSOCIATES
Ecological Consultants
50 years of field notes, exploration, and excellence

Leach's Storm-Petrel *(Hydrobates leucorhous)*

Upwelling ***Oceanic*** ***Davidson***

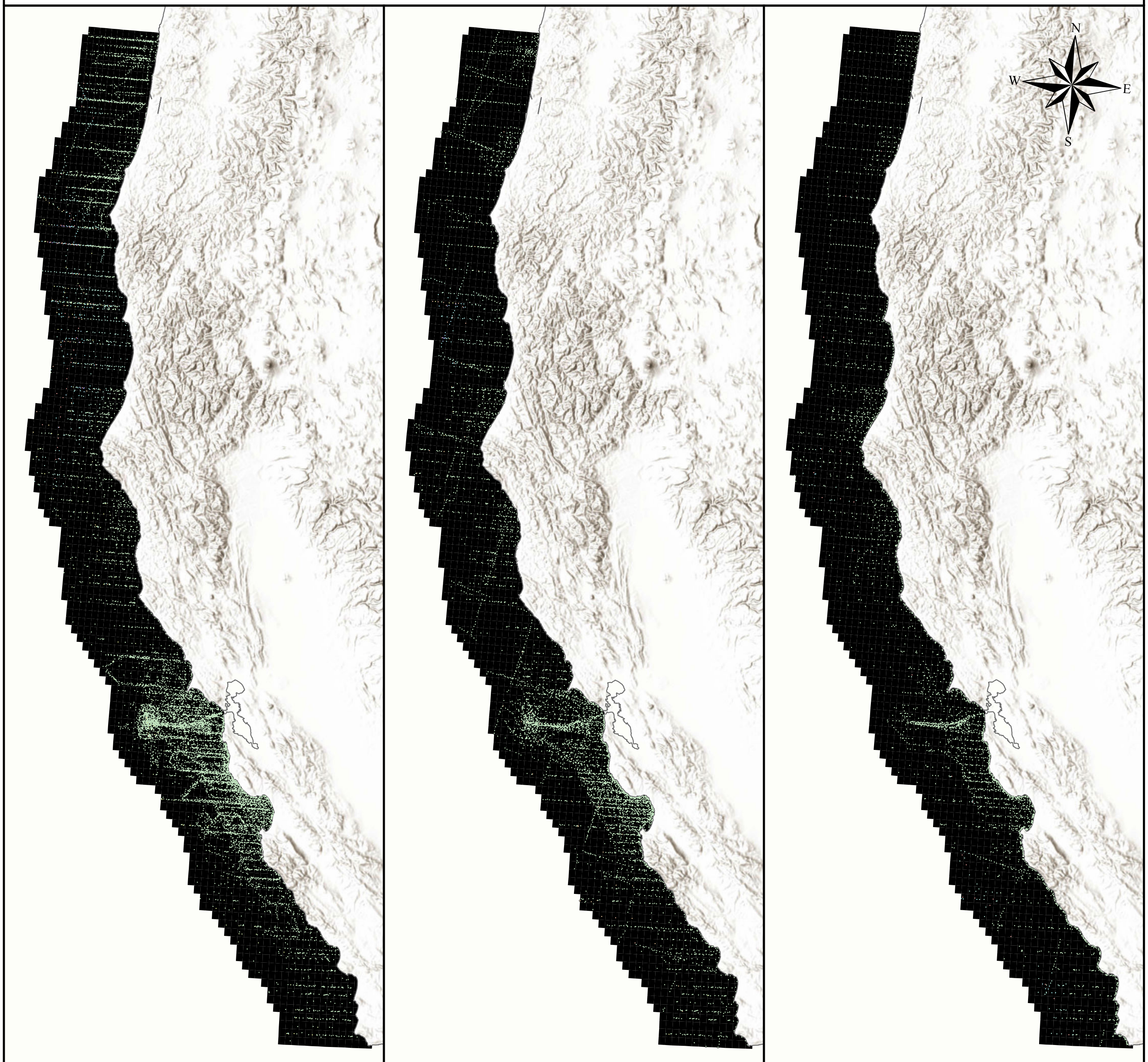

Standardized Residual Value (z-scores)

- x < - 2.75
- -2.75 < x < -2.25
- -2.25 < x < -1.75
- -1.75 < x < -1.25
- -1.25 < x < -0.75
- -0.75 < x < -0.25
- -0.25 < x < 0.25
- 0.25 < x < 0.75
- 0.75 < x < 1.25
- 1.25< x < 1.75
- 1.75 < x < 2.25
- 2.25 < x < 2.75
- x > 2.75
- study area

0 25 50 100
Kilometers

Schatz Energy Research Center

H. T. HARVEY & ASSOCIATES
Ecological Consultants
50 years of field notes, exploration, and excellence

Ashy Storm-Petrel *(Hydrobates homochroa)*

Upwelling	*Oceanic*	*Davidson*

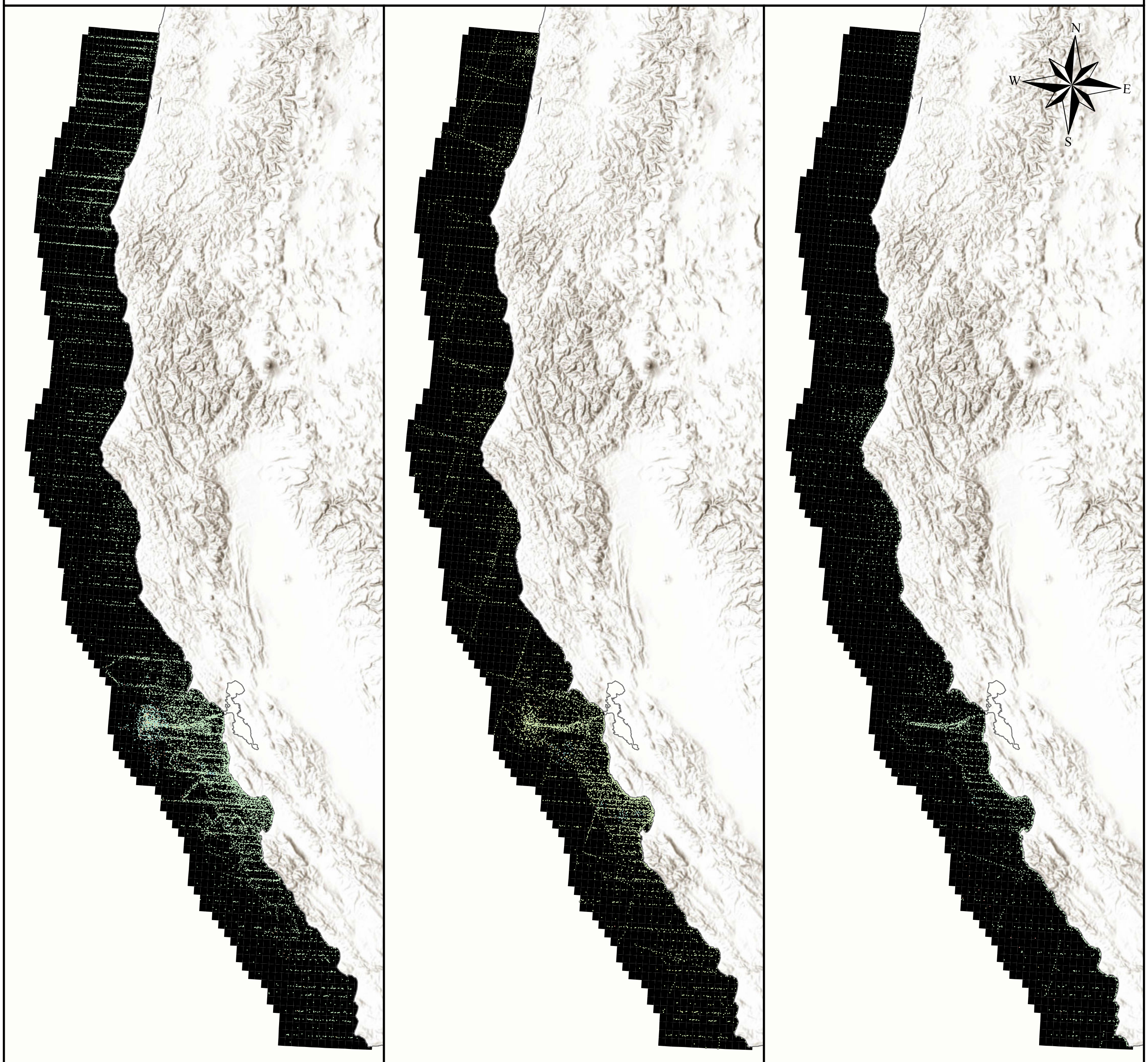

Standardized Residual Value (z-scores)

x < - 2.75	-0.75 < x < -0.25	1.75 < x < 2.25
-2.75 < x < -2.25	-0.25 < x < 0.25	2.25 < x < 2.75
-2.25 < x < -1.75	0.25 < x < 0.75	x > 2.75
-1.75 < x < -1.25	0.75 < x < 1.25	study area
-1.25 < x < -0.75	1.25< x < 1.75	

0 25 50 100 Kilometers

Schatz Energy Research Center

H. T. HARVEY & ASSOCIATES
Ecological Consultants
50 years of field notes, exploration, and excellence

Brown Pelican *(Pelecanus occidentalis)*

Upwelling | *Oceanic* | *Davidson*

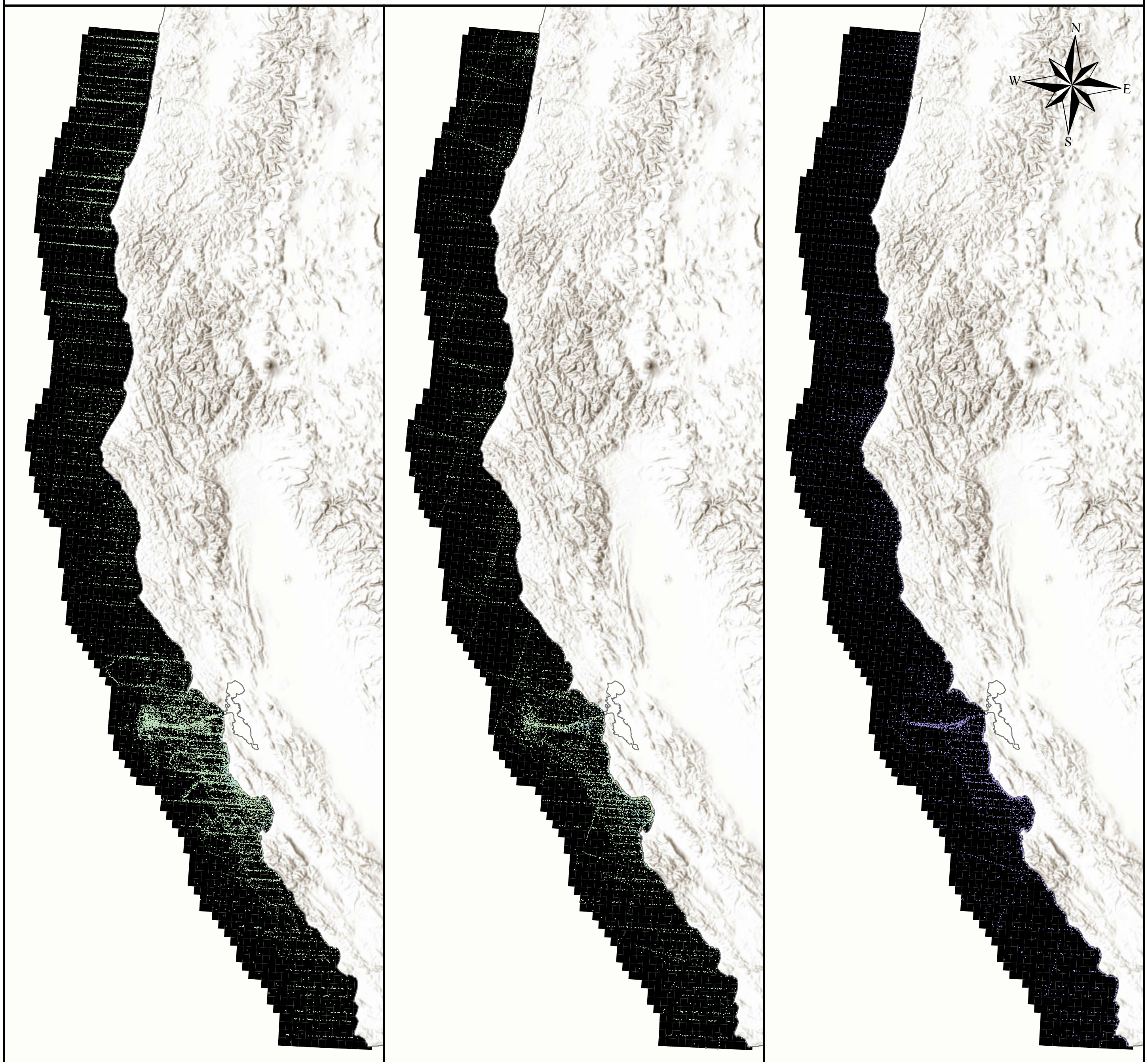

Standardized Residual Value (z-scores)

- x < - 2.75
- -2.75 < x < -2.25
- -2.25 < x < -1.75
- -1.75 < x < -1.25
- -1.25 < x < -0.75
- -0.75 < x < -0.25
- -0.25 < x < 0.25
- 0.25 < x < 0.75
- 0.75 < x < 1.25
- 1.25< x < 1.75
- 1.75 < x < 2.25
- 2.25 < x < 2.75
- x > 2.75
- study area

0 25 50 100 Kilometers

Schatz Energy Research Center

H. T. HARVEY & ASSOCIATES
Ecological Consultants
50 years of field notes, exploration, and excellence

Phalaropes *(Phalaropus sp.)*

Upwelling ***Oceanic*** ***Davidson***

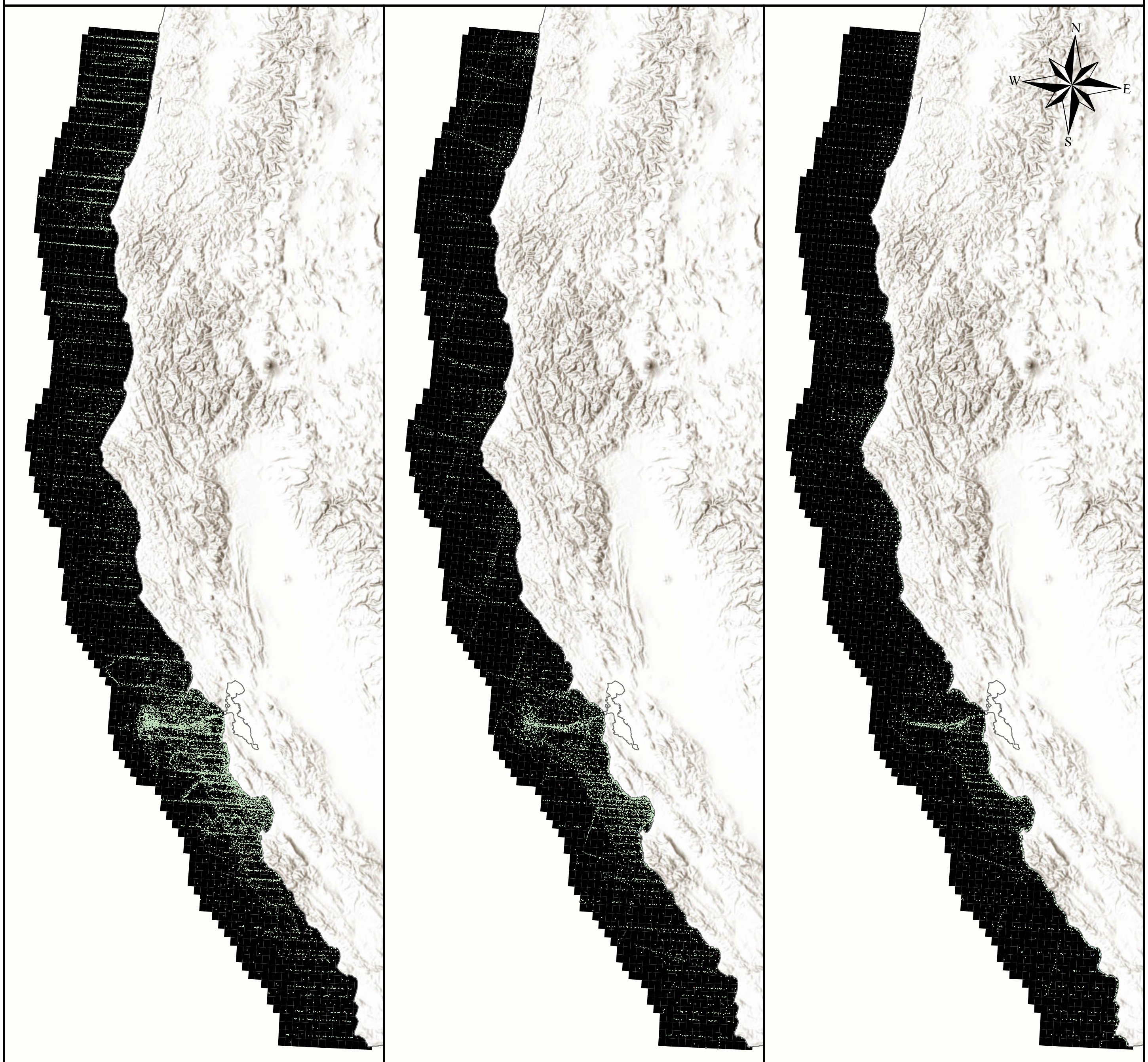

Standardized Residual Value (z-scores)

- x < - 2.75
- -2.75 < x < -2.25
- -2.25 < x < -1.75
- -1.75 < x < -1.25
- -1.25 < x < -0.75
- -0.75 < x < -0.25
- -0.25 < x < 0.25
- 0.25 < x < 0.75
- 0.75 < x < 1.25
- 1.25< x < 1.75
- 1.75 < x < 2.25
- 2.25 < x < 2.75
- x > 2.75
- study area

0 25 50 100
Kilometers

Schatz Energy Research Center

H. T. HARVEY & ASSOCIATES
Ecological Consultants
50 years of field notes, exploration, and excellence

Long-tailed Jaeger *(Stercorarius longicaudus)*

Upwelling ***Oceanic*** ***Davidson***

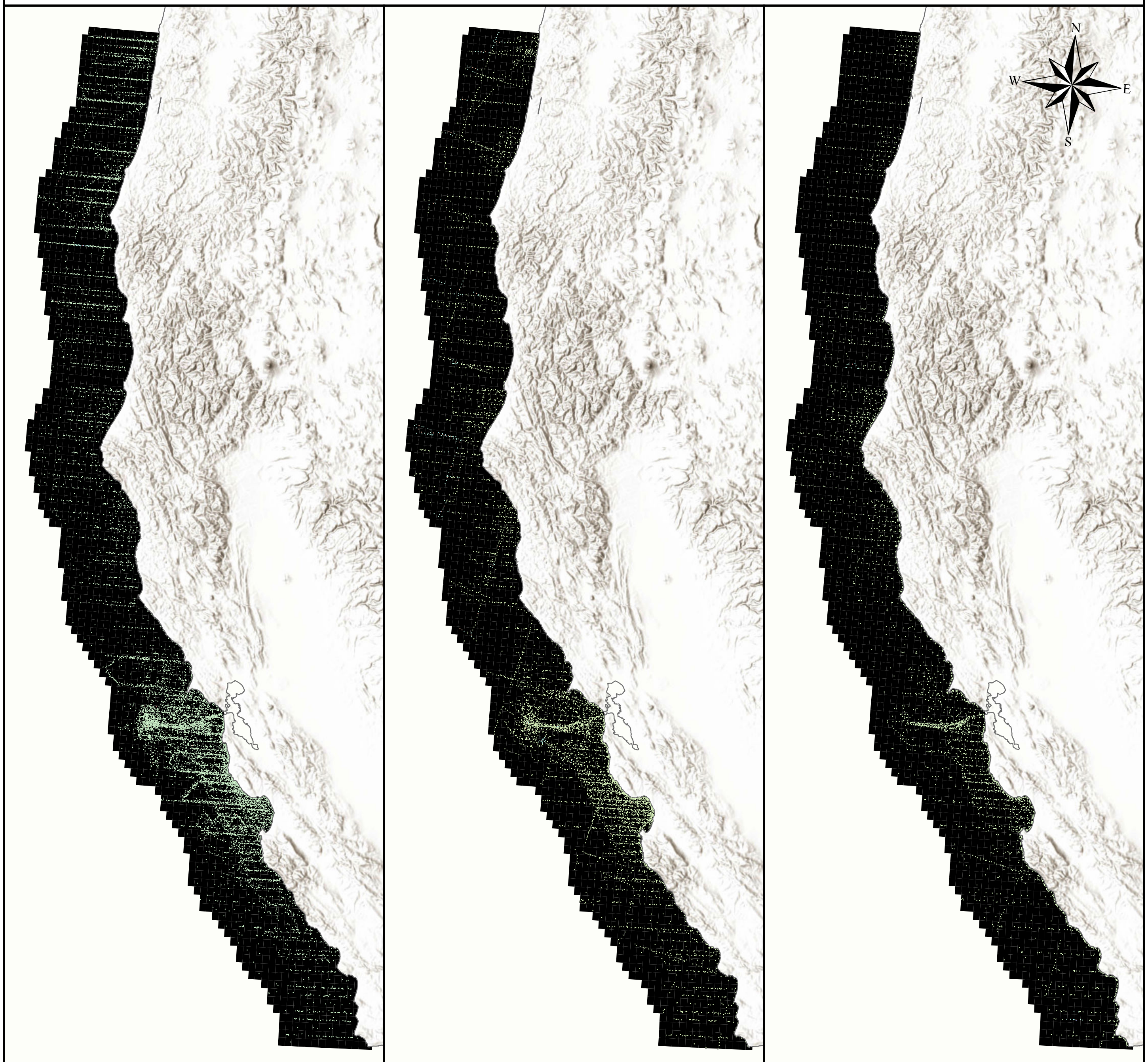

Standardized Residual Value (z-scores)

- x < - 2.75
- -2.75 < x < -2.25
- -2.25 < x < -1.75
- -1.75 < x < -1.25
- -1.25 < x < -0.75
- -0.75 < x < -0.25
- -0.25 < x < 0.25
- 0.25 < x < 0.75
- 0.75 < x < 1.25
- 1.25< x < 1.75
- 1.75 < x < 2.25
- 2.25 < x < 2.75
- x > 2.75
- study area

0 25 50 100
Kilometers

Schatz Energy Research Center

H. T. HARVEY & ASSOCIATES
Ecological Consultants
50 years of field notes, exploration, and excellence

Parasitic Jaeger *(Stercorarius parasiticus)*

Upwelling	*Oceanic*	*Davidson*

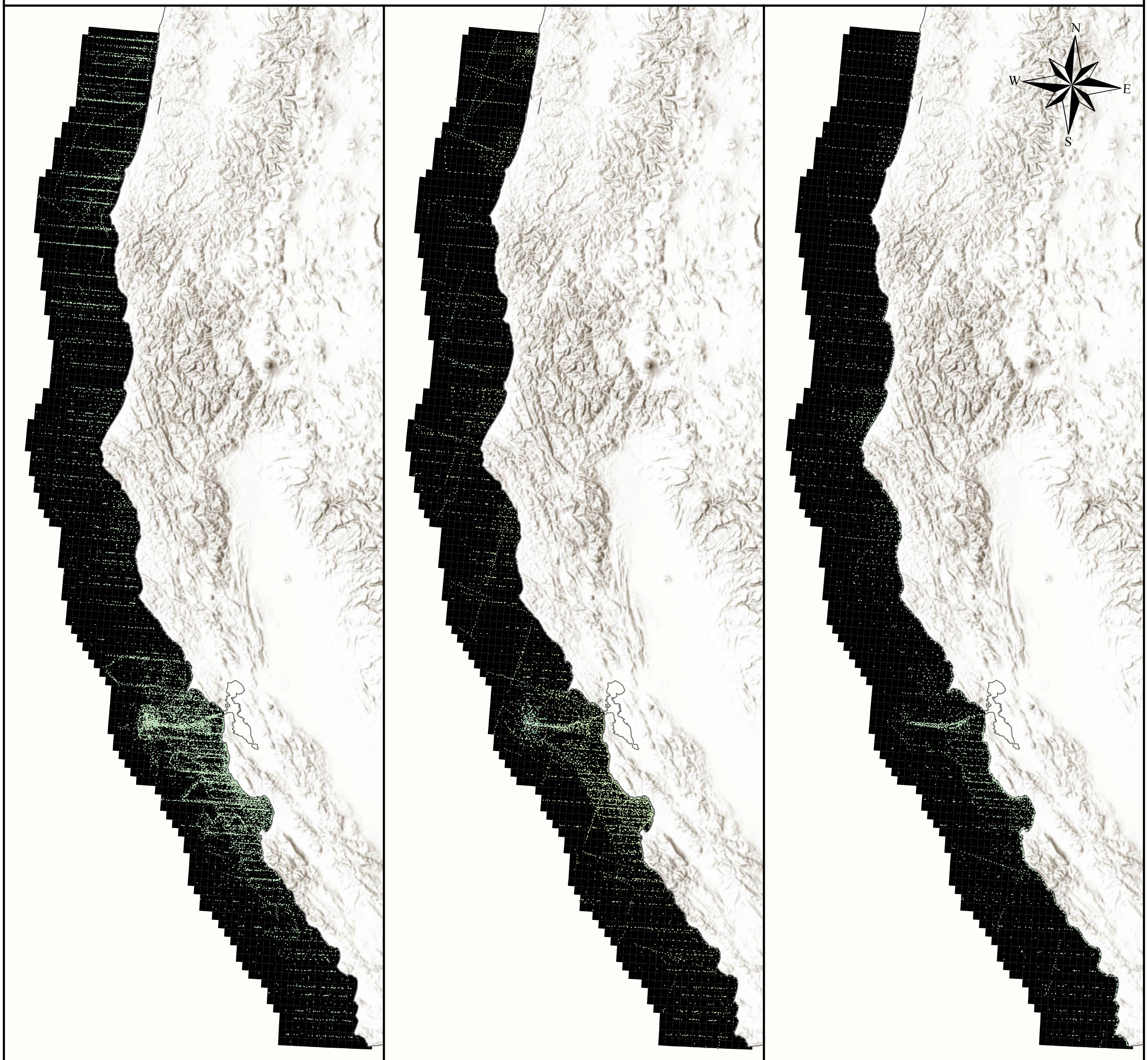

Standardized Residual Value (z-scores)

x < - 2.75
-2.75 < x < -2.25
-2.25 < x < -1.75
-1.75 < x < -1.25
-1.25 < x < -0.75
-0.75 < x < -0.25
-0.25 < x < 0.25
0.25 < x < 0.75
0.75 < x < 1.25
1.25< x < 1.75
1.75 < x < 2.25
2.25 < x < 2.75
x > 2.75
study area

0 25 50 100 Kilometers

Schatz Energy Research Center

H. T. HARVEY & ASSOCIATES
Ecological Consultants
50 years of field notes, exploration, and excellence

Pomarine Jaeger *(Stercorarius pomarinus)*

Upwelling	*Oceanic*	*Davidson*

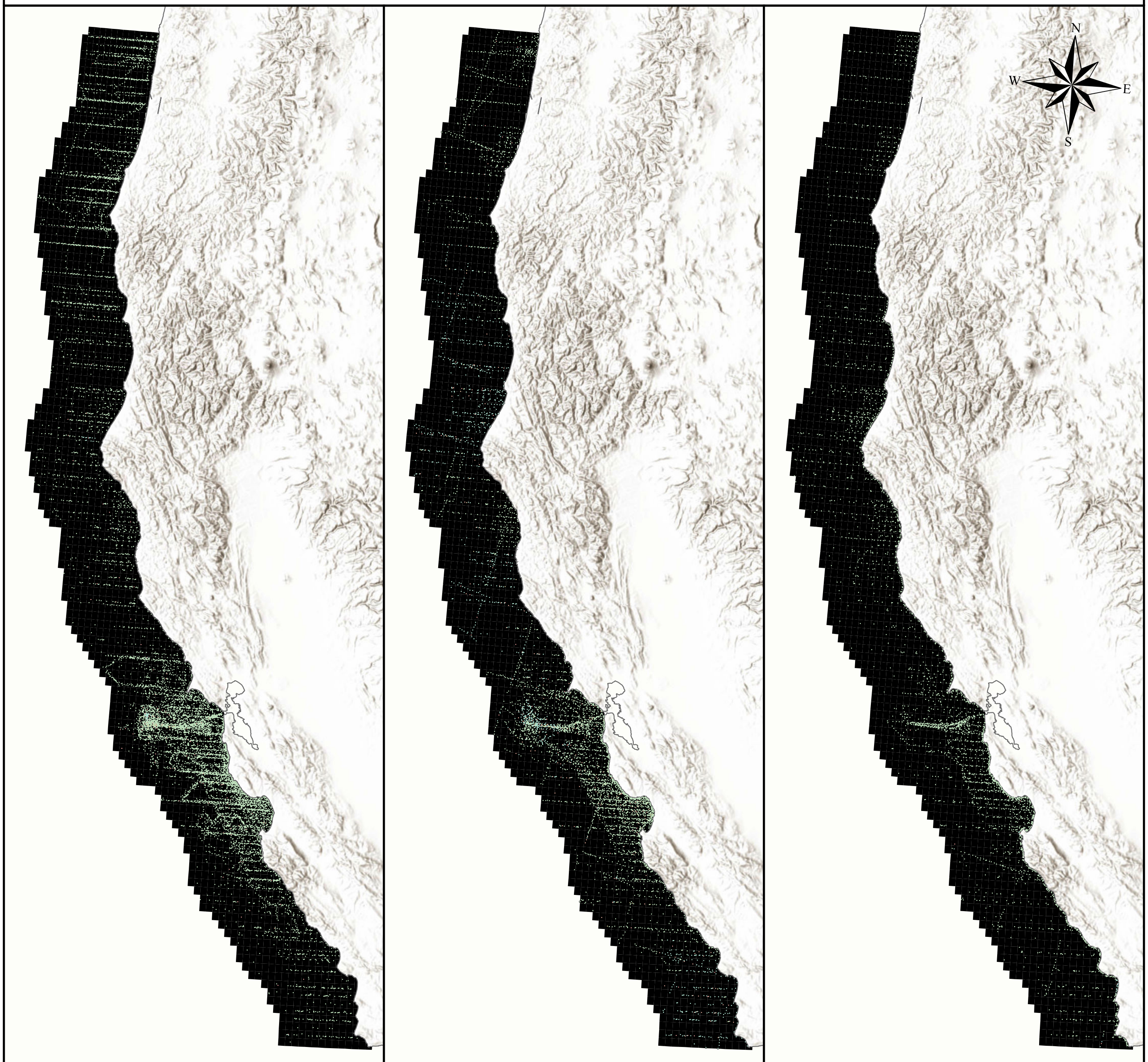

Standardized Residual Value (z-scores)

x < - 2.75	-0.75 < x < -0.25	1.75 < x < 2.25
-2.75 < x < -2.25	-0.25 < x < 0.25	2.25 < x < 2.75
-2.25 < x < -1.75	0.25 < x < 0.75	x > 2.75
-1.75 < x < -1.25	0.75 < x < 1.25	study area
-1.25 < x < -0.75	1.25< x < 1.75	

0 25 50 100
Kilometers

Schatz Energy Research Center

H. T. HARVEY & ASSOCIATES
Ecological Consultants
50 years of field notes, exploration, and excellence

South Polar Skua *(Stercorarius maccormicki)*

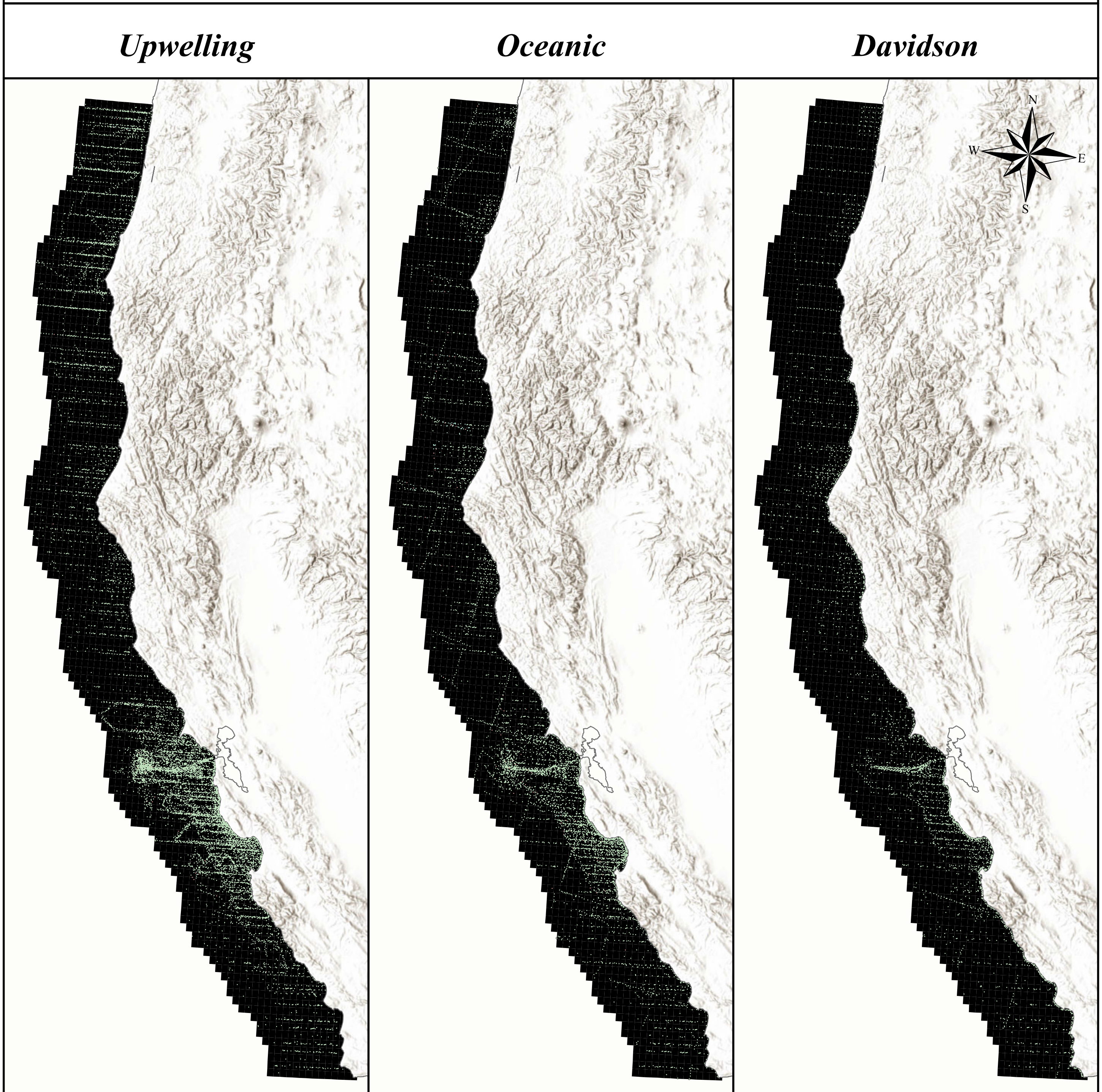

Standardized Residual Value (z-scores)

- x < - 2.75
- -2.75 < x < -2.25
- -2.25 < x < -1.75
- -1.75 < x < -1.25
- -1.25 < x < -0.75
- -0.75 < x < -0.25
- -0.25 < x < 0.25
- 0.25 < x < 0.75
- 0.75 < x < 1.25
- 1.25< x < 1.75
- 1.75 < x < 2.25
- 2.25 < x < 2.75
- x > 2.75
- study area

0 25 50 100 Kilometers

Schatz Energy Research Center

H. T. HARVEY & ASSOCIATES
Ecological Consultants
50 years of field notes, exploration, and excellence

California Gull *(Larus californicus)*

Upwelling | ***Oceanic*** | ***Davidson***

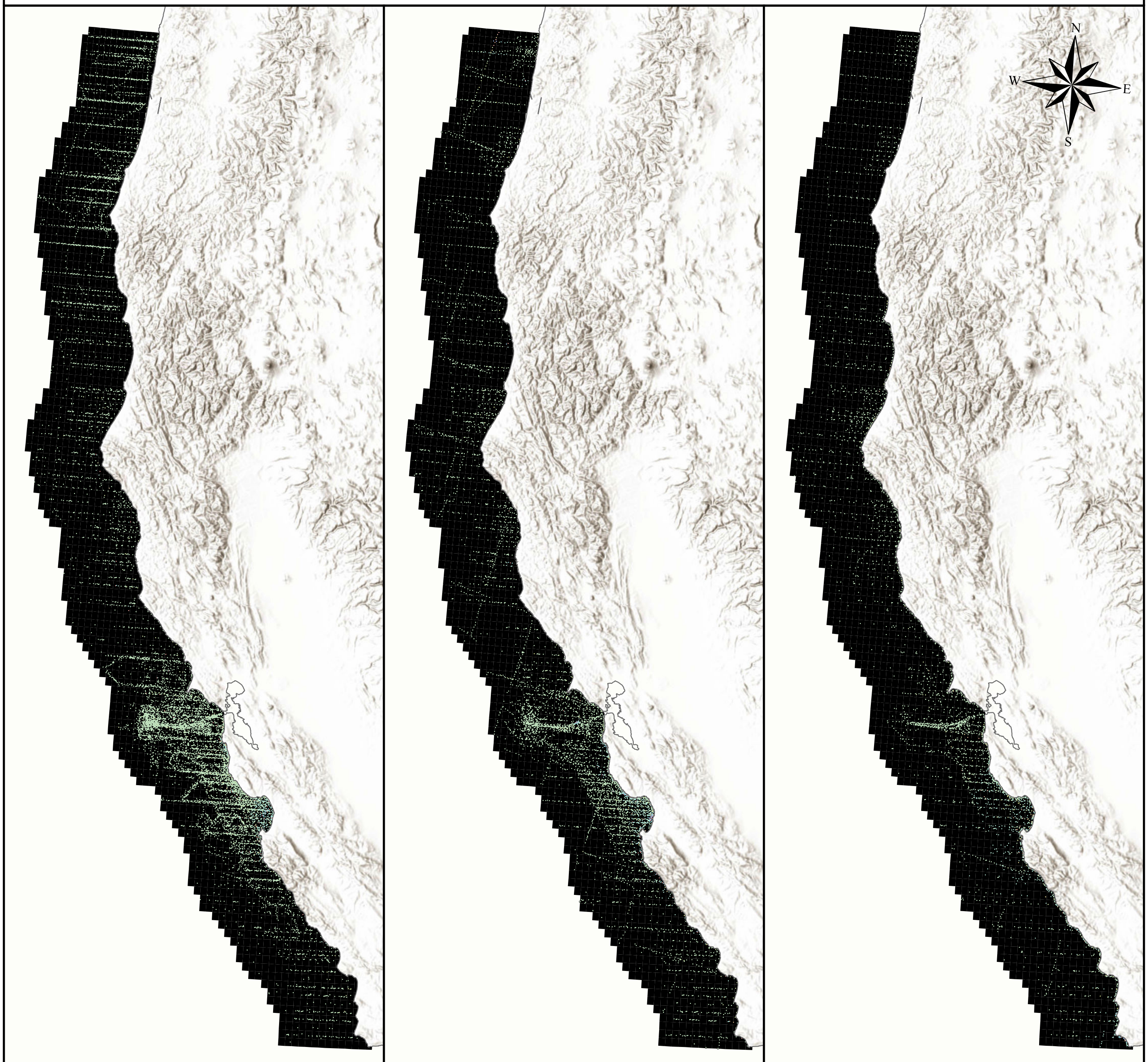

Standardized Residual Value (z-scores)

x < - 2.75
-2.75 < x < -2.25
-2.25 < x < -1.75
-1.75 < x < -1.25
-1.25 < x < -0.75
-0.75 < x < -0.25
-0.25 < x < 0.25
0.25 < x < 0.75
0.75 < x < 1.25
1.25< x < 1.75
1.75 < x < 2.25
2.25 < x < 2.75
x > 2.75
study area

0 25 50 100
Kilometers

Schatz Energy Research Center

H. T. HARVEY & ASSOCIATES
Ecological Consultants
50 years of field notes, exploration, and excellence

Herring Gull *(Larus argentatus)*

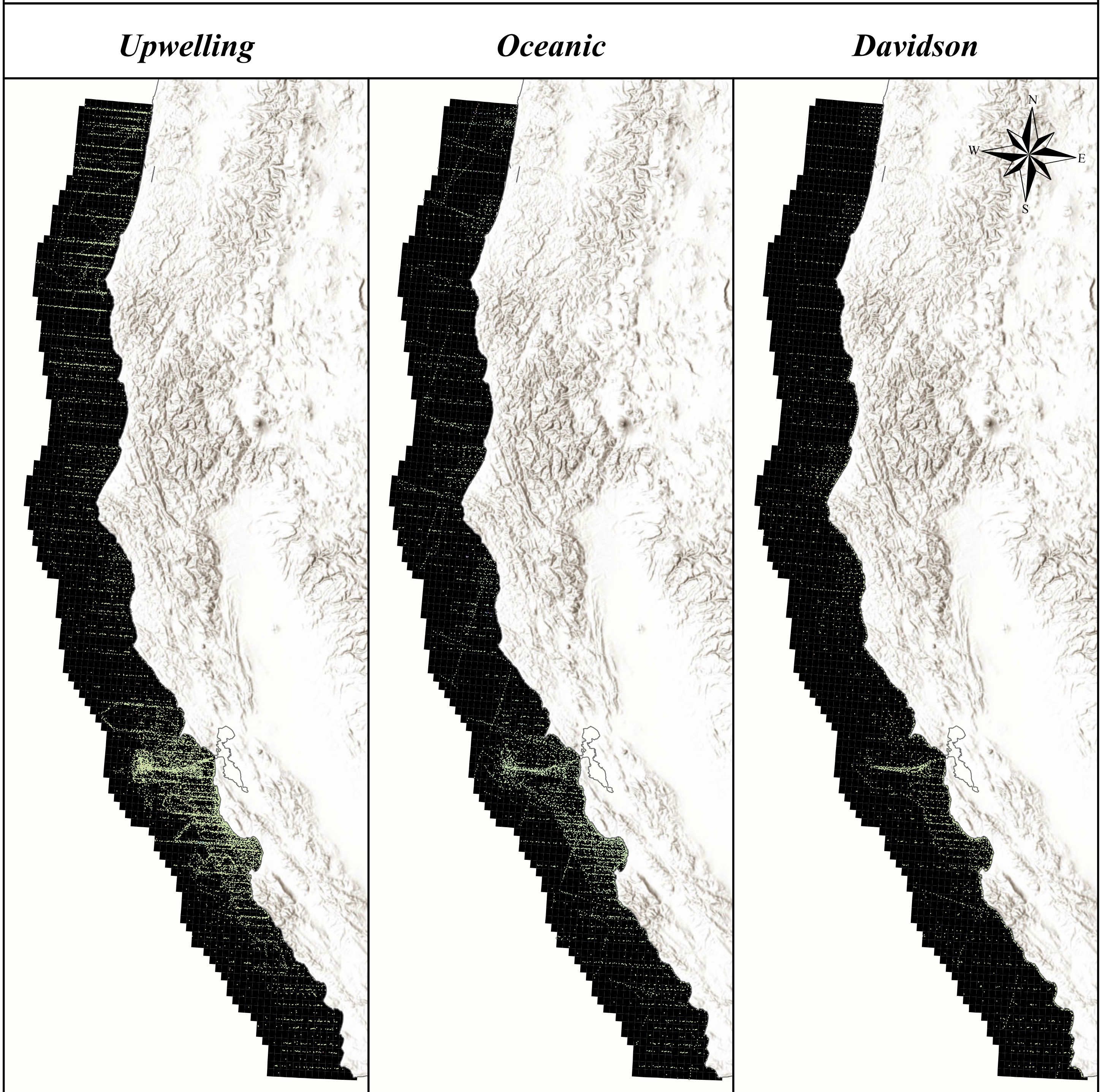

Standardized Residual Value (z-scores)

x < - 2.75	-0.75 < x < -0.25	1.75 < x < 2.25
-2.75 < x < -2.25	-0.25 < x < 0.25	2.25 < x < 2.75
-2.25 < x < -1.75	0.25 < x < 0.75	x > 2.75
-1.75 < x < -1.25	0.75 < x < 1.25	study area
-1.25 < x < -0.75	1.25< x < 1.75	

0 25 50 100 Kilometers

Schatz Energy Research Center

H. T. HARVEY & ASSOCIATES
Ecological Consultants
50 years of field notes, exploration, and excellence

Western Gull *(Larus occidentalis)*

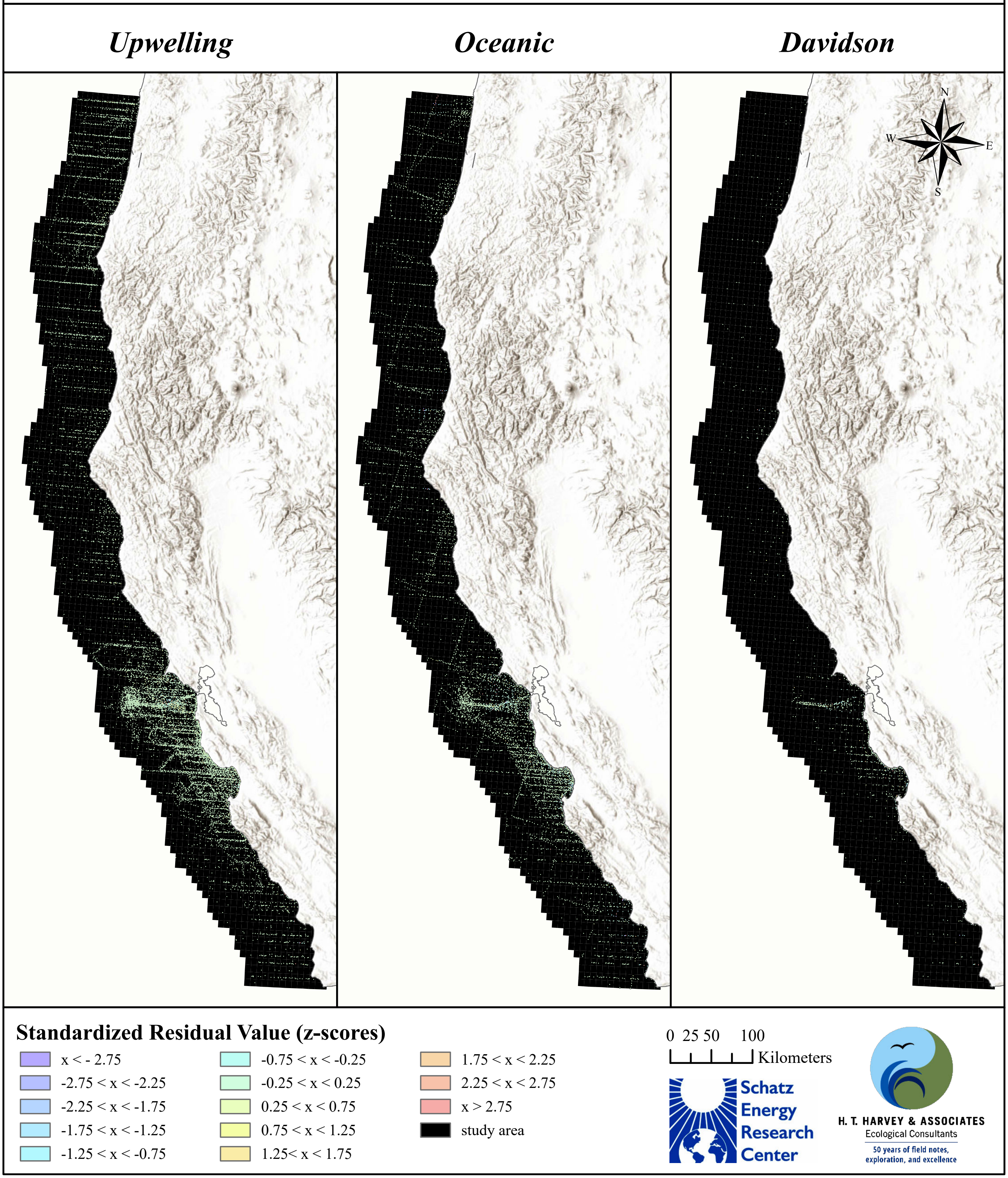

Glaucous-winged Gull *(Larus glaucescens)*

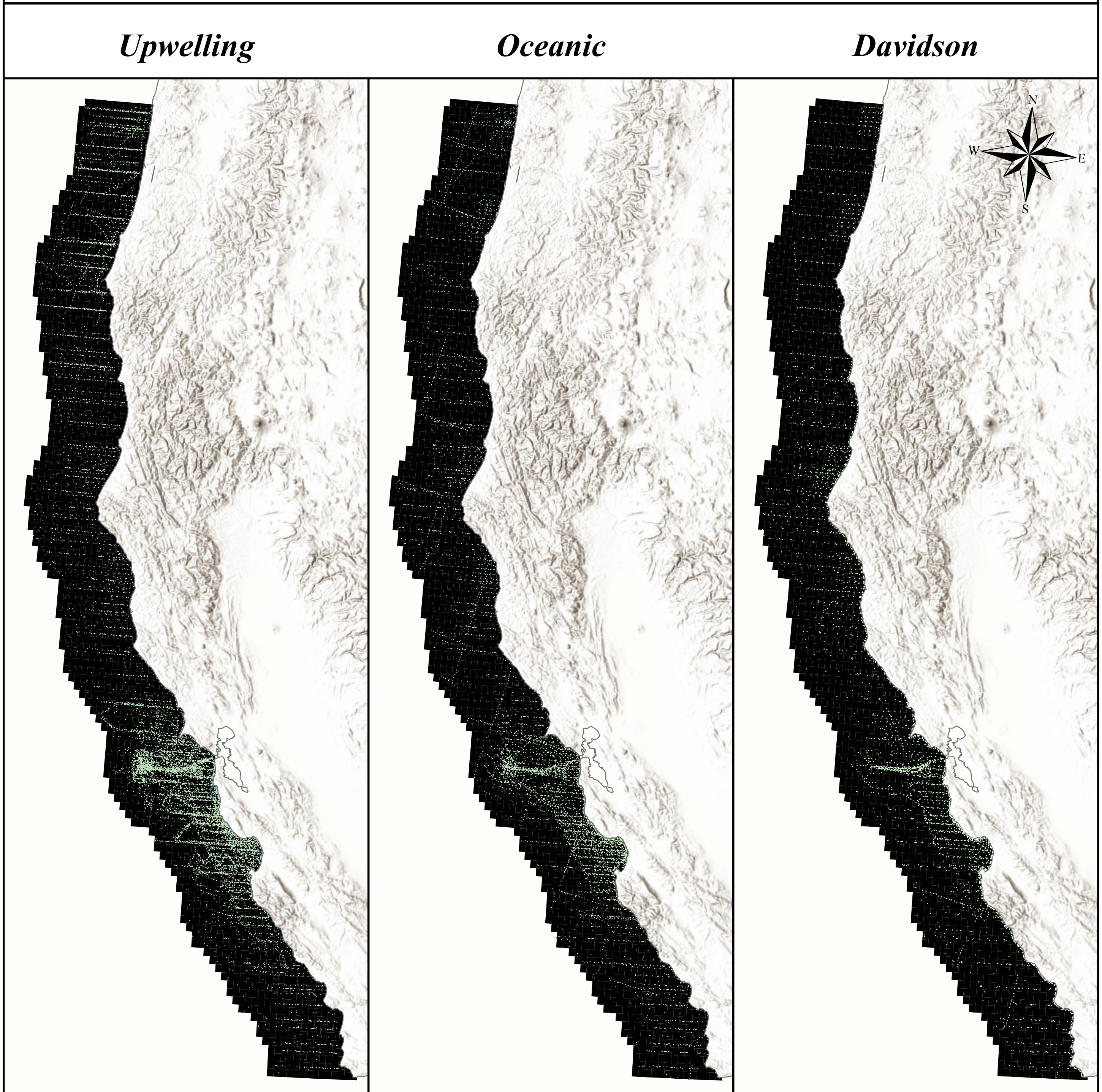

Standardized Residual Value (z-scores)

x < - 2.75	-0.75 < x < -0.25	1.75 < x < 2.25
-2.75 < x < -2.25	-0.25 < x < 0.25	2.25 < x < 2.75
-2.25 < x < -1.75	0.25 < x < 0.75	x > 2.75
-1.75 < x < -1.25	0.75 < x < 1.25	study area
-1.25 < x < -0.75	1.25< x < 1.75	

0 25 50 100
Kilometers

Schatz Energy Research Center

H. T. HARVEY & ASSOCIATES
Ecological Consultants
50 years of field notes, exploration, and excellence

Heermann's Gull *(Larus heermanni)*

Upwelling	***Oceanic***	***Davidson***

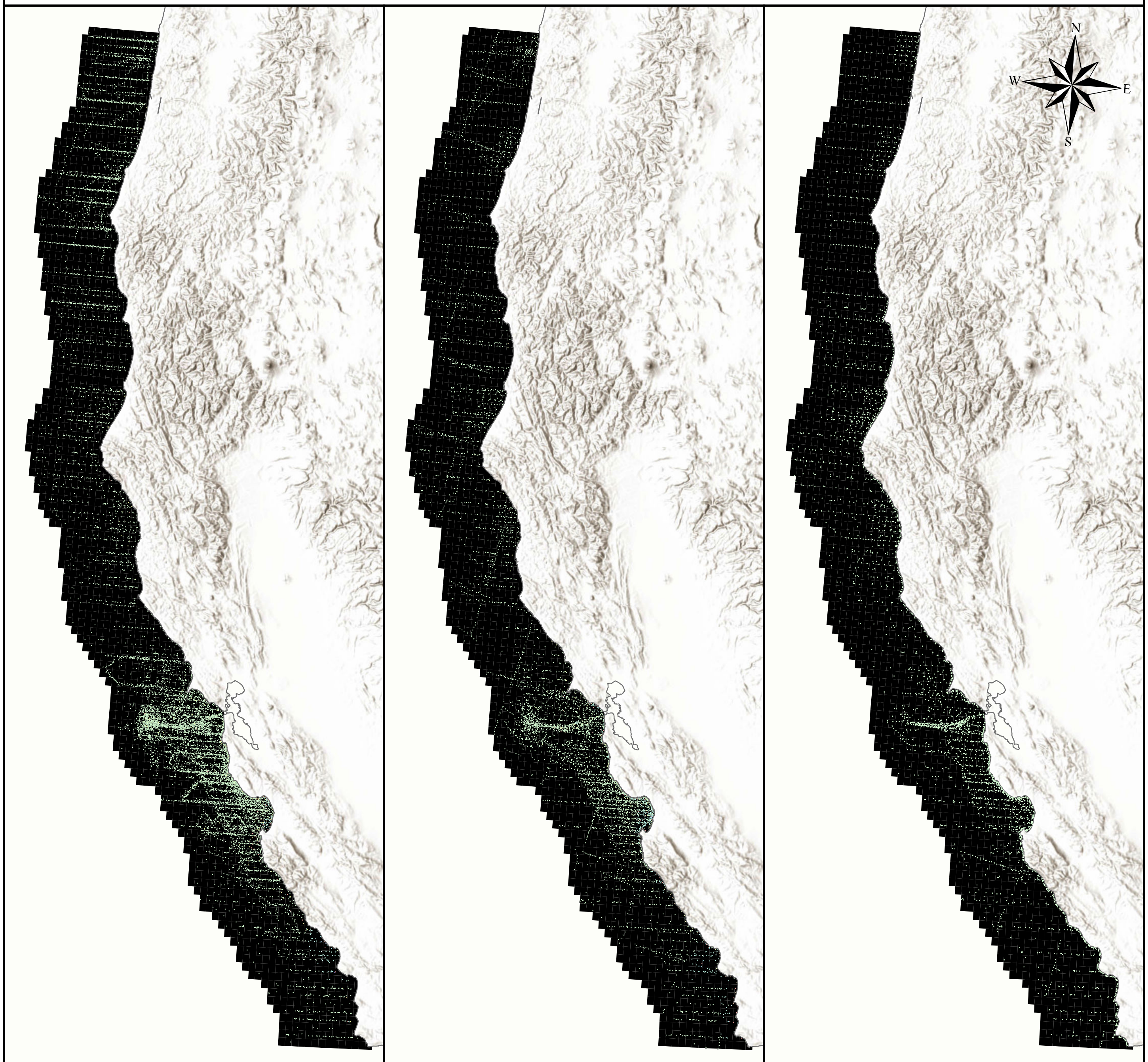

Standardized Residual Value (z-scores)

x < - 2.75	-0.75 < x < -0.25	1.75 < x < 2.25
-2.75 < x < -2.25	-0.25 < x < 0.25	2.25 < x < 2.75
-2.25 < x < -1.75	0.25 < x < 0.75	x > 2.75
-1.75 < x < -1.25	0.75 < x < 1.25	study area
-1.25 < x < -0.75	1.25< x < 1.75	

0 25 50 100
Kilometers

Schatz Energy Research Center

H. T. HARVEY & ASSOCIATES
Ecological Consultants
50 years of field notes, exploration, and excellence

Black-legged Kittiwake *(Rissa tridactyla)*

Upwelling ***Oceanic*** ***Davidson***

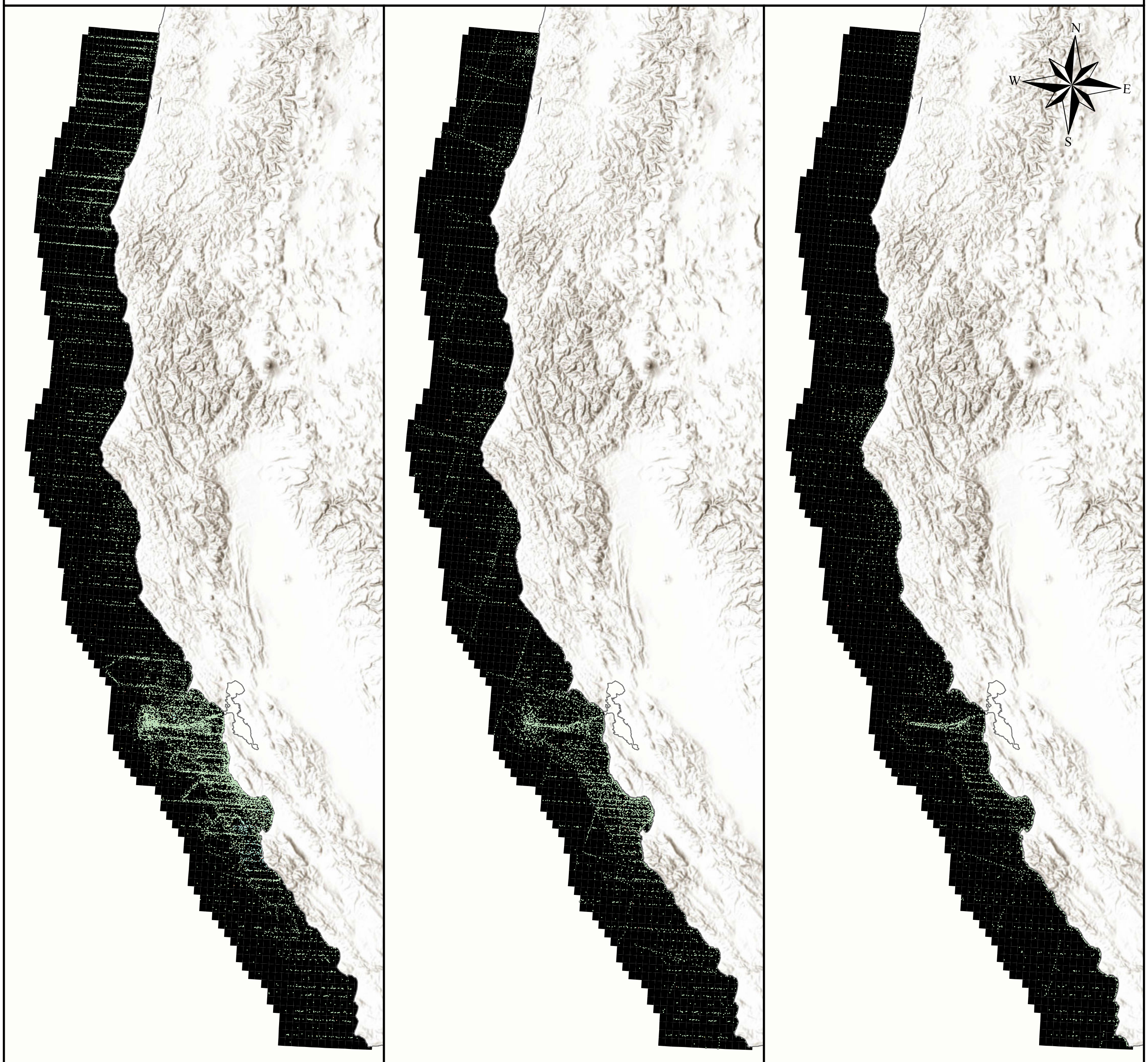

Standardized Residual Value (z-scores)

x < - 2.75	-0.75 < x < -0.25	1.75 < x < 2.25
-2.75 < x < -2.25	-0.25 < x < 0.25	2.25 < x < 2.75
-2.25 < x < -1.75	0.25 < x < 0.75	x > 2.75
-1.75 < x < -1.25	0.75 < x < 1.25	study area
-1.25 < x < -0.75	1.25< x < 1.75	

0 25 50 100 Kilometers

Schatz Energy Research Center

H. T. HARVEY & ASSOCIATES
Ecological Consultants
50 years of field notes, exploration, and excellence

Short-billed Gull *(Larus brachyrhynchus)*

Upwelling	*Oceanic*	*Davidson*

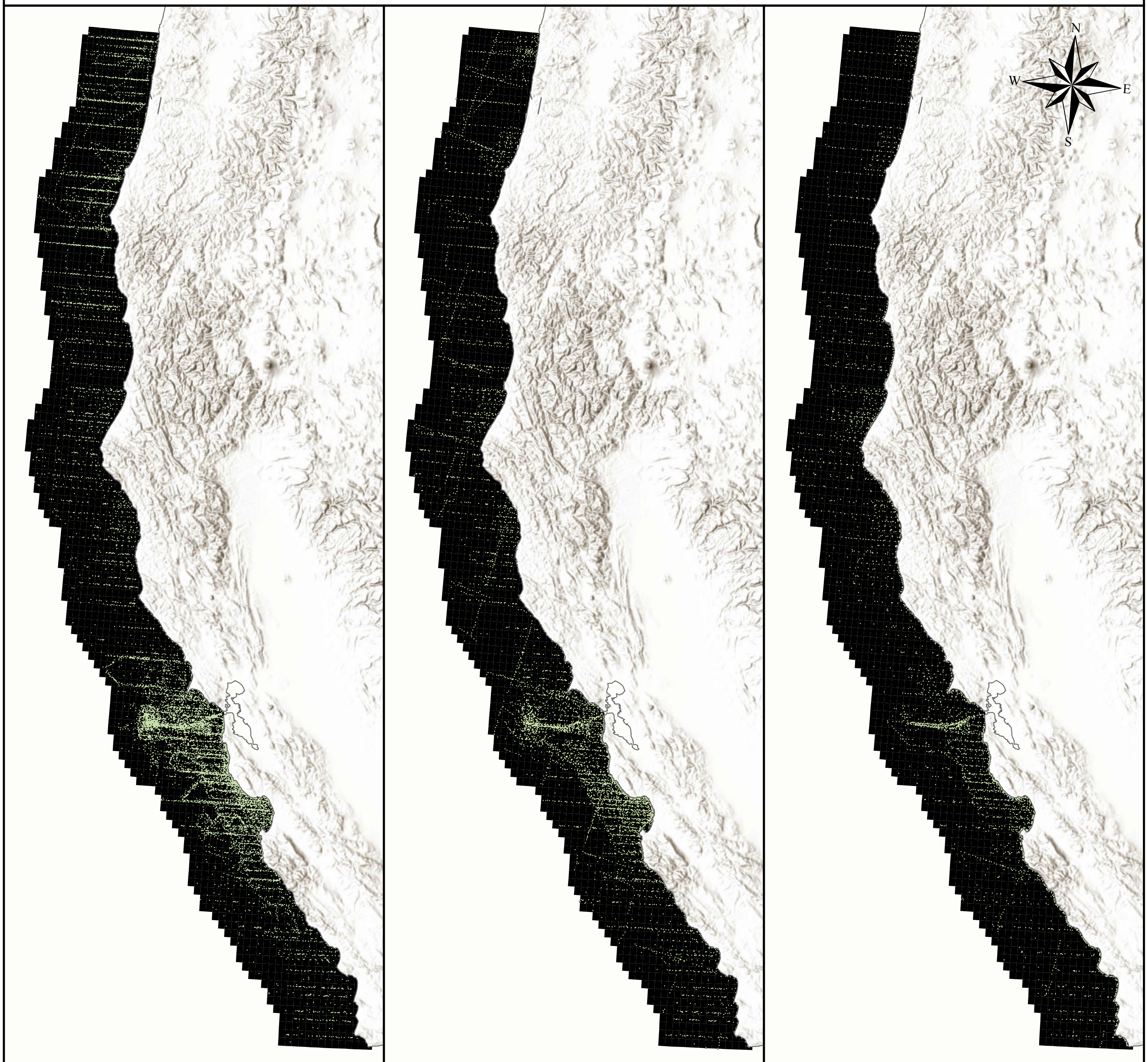

Standardized Residual Value (z-scores)

x < - 2.75	-0.75 < x < -0.25	1.75 < x < 2.25
-2.75 < x < -2.25	-0.25 < x < 0.25	2.25 < x < 2.75
-2.25 < x < -1.75	0.25 < x < 0.75	x > 2.75
-1.75 < x < -1.25	0.75 < x < 1.25	study area
-1.25 < x < -0.75	1.25< x < 1.75	

0 25 50 100 Kilometers

Schatz Energy Research Center

H. T. HARVEY & ASSOCIATES
Ecological Consultants
50 years of field notes, exploration, and excellence

Bonaparte's Gull *(Chroicocephalus philadelphia)*

Upwelling ***Oceanic*** ***Davidson***

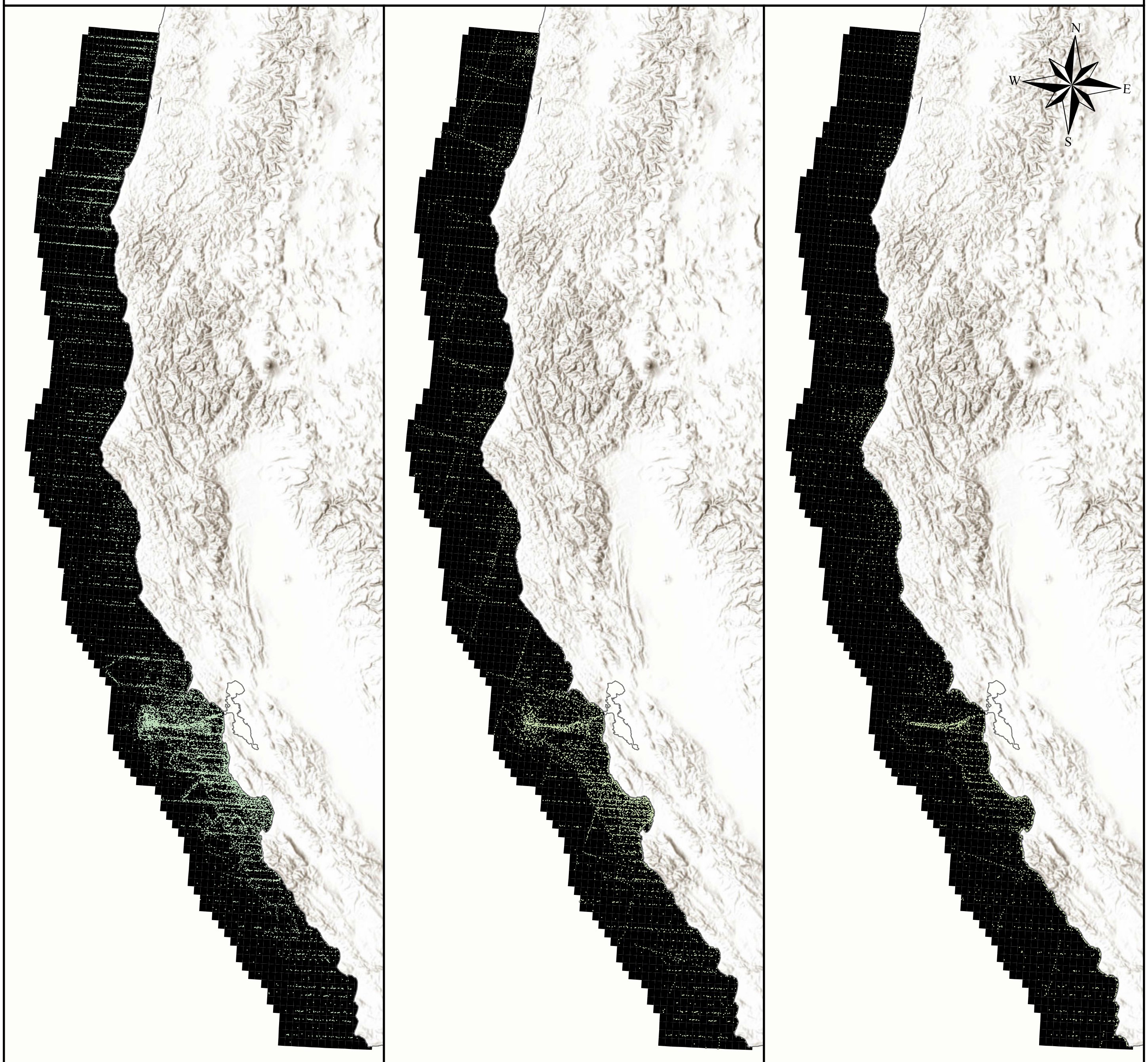

Standardized Residual Value (z-scores)

x < - 2.75	-0.75 < x < -0.25	1.75 < x < 2.25
-2.75 < x < -2.25	-0.25 < x < 0.25	2.25 < x < 2.75
-2.25 < x < -1.75	0.25 < x < 0.75	x > 2.75
-1.75 < x < -1.25	0.75 < x < 1.25	study area
-1.25 < x < -0.75	1.25< x < 1.75	

0 25 50 100 Kilometers

Schatz Energy Research Center

H. T. HARVEY & ASSOCIATES
Ecological Consultants
50 years of field notes, exploration, and excellence

Sabine's Gull *(Xema sabini)*

Upwelling | ***Oceanic*** | ***Davidson***

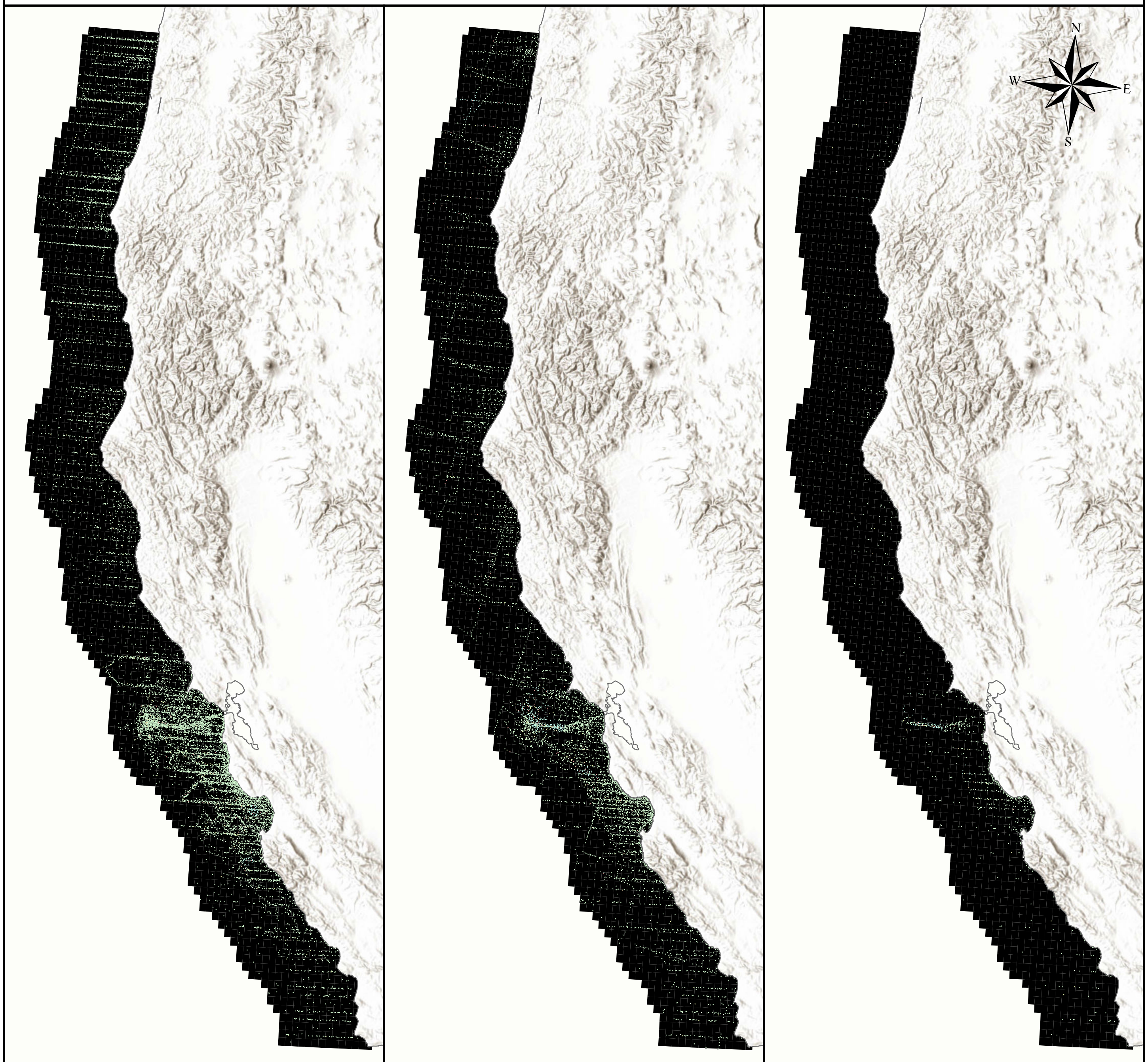

Standardized Residual Value (z-scores)

- x < - 2.75
- -2.75 < x < -2.25
- -2.25 < x < -1.75
- -1.75 < x < -1.25
- -1.25 < x < -0.75
- -0.75 < x < -0.25
- -0.25 < x < 0.25
- 0.25 < x < 0.75
- 0.75 < x < 1.25
- 1.25< x < 1.75
- 1.75 < x < 2.25
- 2.25 < x < 2.75
- x > 2.75
- study area

0 25 50 100 Kilometers

Schatz Energy Research Center

H. T. HARVEY & ASSOCIATES
Ecological Consultants
50 years of field notes, exploration, and excellence

Arctic Tern *(Sterna paradisaea)*

Upwelling | ***Oceanic*** | ***Davidson***

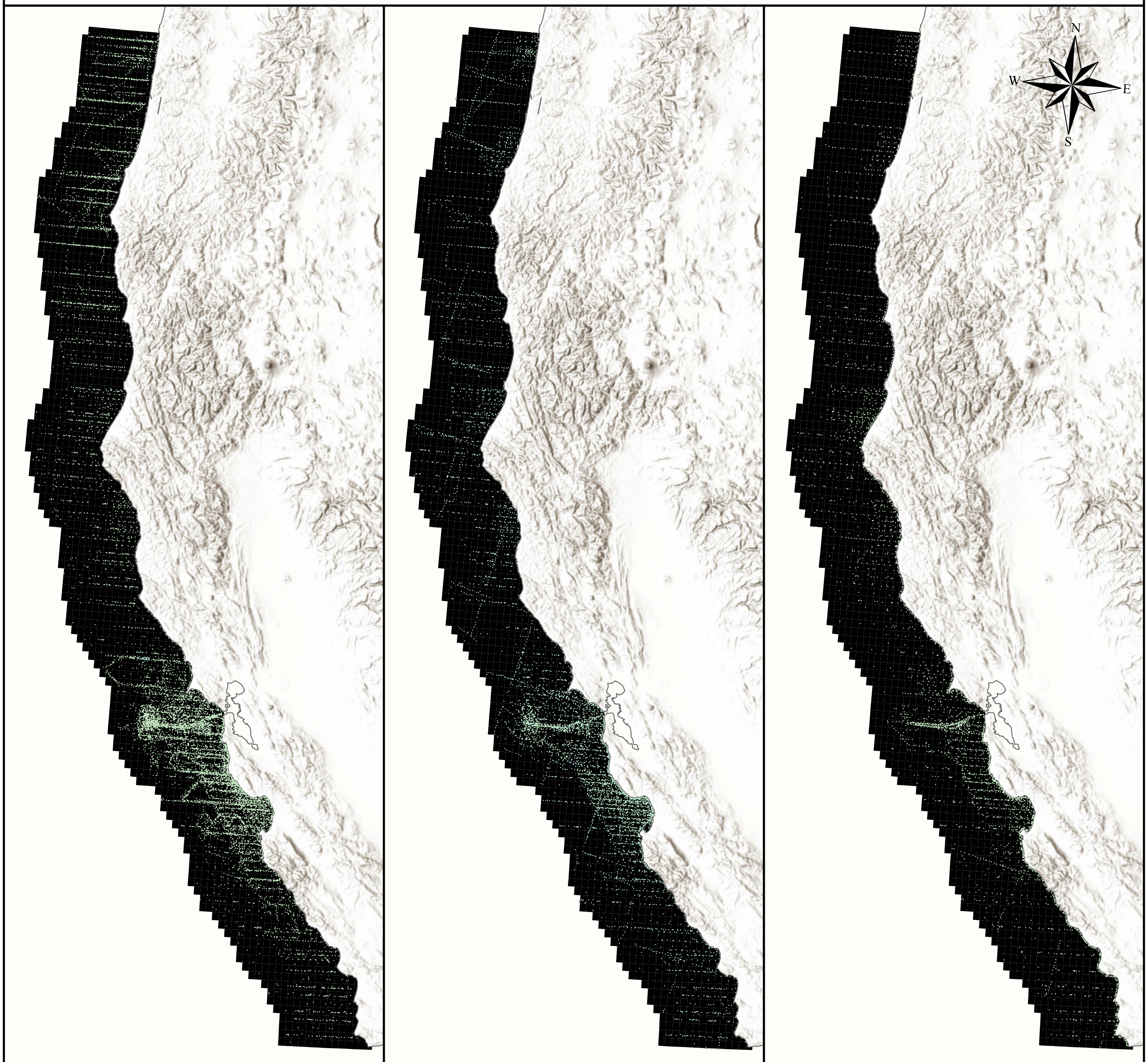

Standardized Residual Value (z-scores)

x < - 2.75	-0.75 < x < -0.25	1.75 < x < 2.25
-2.75 < x < -2.25	-0.25 < x < 0.25	2.25 < x < 2.75
-2.25 < x < -1.75	0.25 < x < 0.75	x > 2.75
-1.75 < x < -1.25	0.75 < x < 1.25	study area
-1.25 < x < -0.75	1.25< x < 1.75	

0 25 50 100 Kilometers

Schatz Energy Research Center

H. T. HARVEY & ASSOCIATES
Ecological Consultants
50 years of field notes, exploration, and excellence

Caspian Tern *(Hydroprogne caspia)*

Upwelling | *Oceanic* | *Davidson*

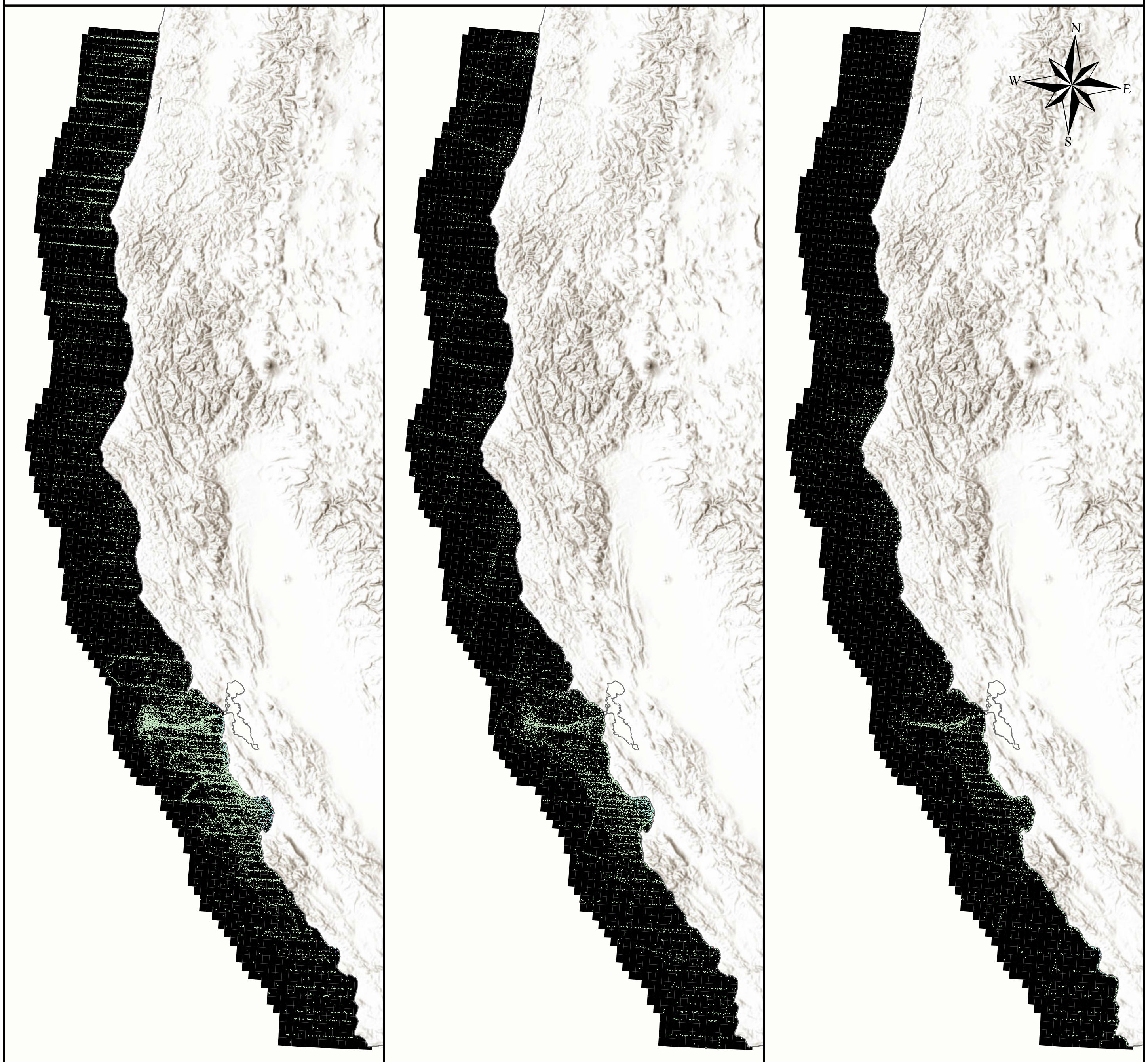

Standardized Residual Value (z-scores)

- x < - 2.75
- -2.75 < x < -2.25
- -2.25 < x < -1.75
- -1.75 < x < -1.25
- -1.25 < x < -0.75
- -0.75 < x < -0.25
- -0.25 < x < 0.25
- 0.25 < x < 0.75
- 0.75 < x < 1.25
- 1.25< x < 1.75
- 1.75 < x < 2.25
- 2.25 < x < 2.75
- x > 2.75
- study area

0 25 50 100 Kilometers

Schatz Energy Research Center

H. T. HARVEY & ASSOCIATES
Ecological Consultants
50 years of field notes, exploration, and excellence

Elegant Tern *(Thalasseus elegans)*

Upwelling ***Oceanic*** ***Davidson***

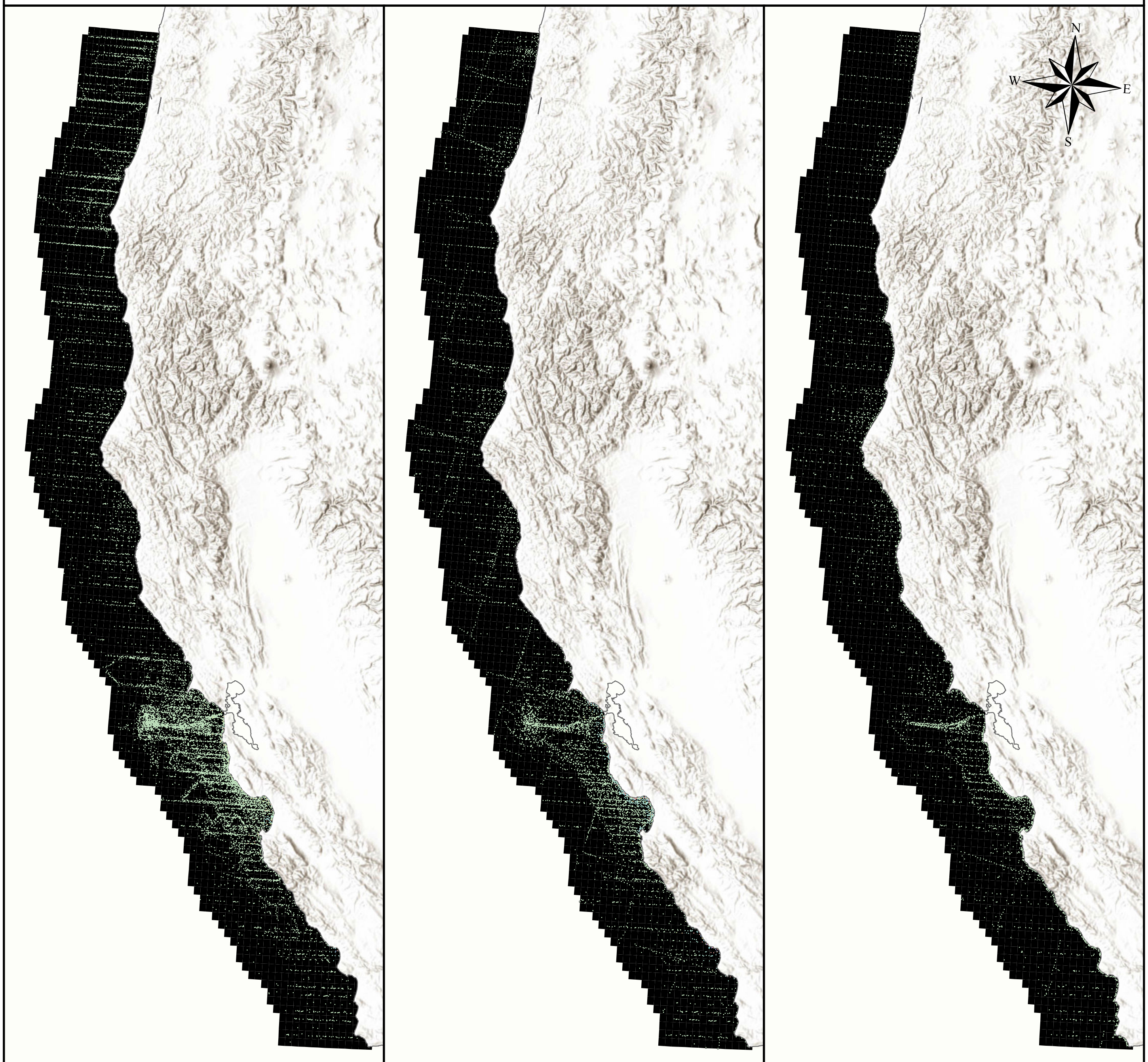

Standardized Residual Value (z-scores)

x < - 2.75	-0.75 < x < -0.25	1.75 < x < 2.25
-2.75 < x < -2.25	-0.25 < x < 0.25	2.25 < x < 2.75
-2.25 < x < -1.75	0.25 < x < 0.75	x > 2.75
-1.75 < x < -1.25	0.75 < x < 1.25	study area
-1.25 < x < -0.75	1.25< x < 1.75	

0 25 50 100 Kilometers

Schatz Energy Research Center

H. T. HARVEY & ASSOCIATES
Ecological Consultants
50 years of field notes, exploration, and excellence

Brandt's Cormorant *(Urile penicillatus)*

Upwelling | ***Oceanic*** | ***Davidson***

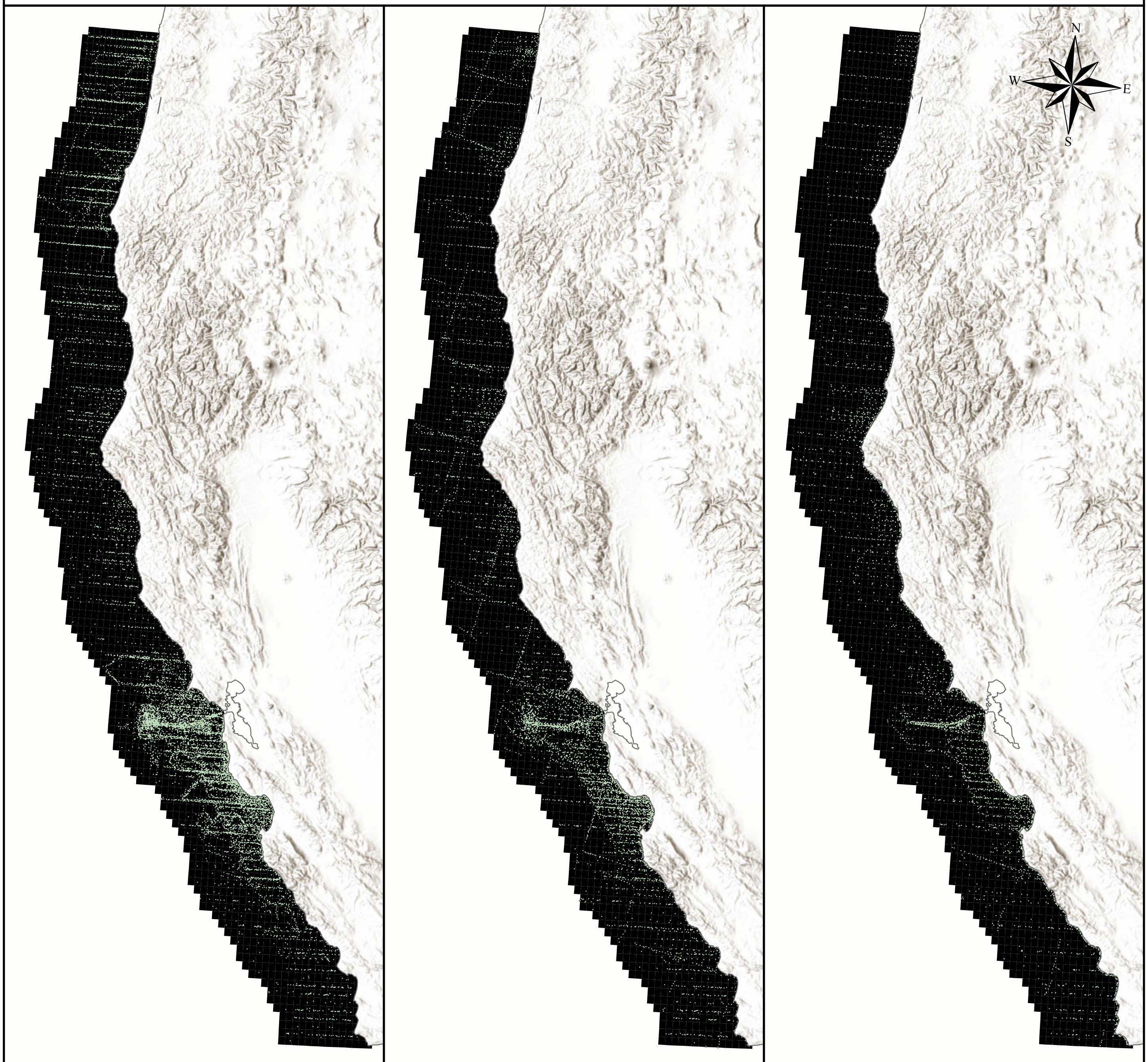

Standardized Residual Value (z-scores)

x < - 2.75	-0.75 < x < -0.25	1.75 < x < 2.25
-2.75 < x < -2.25	-0.25 < x < 0.25	2.25 < x < 2.75
-2.25 < x < -1.75	0.25 < x < 0.75	x > 2.75
-1.75 < x < -1.25	0.75 < x < 1.25	study area
-1.25 < x < -0.75	1.25< x < 1.75	

0 25 50 100 Kilometers

Schatz Energy Research Center

H. T. HARVEY & ASSOCIATES
Ecological Consultants
50 years of field notes, exploration, and excellence

Double-crested Cormorant *(Nannopterum auritum)*

Upwelling	*Oceanic*	*Davidson*

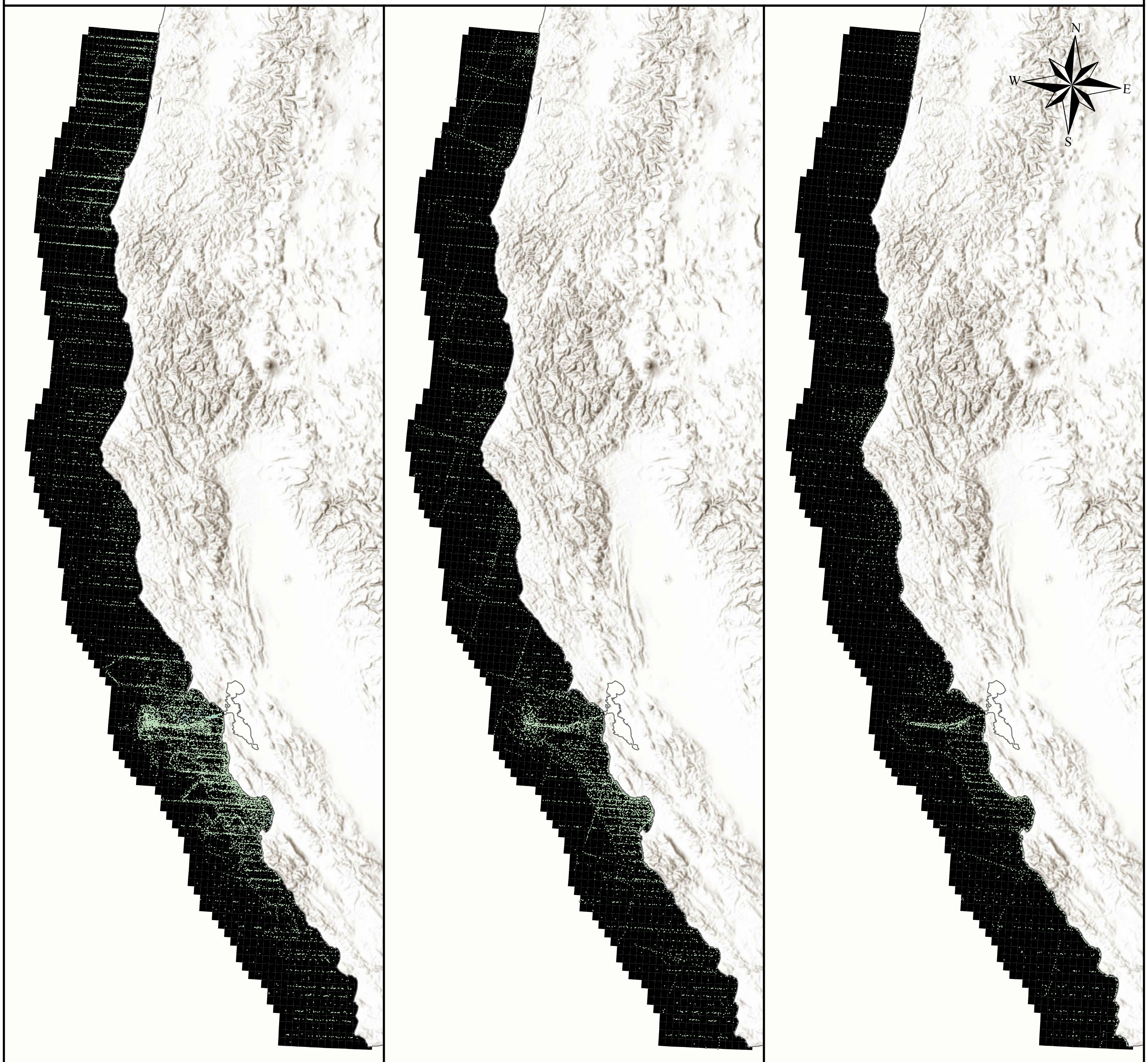

Standardized Residual Value (z-scores)

x < - 2.75	-0.75 < x < -0.25	1.75 < x < 2.25
-2.75 < x < -2.25	-0.25 < x < 0.25	2.25 < x < 2.75
-2.25 < x < -1.75	0.25 < x < 0.75	x > 2.75
-1.75 < x < -1.25	0.75 < x < 1.25	study area
-1.25 < x < -0.75	1.25< x < 1.75	

0 25 50 100 Kilometers

Schatz Energy Research Center

H. T. HARVEY & ASSOCIATES
Ecological Consultants
50 years of field notes, exploration, and excellence

Pelagic Cormorant *(Urile pelagicus)*

Upwelling	*Oceanic*	*Davidson*

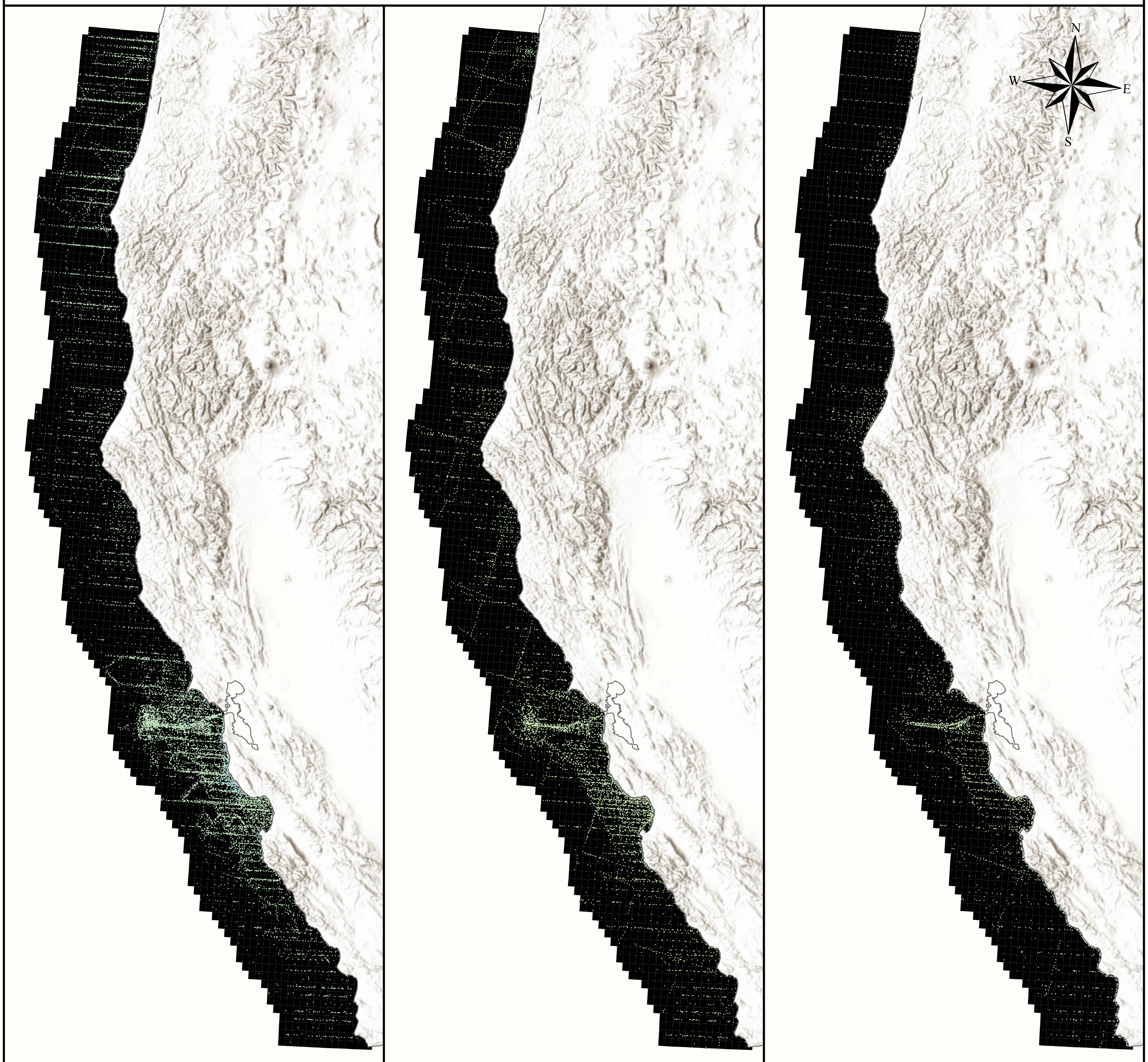

Standardized Residual Value (z-scores)

- x < - 2.75
- -2.75 < x < -2.25
- -2.25 < x < -1.75
- -1.75 < x < -1.25
- -1.25 < x < -0.75
- -0.75 < x < -0.25
- -0.25 < x < 0.25
- 0.25 < x < 0.75
- 0.75 < x < 1.25
- 1.25< x < 1.75
- 1.75 < x < 2.25
- 2.25 < x < 2.75
- x > 2.75
- study area

0 25 50 100 Kilometers

Schatz Energy Research Center

H. T. HARVEY & ASSOCIATES
Ecological Consultants
50 years of field notes, exploration, and excellence

Common Murre *(Uria aalge)*

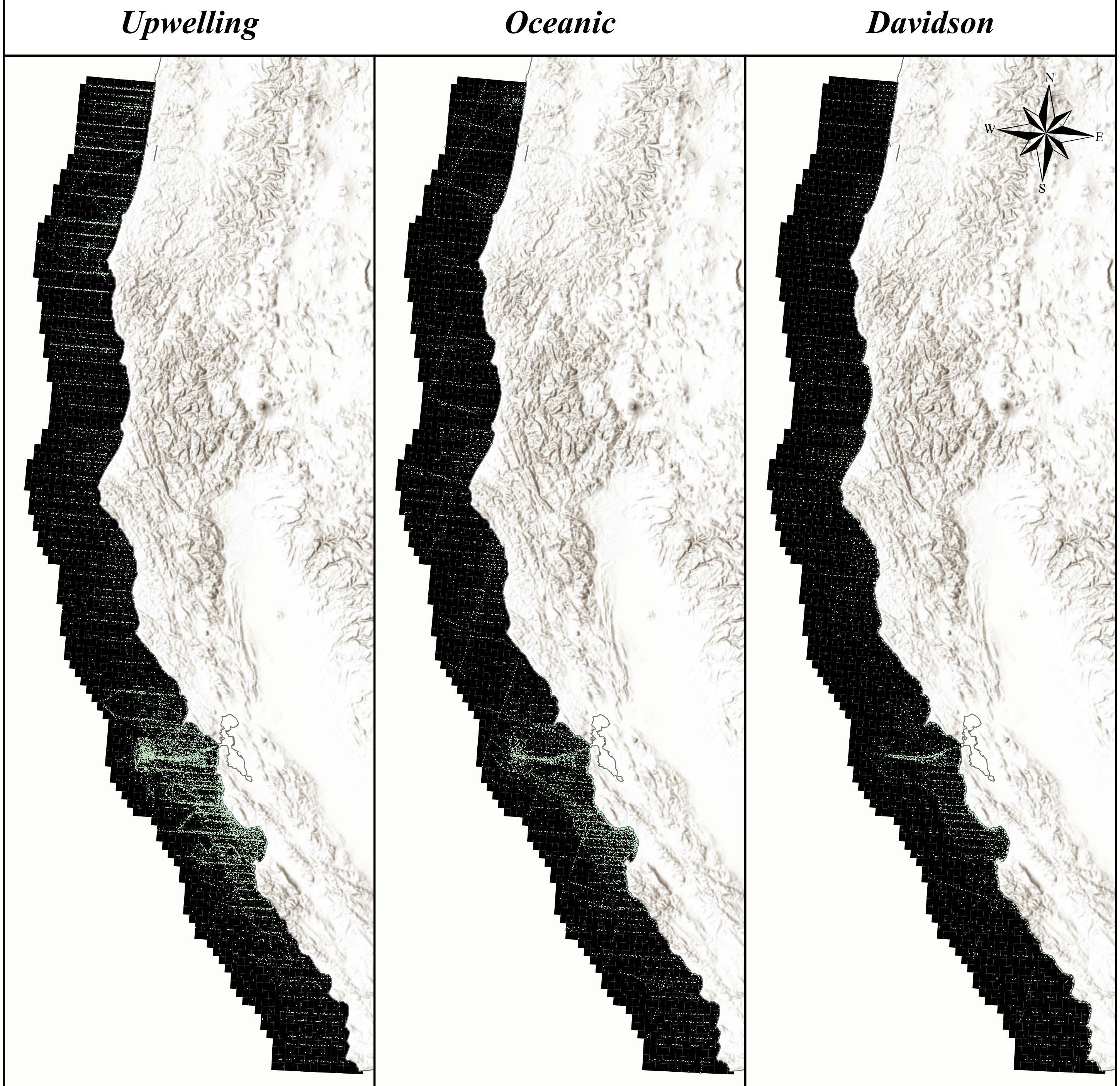

Standardized Residual Value (z-scores)

x < - 2.75	-0.75 < x < -0.25
-2.75 < x < -2.25	-0.25 < x < 0.25
-2.25 < x < -1.75	0.25 < x < 0.75
-1.75 < x < -1.25	0.75 < x < 1.25
-1.25 < x < -0.75	1.25< x < 1.75
1.75 < x < 2.25	
2.25 < x < 2.75	
x > 2.75	
study area	

0 25 50 100 Kilometers

Schatz Energy Research Center

H. T. HARVEY & ASSOCIATES
Ecological Consultants
50 years of field notes, exploration, and excellence

Tufted Puffin *(Fratercula cirrhata)*

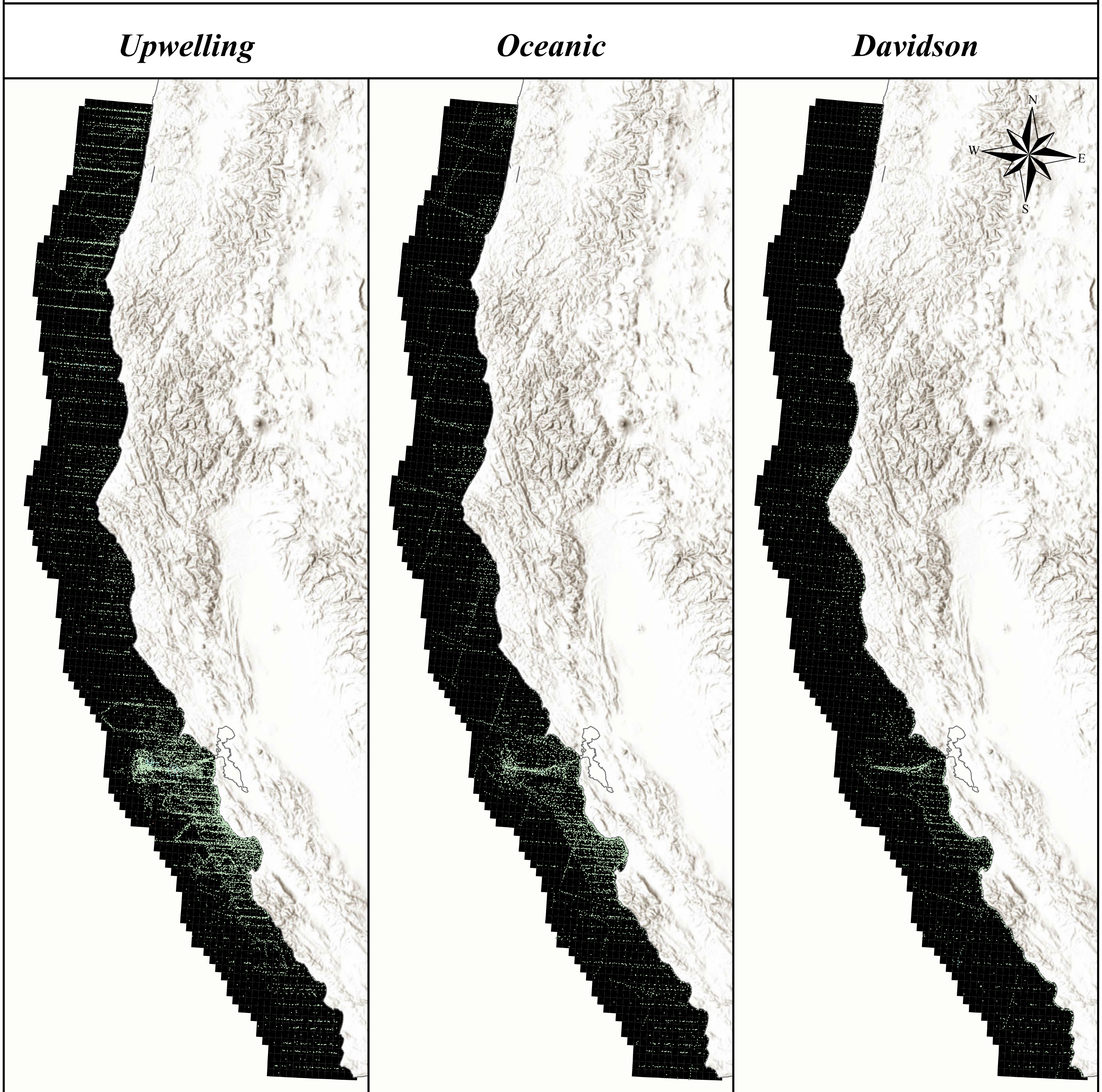

Standardized Residual Value (z-scores)

x < - 2.75	-0.75 < x < -0.25	1.75 < x < 2.25
-2.75 < x < -2.25	-0.25 < x < 0.25	2.25 < x < 2.75
-2.25 < x < -1.75	0.25 < x < 0.75	x > 2.75
-1.75 < x < -1.25	0.75 < x < 1.25	study area
-1.25 < x < -0.75	1.25< x < 1.75	

0 25 50 100 Kilometers

Schatz Energy Research Center

H. T. HARVEY & ASSOCIATES
Ecological Consultants
50 years of field notes, exploration, and excellence

Rhinoceros Auklet *(Cerorhinca monocerata)*

Upwelling	*Oceanic*	*Davidson*

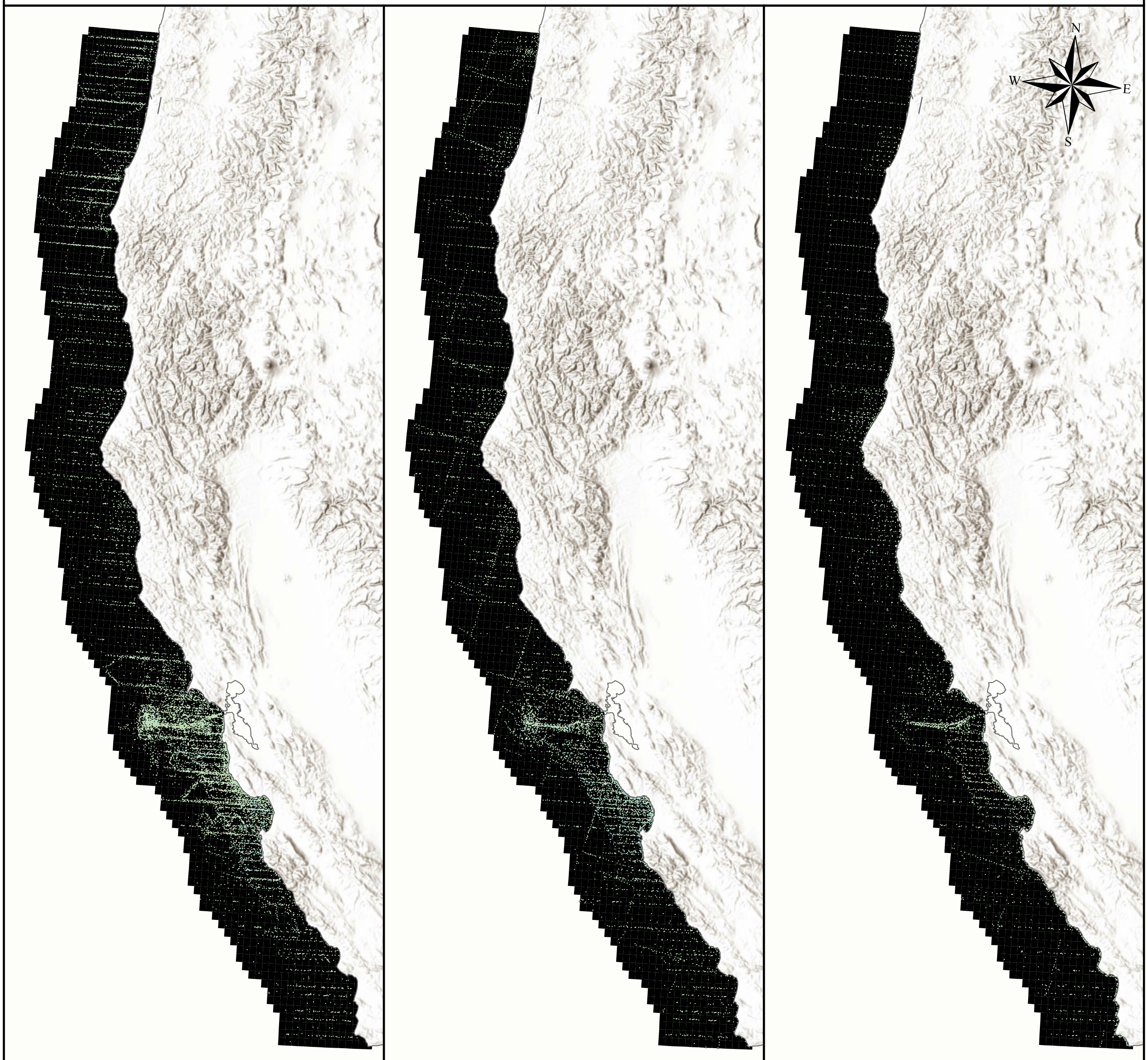

Standardized Residual Value (z-scores)

- x < - 2.75
- -2.75 < x < -2.25
- -2.25 < x < -1.75
- -1.75 < x < -1.25
- -1.25 < x < -0.75
- -0.75 < x < -0.25
- -0.25 < x < 0.25
- 0.25 < x < 0.75
- 0.75 < x < 1.25
- 1.25< x < 1.75
- 1.75 < x < 2.25
- 2.25 < x < 2.75
- x > 2.75
- study area

0 25 50 100 Kilometers

Schatz Energy Research Center

H. T. HARVEY & ASSOCIATES
Ecological Consultants
50 years of field notes, exploration, and excellence

Pigeon Guillemot *(Cepphus columba)*

Upwelling | ***Oceanic*** | ***Davidson***

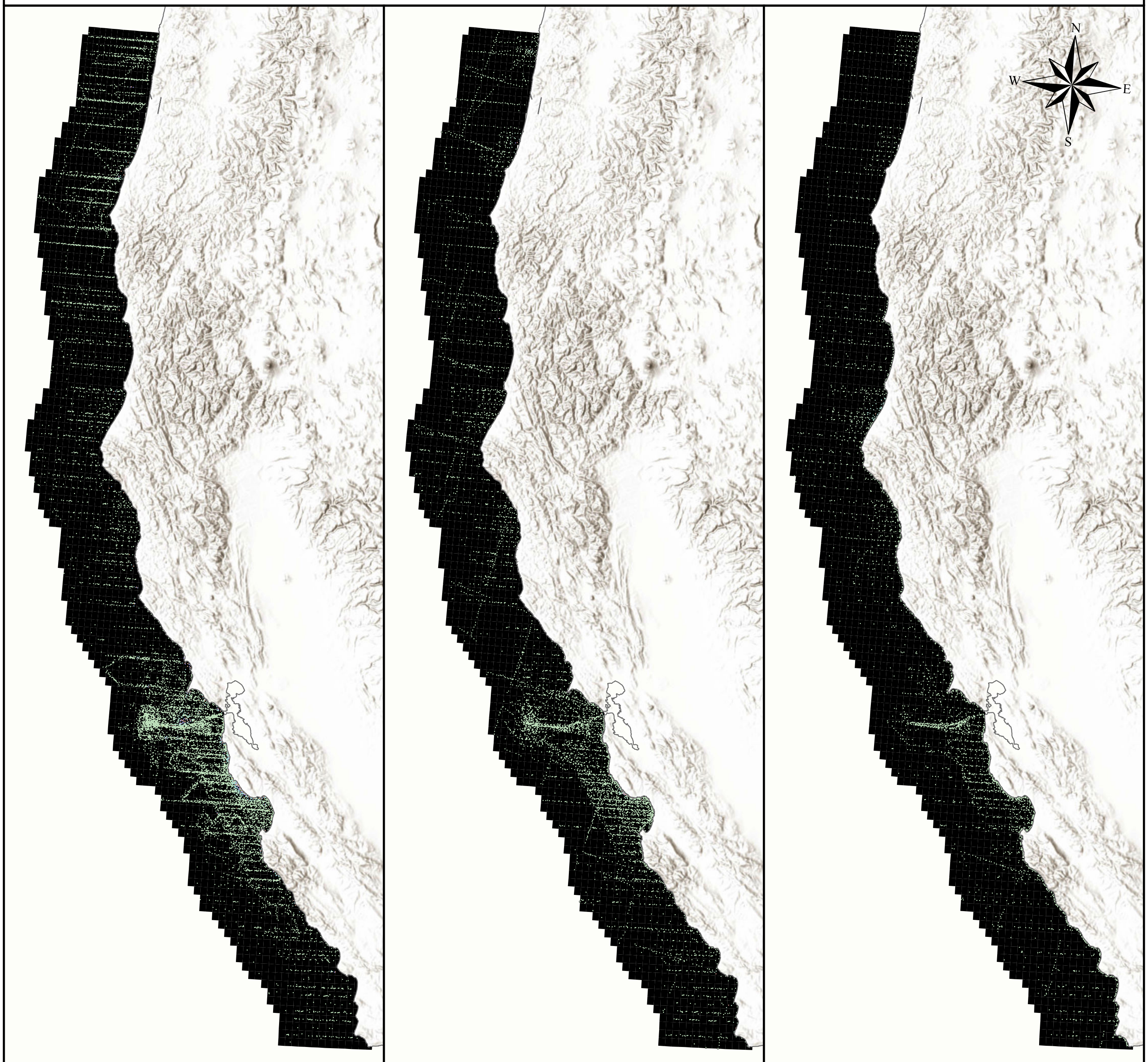

Standardized Residual Value (z-scores)

- x < - 2.75
- -2.75 < x < -2.25
- -2.25 < x < -1.75
- -1.75 < x < -1.25
- -1.25 < x < -0.75
- -0.75 < x < -0.25
- -0.25 < x < 0.25
- 0.25 < x < 0.75
- 0.75 < x < 1.25
- 1.25< x < 1.75
- 1.75 < x < 2.25
- 2.25 < x < 2.75
- x > 2.75
- study area

0 25 50 100 Kilometers

Schatz Energy Research Center

H. T. HARVEY & ASSOCIATES
Ecological Consultants
50 years of field notes, exploration, and excellence

Cassin's Auklet *(Ptychoramphus aleuticus)*

Upwelling	*Oceanic*	*Davidson*

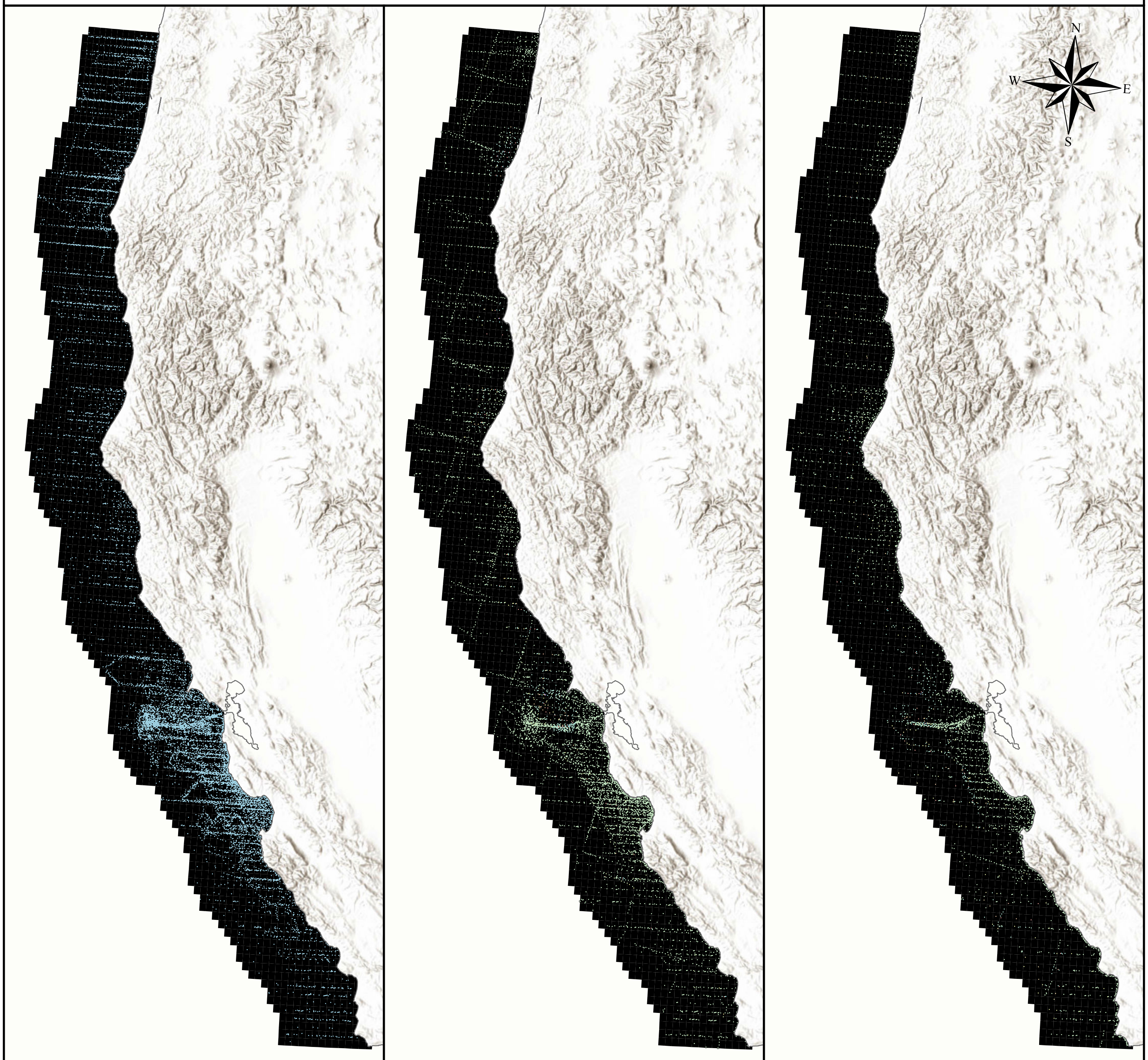

Standardized Residual Value (z-scores)

x < - 2.75	-0.75 < x < -0.25	1.75 < x < 2.25
-2.75 < x < -2.25	-0.25 < x < 0.25	2.25 < x < 2.75
-2.25 < x < -1.75	0.25 < x < 0.75	x > 2.75
-1.75 < x < -1.25	0.75 < x < 1.25	study area
-1.25 < x < -0.75	1.25< x < 1.75	

0 25 50 100 Kilometers

Schatz Energy Research Center

H. T. HARVEY & ASSOCIATES
Ecological Consultants
50 years of field notes, exploration, and excellence

Marbled Murrelet *(Brachyramphus marmoratus)*

Upwelling	*Oceanic*	*Davidson*

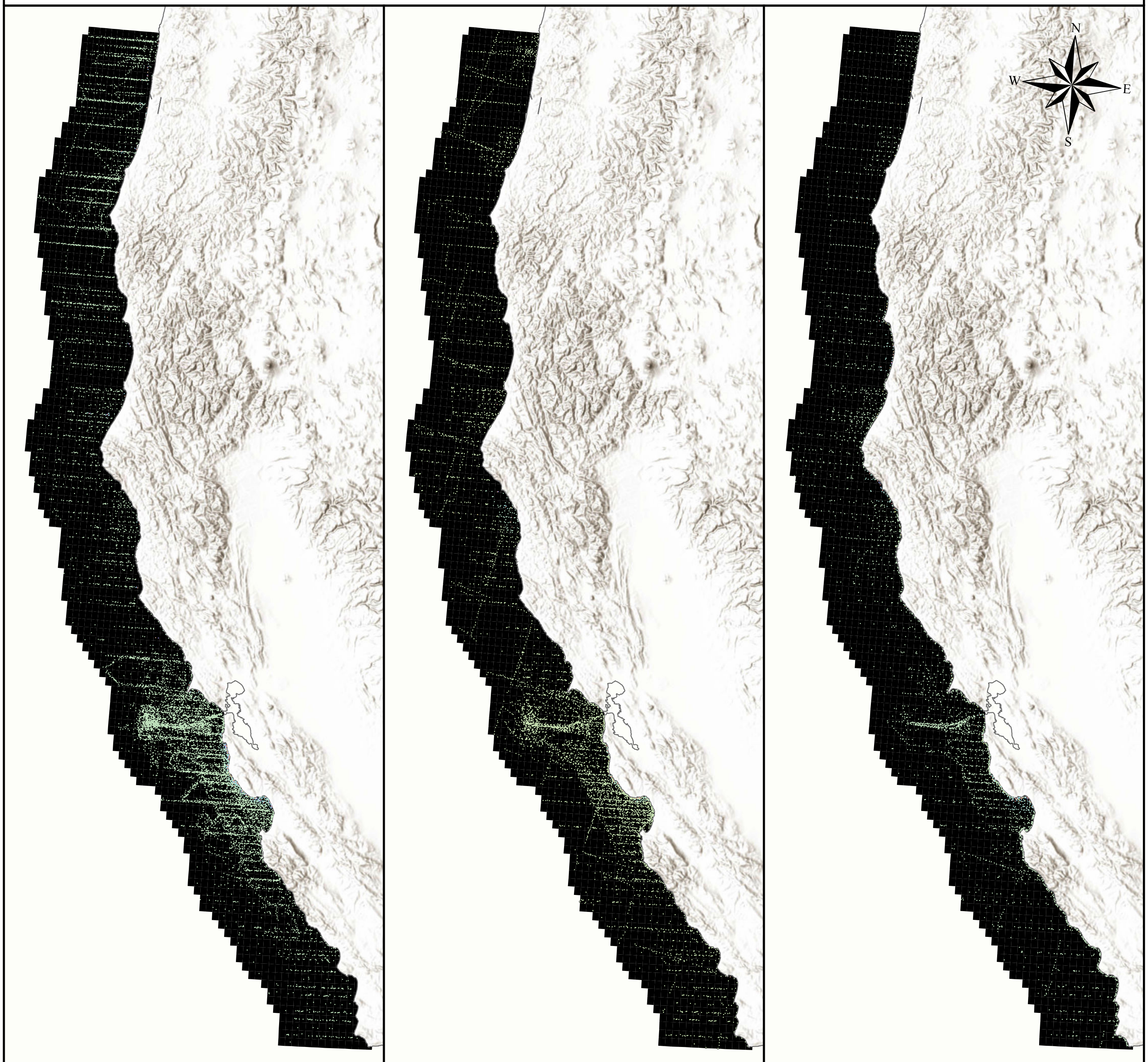

Standardized Residual Value (z-scores)

- x < - 2.75
- -2.75 < x < -2.25
- -2.25 < x < -1.75
- -1.75 < x < -1.25
- -1.25 < x < -0.75
- -0.75 < x < -0.25
- -0.25 < x < 0.25
- 0.25 < x < 0.75
- 0.75 < x < 1.25
- 1.25< x < 1.75
- 1.75 < x < 2.25
- 2.25 < x < 2.75
- x > 2.75
- study area

0 25 50 100
Kilometers

Schatz Energy Research Center

H. T. HARVEY & ASSOCIATES
Ecological Consultants
50 years of field notes, exploration, and excellence

Scripps's/Guadalude/Craveri's Murrelet *(Synthliboramphus sp.)*

Upwelling	***Oceanic***	***Davidson***

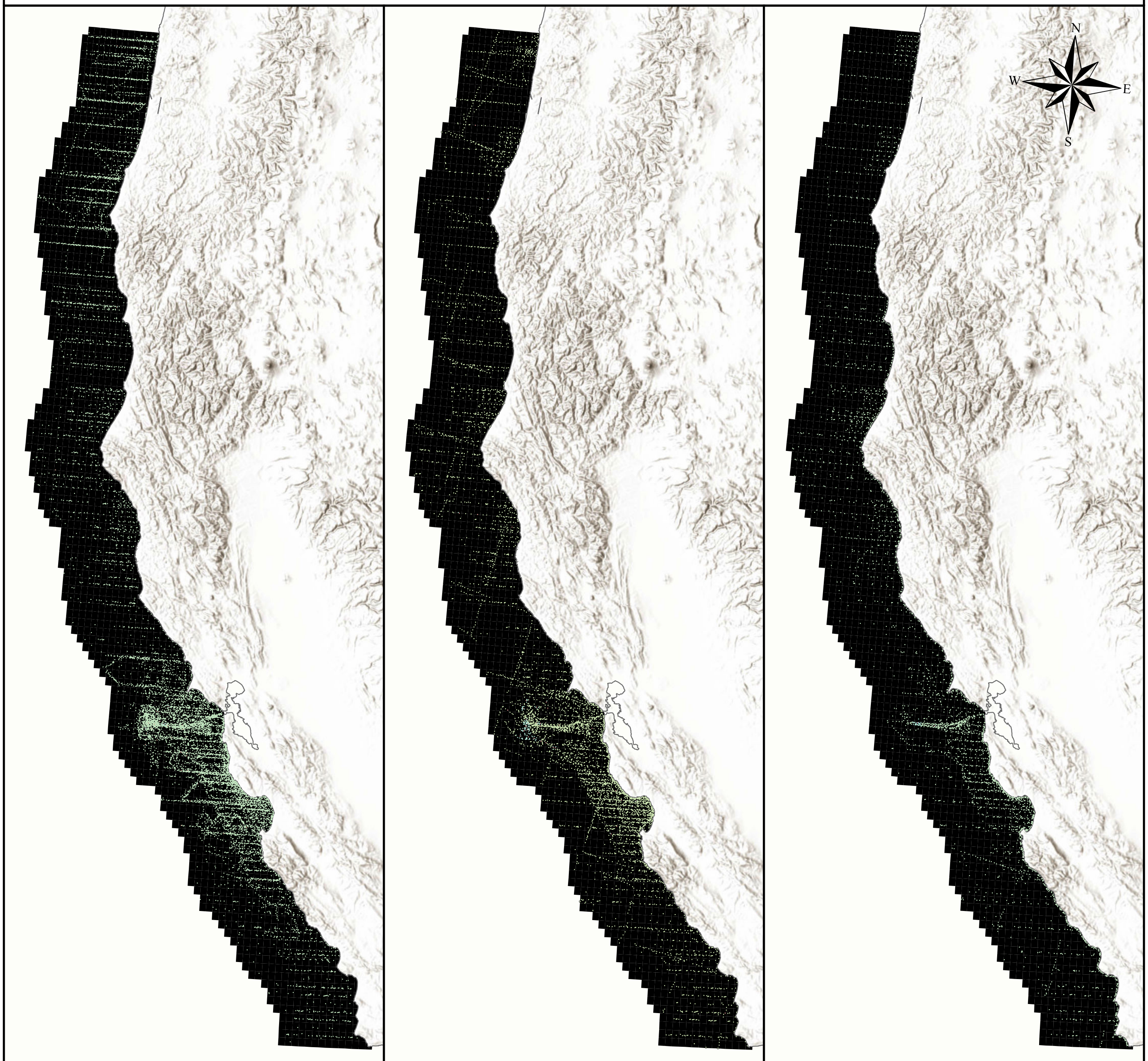

Standardized Residual Value (z-scores)

- x < - 2.75
- -2.75 < x < -2.25
- -2.25 < x < -1.75
- -1.75 < x < -1.25
- -1.25 < x < -0.75
- -0.75 < x < -0.25
- -0.25 < x < 0.25
- 0.25 < x < 0.75
- 0.75 < x < 1.25
- 1.25< x < 1.75
- 1.75 < x < 2.25
- 2.25 < x < 2.75
- x > 2.75
- study area

0 25 50 100 Kilometers

Schatz Energy Research Center

H. T. HARVEY & ASSOCIATES
Ecological Consultants
50 years of field notes, exploration, and excellence

Grebes *(Aechmophorus sp.)*

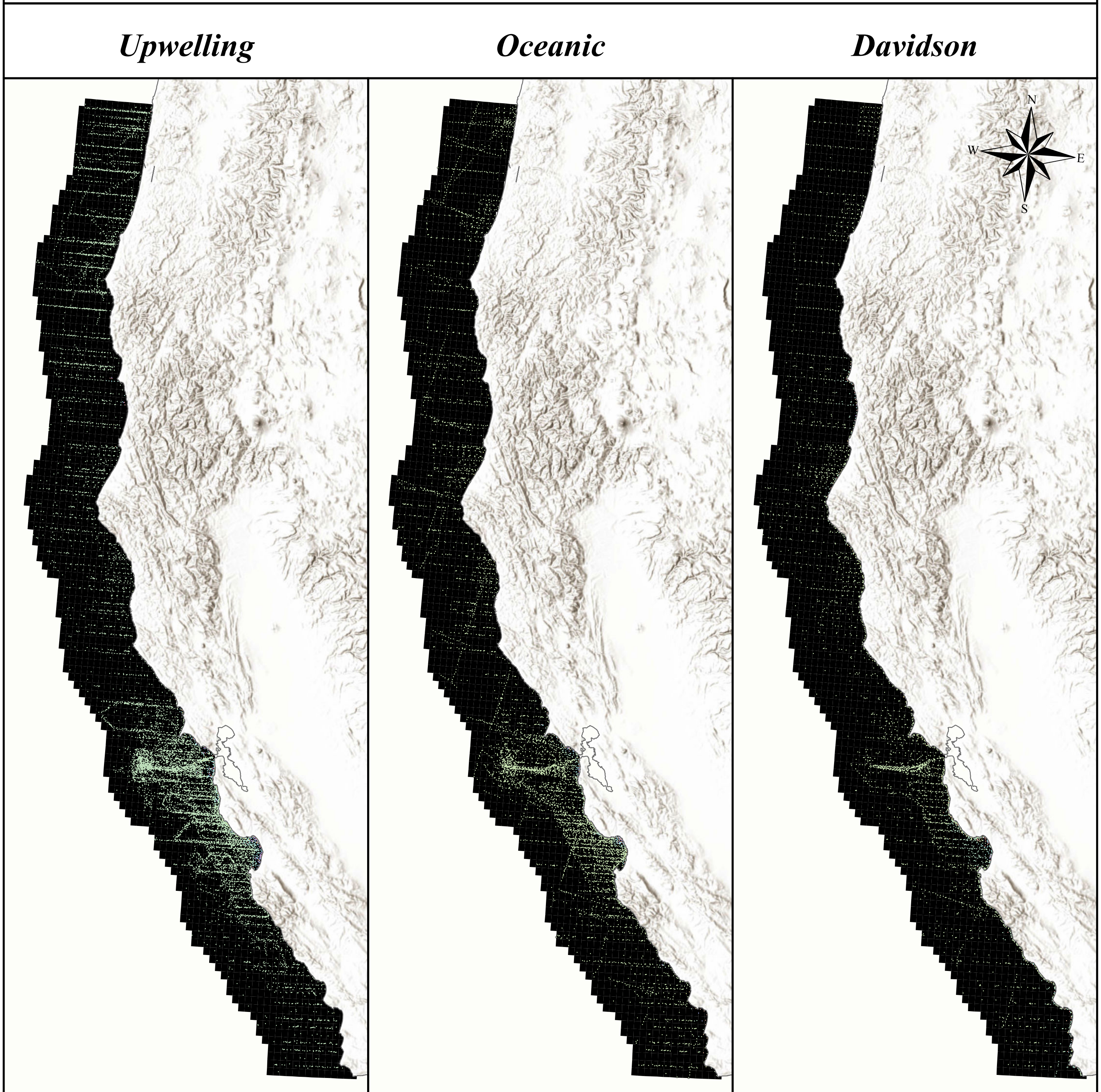

Standardized Residual Value (z-scores)

x < - 2.75	-0.75 < x < -0.25	1.75 < x < 2.25
-2.75 < x < -2.25	-0.25 < x < 0.25	2.25 < x < 2.75
-2.25 < x < -1.75	0.25 < x < 0.75	x > 2.75
-1.75 < x < -1.25	0.75 < x < 1.25	study area
-1.25 < x < -0.75	1.25< x < 1.75	

0 25 50 100
Kilometers

Schatz Energy Research Center

H. T. HARVEY & ASSOCIATES
Ecological Consultants
50 years of field notes, exploration, and excellence

Surf Scoter *(Melanitta perspicillata)*

Upwelling	*Oceanic*	*Davidson*

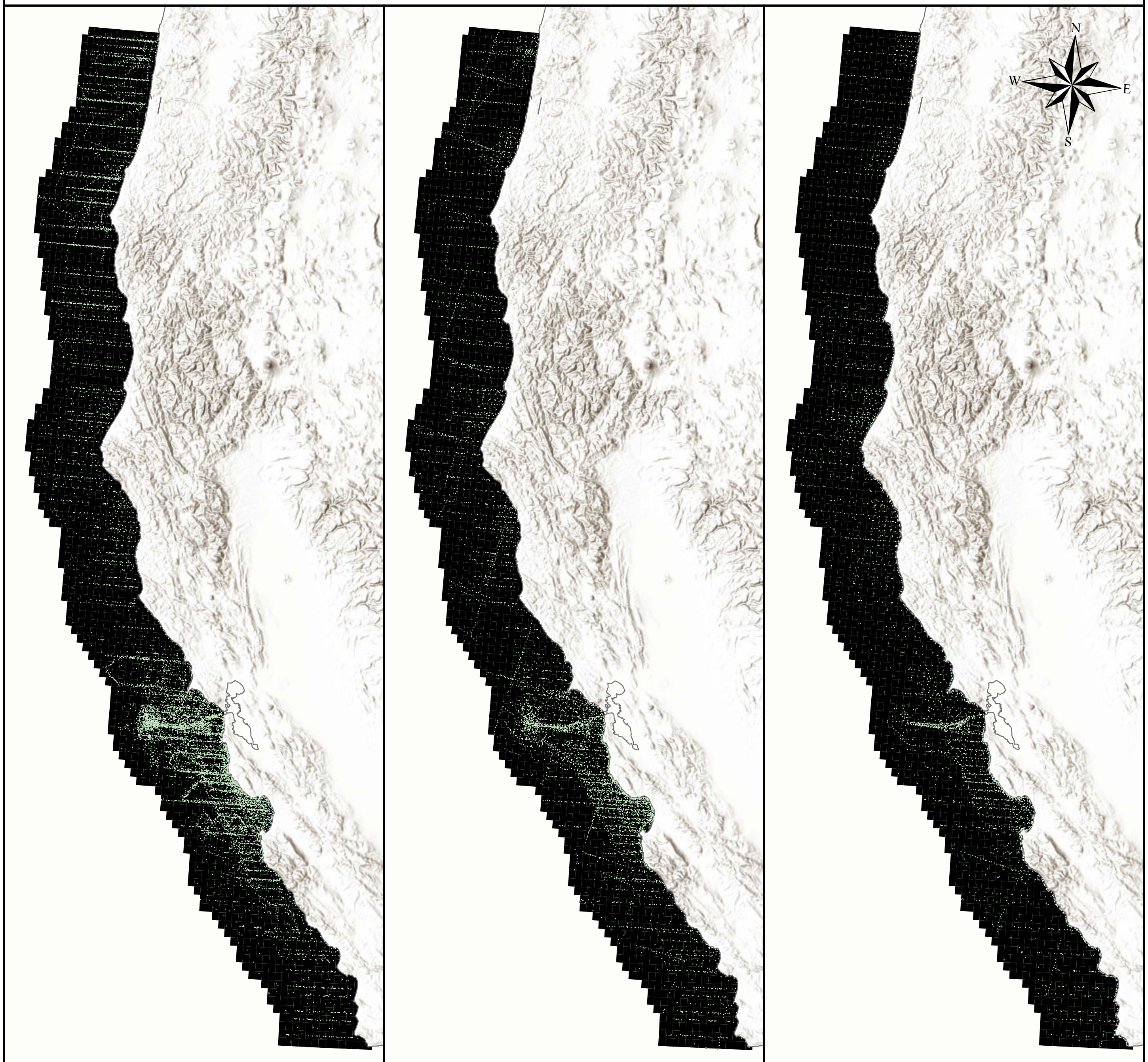

Standardized Residual Value (z-scores)

x < - 2.75	-0.75 < x < -0.25	1.75 < x < 2.25
-2.75 < x < -2.25	-0.25 < x < 0.25	2.25 < x < 2.75
-2.25 < x < -1.75	0.25 < x < 0.75	x > 2.75
-1.75 < x < -1.25	0.75 < x < 1.25	study area
-1.25 < x < -0.75	1.25< x < 1.75	

0 25 50 100 Kilometers

Schatz Energy Research Center

H. T. HARVEY & ASSOCIATES
Ecological Consultants
50 years of field notes, exploration, and excellence

Pacific Loon *(Gavia pacifica)*

Upwelling	*Oceanic*	*Davidson*

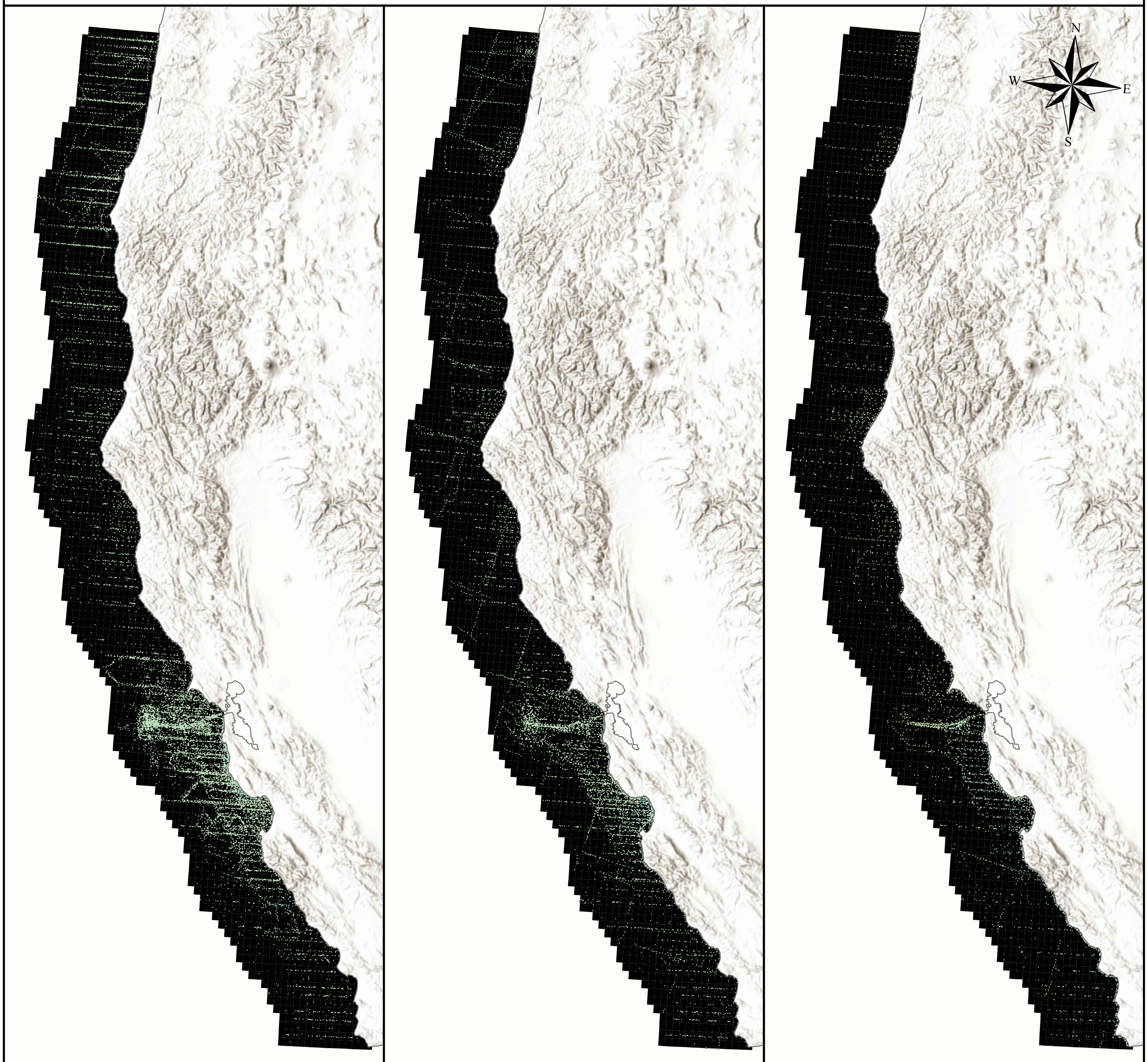

Standardized Residual Value (z-scores)

x < - 2.75	-0.75 < x < -0.25	1.75 < x < 2.25
-2.75 < x < -2.25	-0.25 < x < 0.25	2.25 < x < 2.75
-2.25 < x < -1.75	0.25 < x < 0.75	x > 2.75
-1.75 < x < -1.25	0.75 < x < 1.25	study area
-1.25 < x < -0.75	1.25< x < 1.75	

0 25 50 100
Kilometers

Schatz Energy Research Center

H. T. HARVEY & ASSOCIATES
Ecological Consultants
50 years of field notes, exploration, and excellence

Common Loon *(Gavia immer)*

Upwelling ***Oceanic*** ***Davidson***

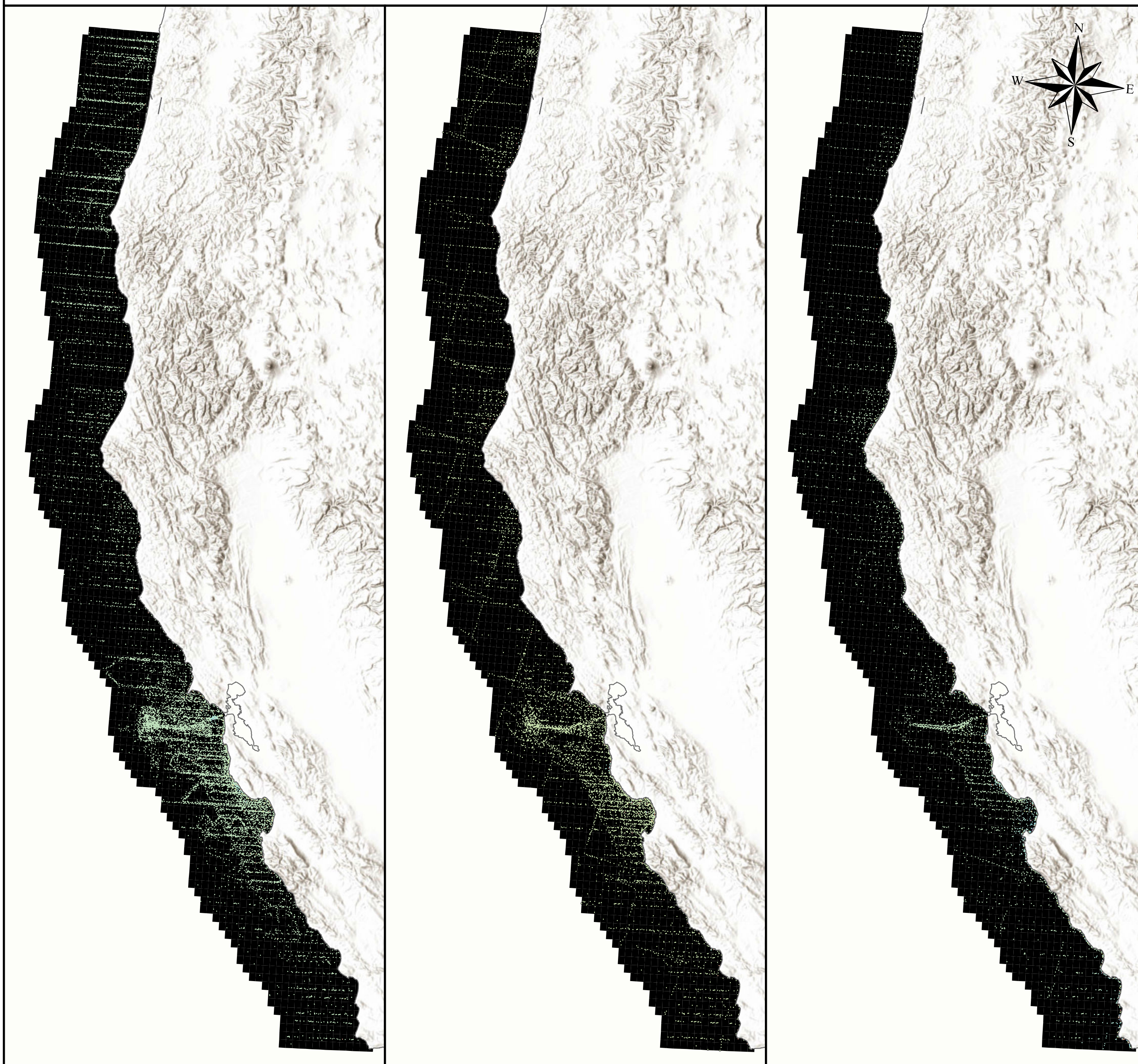

Standardized Residual Value (z-scores)

- x < - 2.75
- -2.75 < x < -2.25
- -2.25 < x < -1.75
- -1.75 < x < -1.25
- -1.25 < x < -0.75
- -0.75 < x < -0.25
- -0.25 < x < 0.25
- 0.25 < x < 0.75
- 0.75 < x < 1.25
- 1.25< x < 1.75
- 1.75 < x < 2.25
- 2.25 < x < 2.75
- x > 2.75
- study area

0 25 50 100
Kilometers

Schatz Energy Research Center

H. T. HARVEY & ASSOCIATES
Ecological Consultants
50 years of field notes, exploration, and excellence

Red-throated Loon *(Gavia stellata)*

Upwelling | ***Oceanic*** | ***Davidson***

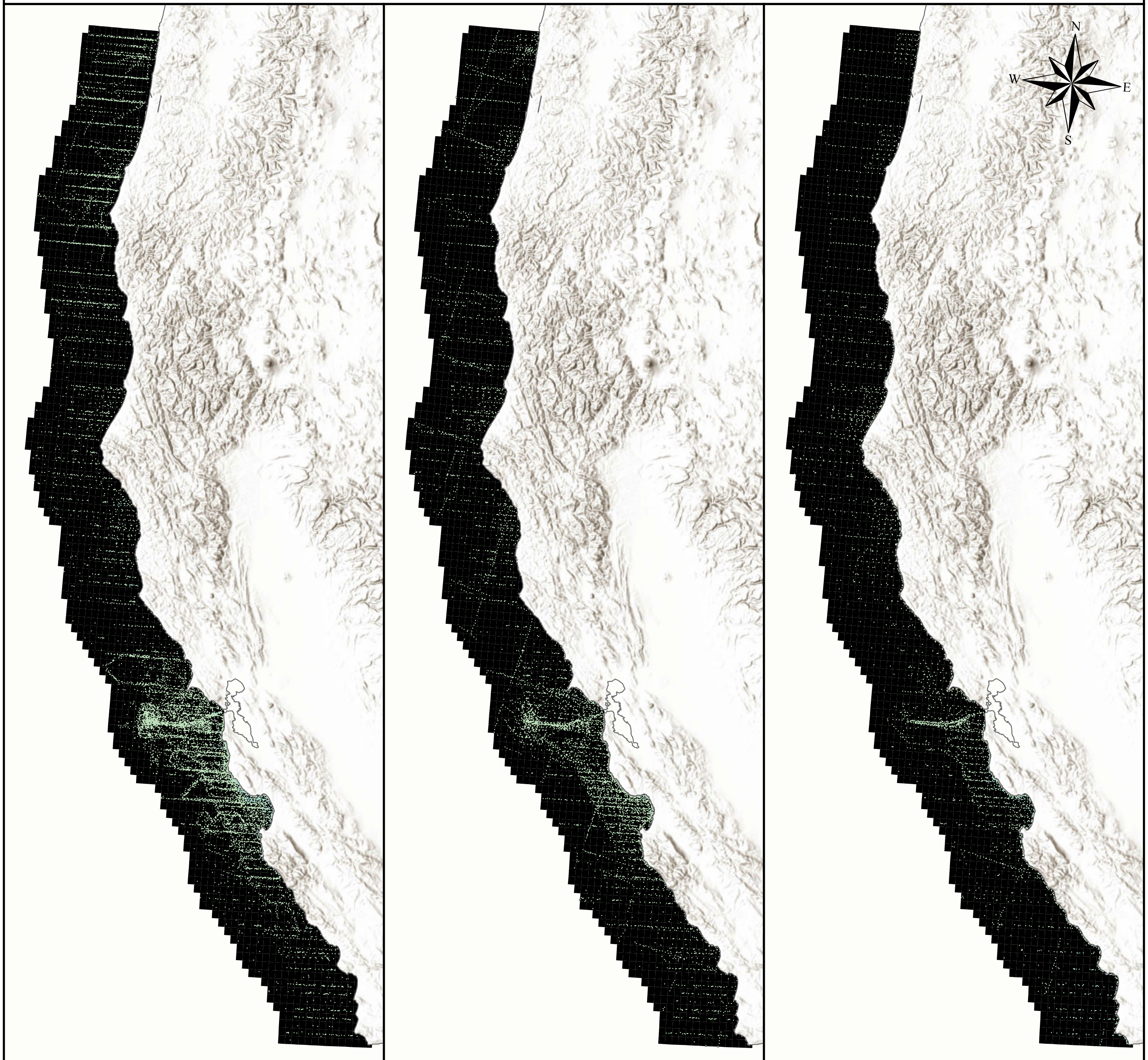

Standardized Residual Value (z-scores)

x < - 2.75	-0.75 < x < -0.25	1.75 < x < 2.25
-2.75 < x < -2.25	-0.25 < x < 0.25	2.25 < x < 2.75
-2.25 < x < -1.75	0.25 < x < 0.75	x > 2.75
-1.75 < x < -1.25	0.75 < x < 1.25	study area
-1.25 < x < -0.75	1.25< x < 1.75	

0 25 50 100
Kilometers

Schatz Energy Research Center

H. T. HARVEY & ASSOCIATES
Ecological Consultants
50 years of field notes, exploration, and excellence

Appendix E. Brief Overview of the Ecology, Morphology, and Flight Behavior of Seabirds Included in the 3D Seabird Collision Vulnerability Framework

Pacific Ocean seabirds can be separated into 29 flight-style groupings (FG) (Spear and Ainley 1997, Ainley et al. 2015). Of these, 18 occur in the California Current System (CCS) in sufficient numbers to devise reliable density estimates using the existing 1980-2016 assembly of at-sea surveys (see Results). Some of these FGs e.g. small albatross , include special status species that are rare but more abundant than other members of the group, and are documented enough to have adequate sample sizes for modeling. Their vulnerability to collision with offshore wind (OSW) turbines can be generally assessed for the FG based on the flight behavior characterizing its group. A few of the 29 FGs (e.g.., large gadfly petrels, small gadfly petrels, boobies, tropicbirds, and frigatebirds), occur but have not been documented enough in the CCS to have a sufficient sample size for analysis (Table A-3) but contain special-status species and are also addressed below.

The information provided herein provides information on seabird flight-style as it relates to their collision vulnerability and can be used to contextualize the results provided by the 3D Seabird Collision Vulnerability Framework (3D Framework). First, we provide an overview of four seabird flight modes. Then, we provide background information on each of the FGs covered in the 3D Framework. Note there is mention of species not modeled by the 3D Framework.

In the data set used in 3D Framework, 18 FGs were analyzed, each composed of species (or taxa) that have similar morphology. Note the species within FGs are consistent with taxonomy (Table E-1) and fall into four overall modes of seabird flight, sequenced by the amount of flapping required to stay aloft: flappers, flap-gliders, glide-flappers, and gliders (Table E-2). These represent the modes of seabirds traveling point-to-point but is not necessarily typical while foraging nor maneuvering to land-at/take-off from colonies or roosts.

Seabirds that travel using flapping flight almost never glide when flying over the open ocean and usually travel close to the ocean surface, as it offers some aerodynamic advantage (i.e., higher air density provides more lift; Pennycuick 1989) (Table E-2). However, when experiencing updrafts along bluffs and cliffs near nesting colonies or roosting sites they glide, i.e., travel without flapping (known as 'slope soaring;' Pennycuick 1987).

Flappers have short and wide wings, with an aspect ratio <10 in most cases (Table E-1) and are very maneuverable. The opposite is true for gliders, which almost never flap when traveling over the open ocean, unless taking off from the sea surface to gain speed (Table E-2). They have long, narrow wings, like an airplane glider, with aspect ratio generally >10 (Table E-1). They need wind to take off, or very large waves that allow down-slope launching. Once aloft, flappers become dynamic soarers (DS).

DS swoop in a circular pattern between the sea surface and height of their swoop. They flap only for quick course alterations and otherwise use gravity to gain speed in the downward portion of their swoop: the higher their swoop, the more speed they can gain in forward flight. As wind increases, their swooping flight height and speed increases. In contrast to flappers, dynamic soarers flap upon approaching or leaving nest or roost sites, needing the flapping for close maneuvering.

Between flappers and gliders are two other styles of flight (Table E-2). Glide-flappers exhibit dynamic soaring interspersed with segments of flapping at the bottom of their 'swoop' near the sea surface to maintain speed for the upward swoop. Glide-flappers have long, narrow wings, and increase their flight height and reduce flapping with higher winds. Flap-gliders are the opposite and mostly flap with interspersed segments of gliding. They, too, generally remain close to the ocean surface, and the gliding segments may be used to conserve energy expended by flapping or maintain the speed needed for gliding. Flappers and flap-gliders often fly in line or V-formation (i.e., slip streaming'), another means to conserve energy.

The following taxonomic and flight-style groups (Table E-1) contain both species that nest along the coast of the study area, as well as species that are seasonal residents or passage migrants. In general, the species most vulnerable to encountering the rotor swept zone (RSZ) and at risk of collision are not California (CA) resident species.

Table E-1. Morphology and Flight-style of Each Seabird Flight-style Group

Flight Group	Species	Body Mass (g)	Wing Span (mm)	Wing Area (cm^2)	Wing Load (newtons per m^2)	Wing Aspect Ratio	Flight-Style*
Small Albatross	6	3449	2170	3456	98	13.6	DS
Fulmars	7	1362	1174	1389	77	10.5	FG
Large Gadfly Petrels	9	360	972	856	42	11.1	DS
Small Gadfly Petrels	7	136	722	524	25	9.9	FG
Surface Feeding Shearwaters	2	391	1019	1044	37	10.0	FG
Large Diving Shearwaters	2	651	978	828	77	11.6	GF
Small Diving Shearwaters	2	632	913	760	68	11.0	GF
Storm-Petrels	2	33	432	244	13	7.7	FL
Pelicans	1	4120	2224	4920	82	10.1	GF
Boobies	5	1746	1590	2202	76	11.5	GF
Cormorants	4	1766	1052	1681	127	6.6	FL
Phalaropes	2	38	388	212	18	7.1	FL
Skuas	6	887	1392	1671	48	9.2	FL
Large Gulls	5	1154	1489	2428	47	9.2	FL
Medium Gulls	4	522	1188	1420	37	10.1	FL
Small Gulls	1	255	1015	945	26	10.9	FL
Terns	5	147	790	617	22	10.2	FL

Flight Group	Species	Body Mass (g)	Wing Span (mm)	Wing Area (cm²)	Wing Load (newtons per m²)	Wing Aspect Ratio	Flight-Style*
Large Alcids	2	1042	729	560	183	9.5	FL
Medium Alcids	6	585	612	440	129	8.6	FL
Small Alcids	8	208	434	238	85	8.1	FL
Loon, Grebes, Ducks	Many	612	591	413	133	8.7	FL

Morphological characteristics of seabirds portioned by flight group are summarized from Spear and Ainley (1997).
* DS = dynamic soarers; FG = flap-gliders; GF = glide-flappers; FL = flappers

Table E-2. Proportion of Individuals that Flap Versus Glide For Each of Four Basic Seabird Flight Strategies

Flight-Style	Proportion Seen Flapping	Proportion Seen Gliding
Flappers	0.71 – 0.92	0.01 – 0.10
Glide-flappers	0.14 – 0.44	0.02 – 0.15
Flap-gliders	0.03 – 0.12	0.21 – 0.53
Gliders/dynamic soarers	0.00 – 0.09	0.73 – 1.00

Table data is derived from 117 cruises in all portions of the Pacific Ocean, 1976-2006 (n >152,000 sightings; Ainley et al. 2015).

Small Albatrosses

These species are visitors to the CCS, and despite being called 'small', they are some of the largest seabirds. Their heavy bodies and wing shape require that they exist in regions where wind is persistent and strong to remain airborne and use dynamic soaring. Black-footed albatross (*Phoebastria nigripes*) are present in the CCS during the spring and summer (Upwelling season). Laysan albatross (*Phoebastria immutabilis*) nest among the Hawaiian Islands and were present in the CCS during the winter, but with recent colonization of some islands off Mexico, their presence has recently extended to be year-round. Both species are listed as near threatened by the IUCN and in Annex I of the Agreement on the Conservation of Albatrosses and Petrels (ACAP). Short-tailed albatross (*Phoebastria albatrus*) are also visitors during the Upwelling season and are listed as endangered under the federal Endangered Species Act (ESA; and so listed by IUCN and ACAP). Their numbers and sightings have been increasing in response to restrictions of long-line fishing in the Gulf of Alaska and recovery of breeding colonies. As DS, small albatrosses are potentially more vulnerable to turbine blade collision than many other CCS species.

Fulmars

While several fulmar species (sometimes called fulmarine petrels) are abundant in the Southern Hemisphere, only the northern fulmar (*Fulmarus glacialis*) is present in the CCS. Northern fulmars nest in the Bering Sea region and typically remain in the Gulf of Alaska but may fly as far south as the CCS in appreciable numbers during the Davidson Current season.

Large Gadfly Petrels

Large gadfly petrels are abundant in the Southern Hemisphere and the eastern tropical Pacific. The Hawaiian petrel (*Pterodroma sandwichensis*) nests among the main islands of Hawaii and forages widely across the Pacific Ocean basin into the CCS. They are listed as endangered under the federal ESA, but populations have been increasing as a result of ongoing conservation measures. The species has been observed routinely in the outer CCS albeit too infrequently to devise meaningful density estimates. A few other species in this FG have been detected in the CCS but at very low frequencies. Like the small albatrosses, the propensity for species in this FG is to engage in dynamic soaring which makes them especially likely to be present at heights overlapping with RSZs and relatively vulnerable to collision with turbine blades.

Small Gadfly Petrels

Small gadfly petrels areanother group abundant in the Southern Hemisphere and the subtropical Pacific (leeward Hawaiian Islands). Numbers of species in the CCS were too sparse to generate density estimates, though one species, Cook's petrel (*Pterodroma cooki*), has been increasingly detected and responding well to conservation measures at nesting colonies in the southwest Pacific.

Surface-feeding Shearwaters

The pink-footed and Buller's shearwaters (*Ardenna creatopus, A. bulleri*) nest in Chile and New Zealand, respectively. The pink-footed shearwater is listed as Vulnerable by IUCN, and endangered in the waters of Chile and Canada and under Annex I of ACAP. Appreciable numbers visit the CCS during the Oceanic season, and occur mainly offshore at the edge of subtropical waters in association with tuna. When flap-gliding, they mostly occur close to the sea surface.

Larger Diving Shearwaters

The sooty and short-tailed shearwaters (*Ardenna grisea*, *A. tenuirostris*) nest in New Zealand, Patagonia and Australia, respectively. Their populations number in the millions, although they are decreasing primarily from resource competition with commercial fisheries. Large numbers of sooty shearwaters spend their non-breeding period in the CCS and occur at greatest concentrations during the Upwelling season. Short-tailed shearwaters occur more in the Oceanic season. Owing to their relatively large body size, both species switch from a flap-gliding flight style to a dynamic soaring flight style in high winds (>15 m/s) to reach appreciable heights above the sea surface.

Smaller Diving Shearwaters

Black-vented shearwaters (*Puffinus opisthomelas*) nest in colonies off Mexico and Central America, only visiting the CCS in small numbers during the Oceanic and Davidson Current seasons. They remain close to the sea surface as they transit using a glide-flapping style of flight.

Storm-Petrels

Leach's, ashy, and fork-tailed storm-petrels (*Hydrobates homochroa, H. leucorhous, and H. furcatus*) are abundant in the CCS, especially along the shelf break and offshore waters. All three species nest in colonies on various CA islands, with the ashy (and black storm-petrel [*H. Melania*]) more in the south and Leach's and fork-tailed in the north. Ashy and fork-tailed storm-petrels occur in the CCS year-round, while Leach's storm-petrels migrate south in autumn and back in spring. A portion of the Leach's storm-petrels are passage migrants that nest in abundance from British Columbia to the Aleutian Islands but also travel to eastern tropical Pacific waters for the non-breeding period. A few other storm-petrel species visit CCS waters, especially the black storm-petrel, which mostly nests in islands of Baja CA but also in the CA Channel Islands. Black storm-petrels disperse north to central CA waters in fall after the breeding season. Storm-petrels fly by flapping close to the sea surface or at times using 'sea-anchor soaring' and pushing off the water with their feet to then glide and flap (Spear and Ainley 1997). Ashy, fork-tailed and black storm-petrels are listed by the state of CA as Species of Special Concern.

Pelicans

The brown pelican (*Pelecanus occidentalis*) is a very large, heavy bird with broad wings. It flies by glide-flapping, often in follow-the-leader flocks, but is otherwise very maneuverable. It flies higher than 10 m in waters over the continental shelf and closer to shore, especially when searching for food. The species once was listed as endangered under federal and CA ESA but was delisted. It mostly nests on islands of Baja CA, though colonies exist in the CA Channel Islands as well. Within our study area, it is a seasonal resident mainly during the late Upwelling and Oceanic seasons. However, its presence can be variable, depending on ocean climate (El Niño – La Niña). Brown pelicans may be more abundant for longer parts of the year during El Niño, as. they generally do notnest during El Niño due to insufficient food resources. During that period can be present in the study area year-round.

Boobies

Prehistorically abundant in the CCS, a few species of boobies have recently returned in low numbers to nest in the CA Channel Islands. Numbers are increasing but were too low in our study area during the survey periods to be included in the 3D Framework. Like pelicans, boobies fly by glide-flapping and reach appreciable heights when foraging.

Phalaropes

The red and red-necked phalaropes (*Phalaropus fulicarius, P. lobatus*) are grouped in the 3D Framework as it is difficult to differentiate them quickly in the field, especially in aerial surveys. Both are migrants present in the shelf break as they pass through the CCS from Arctic breeding grounds and the Humboldt Current off of South America.. They likely number in the millions as they head southward during the Oceanic season and Northward during Upwelling. During the latter, they wait for periodic lulls in the otherwise persistent, strong upwelling headwinds. They fly by flapping and remain very close to the sea surface.

Skuas

Skuas include four members of the genus *Stercorarius*, of which one (south polar skua [*S. maccormicki*]) is a seasonal resident from the polar south, and three are seasonal residents or passage migrants from the Arctic. South polar skuas are present in the CCS during the Oceanic season. All skuas fly by flapping and are highly maneuverable. They harass other species into dropping prey which they subsequently steal. At times they fly relatively high, possibly expanding their ability to locate multi-species feeding flocks.

Large Gulls

This group is dominated by western and glaucous-winged gulls (and hybrids; *Larus occidentalis, L. glaucescens*). Both are year-round residents, with western gulls present more in the southern portion and glaucous-winged gulls more in the northern portion of the study area. They are most densely concentrated near the coast, especially during the non-breeding period (Davidson Current season) and nest on islands, islets, and warehouses. Herring and Iceland Gulls (*L. argentatus*, *L. glaucoides*) are seasonal residents from subarctic and Arctic breeding sites, mainly during the Davidson Current season. Large gulls typically remain close to the water at they travel by flapping flight and are highly maneuverable.

Medium Gulls

This is one of the most species-rich FGs in the study area and includes Heermann's, California, ring-billed gulls (*L. heermanni*, *L. californicus*, *L. delawarensis*), and black-legged kittiwakes (*Rissa tridactyla*). California gulls are year-round residents that nest in CA at fresh or brackish water sites. The remaining species are seasonal residents. Medium gulls are most abundant in CCS waters during the Davidson Current season, their non-breeding season. Heermann's gull nests mostly on islands of Baja CA while the remainder are subarctic nesters. The abundance of Heermann's gull, which often feed by stealing from brown pelicans, varies greatly depending on ocean climate in the Gulf of CA and they can forgo breeding altogether during strong El Niño events.

Small Gulls

Sabine's and Bonaparte's gulls (*Xema sabini* and *Chroicocephalus philadephia*) are migrants that pass through the CCS study area and primarily occur at or beyond the outer continental shelf during migrations. Their southward migration occurs during the Oceanic season and northward migration during the Upwelling season with most of their progress being made during lulls in headwinds. They travel by flapping flight close to the sea surface. Short-billed gulls (*L. brachyrhynchus*) breed in Alaska and Canada and winter primarily in nearshore habitats. They are most common in coastal areas but can occur offshore as well.

Terns

There are several genera in this group. The smallest in size is the California least tern (*Sternula antillarum*), which is listed as endangered by the federal ESA. A small colony exists on the coast of the southern portion of the study area, generally foraging in continental shelf waters. It is present mostly during the upwelling period, likely wintering off South America. The slightly larger *Sterna* species include the Arctic and common terns (*S. Paradisaea, S. hirundo*). Arctic and common terns in the study area are passage migrants, moving between Arctic nesting areas and Southern Hemisphere waters. They move south during the Oceanic season and north during Upwelling, mainly along the shelf break and waters to the west. Lastly, there are the larger *Hydroprogne and Thalasseus* species. These include the Caspian, elegant, and royal terns (*Hydroprogne caspia, Thalasseus elegans, T. maximus*). Caspian terns nest at inland river bars and lake islands while elegant terns nest largely on islands in the Gulf of CA. They are seasonal residents in the study area during their non-breeding period (Oceanic and Davidson Current seasons). They mainly frequent waters overlying the continental shelf, flying by flapping at relatively high altitudes at times to search for fish schools. All terns are highly maneuverable flappers.

Cormorants

Brandt's, double-crested and pelagic cormorants (*Urile penicillatus, Nannopterum auritum, U. pelagicus)* all nest on CA islands, coastal islets or headlands. They frequent waters of the continental shelf and are capable of diving to the ocean bottom to reach prey. All are heavy flappers and often travel in follow-the-leader flocks, staying close to the sea surface.

Large Alcids

In the CCS study area, this FG is represented by one species: the common murre (*U. aalge*). The common murre is one of the two most abundant species in the seabird observation data set. It is a year-round resident, concentrated largely in continental shelf waters from central to northern CA and nesting on islands and headlands from the CA Channel Islands north into central Oregon. Recovering from human impacts, the overall population of the common murre has been steadily increasing during recent decades. Common murres have short, stubby wings with high body mass and wing loading, which require very rapid flapping flight. They use their wings for under-water 'flight' as well. Unless approaching or leaving elevated nesting colonies, they generally fly close to the sea surface. They are flightless during molt, which occurs during the Oceanic season.

Medium Alcids

This group includes pigeon guillemots (*Cepphus columba*), tufted puffins (*Fratercula cirrhata*) and rhinoceros auklets (*Cerorhinca monocerata*;). Pigeon guillemot and tufted puffin are only residents in the study area during the breeding season and reside in waters of British Columbia and Gulf of Alaska during the remainder of the year. The rhinoceros auklet is the only year-round resident, frequenting the shelf break waters when not associated with nesting islands from central CA to the Pacific Northwest. All have short, stubby wings used for diving and must stay aloft by flapping flight (i.e., requiring a high wing-beat frequency), and remain very close to the sea surface except when approaching and leaving elevated nesting sites.

Small Alcids

Small alcids are another specious FG in the study area and include the taxon composed of three closely related *Synthliboramphus* murrelets: Scripps's, Guadalupe, and Craveri's, which were formerly lumped as one species; the Xantus's murrelet; marbled murrelet (*Brachyramphus marmoratus)*; ancient murrelet (also a *Synthliboramphus antiquum*) murrelets; and Cassin's auklet (*Ptychoramphus aleuticus*). Ancient murrelets area visitors to the CCS from the Pacific Northwest during the Oceanic and Davidson seasons. The others are year-round residents off CA, though the *Synthliboramphus* 'Xantus's' group nests to the south of the study area. The latter disperses northward during the post-breeding season, swimming north and remaining in the shelf break and more westerly waters. Marbled murrelets rarely stray farther than a few kilometers (km) from shore, while the Cassin's Auklet frequents the outer shelf and shelf break waters. The marbled murrelet is listed as threatened under the federal ESA and endangered under CA ESA, and the Scripps's and Guadalupe murrelets are listed as threatened under CA ESA. All members of this group have short, stubby wings used in diving and generally remain very close to the sea surface when flying.

Loons, Grebes, Ducks

There are four loon species (common, red-throated, Pacific and Arctic [*Gavia immer, G. stellata, G. pacifica, arctica*]) in this FG. These species are all flappers and nest in the subarctic/arctic. They frequent CCS coastal waters largely during the Davidson Current season but some winter in coastal Mexican waters and can also be passage migrants. Also included are Clark's and western grebes. Both nest in marshes of the CA interior, coming to the coast during the Oceanic and Davidson Current seasons, where they remain close to shore. They difficult to identify in the field and were treated as one taxa for purposes of this study. Ducks included in this FG are surf scoters (*Melanitta perspicillata*) and black brant (*Branta bernicla*) that range between passage migrants and seasonal residents during the Davidson Current season. All species in this FG generally travel in large, single-species flocks, sometimes in V-formation, at low to medium heights above the sea surface. Unlike alcids, they propel themselves underwater using their feet rather than their wings, and thus are more rapid, agile fliers.

Appendix E References

Ainley, D. G., E. Porzig, D. Zajanc, and L. B. Spear. 2015. Seabird flight behavior and height in response to altered wind strength and direction. Marine Ornithology 43:25-36.

Pennycuick, C. J. 1987. Flight of Seabirds. Pages 43-62 *in* J. P. Croxall, Seabirds: Feeding Biology and Role in Marine Ecosystems. Cambridge University Press, UK.

Pennycuick, C. J. 1989. Bird Flight Performance: A Practical Calculation Manual. Oxford University Press, Oxford, UK.

Spear, L. B., and D. G. Ainley. 1997. Flight behaviour of seabirds in relation to wind direction and wing morphology. Ibis 139:221-233.